ISSN 2500-316X (Online)

RUSSIAN TECHNOLOGICAL JOURNAL

РОССИЙСКИЙ ТЕХНОЛОГИЧЕСКИЙ ЖУРНАЛ

Information systems.
Computer sciences.
Issues of information security

Multiple robots (robotic centers) and systems.
Remote sensing and nondestructive testing

Modern radio engineering and telecommunication systems

Micro- and nanoelectronics.
Condensed matter physics

Analytical instrument engineering and technology

Mathematical modeling

Economics of knowledge-intensive and high-tech enterprises and industries.
Management in organizational systems

Product quality management. Standardization

Philosophical foundations of technology and society

12+
www.rtj-mirea.ru

13(4) 2025

ISSN 2500-316X (Online)

RUSSIAN TECHNOLOGICAL JOURNAL

РОССИЙСКИЙ ТЕХНОЛОГИЧЕСКИЙ ЖУРНАЛ

- Information systems. Computer sciences. Issues of information security
- Multiple robots (robotic centers) and systems. Remote sensing and nondestructive testing
- Modern radio engineering and telecommunication systems
- Micro- and nanoelectronics. Condensed matter physics
- Analytical instrument engineering and technology
- Mathematical modeling
- Economics of knowledge-intensive and high-tech enterprises and industries. Management in organizational systems
- Product quality management. Standardization
- Philosophical foundations of technology and society

- Информационные системы. Информатика. Проблемы информационной безопасности
- Роботизированные комплексы и системы. Технологии дистанционного зондирования и неразрушающего контроля
- Современные радиотехнические и телекоммуникационные системы
- Микро- и наноэлектроника. Физика конденсированного состояния
- Аналитическое приборостроение и технологии
- Математическое моделирование
- Экономика наукоемких и высокотехнологичных предприятий и производств. Управление в организационных системах
- Управление качеством продукции. Стандартизация
- Мировоззренческие основы технологии и общества

Russian Technological Journal
2025, Vol. 13, No. 4

Russian Technological Journal
2025, том 13, № 4

https://www.rtj-mirea.ru

https://doi.org/10.32362/2500-316X

ISSN 2500-316X (Online)

Russian Technological Journal
2025, Vol. 13, No. 4

Publication date July 31, 2025.

The peer-reviewed scientific and technical journal highlights the issues of complex development of radio engineering, telecommunication and information systems, electronics and informatics, as well as the results of fundamental and applied interdisciplinary researches, technological and economical developments aimed at the development and improvement of the modern technological base.

Periodicity: bimonthly.
The journal was founded in December 2013. The titles were «Herald of MSTU MIREA» until 2016 (ISSN 2313-5026) and «Rossiiskii tekhnologicheskii zhurnal» from January 2016 until July 2021 (ISSN 2500-316X).

Founder and Publisher:
Federal State Budget
Educational Institution of Higher Education
«MIREA – Russian Technological University»
78, Vernadskogo pr., Moscow, 119454 Russia.

The journal is included into the List of peer-reviewed science press of the State Commission for Academic Degrees and Titles of Russian Federation. The Journal is included in Russian Science Citation Index (RSCI), Russian State Library (RSL), Science Index, eLibrary, Directory of Open Access Journals (DOAJ), Directory of Open Access Scholarly Resources (ROAD), Google Scholar, Ulrich's International Periodicals Directory.

The registration number ПИ № ФС 77 - 81733 was issued in August 19, 2021 by the Federal Service for Supervision of Communications, Information Technology, and Mass Media of Russia.

The subscription index of *Pressa Rossii*: **79641**.

Russian Technological Journal
2025, том 13, № 4

Дата опубликования 31 июля 2025 г.

Научно-технический рецензируемый журнал освещает вопросы комплексного развития радиотехнических, телекоммуникационных и информационных систем, электроники и информатики, а также результаты фундаментальных и прикладных междисциплинарных исследований, технологических и организационно-экономических разработок, направленных на развитие и совершенствование современной технологической базы.

Периодичность: один раз в два месяца.
Журнал основан в декабре 2013 года. До 2016 г. издавался под названием «Вестник МГТУ МИРЭА» (ISSN 2313-5026), а с января 2016 г. по июль 2021 г. под названием «Российский технологический журнал» (ISSN 2500-316X).

Учредитель и издатель:
федеральное государственное бюджетное образовательное учреждение высшего образования «МИРЭА – Российский технологический университет»
119454, РФ, г. Москва, пр-т Вернадского, д. 78.

Журнал входит в Перечень ведущих рецензируемых научных журналов ВАК РФ, в которых должны быть опубликованы основные научные результаты диссертаций на соискание ученой степени кандидата наук и доктора наук, входит в RSCI, РГБ, РИНЦ, eLibrary, Directory of Open Access Journals (DOAJ), Directory of Open Access Scholarly Resources (ROAD), Google Scholar, Ulrich's International Periodicals Directory.

Регистрационный номер и дата принятия решения о регистрации СМИ ПИ № ФС 77 - 81733 от 19.08.2021 г. СМИ зарегистрировано Федеральной службой по надзору в сфере связи, информационных технологий и массовых коммуникаций (Роскомнадзор).

Индекс по объединенному каталогу «Пресса России» **79641**.

Editorial Board

Редакционная коллегия

Contents

Содержание

Information systems. Computer sciences. Issues of information security
Информационные системы. Информатика. Проблемы информационной безопасности

UDC 004.422.8:53.043
https://doi.org/10.32362/2500-316X-2025-13-4-7-24
EDN WLFGJJ

RESEARCH ARTICLE

Programming and computing suite for simulating the therapeutic absorbed dose in radiotherapy

Aleksei N. Solovev [1, 2, @], Yana V. Kizilova [1], Evgeniy I. Kazakov [1], Sergey N. Koryakin [1, 2]

[1] *A. Tsyb Medical Radiological Research Center – Branch of the National Medical Research Radiological Center of the Ministry of Health of the Russian Federation, Kaluga oblast, Obninsk, 249031 Russia*
[2] *Obninsk Institute for Nuclear Power Engineering, Kaluga oblast, Obninsk, 249039 Russia*
[@] *Corresponding author, e-mail: salonf@mrrc.obninsk.ru*

• **Submitted:** 27.09.2024 • **Revised:** 06.02.2025 • **Accepted:** 20.05.2025

Abstract

Objectives. Simulation of the absorbed dose is an essential part of radiation therapeutic treatment, performed not only for its correct evaluation, but also for assuring quality control and retrospective evaluation of the provided cure. From the technological point of view, strict requirements are imposed on the software applications and hardware units that support a successful decision-making process before, during, or after the provided therapy. This paper reports an R&D project aimed at technological support of radiation treatment planning systems coupled with the creation of a mathematical framework for estimating the absorbed dose for radiobiological and medical therapeutic purposes.

Methods. A dedicated automated software suite for executing multipurpose Monte Carlo simulations was developed. The suite is backed up with virtualization techniques for structured hardware access, data intercommunication using diverse connection channels, various physical interaction engines, and coupled end-user software.

Results. The developed suite facilitates a wide array of tasks in the realm of radiobiological research conducted using radiation beams of different qualities. Additionally, it serves as a foundation toolkit for developing radiotherapy planning systems for both existing and new therapeutic facilities, as well as software packages for estimation of the long-term effects of the conducted radiotherapy.

Conclusions. The developed programming and computing suite is an effective tool for organizing a specialized environment for multipurpose estimation of the absorbed dose of radiation for therapeutic applications of radiation beams of different qualities. The suite can be updated and extended upon end-user needs and modified by skilled software developers for specific purposes.

Keywords: programming and computing suite, physics-based simulation, absorbed dose, radiotherapy, proton therapy, neutron therapy, Monte Carlo method

For citation: Solovev A.N., Kizilova Ya.V., Kazakov E.I., Koryakin S.N. Programming and computing suite for simulating the therapeutic absorbed dose in radiotherapy. *Russian Technological Journal.* 2025;13(4):7–24. https://doi.org/10.32362/2500-316X-2025-13-4-7-24, https://www.elibrary.ru/WLFGJJ

Financial disclosure: The authors have no financial or proprietary interest in any material or method mentioned.

The authors declare no conflicts of interest.

НАУЧНАЯ СТАТЬЯ

Комплекс программно-вычислительных средств моделирования терапевтических величин поглощенных доз в задачах лучевой терапии

А.Н. Соловьев [1, 2, @], Я.В. Кизилова [1], Е.И. Казаков [1], С.Н. Корякин [1, 2]

[1] *Медицинский радиологический научный центр имени А.Ф. Цыба – филиал ФГБУ «Национальный медицинский исследовательский центр радиологии» Министерства здравоохранения Российской Федерации, Обнинск, Калужская область, 249031 Россия*

[2] *Обнинский институт атомной энергетики — филиал ФГАОУ ВО «Национальный исследовательский ядерный университет «МИФИ», Обнинск, Калужская область, 249039 Россия*

[@] *Автор для переписки, e-mail: salonf@mrrc.obninsk.ru*

• **Поступила:** 27.09.2024 • **Доработана:** 06.02.2025 • **Принята к опубликованию:** 20.05.2025

Резюме

Цели. Моделирование поглощенных доз в радиотерапии является ключевым процессом в ходе лечения пациентов, а также выполняется с целью обеспечения гарантий качества терапии и ретроспективных оценок успешности проведенного лечения. С технической точки зрения предъявляемые требования к программному и аппаратному обеспечению весьма строгие для того, чтобы обеспечить успешный процесс принятия решения до, во время или после проведения терапии. Цель статьи – разработка и апробация технологического процесса обеспечения систем планирования лучевой терапии, а также создание расчетных модулей оценок поглощенных доз радиобиологического и терапевтического назначения.

Методы. Специализированное автоматизированное программное обеспечение, разработанное и поддерживаемое для обеспечения многоцелевых расчетов методом Монте-Карло, построено на основе технологий виртуализации для структурированного доступа к оборудованию, технологий передачи данных по разнородным каналам связи, различных физических моделей расчета взаимодействий излучения, которые совмещены в продукты для конечного пользователя.

Результаты. Комплекс позволяет решать широкий круг задач в интересах радиобиологических исследований, проводимых на пучках излучений разного качества, а также служить основой как для построения систем планирования лучевой терапии для действующих и вновь создаваемых установок, так и в интересах оценки отдаленных последствий действия терапевтического излучения.

Выводы. Разработанный комплекс программно-вычислительных средств является мощным инструментом, служащим для дальнейшего создания специализированных многоцелевых сред оценок поглощенных доз, необходимых для терапевтического применения широкого круга радиационных технологий. Комплекс может быть модернизирован под потребности пользователей, а также дорабатываться разработчиками программного обеспечения под собственные нужды.

Ключевые слова: программно-аппаратный комплекс, моделирование физических величин, поглощенная доза, лучевая терапия, протонная терапия, нейтронная терапия, метод Монте-Карло

Для цитирования: Соловьев А.Н., Кизилова Я.В., Казаков Е.И., Корякин С.Н. Комплекс программно-вычислительных средств моделирования терапевтических величин поглощенных доз в задачах лучевой терапии. *Russian Technological Journal*. 2025;13(4):7–24. https://doi.org/10.32362/2500-316X-2025-13-4-7-24, https://www.elibrary.ru/WLFGJJ

Прозрачность финансовой деятельности: Авторы не имеют финансовой заинтересованности в представленных материалах или методах.

Авторы заявляют об отсутствии конфликта интересов.

INTRODUCTION

The computational and mathematical problems that need to be solved within the framework of radiation therapy procedures can be conventionally divided into two main classes.

The problems of the first class include those of pretreatment patient preparation. At this stage, it is necessary to ensure the fulfillment of model therapeutic criteria of effectiveness and safety of the patient's treatment with the necessary accuracy and promptness for making a grounded medical decision. The resulting solution consists in the formation of recommendations about the admissibility of the course of therapy by the system supporting medical decision making.

The problems of the second class, conversely, are not directly linked to the decision to prescribe therapy to a particular patient; instead, they are aimed at verification and confirmation of the characteristics of the previously prescribed treatment scheme, including the criteria for the formation of early and late radiation complications, retrospective analysis of groups of treated patients in order to form a survival prognosis and assess the quality of the previously performed planning, or to form alternative scenarios for assessing the success of the therapy.

The systems that solve the first class of problems are conventionally referred to as treatment planning systems (TPS). Among them, commercially available systems include *Raystation*[1] by RaysearchLabs, *Eclipse*[2] by Varian (Germany), *Pinnacle*[3] by Philips (Netherlands), *One*[4] in *XiO* and *Monaco* versions by Elekta (Sweden); *PLANB*[5] complex by RT-7, *Amfora*[6] by Medico-Physical Center (Russia). As a general rule, the planning system is not a separate versatile product; rather, such a system is an element of the final physical installation, e.g., the planning system for the neutron therapy complex based on the NG-24MT generator (neutron generator based on the D(T, ^{4}He)n reaction, neutron energy 14 MeV) [1] and for the domestic 6 MeV conventional accelerator (electron drift tube with energy up to 6 MeV suited for medical application using a bremsstrahlung on a tungsten target) [2], *XiDose* for carbon therapy centers in Japan [3], *TRiP98* for carbon therapy centers in Darmstadt and Heidelberg, Germany [4], projects of *NCTPlan* use at Massachusetts Institute for neutron capture therapy at reactors of National Research Nuclear University "MEPhI" [5]. Specialized tools also include the *NeuCure* [6] and *NeuMANTA* [7] systems used for neutron capture therapy purposes.

In the classical scheme of radiation therapy, planning systems has the specific feature associated with the time of obtaining a solution to the dosimetric planning problem. Tasks related to the assessment of long-term (relative to the course of therapy) consequences of treatment and dosimetric features of dose formation are simulated, as a rule, using more conventional means and methods of Monte Carlo modeling of radiation interactions with matter, which include, e.g., *Geant4* [8], *FLUKA* [9], *MCNP* [10], *PHITS* [11], and *SHIELD-HIT* [12]. All these simulation tools have been approved by the world community as those intended for a reliably accurate prediction of, in particular, the values of absorbed doses in target media. Although the results of such models have proved useful in clinical and research practice, a number of issues remain to be resolved [13], primarily those related to elucidating the response of biological

[1] https://www.raysearchlabs.com/raystation/. Accessed May 19, 2025.

[2] https://www.varian.com/products/radiotherapy/treatment-planning/eclipse. Accessed May 19, 2025.

[3] https://www.usa.philips.com/healthcare/solutions/radiation-oncology/radiation-treatment-planning. Accessed May 19, 2025.

[4] https://www.elekta.com/products/oncology-informatics/elekta-one/treatment-applications/planning/. Accessed May 19, 2025.

[5] https://rt-7.ru/planb (in Russ.). Accessed May 19, 2025.

[6] http://mphc.ru/catalog/amphora/ (in Russ.). Accessed May 19, 2025.

systems with various levels of organization to complex mechanisms of radiation action on cell cultures [14–17]. Such systems are also used in *in vivo* studies [18, 19], for safety assessment of radioactive waste landfills [20] and space flights [21, 22], and for verifying the radiation safety for the personnel of the radiotherapy facilities [23].

In this paper, we set out to develop a versatile suite of computational tools capable of solving problems of both classes described above and having wide possibilities for interchangeability of components and their modernization. We also describe the characteristics and specific features of technological implementation of the developed suite for the tasks of pre-radiation preparation of radiobiological studies, dosimetric planning of radiation therapy, retrospective assessment of biological effects on the basis of equivalent precision calculation of absorbed doses, as well as for building predictive models to describe the damaging effects of radiation and present the results obtained in accordance with the international requirements of the IAEA[7] and ICRP[8] for specific types of radiation (ion radiation ICRU 93[9], neutron capture therapy CRCP/BOR/002[10]).

MATERIALS AND METHODS

For efficient operation of a hardware and software suite, which is capable of functioning in an automated mode, an integrative connectivity between its individual components, as well as the possibility of their controlled launch depending on the availability of relevant input data, should be ensured. Figure 1 presents the architecture of the developed suite and displays the interconnection between the components, as well as the roles and places of individual users. The solid lines show module affiliations; the dotted lines show communication links.

While developing the suite, the main requirement was related to the possibility of rapid deployment of its components on a new hardware platform, geographically separated from other components of the suite. At the same time, the initial construction of the software included in the suite and its implementation were carried out on a single hardware base represented by a means of high-performance computing, including a dual-processor system based on Intel Xeon Gold E5506 (Intel, USA) with 380 GB of connected random access memory (RAM), NVIDIA Tesla V100 graphics processor (NVIDIA, USA), and a data storage system based on server hard disk drives (HDD) manufactured by Toshiba (Japan). The platform is connected to the local area network of the experimental sector of the A. Tsyb MRRC[11] based on MikroTik switches (Latvia), providing bandwidth at a level of 1 Gbps. The external communication channel used during the testing of the software in a geographically distributed setup mode provided data transmission speeds of up to 70 Mbit/s. Terminal workplaces of the complex operators were connected both in the internal network mode with full capacity (1 Gbit/s) and in the modes of artificially limited typical network (100 Mbit/s) and remote network (Internet channel).

CONTROL ARCHITECTURE

Since the architecture under development was required to enable shared component work, and since the physical means for organizing server interaction was presented as a single entity, the main technological approach was the organization of virtualization. To that end, Proxmox[12] was used as the base operating system of the server. This distribution is based on Debian GNU/Linux, developed and supported by the Internet Foundation Austria. Initially, the Proxmox VE 6 version was developed followed by its modification to Proxmox VE 7.1-11. At present, a stable version of Proxmox VE 8.2 is available.

The system fast data storage (solid-state drive, SSD) is divided into the main sector (for installing the Proxmox base environment) and sectors of managed application servers. In this case, each storage is a separate disk space with the possibility of expanding the address space, including during physical migration of the storage medium. The long-term storage is organized by addressing the whole pool of disk space of physical devices of the system into the created Proxmox container managed by TrueNAS[13] operating system. On the basis of TrueNAS, a software RAID array of level 5 with access via CIFS[14], SSH[15], and NFS[16] protocols is organized.

[7] International Atomic Energy Agency. https://www.iaea.org. Accessed May 19, 2025.

[8] International Commission on Radiation Units and Measurements. https://www.icru.org/. Accessed May 19, 2025.

[9] ICRU Report 93: Prescribing, Recording, and Reporting Light Ion Beam Therapy. https://www.icru.org/report/icru-report-93-prescribing-recording-and-reporting-light-ion-beam-therapy/. Accessed May 19, 2025.

[10] IAEA. Advanced in Boron Neutron Capture Therapy. Non-serial Publication. https://www.iaea.org/publications/15339/advances-in-boron-neutron-capture-therapy. Accessed May 19, 2025.

[11] A. Tsyb Medical Radiological Research Center. https://new.nmicr.ru/en/mrrc/. Accessed May 19, 2025.

[12] https://www.proxmox.com/en/. Accessed May 19, 2025.

[13] http://www.truenas.com/. Accessed May 19, 2025.

[14] https://learn.microsoft.com/ru-ru/windows/win32/fileio/microsoft-smb-protocol-and-cifs-protocol-overview (in Russ.). Accessed May, 19, 2025.

[15] https://www.rfc-editor.org/info/rfc4251. Accessed May 19, 2025.

[16] https://www.rfc-editor.org/info/rfc3010. Accessed May 19, 2025.

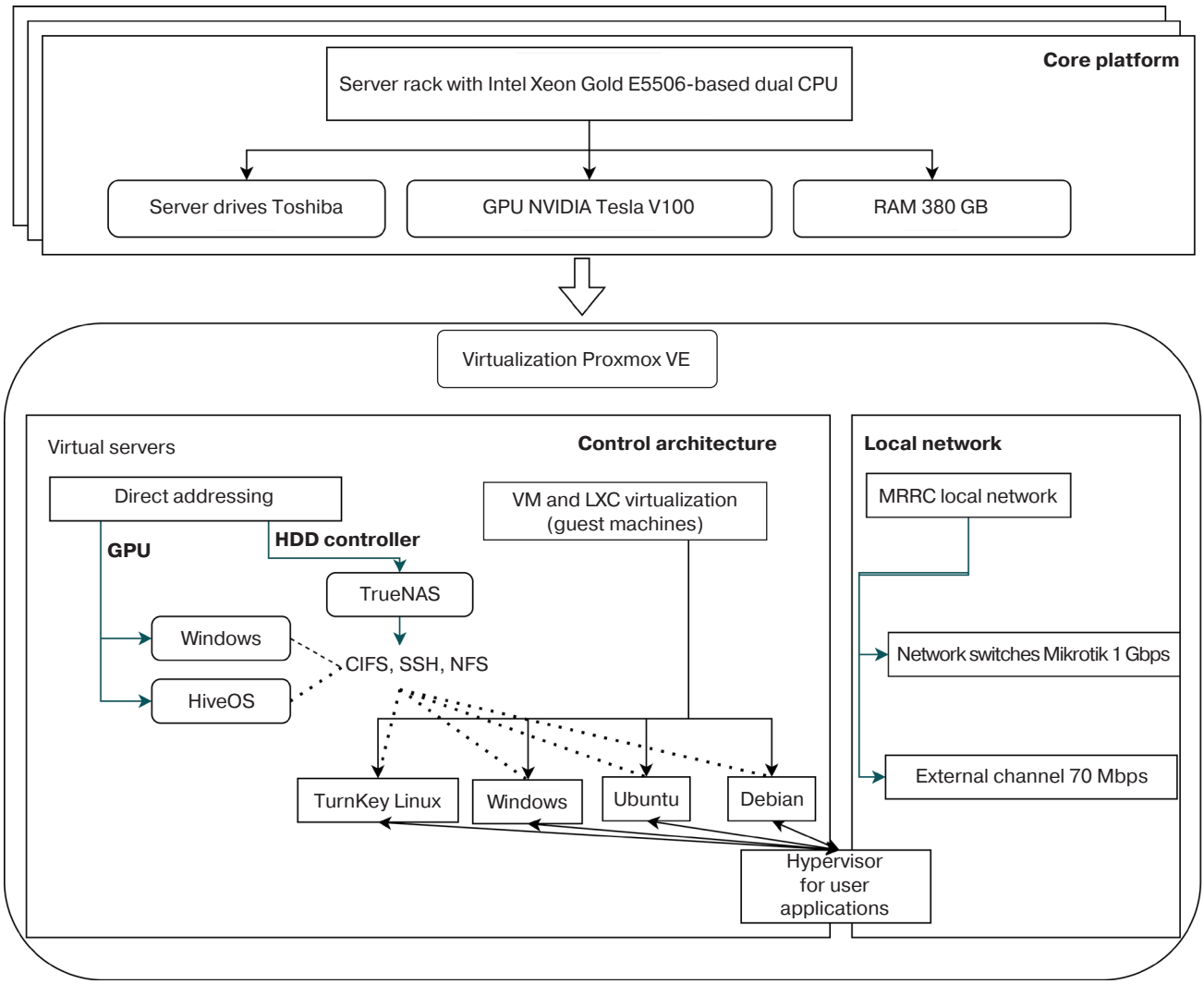

Fig. 1. Structural diagram of the software-computing complex.
GPU—graphics processing unit, HDD—hard-disk drives, VM—virtual machine, LXC—simplified Linux containerization scheme

Support for iSCSI[17] in the implementation [1] is used only as part of the terminal equipment of automated workstations. Thus, it is assumed that all further created components of the server architecture use at least their address space of fast storage and have a common configurable access to the common file space of long-term storage.

RAM allocation for each of the subsequent managed servers in Proxmox virtualization is carried out at the stage of creation of a virtualization server, and, depending on specific needs, the parameters cannot always be dynamically expanded without recreating the server. In this regard, for each task solved by the server computers, an understanding of the actual resource consumption by the system architect and system programmer is needed. It should borne in mind that the tasks of modeling a direct radiation response (e.g., a tumor) and the entire therapy course with different variants of treatment responses are undoubtedly large-scale computing tasks. Thus, the task solved by a person when organizing the control level of the control architecture is, among other things, the choice of optimal parameters of the physical computing means.

Finally, a separate technological solution was developed as part of the solution to the problem of controlled, configurable launching of end-user applications on individual system servers. It represents its own hypervisor, launched by the command of the end-user tool, providing further automatic start, management, control, receipt, and transfer of the results of execution of computing tools on one target server. The target server can be any server running an *nix family of operating systems; connection and communication is performed via the secure SSH protocol. The configuration of managed applications is specified by a text file of JSON[18] syntax.

[17] https://www.rfc-editor.org/info/rfc7143. Accessed May 19, 2025.

[18] https://dx.doi.org/10.17487/RFC4627. Accessed May 19, 2025.

SERVER COMPUTING HARDWARE ARCHITECTURE

In the developed suite, all server computing facilities are divided into two classes. The first class includes systems that are deployed only within the Proxmox virtual environment, requiring no physical addressing of server devices. In general, this simply includes individual compute nodes for tasks that require only a central processing unit (CPU). The second class of systems are those that require the virtualization server administrator to configure physical addressing, which primarily refers to the graphics processing unit (GPU). The implementation of such means implies that at a particular moment in time, the access of such a system to the addressed physical entity is exclusive. Thus, e.g., all computational models and tools using a graphics card must either connect to the currently active server using the GPU or wait their turn for their server exclusive access to a physical resource on the host machine. When implementing system components outside of a virtualization environment, e.g., when there are separate physical compute machines and graphics card machines, such a task can be excluded from consideration.

The stages of deployment of server computing environment are built according to the classical scheme. First of all, after installing and assembling the operating system on the dedicated node and installing the appropriate updates, the target software of the node is assembled. For the computational nodes involved in the described suite for simulating the effects of ionizing radiation, the main package of computational software was *Geant4* [8] developed by CERN[19] (Switzerland), with versions from 4-9.5.0 (2016) to 4-11.2.2 (2024) being used during the period of the target use of the suite. One of the features of the package is the allocation of components of section libraries in separate downloadable files with the possibility of automatic linking at the stage of building the program. The *Geant4* build system is completely based on CMake[20], and versions from 4-10.0 can be built on any target platform compilers gcc, clang, and msvc, depending on the preferences of the developer. In this case, unlike the vast majority of similar Monte Carlo codes, *Geant4* is not a final executable file, but rather a set of libraries of dynamic or static linking for further creation of the programmer's own application. However, it should be noted that there are ready-made executables based on *Geant4*, which the user already manages only by providing input data, similar to other environments. Such solutions include *TOPAS*[21], *GATE*[22], and *GAMOS*[23]. The Table shows characteristic

[19] Conseil Européen pour la Recherche Nucléaire, CERN.
[20] https://cmake.org/. Accessed May 19, 2025.
[21] https://www.topasmc.org/. Accessed May 19, 2025.
[22] http://www.opengatecollaboration.org/. Accessed May 19, 2025.
[23] https://fismed.ciemat.es/GAMOS/. Accessed May 19, 2025.

Table. Performance evaluation of different *Geant4* versions

Geant4 version (*Geant4* year of issue)	Archive unpacking, ms	CMake configuration, ms	Make		
			1 thread, ms	16 threads, ms	32 threads, ms
9.6.4 (2016)	1392	6275	1321462	116047	85899
10.0.0 (2016)	1504	7737	1721182	106263	82304
10.3.0 (2016)	1760	5497	3124605	164876	127049
10.4.0 (2017)	1636	2911	3538766	179560	138334
10.5.0 (2018)	1764	1761	2814052	216675	163520
10.7.0 (2020)	1787	6147	3715283	239053	185224
10.7.4 (2022)	1708	3612	3057118	256715	201234
11.0.0 (2021)	1599	9720	6450537	277412	211570
11.1.0 (2022)	1745	6532	4831937	299245	238212
11.2.0 (2023)	1662	4732	5031802	306279	238548
11.2.2 (2024)	1688	8582	3813355	306803	246890

installation times of different *Geant4* versions on one of the currently functioning dedicated servers. All measurements were made in automatic mode by means of bash interpreter and *nix system time utility. The data is presented as a single measurement of calendar (wall time) time of the build procedure execution.

When implementing computational packages within the suite, one or another version of the software was used, depending on the specific task. For example, to solve the problem of dosimetric planning as part of the neutron therapy complex [1], the stable version 10.6.2 was used, which was not updated further. For a number of other tasks, in particular those described in [24], the then current version 10.3.1 was used. All routine simulations of the tasks arising in the course of the activities of the Department of Radiation Biophysics of the A. Tsyb MRRC are always performed on the latest stable version at the time of problem statement. It should be noted that backward compatibility of the user code is not always guaranteed by the developers of the *Geant4* environment, including compatibility with new versions of compilers. This is especially true in the case of explicit requirements for cross-platform end-applications.

It should be noted that the use of a specific tool for mathematical simulation of radiation action is not a limiting factor. It was earlier shown in [25] that heterogeneous tools can be used both in solving the task of radiation therapy planning and integrated under a common architecture of control commands. Thus, in the present work, the launch of the functionality executed on video cards can be performed both directly from the *Geant4* environment application and separately on a standalone virtual machine using the output of the *Geant4* application as its own input data transmitted via the previously described communication channels.

ARCHITECTURE OF A STANDARDIZED DATA TRANSMISSION FORMAT

In the presented suite, JSON is the main format of configuration files. This convenient format allows cross-platform transfer of "key-value" pairs, and the values can be both separate data types and lists and dictionaries of values. However, due to the specificity of user data, which are conventionally represented in such systems in the DICOM[24] industrial format, the internal format of data exchange in applications should effectively support the transfer of binary data. Thus, during the implementation of the project, it was decided to implement a separate format for storing user intermediate data. As the main format for such tasks, the protobuf[25] message transmission description by Google[26] was selected. After that, versatile tools for transforming tomographic images and associated contours [26], phase spaces for general-purpose Monte Carlo codes [27], and associated output formats were written. The format and the messages themselves are fully portable between operating systems, while message writing and reading functionality implemented for a vast amount of programming languages. The only limitation of the used solution consists in the maximum message size, which cannot be larger than 2.14 GB due to the addressing of the binary file in a 32-bit memory region. Such target files may occur, e.g., when working with tomographic images with the pixel number of 1024 × 1024 and the slice number of more than 200 and simultaneously with the associated number of contours more than 32. To solve this problem, a backup format based on serialization libraries in Boost[27] was implemented; however, the associated disadvantage involves the impossibility of transferring the final target files between Linux and Windows operating systems.

ARCHITECTURE OF END-USER TERMINAL FACILITIES

In contrast to server-based settlement tools, which should be deployed only on the basis of Linux or BSD operating systems, the requirements for endpoint workstations and client machines may be not as strict. In general, deployment should be available on any operating system, including Windows, Linux, and macOS. In addition, any endpoint user environment should be easily upgradeable. Thus, it was decided to use the Python[28] programming language for the work of creating the final user interface, and the final executable files were built for the specific operating system of the target endpoint using publicly available tools for building executable files (e.g., pyinstaller[29]). In this case, separate modules of the final software, which have their own separate input and output data, are realized as ready executable files, and integrative access is provided by means of the end environment file system and network file system, linked by servers according to the scheme described above. Some examples of this approach include specific modules for the pre-radiation preparation stage [28] and an external system for field optimization in the mode of 3D conformal radiation therapy [29].

[24] Digital Imaging and Communications in Medicine is a medical industry standard for creating, storing, transmitting, and visualizing digital medical images and documents of examined patients.

[25] https://protobuf.dev/reference/protobuf/edition-2023-spec/. Accessed May 19, 2025.

[26] https://about.google/. Accessed May 19, 2025.

[27] https://www.boost.org/. Accessed May 19, 2025.

[28] https://python.org/. Accessed May 19, 2025.

[29] https://pyinstaller.org/. Accessed May 19, 2025.

Figure 2 presents the architecture of using end-user tools as part of the considered suite when realized within the framework of neutron therapy tasks (variant 1), prospective planning tasks (variant 2), and related integration tasks (variant 3). The client application in C# language can call separate modules of Python language and executable files of additional applications (*NGPlan.Visual.Client* and *ROReview*); it also has interfaces of exchange with third-party services and tracking the progress of server tasks. Within the framework of providing data flows on the server, three variants of execution of Monte Carlo calculations are realized, the main technological components of which are presented in their order of invocation. Figure 3 shows a number of screenshots illustrating the appearance of the software products.

SUITE APPROBATION IN FIELD STUDIES

The primary evaluation of the technological connectivity of the components was carried out within the framework of related work on the assessment of the radiation hardening of products to heavy ions [30]. In the process of performing the simulations that serve as a basis for subsequent estimates of the values of linear energy transfer of various ions through scatterers and a low (10 torr) density atmosphere, the calculation server, deployed as described earlier, was used. The results obtained were automatically analyzed in the form of histograms in the *ROOT* package [31] developed by CERN. The communication mechanisms between the calculation server with *Geant4* and typical clients in the form of the Windows file system explorer and the root client application were tested.

One of the main applications of the suite software consists in obtaining comprehensive estimates of the values of biological effectiveness of radiation. Primary results related to the medical application of the suite were described in [32], where the components of the suite, including the GPU, were used in an automated mode to perform retrospective estimates of the contribution to the biological dose of the proton component in fast neutron irradiation.

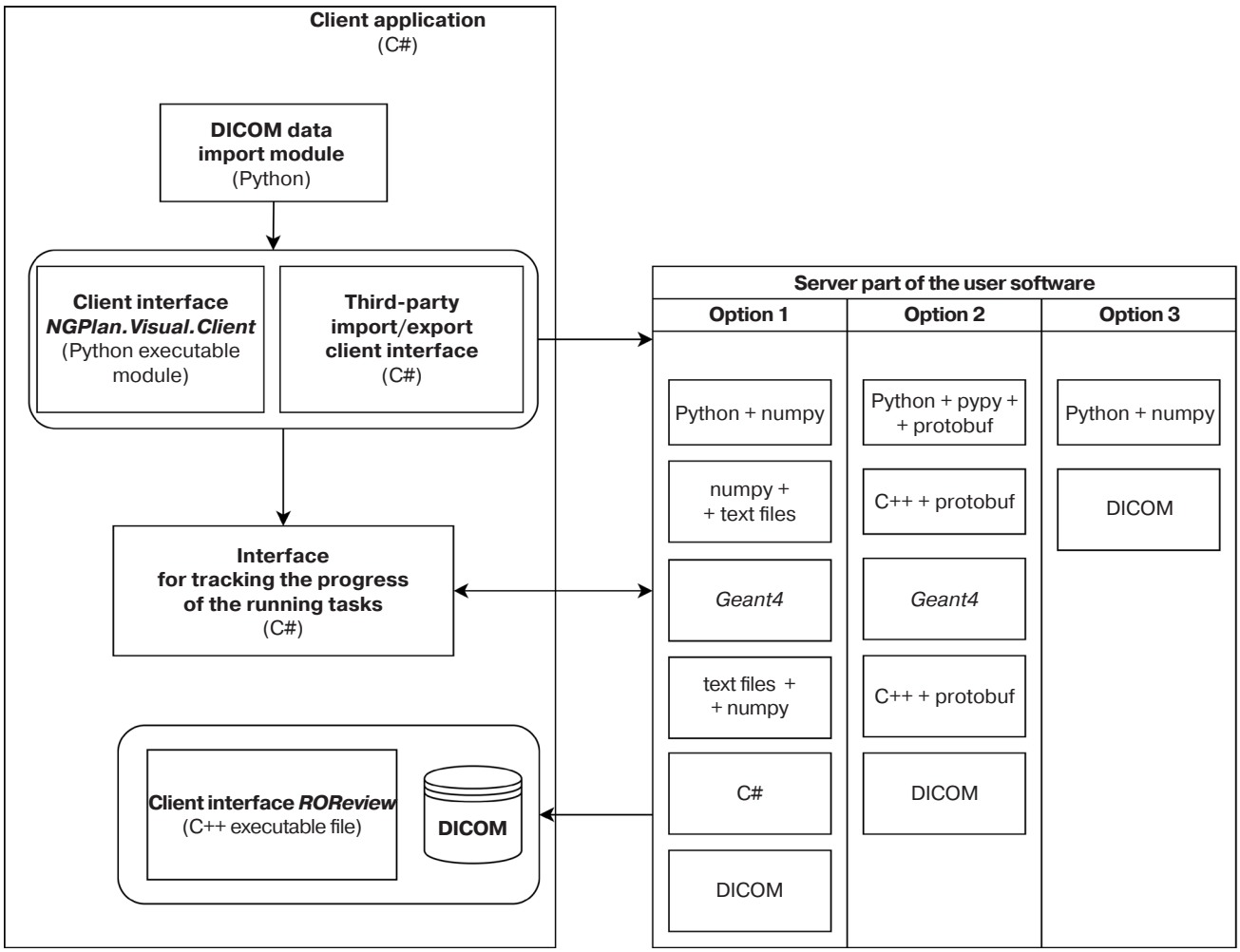

Fig. 2. Principal diagram of the end-user application organization

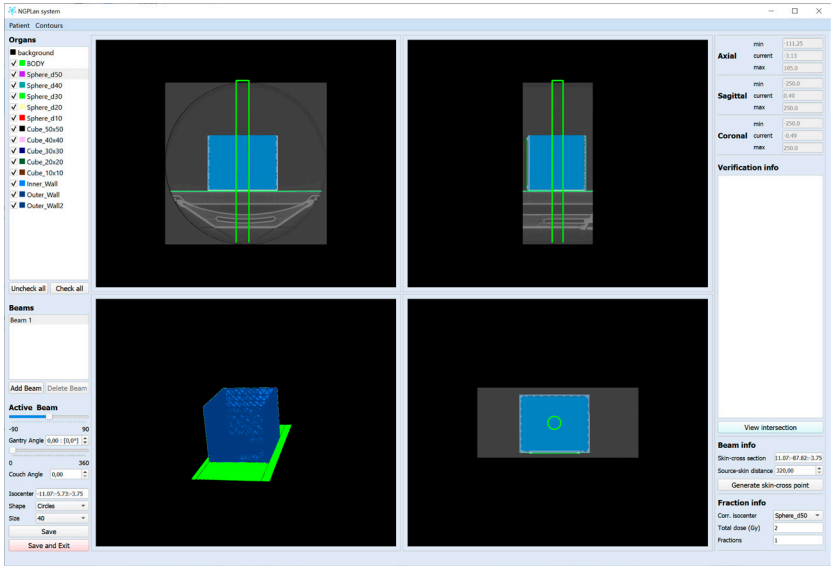

(a)

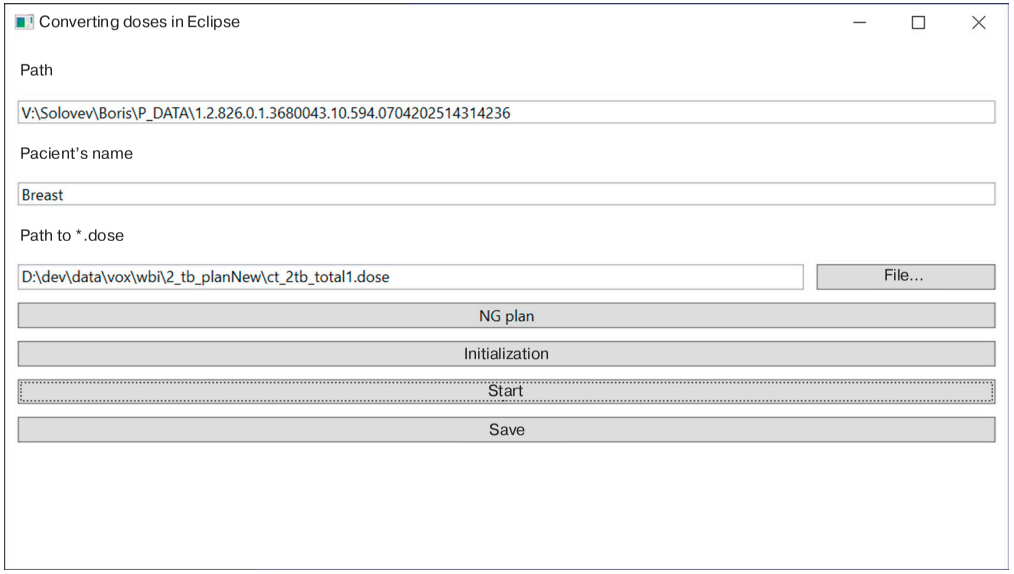

(b)

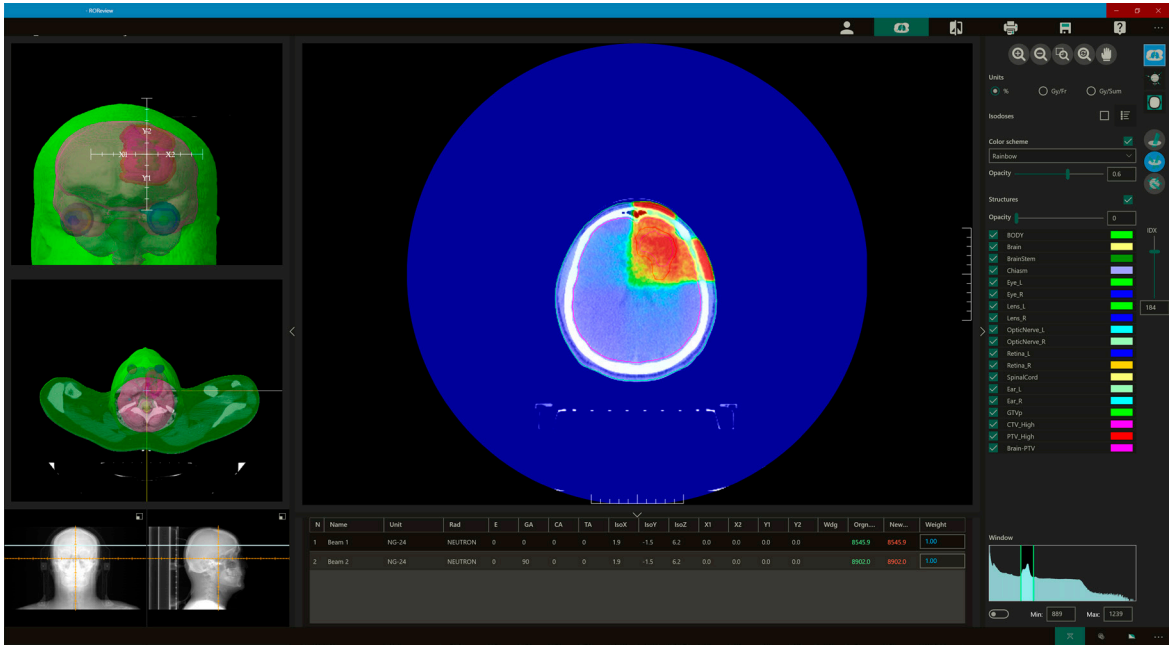

(c)

Fig. 3. Appearance of some software tools of the developed suite:
(a) *NGPlan.Visual.Client* interface for working with the irradiator location at the stage of pre-radiation preparation;
(b) interface of the third-party import/export utility;
(c) interface of the *ROReview* software package in the dose field display mode

A similar application domain[30] was the modification of the presented suite for the purposes of estimation of relative biological effectiveness (RBE) of proton radiation in comparison with the conventional RBE 1.1 used in routine clinical practice. When building such models, Hounsfield number transformations of the original tomograms based on the optimized model of material densities [33] were used, but all operations within the presented suite are configurable. Work is underway to create an ergonomic user interface for convenient data input at the commissioning stage of the planning systems implemented or intended to be implemented as part of the described suite.

The results of field testing of mathematical models for optimizing the dose deposit of a modified Bragg peak for protons in the form of a task file for the accelerator of the Prometheus proton therapeutic facility (Obninsk, Russia) were presented in [34]. The above-described approaches to mathematical simulation of proton radiation action were used to develop control commands, which were then transmitted to the control system of the accelerator [35]. A similar task of creating control commands was solved in [36] to detect morphological changes in tumor cells after implantation in a tumor-bearing animal. In general, such an approach to the automation of radiobiological studies shows its effectiveness and makes it possible to significantly reduce the time of preparation for the experiment by unifying typical solutions.

Finally, the computing and programming suite proved feasible in the tasks of experimental activities at the temporary radiobiological stand [37], and later—within the framework of the collective use center of the U-70 accelerator facility (CCU "RBS on U-70"[31]). When carrying out an initial assessment of the biological efficiency of carbon ion beams [38], data on the dose-averaged values of linear energy transfer calculated in a detailed model of the irradiated object for various experimental conditions were used. The approaches to the creation of means for passive modification of carbon radiation described earlier [39] and realized later as a software package as part of the described suite and directly fabricated ridge filters were used by other researchers [40, 41]. The operations of the radiobiological stand of the U-70 facility were described in [42]; approaches to the implementation of channels for medical and therapeutic purposes were reported in [43].

[30] Smyk D.I. *Proton therapy in re-irradiation of recurrent tumors of head and neck organs*. Thesis for a Candidate Degree in Medical Sciences. https://new.nmicr.ru/wp-content/uploads/2024/05/dissertacija-smyk.pdf (in Russ.).

[31] http://ihep.ru/pages/main/6580/8769/index.shtml (in Russ.). Accessed May 19, 2025.

DISCUSSION

One essential aspect of radiotherapy planning systems in clinical practice involves the organization of data transfer between different systems and the connectivity of software components within the system. Thus, the work [44] showed that even when transferring the same DICOM-data set, different planning systems (in [44]—*MRIdian TPS* and *Eclipse*) differ significantly (up to 16%) in terms of interpretation of structure volumes and, consequently, dose-volume parameters. At the same time, taking into account the abundance of systems both available on the market and proprietary (in-house) systems of individual clinics [45–49], the question of ensuring coherence and equivalence of the reported clinical results remains relevant. As clinical practice shows, even in the same hospital, two [50] or more planning systems may be used for the same accelerator or treatment cabin, and the decision to prescribe therapy is achieved after all alternative proposed scenarios have been analyzed by the attending radiotherapist or a board of specialists.

The main direction in the development of calculation systems carrying out simulation of the absorbed dose of radiation therapy consists in a multiple increase of their calculation performance while maintaining the accuracy at the level of precision provided by Monte Carlo systems. In this context, calculations with the use of GPUs are increasingly attracting attention. GPUs have long been used for simulating radiobiological response at the DNA, cellular, and intercellular levels of matter organization, including water radiolysis [51, 52]. At the same time, simulations for the purposes of radiation therapy have emerged only in recent years. For example, the researchers in [53] developed *goCMC*, including the support of a computational module for carbon ion therapy, which allows a computational speed of one plan within 40 min. At the same time, the manufacturers enable the integration of their approach into the *Eclipse* commercial planning system. A similar problem, applied to intraoperative high-energy electron therapy, was solved in [54], with calculation speeds of up to 10 s on a video card. Earlier solutions, such as the one described for proton therapy in [55], become the basis for experimental validation of the approaches used, showing not only times of 3.5 to 11.5 s per beam versus 20 s for the CPU-based solution, but also excellent agreement with measured values according to gamma index criteria (more than 95% passing points according to the 3%/1 mm criterion). The *VQA Plan* [56] system by Hitachi, developed specifically for the ion center in Osaka (Japan), is another solution proposed for the operational calculation of scanning ion beams.

According to the authors, the distinguishing feature of the presented system in comparison with the simplified analogs in *XiDose* and *RayStation* consists in the calculation of the biological component of the dose of carbon beams. The implementation of fast computational algorithms for such systems based on GPUs seems to be a challenging task, the solution of which requires the efforts of a wide range of specialists [57, 58].

CONCLUSIONS

Modern approaches to radiation therapy should not only meet the quality criteria of medical services, but also ensure the required safety of treatment. Organization of an effective software computing environment for a wide range of purposes facilitates, among other things, coordination of efforts of various medical specialists, software developers, radiation technologists. As part of promising development directions, mechanisms for the introduction of quantum computing and artificial intelligence technologies can be considered. Work on the mass-scale introduction of the developed technologies is underway.

ACKNOWLEDGMENTS

The authors thank R.V. Shershnev and U.A. Stepanova for their contribution to the development of the suite during their work in the Laboratory; V.O. Saburov, Acting Head of the Laboratory of the Development and Operation of Irradiation equipment, and A.A. Pechenin, System Administrator, for their help in organizing the technological process; the Directorate of the A. Tsyb MRRC represented by Director S.A. Ivanov for the constructive approach to the implementation of medical tasks; the Directorate of NMRRC Radiology represented by Deputy Director for Science P.V. Shegay and General Director A.D. Kaprin for extensive discussions on the subject of the problem and beyond.

Authors' contributions

A.N. Solovev—writing the original draft, software, conceptualization, project administration, methodology, and investigation.

Ya.V. Kizilova—visualization, formal analysis, data curation, software, investigation, writing the review, and editing.

E.I. Kazakov—investigation, resources, validation, and methodology.

S.N. Koryakin—resources, supervision, validation, funding acquisition, writing the review, and editing.

REFERENCES

1. Mardynsky Yu.S., Gulidov I.A., Gordon K.B., Koryakin S.N., Solovyov A.N., Saburov V.O., Ivanov S.A., Kaprin A.D., Lobzhanidze T.K., Markov N.V., Zheleznov I.M., Yurkov D.I., Gerasimchuk O.A., Presnyakov A.Yu., Zverev V.I., Smirnov V.P. External-Beam Neutron Therapy: The First Domestic Medical Unit. *Vestnik Rossiiskoi Akademii Nauk* (*Herald of the Russian Academy of Sciences*). 2024;94(1):80–86 (in Russ.). https://doi.org/10.31857/S0869587324010098
2. Rod'ko I.I., Sarychev G.A., Balakirev P.V., et al. Development of a Radiotherapy System Based on 6 MeV Linac and Cone-Beam Computer Tomograph. *At. Energy*. 2019;125(5):333–337. https://doi.org/10.1007/s10512-019-00490-9
3. Inaniwa T., Kanematsu N., Noda K., Kamada T. Treatment planning of intensity modulated composite particle therapy with dose and linear energy transfer optimization. *Phys. Med. Biol.* 2017;62(12):5180–5197. https://doi.org/10.1088/1361-6560/aa68d7
4. Krämer M. Swift ions in radiotherapy – Treatment planning with TRiP98. *Nuclear Instruments and Methods in Physics Research Section B: Beam Interactions with Materials and Atoms* 2009;267(6):989–992. https://doi.org/10.1016/j.nimb.2009.02.015
5. Elyutina A.S., Kiger W.S., Portnov A.A. NCTPlan application for neutron capture therapy dosimetric planning at MEPhI nuclear research reactor. *Appl. Radiat. Isot.* 2011;69(12):1888–1891. https://doi.org/10.1016/j.apradiso.2011.04.018
6. Takeuchi A., Hirose K., Kato R., Komori S., Sato M., Motoyanagi T., Yamazaki Y., Narita Y., Takai Y., Kato T. Evaluation of calculation accuracy and computation time in a commercial treatment planning system for accelerator-based boron neutron capture therapy. *Radiol. Phys. Technol.* 2024;17(4):907–917. https://doi.org/10.1007/s12194-024-00833-7
7. Tenk Y.C., Chen J., Zhong W.B., Lio Y.H. HU-based material conversion for BNCT accurate dose estimation. *Sci. Rep.* 2023;13:15701 https://doi.org/10.1038/s41598-023-42508-0
8. Allison J., Amako K., Apostolakis J., et al. Recent developments in Geant4. *Nuclear Instruments and Methods in Physics Research Section A: Accelerators, Spectrometers, Detectors and Associated Equipment*. 2016;835:186–225. https://doi.org/10.1016/j.nima.2016.06.125
9. Ahdida C., Bozzato D., Calzolari D., et al. New Capabilities of the FLUKA Multi-Purpose Code. *Front. Phys.* 2022;9:788253. https://doi.org/10.3389/fphy.2021.788253
10. Rising M.E., Armstrong J.C., Bolding S.R., et al. MCNP® Code V.6.3.0 Release Notes. *Tech. Rep. LA-UR-22-33103, Rev. 1.* Los Alamos National Laboratory, Los Alamos, NM, USA. 2023. 55 p. URL: CoverSheet
11. Sato T., Iwamoto Y., Hashimoto S., et al. Recent improvements of the particle and heavy ion transport code system – PHITS version 3.33. *J. Nuclear Sci. Technol.* 2023;61(1):127–135. https://doi.org/10.1080/00223131.2023.2275736

12. Bassler N., Hansen D.C., Lühr A., Thomsen B., Petersen J.B., Sobolevsky N. SHIELD-HIT12A – a Monte Carlo particle transport program for ion therapy research. *J. Phys.: Conf. Ser.* 2014;489:012004. https://doi.org/10.1088/1742-6596/489/1/012004
13. Muraro S., Battistoni G., Kraan A.C. Challenges in Monte Carlo Simulations as Clinical and Research Tool in Particle Therapy: A Review. *Front. Phys.* 2020;8:567800. https://doi.org/10.3389/fphy.2020.567800
14. Petringa G., Romano F., Manti L., et al. Radiobiological quantities in proton-therapy: Estimation and validation using Geant4-based Monte Carlo simulations. *Phys. Med*. 2019;58:72–80. https://doi.org/10.1016/j.ejmp.2019.01.018
15. Troshina M.V., Koryakina E.V., Potetnya V.I., Koryakin S.N., Pikalov V.A., Antipov Yu.M. Induction of chromosome aberrations in B14-150 cells following carbon ions irradiation at low doses. *J. Phys.: Conf. Ser.* 2020;1701:012029. https://doi.org/10.1088/1742-6596/1701/1/012029
16. Kyriakou I., Sakata D., Tran H.N., et al. Review of the Geant4-DNA simulation toolkit for radiobiological applications at the cellular and DNA level. *Cancers.* 2022;14(1):35. https://doi.org/10.3390/cancers14010035
17. Chatzipapas K., Dordevic M., Zivkovic S., et al. Geant4-DNA simulation of human cancer cells irradiation with helium ion beams. *Phys. Med*. 20233;112:102613. https://doi.org/10.1016/j.ejmp.2023.102613
18. Pisciotta P., Cammarata F.P., Stefano A., et al. Monte Carlo GEANT4-based application for *in vivo* RBE study using small animals at LNS-INFN preclinical hadrontherapy facility. *Phys. Med*. 2018;54:173–178. https://doi.org/10.1016/j.ejmp.2018.07.003
19. Taha E., Djouider F., Banoqitah E. Monte Carlo simulations for dose enhancement in cancer treatment using bismuth oxide nanoparticles implanted in brain soft tissue. *Australas. Phys. Eng. Sci. Med*. 2018;41:363–370. https://doi.org/10.1007/s13246-018-0633-z
20. Cadini F., De Sanctis J., Girotti T., Zio E., Luce A., Taglioni A. Monte Carlo-based assessment of the safety performance of a radioactive waste repository. *Reliability Engineering & System Safety* (*RESS*). 2010;95(8):859–865. https://doi.org/10.1016/j.ress.2010.04.002
21. Geng C., Tang X., Gong C., Guan F., Johns J., Shu D., Chen D. A Monte Carlo-based radiation safety assessment for astronauts in an environment with confined magnetic field shielding. *J. Radiol. Prot.* 2015;35(4):777. https://doi.org/10.1088/0952-4746/35/4/777
22. Archer J.W., Large M.J., Bolst D., et al. A multiscale nanodosimetric study of GCR protons and alpha particles in the organs of astronauts on the lunar surface *Rad. Phys. Chem.* 2025;229:112448. https://doi.org/10.1016/j.radphyschem.2024.112448
23. Chernukha A.E., Saburov V.O., Adarova A.I., Solovev A.N., Kizilova Yu.V., Koryakin S.N. Three-Dimensional Models and Complimentary Geometry for Dose Evaluation in NG-24MT Based Neutron Radiotherapy Cabinet. *Izvestiya vuzov. Yadernaya energetika*. 2022;3:158–167 (in Russ.). https://doi.org/10.26583/npe.2022.3.14
24. Koryakin S., Isaeva E., Beketov E., Solovev A., Ulyanenko L., Fedorov V., Lityaev V., Ulyanenko S. The photon capture therapy model for *in vivo* and *in vitro* studies using Au nanocomposites with the hyaluronic acid based compounds. *RAD Journal.* 2017;2(2):86–89. http://doi.org/10.21175/RadJ.2017.02.019
25. Solovyev A.N., Fedorov V.V., Kharlov V.I., Stepanova U.A. Comparative analysis of MCNPX and GEANT4 codes for fast-neutron radiation treatment planning. *Nuclear Energy Technol.* 2015;1(1):14–19. https://doi.org/10.1016/j.nucet.2015.11.004
26. Solovev A.N., Kizilova Ya.V., Koryakin S.N. *A Software Toolkit for DICOM Medical Standard Images Conversion to Rapid Access Formats:* computer program. Registration number (certificate) 2023685423 RF. Publ. 27.11.2023 (in Russ.).
27. Solovev A.N., Kizilova Ya.V., Chernukha A.E., Merzlikin G.V., Koryakin S.N. *Software Toolkit for General-Purpose Phase Space Conversion to Rapid Access Formats*: computer program. Registration number (certificate) 2024660249 RF. Publ. 03.05.2024 (in Russ.).
28. Solovev A.N., Kizilova Ya.V., Zverev V.I., Presnyakov A.Yu., Koryakin S.N. *A Supplementary Tool for Visual-Based Verification of Cross-Section of Collimator Slice with Patient Body in the Pre-Treatment Stage*: computer program. Registration number (certificate) 2024665975 RF. Publ. 09.07.2024 (in Russ.).
29. Solovev A.N., Chernukha A.E., Koryakin S.N., Presnyakov A.Yu., Zverev V.I. *Automated Optimization Tool for Fast Neutron Therapy Using 3D-CRT Regime by Root Mean Square Deviation with Broyden-Fletcher-Goldfarb-Shanno Algorithm Implemented in Pytorch*: computer program. Registration number (certificate) 2024664787 RF. Publ. 09.07.2024 (in Russ.).
30. Butenko A.V., Syresin E.M., Tyutyunnikov S.I., et al. Analysis of Metrological Provision Problems of a Test Stand for Testing Radio-Electronic Products for Resistance to Irradiation with High-Energy Heavy Ions. *Phys. Part. Nuclei Lett.* 2019;16:734–743. https://doi.org/10.1134/S1547477119060098
31. Brun R., Rademakers F. ROOT — An object oriented data analysis framework. *Nuclear Instruments and Methods in Physics Research Section A: Accelerators, Spectrometers, Detectors and Associated Equipment.* 1997;389(1–2):81–86. https://doi.org/10.1016/S0168-9002(97)00048-X
32. Gordon K.B., Saburov V.O., Koryakin S.N., et al. Calculation of the Biological Efficiency of the Proton Component from 14.8 MeV Neutron Irradiation in Computational Biology with Help of Video Cards. *Bull. Exp. Biol. Med.* 2022;173:281–285. https://doi.org/10.1007/s10517-022-05534-y
[Original Russian Text: Gordon K.B., Saburov V.O., Koryakin S.N., Gulidov I.A., Fatkhudinov T.Kh., Arutyunyan I.V., Kaprin A.D., Solov'ev A.N. Calculation of the Biological Efficiency of the Proton Component from 14.8 MeV Neutron Irradiation in Computational Biology with Help of Video Cards. *Byulleten' eksperimental'noi biologii i meditsiny*. 2022;173(2):263–267 (in Russ.). https://doi.org/10.47056/0365-9615-2022-173-2-263-267]

33. Schneider W., Bortfeld T., Schlegel W. Correlation between CT numbers and tissue parameters needed for Monte Carlo simulations of clinical dose distributions *Phys. Med. Biol.* 2000;45(2):459. https://doi.org/10.1088/0031-9155/45/2/314
34. Kotb O.M., Solovev A.N., Saburov V.O., et al. Response of the FBX aqueous chemical dosimeter to high energy proton and electron beams used for radiotherapy research. *Radiat. Phys. Chem.* 2024;216:111451. https://doi.org/10.1016/j.radphyschem.2023.111451
35. Balakin V.E., Bazhan A.I., Alexandrov V.A., et al. Updated Status of Protom Synchrotrons for Radiation Therapy. In: *27 Russian Particle Acc. Conf.* (*Proc. RuPAC'21, Alushta, Russia*). *J. Accelerator Conferences Website* (*JACoW*) *Publishing*. 2021. P. 120–123. https://doi.org/10.18429/JACoW-RuPAC2021-FRB05
36. Yuzhakov V.V., Korchagina K.S., Fomina N.K., Koryakin S.M., Solovev A.N., Ingel I.E., Koretskaya A.E., Sevankaeva L.E., Yakovleva N.D., Tsyganova M.G. Effect of gamma-radiation and scanning proton beam on the morphofunctional characteristics of rat sarcoma M-1. *Radiatsiiya i risk = Radiation and Risk.* 2020;29(2):101–114 (in Russ.). https://doi.org/10.21870/0131-3878-2020-29-2-101-114
37. Solovev A.N., Chernukha A.E., Potetnya V.I. *The Radiobiological Experiments Decision Making Support System for Temporary Radiobiological Stand of the U-70 Accelerator Facility*: computer program. Registration number (certificate) 2020615172 RF. Publ. 18.05.2020 (in Russ.).
38. Beketov E., Isaeva E., Malakhov E., Nasedkina N., Koryakin S., Ulyanenko S., Solovev A., Lychagin A. The study of biological effectiveness of U-70 accelerator carbon ions using melanoma B-16 clonogenic assay. *RAD Journal.* 2017;2(2):90–93. https://doi.org/10.21175/RadJ.2017.02.020
39. Solovev A.N., Chernukha A.E., Troshina M.V., Lychagin A.A. Pikalov V.A., Kharlov V.I. Design of passive beam modifiers in carbon ion beam at U-70 synchrotron facility for radiobiological studies. *Meditsinskaya Fizika = Medical Physics*. 2016;4(72):47–54 (in Russ.). https://elibrary.ru/item.asp?id=27428891
40. Zaichkina S.I., Rozanova O.M., Smirnova E.N., et al. Assessment of the Biological Efficiency of 450 MeV/Nucleon Accelerated Carbon Ions in the U-70 Accelerator According to the Criterion of Mouse Survival. *BIOPHYSICS*. 2019;64:991–998. https://doi.org/10.1134/S000635091906023X
[Original Russian Text: Zaichkina S.I., Rozanova O.M., Smirnova E.N., Dyukina A.R., Belyakova T.A., Strelnikova N.S., Sorokina S.S., Pikalov V.A. Assessment of the Biological Efficiency of 450 MeV/Nucleon Accelerated Carbon Ions in the U-70 Accelerator According to the Criterion of Mouse Survival. *Biofizika*. 2019;64(4):1208–1215 (in Russ.). http://dx.doi.org/10.1134/S0006302919060206]
41. Kuznetsova E.A., Sirota N.P., Mitroshina I.Yu., Pikalov V.A., Smirnova E.N., Rozanova O.M., Glukhov S.I., Sirota T.V., Zaichkina S.I. DNA damage in blood leukocytes from mice irradiated with accelerated carbon ions with an energy of 450 MeV/nucleon. *Int. J. Radiat. Biol*. 2020;96(10):1245–1253. https://doi.org/10.1080/09553002.2020.1807640
42. Pikalov V.A., Alexeev A.G., Antipov Y.M., Kalinin V.A., Koshelev A.V., Maximov A.V., Ovsienko M.P., Polkovnikov M.K., Soldatov A.P. The Results Obtained on "Radiobiological Stand" Facility, Working with the Extracted Carbon Ion Beam of the U-70 Accelerator. In: *27 Russian Particle Acc. Conf.* (*Proc. RuPAC'21, Alushta, Russia*). *J. Accelerator Conferences Website* (*JACoW*) *Publishing*. 2021. P. 124–126. https://doi.org/10.18429/JACoW-RuPAC2021-FRB06
43. Garkusha V.I., Ivanov S.V., Kalinin V.A., et al. Status of work on creating carbon ion beam channels for radiobiological and preclinical studies at the U-70 accelerator complex. *Instrum. Exp. Tech.* 2024;64(Suppl.2):S256–S241. https://doi.org/10.1134/S0020441224701768
[Original Russian Text: Garkusha V.I., Ivanov S.V., Kalinin V.A., Maksimov A.V., Markin A.M., Novoskol'tsev F.N., Pikalov V.A., Soldatov A.P., Sinyukov R.Yu. Status of work on creating carbon ion beam channels for radiobiological and preclinical studies at the U-70 accelerator complex. *Pribory i tekhnika eksperimenta.* 2024;8(S2):14 (in Russ.).]
44. Meffe G., Votta C., Turco G., Chillè E., et al. Impact of data transfer between treatment planning systems on dosimetric parameters. *Phys. Med.* 2024;121:103369. https://doi.org/10.1016/j.ejmp.2024.103369
45. Mosleh Shirazi M.A., Faghihi R., Siavashpour Z., Nedaie H.A., Mehdizadeg S., Sina S. Independent evaluation of an *in-house* brachytherapy treatment planning system using simulation, measurement and calculation methods. *J. Appl. Clin. Med. Phys*. 2012;13(2):103–112. https://doi.org/10.1120/jacmp.v13i2.3687
46. Kumada H., Takada K., Aihara T., Matsumura A., Sakurai H., Sakae T. Verification for dose estimation performance of a Monte-Carlo based treatment planning system in University of Tsukuba. *Appl. Radiat. Isot.* 2021;166:109222. https://doi.org/10.1016/j.apradiso.2020.109222
47. Moyers M.F., Lin J., Li J., Chen H., Shen Z. Optimization of the planning process with an *in-house* treatment information, management, and planning system. *Radiat. Med. Protect.* 2022;3(3):102–107. https://doi.org/10.1016/j.radmp.2022.07.004
48. Shao Y., Gui J., Wang J., et al. Novel *in-house* knowledge-based automated planning system for lung cancer treated with intensity-modulated radiotherapy. *Strahlenther. Onkol*. 2023;200(11):967–982. https://doi.org/10.1007/s00066-023-02126-1
49. Guo Y., Liu Z., Feng S., Cai H., Zhang Q. Clinical Viability of an Active Spot Scanning Beam Delivery System with a Newly Developed Carbon-Ion Treatment Planning System. *Adv. Radiat. Oncol.* 2024;9(7):101503. https://doi.org/10.1016/j.adro.2024.101503
50. Kalyganova N.V., Kiselev V.A., Kashentseva N.V., Udalov Yu.D., Gritsenko S.E. Comparison of dosimetric properties of proton and intensity modulated radiotherapy for glioblastomes. In: *Il'inskie chteniya 2022: Proceedings of the School-Conference of Young Scientists and Specialists.* Moscow, 2022. P. 141–142 (in Russ.). https://elibrary.ru/item.asp?id=49488724
51. Okada S., Murakami K., Amako K., et al. GPU Acceleration of Monte Carlo Simulation at the Cellular and DNA Levels. In book series: Chen Y.W., Torro C., Tanaka S., Howlett R. (Eds.). *Innovation in Medicine and Healthcare 2015*. *Smart Innovation, Systems and Technologies.* Springer; 2016. V. 45. P. 323–332. http://dx.doi.org/10.1007/978-3-319-23024-5_29

52. Okada S., Murakami K., Incerti S., Amako K., Sasaki T. MPEXS-DNA, A new GPU-based Monte Carlo simulator for track structure and radiation chemistry at subcellular scale. *Med. Phys.* 2019;46(3):1483–1500. https://doi.org/10.1002/mp.13370
53. Qin N., Shen C., Tasi M.Y., et al. Full Monte Carlo–Based Biologic Treatment Plan Optimization System for Intensity Modulated Carbon Ion Therapy on Graphics Processing Unit. *Int. J. Radiat. Oncol. Biol. Phys*. 2018;100(1):235–243. https://doi.org/10.1016/j.ijrobp.2017.09.002
54. Franciosini G., Carlotti D., Cattani F., et al. IOeRT conventional and FLASH treatment planning system implementation exploiting fast GPU Monte Carlo: The case of breast cancer. *Phys. Med.* 2024;121:103346. https://doi.org/10.1016/j.ejmp.2024.103346
55. Magro G., Mein S., Kopp B., et al. FRoG dose computation meets Monte Carlo accuracy for proton therapy dose calculation in lung. *Phys. Med.* 2021;88;66–74. https://doi.org/10.1016/j.ejmp.2021.05.021
56. Yagi M., Tsubouchi T., Hamatani N., Takashina M., Maruo H., Fujitaka S., et al. Commissioning a newly developed treatment planning system, VQA Plan, for fast-raster scanning of carbon-ion beams. *PLoS ONE*. 2022;17(5):e0268087. https://doi.org/10.1371/journal.pone.0268087
57. Lu Y., Sigov A., Ratkin L, Ivanov L.A., Zuo M. Quantum computing and industrial information integration: A review. *J. Ind. Inform. Integr*. 2023;35:100511. https://doi.org/10.1016/j.jii.2023.100511
58. Giraud P., Bibault J.E. Artificial intelligence in radiotherapy: Current applications and future trends. *Diagn. Interv. Imaging*. 2024;105(12):475–480. https://doi.org/10.1016/j.diii.2024.06.001

СПИСОК ЛИТЕРАТУРЫ

1. Мардынский Ю.С., Гулидов И.А., Гордон К.Б., Корякин С.Н., Соловьёв А.Н., Сабуров В.О., Иванов С.А., Каприн А.Д., Лобжанидзе Т.К., Марков Н.В., Железнов И.М., Юрков Д.И., Герасимчук О.А., Пресняков А.Ю., Зверев В.И., Смирнов В.П. Дистанционная нейтронная терапия: первый отечественный медицинский комплекс. *Вестник Российской Академии Наук*. 2024;94(1):80–86. https://doi.org/10.31857/S0869587324010098
2. Rod'ko I.I., Sarychev G.A., Balakirev P.V., et al. Development of a Radiotherapy System Based on 6 MeV Linac and Cone-Beam Computer Tomograph. *At. Energy*. 2019;125(5):333–337. https://doi.org/10.1007/s10512-019-00490-9
3. Inaniwa T., Kanematsu N., Noda K., Kamada T. Treatment planning of intensity modulated composite particle therapy with dose and linear energy transfer optimization. *Phys. Med. Biol.* 2017;62(12):5180–5197. https://doi.org/10.1088/1361-6560/aa68d7
4. Krämer M. Swift ions in radiotherapy – Treatment planning with TRiP98. *Nuclear Instruments and Methods in Physics Research Section B: Beam Interactions with Materials and Atoms* 2009;267(6):989–992. https://doi.org/10.1016/j.nimb.2009.02.015
5. Elyutina A.S., Kiger W.S., Portnov A.A. NCTPlan application for neutron capture therapy dosimetric planning at MEPhI nuclear research reactor. *Appl. Radiat. Isot.* 2011;69(12):1888–1891. https://doi.org/10.1016/j.apradiso.2011.04.018
6. Takeuchi A., Hirose K., Kato R., Komori S., Sato M., Motoyanagi T., Yamazaki Y., Narita Y., Takai Y., Kato T. Evaluation of calculation accuracy and computation time in a commercial treatment planning system for accelerator-based boron neutron capture therapy. *Radiol. Phys. Technol.* 2024;17(4):907–917. https://doi.org/10.1007/s12194-024-00833-7
7. Tenk Y.C., Chen J., Zhong W.B., Lio Y.H. HU-based material conversion for BNCT accurate dose estimation. *Sci. Rep.* 2023;13:15701. https://doi.org/10.1038/s41598-023-42508-0
8. Allison J., Amako K., Apostolakis J., et al. Recent developments in Geant4. *Nuclear Instruments and Methods in Physics Research Section A: Accelerators, Spectrometers, Detectors and Associated Equipment*. 2016;835:186–225. https://doi.org/10.1016/j.nima.2016.06.125
9. Ahdida C., Bozzato D., Calzolari D., et al. New Capabilities of the FLUKA Multi-Purpose Code. *Front. Phys.* 2022;9:788253. https://doi.org/10.3389/fphy.2021.788253
10. Rising M.E., Armstrong J.C., Bolding S.R., et al. MCNP® Code V.6.3.0 Release Notes. *Tech. Rep. LA-UR-22-33103, Rev. 1.* Los Alamos National Laboratory, Los Alamos, NM, USA. 2023. 55 p. URL: CoverSheet
11. Sato T., Iwamoto Y., Hashimoto S., et al. Recent improvements of the particle and heavy ion transport code system – PHITS version 3.33. *J. Nuclear Sci. Technol.* 2023;61(1):127–135. https://doi.org/10.1080/00223131.2023.2275736
12. Bassler N., Hansen D.C., Lühr A., Thomsen B., Petersen J.B., Sobolevsky N. SHIELD-HIT12A – a Monte Carlo particle transport program for ion therapy research. *J. Phys.: Conf. Ser.* 2014;489:012004. https://doi.org/10.1088/1742-6596/489/1/012004
13. Muraro S., Battistoni G., Kraan A.C. Challenges in Monte Carlo Simulations as Clinical and Research Tool in Particle Therapy: A Review. *Front. Phys.* 2020;8:567800. https://doi.org/10.3389/fphy.2020.567800
14. Petringa G., Romano F., Manti L., et al. Radiobiological quantities in proton-therapy: Estimation and validation using Geant4-based Monte Carlo simulations. *Phys. Med*. 2019;58:72–80. https://doi.org/10.1016/j.ejmp.2019.01.018
15. Troshina M.V., Koryakina E.V., Potetnya V.I., Koryakin S.N., Pikalov V.A., Antipov Yu.M. Induction of chromosome aberrations in B14-150 cells following carbon ions irradiation at low doses. *J. Phys.: Conf. Ser.* 2020;1701:012029. https://doi.org/10.1088/1742-6596/1701/1/012029
16. Kyriakou I., Sakata D., Tran H.N., et al. Review of the Geant4-DNA simulation toolkit for radiobiological applications at the cellular and DNA level. *Cancers.* 2022;14(1):35. https://doi.org/10.3390/cancers14010035
17. Chatzipapas K., Dordevic M., Zivkovic S., et al. Geant4-DNA simulation of human cancer cells irradiation with helium ion beams. *Phys. Med*. 20233;112:102613. https://doi.org/10.1016/j.ejmp.2023.102613

18. Pisciotta P., Cammarata F.P., Stefano A., et al. Monte Carlo GEANT4-based application for *in vivo* RBE study using small animals at LNS-INFN preclinical hadrontherapy facility. *Phys. Med*. 2018;54:173–178. https://doi.org/10.1016/j.ejmp.2018.07.003
19. Taha E., Djouider F., Banoqitah E. Monte Carlo simulations for dose enhancement in cancer treatment using bismuth oxide nanoparticles implanted in brain soft tissue. *Australas. Phys. Eng. Sci. Med*. 2018;41:363–370. https://doi.org/10.1007/s13246-018-0633-z
20. Cadini F., De Sanctis J., Girotti T., Zio E., Luce A., Taglioni A. Monte Carlo-based assessment of the safety performance of a radioactive waste repository. *Reliability Engineering & System Safety* (*RESS*). 2010;95(8):859–865. https://doi.org/10.1016/j.ress.2010.04.002
21. Geng C., Tang X., Gong C., Guan F., Johns J., Shu D., Chen D. A Monte Carlo-based radiation safety assessment for astronauts in an environment with confined magnetic field shielding. *J. Radiol. Prot.* 2015;35(4):777. https://doi.org/10.1088/0952-4746/35/4/777
22. Archer J.W., Large M.J., Bolst D., et al. A multiscale nanodosimetric study of GCR protons and alpha particles in the organs of astronauts on the lunar surface *Rad. Phys. Chem.* 2025;229:112448. https://doi.org/10.1016/j.radphyschem.2024.112448
23. Чернуха А.Е., Сабуров В.О., Адарова А.И., Соловьев А.Н., Кизилова Я.В., Корякин С.Н. Трехмерные модели и дополнение геометрии для оценки доз в лучевой кабине нейтронной терапии на базе генератора НГ-24МТ. *Известия вузов. Ядерная энергетика*. 2022;3:158–167. https://doi.org/10.26583/npe.2022.3.14
24. Koryakin S., Isaeva E., Beketov E., Solovev A., Ulyanenko L., Fedorov V., Lityaev V., Ulyanenko S. The photon capture therapy model for *in vivo* and *in vitro* studies using Au nanocomposites with the hyaluronic acid based compounds. *RAD Journal.* 2017;2(2):86–89. http://doi.org/10.21175/RadJ.2017.02.019
25. Solovyev A.N., Fedorov V.V., Kharlov V.I., Stepanova U.A. Comparative analysis of MCNPX and GEANT4 codes for fast-neutron radiation treatment planning. *Nuclear Energy Technol.* 2015;1(1):14–19. https://doi.org/10.1016/j.nucet.2015.11.004
26. Соловьев А.Н., Кизилова Я.В., Корякин С.Н. *Программное средство преобразования медицинских изображений отраслевого стандарта DICOM в форматы оперативного доступа*: программа для ЭВМ. Номер регистрации (свидетельства) 2023685423 РФ. Номер заявки 2023683925; заявл. 13.11.2023; опубл. 27.11.2023. Бюл. № 12. https://www.elibrary.ru/item.asp?id=56012725.
27. Соловьев А.Н., Кизилова Я.В., Чернуха А.Е., Мерзликин Г.В., Корякин С.Н. *Программное средство универсального преобразования фазовых пространств в форматы оперативного доступа:* программа для ЭВМ. Номер регистрации (свидетельства) 2024660249 РФ. Номер заявки 2024618897; заявл. 24.04.2024; опубл. 03.05.2024. Бюл. № 5. https://www.elibrary.ru/item.asp?id=67263924.
28. Соловьев А.Н., Кизилова Я.В., Зверев В.И., Пресняков А.Ю., Корякин С.Н. *Вспомогательная утилита визуальной верификации пересечений среза коллиматора с телом пациента на стадии предлучевой подготовки*: программа для ЭВМ. Номер регистрации (свидетельства) 2024665975 РФ. Номер заявки 2024665975; заявл. 28.06.2024; опубл. 09.07.2024. Бюл. № 7.
29. Соловьев А.Н., Чернуха А.Е., Корякин С.Н., Пресняков А.Ю., Зверев В.И. *Автоматизированное средство оптимизации полей быстрой нейтронной терапии в режиме 3D-CRT по среднеквадратичному отклонению на основе алгоритма Бройдена-Флетчера-Гольдфарба-Шанно в реализации pytorch*: программа для ЭВМ. Номер регистрации (свидетельства) 2024666070 РФ. Номер заявки 2024664787; заявл. 28.06.2024; опубл. 09.07.2024. Бюл. № 7.
30. Butenko A.V., Syresin E.M., Tyutyunnikov S.I., et al. Analysis of Metrological Provision Problems of a Test Stand for Testing Radio-Electronic Products for Resistance to Irradiation with High-Energy Heavy Ions. *Phys. Part. Nuclei Lett.* 2019;16:734–743. https://doi.org/10.1134/S1547477119060098
31. Brun R., Rademakers F. ROOT — An object oriented data analysis framework. *Nuclear Instruments and Methods in Physics Research Section A: Accelerators, Spectrometers, Detectors and Associated Equipment.* 1997;389(1–2):81–86. https://doi.org/10.1016/S0168-9002(97)00048-X
32. Гордон К.Б., Сабуров В.О., Корякин С.Н., Гулидов И.А., Фатхудинов Т.Х., Арутюнян И.В., Каприн А.Д., Соловьев А.Н. Расчет биологической эффективности протонной компоненты при нейтронном облучении 14.8 МэВ методами вычислительной биологии с использованием видеокарт. *Бюллетень экспериментальной биологии и медицины.* 2022;173(2):263–267. https://doi.org/10.47056/0365-9615-2022-173-2-263-267
33. Schneider W., Bortfeld T., Schlegel W. Correlation between CT numbers and tissue parameters needed for Monte Carlo simulations of clinical dose distributions *Phys. Med. Biol.* 2000;45(2):459. https://doi.org/10.1088/0031-9155/45/2/314
34. Kotb O.M., Solovev A.N., Saburov V.O., et al. Response of the FBX aqueous chemical dosimeter to high energy proton and electron beams used for radiotherapy research. *Radiat. Phys. Chem.* 2024;216:111451. https://doi.org/10.1016/j.radphyschem.2023.111451
35. Balakin V.E., Bazhan A.I., Alexandrov V.A., et al. Updated Status of Protom Synchrotrons for Radiation Therapy. In: *27 Russian Particle Acc. Conf.* (*Proc. RuPAC'21, Alushta, Russia*). *J. Accelerator Conferences Website* (*JACoW*) *Publishing*. 2021. P. 120–123. https://doi.org/10.18429/JACoW-RuPAC2021-FRB05
36. Южаков В.В., Корчагина К.С., Фомина Н.К., Корякин С.М., Соловьев А.Н., Ингель И.Э., Корецкая А.Е., Севанькаева Л.Е., Яковлева Н.Д., Цыганова М.Г. Действие гамма-излучения и сканирующего пучка протонов на морфофункциональные характеристики саркомы М-1 крыс. *Радиация и риск.* 2020;29(2):101–114. https://doi.org/10.21870/0131-3878-2020-29-2-101-114

37. Соловьев А.Н., Чернуха А.Е., Потетня В.И. *Программа поддержки принятия решений по радиобиологическим экспериментам на временном радиобиологическом стенде ускорительного комплекса У-70*: программа для ЭВМ. Номер регистрации (свидетельства) 2020615172 РФ. Номер заявки 2020614229; заявл. 14.05.2020; опубл. 18.05.2020. Бюл. № 5. https://elibrary.ru/item.asp?id=43880348.
38. Beketov E., Isaeva E., Malakhov E., Nasedkina N., Koryakin S., Ulyanenko S., Solovev A., Lychagin A. The study of biological effectiveness of U-70 accelerator carbon ions using melanoma B-16 clonogenic assay. *RAD Journal.* 2017;2(2): 90–93. https://doi.org/10.21175/RadJ.2017.02.020
39. Соловьев А.Н., Чернуха А.Е., Трошина М.В., Лычагин А.А., Пикалов В.А., Харлов В.И., Ульяненко С.Е. Разработка средств пассивной модификации пучка ионов углерода ускорительного комплекса У-70 для радиобиологических исследований. *Медицинская физика*. 2016;4(72):47–54. https://elibrary.ru/item.asp?id=27428891
40. Заичкина С.И., Розанова О.М., Смирнова Е.Н., Дюкина А.Р., Белякова Т.А., Стрельникова Н.С., Сорокина С.С., Пикалов В.А. Оценка биологической эффективности ускоренных ионов углерода с энергией 450 МэВ/нуклон в ускорительном комплексе У-70 по критерию выживаемости мышей. *Биофизика*. 2019;64(6):1208–1215. http://doi.org/10.1134/S0006302919060206
[Zaichkina S.I., Rozanova O.M., Smirnova E.N., Dyukina A.R., Belyakova T.A., Strelnikova N.S., Sorokina S.S., Pikalov V.A. Assessment of the Biological Efficiency of 450 MeV/Nucleon Accelerated Carbon Ions in the U-70 Accelerator According to the Criterion of Mouse Survival. *BIOPHYSICS*. 2019;64:991–998. https://doi.org/10.1134/S000635091906023X]
41. Kuznetsova E.A., Sirota N.P., Mitroshina I.Yu., Pikalov V.A., Smirnova E.N., Rozanova O.M., Glukhov S.I., Sirota T.V., Zaichkina S.I. DNA damage in blood leukocytes from mice irradiated with accelerated carbon ions with an energy of 450 MeV/nucleon. *Int. J. Radiat. Biol*. 2020;96(10):1245–1253. https://doi.org/10.1080/09553002.2020.1807640
42. Pikalov V.A., Alexeev A.G., Antipov Y.M., Kalinin V.A., Koshelev A.V., Maximov A.V., Ovsienko M.P., Polkovnikov M.K., Soldatov A.P. The Results Obtained on "Radiobiological Stand" Facility, Working with the Extracted Carbon Ion Beam of the U-70 Accelerator. In: *27 Russian Particle Acc. Conf.* (*Proc. RuPAC'21, Alushta, Russia*). *J. Accelerator Conferences Website* (*JACoW*) *Publishing*. 2021. P. 124–126. https://doi.org/10.18429/JACoW-RuPAC2021-FRB06
43. Гаркуша В.И., Иванов С.В., Калинин В.А., Максимов А.В., Маркин А.М., Новоскольцев Ф.Н., Пикалов В.А., Солдатов А.П., Синюков Р.Ю. Создание каналов пучков ионов углерода для проведения радиобиологических и предклинических исследований на ускорительном комплексе У-70. *Приборы и техника эксперимента* 2024;8(S2):14.
44. Meffe G., Votta C., Turco G., Chillè E., et al. Impact of data transfer between treatment planning systems on dosimetric parameters. *Phys. Med.* 2024;121:103369. https://doi.org/10.1016/j.ejmp.2024.103369
45. Mosleh Shirazi M.A., Faghihi R., Siavashpour Z., Nedaie H.A., Mehdizadeg S., Sina S. Independent evaluation of an *in-house* brachytherapy treatment planning system using simulation, measurement and calculation methods. *J. Appl. Clin. Med. Phys*. 2012;13(2):103–112. https://doi.org/10.1120/jacmp.v13i2.3687
46. Kumada H., Takada K., Aihara T., Matsumura A., Sakurai H., Sakae T. Verification for dose estimation performance of a Monte-Carlo based treatment planning system in University of Tsukuba. *Appl. Radiat. Isot.* 2021;166:109222. https://doi.org/10.1016/j.apradiso.2020.109222
47. Moyers M.F., Lin J., Li J., Chen H., Shen Z. Optimization of the planning process with an *in-house* treatment information, management, and planning system. *Radiat. Med. Protect.* 2022;3(3):102–107. https://doi.org/10.1016/j.radmp.2022.07.004
48. Shao Y., Gui J., Wang J., et al. Novel *in-house* knowledge-based automated planning system for lung cancer treated with intensity-modulated radiotherapy. *Strahlenther. Onkol*. 2023;200(11):967–982. https://doi.org/10.1007/s00066-023-02126-1
49. Guo Y., Liu Z., Feng S., Cai H., Zhang Q. Clinical Viability of an Active Spot Scanning Beam Delivery System with a Newly Developed Carbon-Ion Treatment Planning System. *Adv. Radiat. Oncol.* 2024;9(7):101503. https://doi.org/10.1016/j.adro.2024.101503
50. Калыганова Н.В., Киселев В.А., Кашенцева Н.В., Удалов Ю.Д., Гриценко С.Е. Сравнение дозиметрических характеристик планов протонной и лучевой терапии с модуляцией интенсивности при глиобластоме головного мозга. В сб.: *Ильинские чтения 2022*: *Сборник материалов школы-конференции молодых ученых и специалистов*. М., 2022. С. 141–142. https://elibrary.ru/item.asp?id=49488724
51. Okada S., Murakami K., Amako K., et al. GPU Acceleration of Monte Carlo Simulation at the Cellular and DNA Levels. In: Chen Y.W., Torro C., Tanaka S., Howlett R. (Eds.). *Innovation in Medicine and Healthcare 2015*. *Smart Innovation, Systems and Technologies.* Springer; 2016. V. 45. P. 323–332. http://dx.doi.org/10.1007/978-3-319-23024-5_29
52. Okada S., Murakami K., Incerti S., Amako K., Sasaki T. MPEXS-DNA, A new GPU-based Monte Carlo simulator for track structure and radiation chemistry at subcellular scale. *Med. Phys.* 2019;46(3):1483–1500. https://doi.org/10.1002/mp.13370
53. Qin N., Shen C., Tasi M.Y., et al. Full Monte Carlo–Based Biologic Treatment Plan Optimization System for Intensity Modulated Carbon Ion Therapy on Graphics Processing Unit. *Int. J. Radiat. Oncol. Biol. Phys*. 2018;100(1):235–243. https://doi.org/10.1016/j.ijrobp.2017.09.002
54. Franciosini G., Carlotti D., Cattani F., et al. IOeRT conventional and FLASH treatment planning system implementation exploiting fast GPU Monte Carlo: The case of breast cancer. *Phys. Med.* 2024;121:103346. https://doi.org/10.1016/j.ejmp.2024.103346
55. Magro G., Mein S., Kopp B., et al. FRoG dose computation meets Monte Carlo accuracy for proton therapy dose calculation in lung. *Phys. Med.* 2021;88;66–74. https://doi.org/10.1016/j.ejmp.2021.05.021

56. Yagi M., Tsubouchi T., Hamatani N., Takashina M., Maruo H., Fujitaka S., et al. Commissioning a newly developed treatment planning system, VQA Plan, for fast-raster scanning of carbon-ion beams. *PLoS ONE.* 2022;17(5):e0268087. https://doi.org/10.1371/journal.pone.0268087
57. Lu Y., Sigov A., Ratkin L, Ivanov L.A., Zuo M. Quantum computing and industrial information integration: A review. *J. Ind. Inform. Integr*. 2023;35:100511. https://doi.org/10.1016/j.jii.2023.100511
58. Giraud P., Bibault J.E. Artificial intelligence in radiotherapy: Current applications and future trends. *Diagn. Interv. Imaging*. 2024;105(12):475–480. https://doi.org/10.1016/j.diii.2024.06.001

About the Authors

Aleksei N. Solovev, Cand. Sci. (Phys.-Math.), Head of Laboratory of Medical Radiation Physics, Radiation Biophysics Department, A. Tsyb Medical Radiological Research Center – Branch of the National Medical Research Radiological Center (10, Marshala Zhukova ul., Obninsk, Kaluga oblast, 249031 Russia); Associate Professor, Radionuclide Medicine Department, Obninsk Institute for Nuclear Power Engineering (1, Studgorodok, Obninsk, Kaluga oblast, 249039 Russia). E-mail: salonf@mrrc.obninsk.ru. Scopus Author ID 57215856302, ResearcherID O-6340-2014, https://orcid.org/0000-0002-4386-3725

Yana V. Kizilova, Researcher, Laboratory of Medical Radiation Physics, Radiation Biophysics Department, A. Tsyb Medical Radiological Research Center – Branch of the National Medical Research Radiological Center (10, Marshala Zhukova ul., Obninsk, Kaluga oblast, 249031 Russia). E-mail: cobaltcorsair@yandex.ru. https://orcid.org/0009-0001-0404-820X

Evgeniy I. Kazakov, Engineer, Laboratory of Development and Operation of Radiation Equipment, Radiation Biophysics Department, A. Tsyb Medical Radiological Research Center – Branch of the National Medical Research Radiological Center (10, Marshala Zhukova ul., Obninsk, Kaluga oblast, 249031 Russia). E-mail: ekazakof@ya.ru. https://orcid.org/0009-0009-4178-6242

Sergey N. Koryakin, Cand. Sci. (Biol.), Head of Radiation Biophysics Department, A. Tsyb Medical Radiological Research Center – Branch of the National Medical Research Radiological Center (10, Marshala Zhukova ul., Obninsk, Kaluga oblast, 249031 Russia); Associate Professor, Radionuclide Medicine Department, Obninsk Institute for Nuclear Power Engineering (1, Studgorodok, Obninsk, Kaluga oblast, 249039 Russia). E-mail: korsernic@mail.ru. Scopus Author ID 6603357340, https://orcid.org/0000-0003-0128-4538

Об авторах

Соловьев Алексей Николаевич, к.ф.-м.н., заведующий лабораторией медицинской радиационной физики отдела радиационной биофизики, Медицинский радиологический научный центр имени А.Ф. Цыба – филиал ФГБУ «Национальный медицинский исследовательский центр радиологии» Минздрава Российской Федерации (249031, Россия, Калужская область, Обнинск, ул. Маршала Жукова, д. 10); доцент, кафедра радионуклидной медицины, Обнинский институт атомной энергетики — филиал ФГАОУ ВО «Национальный исследовательский ядерный университет «МИФИ» (249039, Россия, Калужская область, городской округ «Город Обнинск», тер. Студгородок, д. 1). E-mail: salonf@mrrc.obninsk.ru. Scopus Author ID 57215856302, ResearcherID O-6340-2014, https://orcid.org/0000-0002-4386-3725

Кизилова Яна Владимировна, научный сотрудник, лаборатория медицинской радиационной физики отдела радиационной биофизики, Медицинский радиологический научный центр имени А.Ф. Цыба – филиал ФГБУ «Национальный медицинский исследовательский центр радиологии» Минздрава Российской Федерации (249031, Россия, Калужская область, Обнинск, ул. Маршала Жукова, д. 10). E-mail: cobaltcorsair@yandex.ru. https://orcid.org/0009-0001-0404-820X

Казаков Евгений Игоревич, инженер, лабораториия разработки и эксплуатации облучающей техники отдела радиационной биофизики, Медицинский радиологический научный центр имени А.Ф. Цыба – филиал ФГБУ «Национальный медицинский исследовательский центр радиологии» Минздрава Российской Федерации (249031, Россия, Калужская область, Обнинск, ул. Маршала Жукова, д. 10). E-mail: ekazakof@ya.ru. https://orcid.org/0009-0009-4178-6242

Корякин Сергей Николаевич, к.б.н., заведующий отделом радиационной биофизики, Медицинский радиологический научный центр имени А.Ф. Цыба – филиал ФГБУ «Национальный медицинский исследовательский центр радиологии» Минздрава Российской Федерации (249031, Россия, Калужская область, Обнинск, ул. Маршала Жукова, д. 10); доцент, кафедра радионуклидной медицины, Обнинский институт атомной энергетики — филиал ФГАОУ ВО «Национальный исследовательский ядерный университет «МИФИ» (249039, Россия, Калужская область, городской округ «Город Обнинск», тер. Студгородок, д. 1). E-mail: korsernic@mail.ru. Scopus Author ID 6603357340, https://orcid.org/0000-0003-0128-4538

Translated from Russian into English by Lyudmila O. Bychkova
Edited for English language and spelling by Dr. David Mossop

Modern radio engineering and telecommunication systems

Современные радиотехнические и телекоммуникационные системы

UDC 004.93'1
https://doi.org/10.32362/2500-316X-2025-13-4-25-36
EDN WVWVCJ

RESEARCH ARTICLE

Efficiency of YOLO neural network models applied for object recognition in radar images

Alena S. Krasnoperova [@], Alexander S. Tverdokhlebov, Alexey A. Kartashov, Vladislav I. Weber, Vladimir Y. Kuprits

Tomsk State University of Control Systems and Radioelectronics, Tomsk, 634050 Russia
[@] Corresponding author, e-mail: alenacergeevna2@icloud.com

• **Submitted:** 10.10.2024 • **Revised:** 24.02.2025 • **Accepted:** 21.05.2025

Abstract

Objectives. The paper addresses the problem of applying neural networks for object detection in radar images and their recognition under conditions of limited computational resources. The aim was to investigate the speed and recognition quality of YOLO[1] neural network models in solving object detection and classification tasks in radar images in order to evaluate the feasibility of their practical implementation on a microcomputer with a neural processor.

Methods. Machine learning, object detection, and classification techniques were used to detect and classify objects in a radar image.

Results. The study compared the speed and recognition quality of the 5th, 8th, and 11th generation YOLO neural network models with varying numbers of trainable parameters (nano-, small-, medium-, large-, and extra-large-sized) to assess their potential use on a microcomputer with a neural processor. As a result of comparing various YOLO models using evaluation metrics, YOLOv11n (0.925), YOLOv5l (0.889), and YOLOv11s (0.883) showed the highest precision metric; YOLOv5n (0.932), YOLOv11n (0.928), and YOLOv11s (0.914) showed the highest recall metric; YOLOv11s (0.961), YOLOv5n (0.954), and YOLOv11n (0.953) showed the highest mAP50 metric; and YOLOv5n (0.756), YOLOv11s (0.74), and YOLOv5l (0.727) showed the highest mAP50-95 metric.

Conclusions. The conducted research confirmed the feasibility of running YOLO neural network models on a microcomputer with a neural processor, provided that the computational resources of the microcomputer match the computational requirements of the neural networks. The ROC-RK3588S-PC microcomputer (Firefly Technology Co., China) provides up to 6 TOPS of performance, allowing the use of YOLOv5n (7.1 GFLOPs), YOLOv11n (6.3 GFLOPs), and YOLOv11s (21.3 GFLOPs) models.

Keywords: pattern recognition systems, neural networks, radar images, machine learning algorithms

[1] You Only Look Once is a series of neural network models for the real-time object detection.

For citation: Krasnoperova A.S., Tverdokhlebov A.S., Kartashov A.A., Weber V.I., Kuprits V.Y. Efficiency of YOLO neural network models applied for object recognition in radar images. *Russian Technological Journal.* 2025;13(4):25–36. https://doi.org/10.32362/2500-316X-2025-13-4-25-36, https://www.elibrary.ru/WWWCJ

Financial disclosure: The authors have no financial or proprietary interest in any material or method mentioned.

The authors declare no conflicts of interest.

НАУЧНАЯ СТАТЬЯ

Исследование эффективности применения моделей нейронных сетей YOLO для распознавания объектов на радиолокационных изображениях

А.С. Красноперова [@], А.С. Твердохлебов, А.А. Карташов, В.И. Вебер, В.Ю. Куприц

Томский государственный университет систем управления и радиоэлектроники», Томск, 634050 Россия
[@] *Автор для переписки, e-mail: alenacergeevna2@icloud.com*

• **Поступила:** 10.10.2024 • **Доработана:** 24.02.2025 • **Принята к опубликованию:** 21.05.2025

Резюме

Цели. В статье рассматривается проблема применения нейронных сетей для обнаружения и классификации объектов на радиолокационных изображениях в условиях ограниченных вычислительных ресурсов. Целью работы является исследование быстродействия и точности моделей нейронных сетей YOLO[2] при решении задач обнаружения и классификации объектов на радиолокационных изображениях для оценки возможностей практической реализации на микрокомпьютере с нейронным процессором.

Методы. В работе использовались методы машинного обучения, обнаружения и классификации объектов на изображении.

Результаты. Результатом работы является оценка и сравнение быстродействия и точности моделей нейронных сетей YOLO 5-го, 8-го и 11-го поколений с разным количеством обучаемых параметров (модели nano, small, medium, large, extra large) для исследования возможности их использования на микрокомпьютере с нейронным процессором. При сравнении различных моделей YOLO по метрике оценки точности лучшие результаты показали модели YOLOv11n (0.925), YOLOv5l (0.889), YOLOv11s (0.883); по метрике полноты – YOLOv5n (0.932), YOLOv11n (0.928), YOLOv11s (0.914); по метрике mAP50 – YOLOv11s (0.961), YOLOv5n (0.954), YOLOv11n (0.953); по метрике mAP50-95 – YOLOv5n (0.756), YOLOv11s (0.74), YOLOv5l (0.727).

Выводы. Проведенные исследования показывают возможность применения моделей нейронных сетей YOLO на микрокомпьютере с нейронным процессором при соответствии вычислительных ресурсов микрокомпьютера и вычислительных требований нейронных сетей. Микрокомпьютер ROC-RK3588S-PC (Firefly Technology Co., Китай) обеспечивает быстродействие до 6 TOPS (Тера-операций в секунду), что позволяет применять модели YOLOv5n (7.1 GFLOPs), YOLOv11n (6.3 GFLOPs), YOLOv11s (21.3 GFLOPs).

[2] You only look once (YOLO) – серия нейросетевых моделей для задачи детекции объектов. [You Only Look Once is a series of neural network models for the real-time object detection.]

Ключевые слова: системы распознавания образов, нейронные сети, радиолокационное изображение, алгоритмы машинного обучения

Для цитирования: Красноперова А.С., Твердохлебов А.С., Карташов А.А., Вебер В.И., Куприц В.Ю. Исследование эффективности применения моделей нейронных сетей YOLO для распознавания объектов на радиолокационных изображениях. *Russian Technological Journal*. 2025;13(4):25–36. https://doi.org/10.32362/2500-316X-2025-13-4-25-36, https://www.elibrary.ru/WWVCJ

Прозрачность финансовой деятельности: Авторы не имеют финансовой заинтересованности в представленных материалах или методах.

Авторы заявляют об отсутствии конфликта интересов.

INTRODUCTION

At present, airborne synthetic aperture radar (SAR) systems are widely used to obtain radar images of terrain [1, 2]. The examples of practical applications of radar imagery produced by SAR airborne radar systems installed on unmanned aerial vehicles (UAVs) include the following:

- vehicle location during search and rescue operations, movement control and security of production plants, storage terminals, fields, ports, and urban areas (parks, water conservation areas), as well as flood detection;
- remote monitoring of extended infrastructure, particularly in remote areas, including oil and gas pipelines, power lines, and railway infrastructure;
- automated creation of digital elevation maps (3D models) of the Earth's surface and classification of the Earth's cover, such as farmland, town, village, water, forest, and road objects.

As a rule, data processing and formation of radar images is performed in stationary conditions using high performance computers. However, in cases where a higher efficiency is required, radar image processing can be carried out on board the UAV. For example, the efficiency of search and rescue operations can be improved by onboard radar image processing and formation by significantly reducing the duration of vehicle search and increasing the efficiency of assistance. This operation can be implemented using neural networks installed on the microcomputers (MC) of the onboard equipment.

The efficiency of ground object detection can be enhanced using various-purpose sensors on the UAV. A new approach to the creation of a multifunctional airborne radioelectronic complex includes the use of various radar modes, the integration of the locator with optoelectronic means, including infrared, as well as the use of airborne radar stations based on synthetic aperture. Modern radar stations ensure high resolution and are capable of performing the tasks of detection and recognition of hidden objects, thus supplementing optical and infrared systems [3].

Radar surveillance using SAR technology is currently considered to be an effective method of remote monitoring of objects of interest, resulting in highly informative 2D radar images. The possibility of obtaining these images is not limited by time of day or meteorological conditions [4, 5].

The basic principles of radar image formation are well known and have been thoroughly discussed previously[3] [6, 7]. When processing SAR data, account should be taken of the specifics of radar imaging, such as:

- geometric and radiometric distortions on the formed radar images;
- the presence of radar shadows;
- speckle noise formed as a result of coherent summation of reflected electromagnetic waves from spatially random scattering sources falling within the SAR resolution element;
- the difference in reflective properties of objects in different frequency ranges;
- radar imaging mode;
- operating frequency range and signal polarization.

At the same time, the basic principles and characteristics of radar image formation are important for the creation of image databases to be further used for training, validation, and testing of neural network models.

The relevance of the research presented in our paper is confirmed by a number of publications. The effectiveness of neural networks for maritime object detection and recognition was investigated in [8–10]. Thus, the work [8] provided accuracy estimates of the YOLOv5x neural network[4] based on the SAR Ship Dataset database [11] using appropriate metrics to evaluate the accuracy of its performance, while [9] investigated neural networks for ship detection and recognition. The results of different neural network

[3] Fundamentals of processing radar data from Earth remote sensing. https://habr.com/ru/articles/787074 (in Russ.). Accessed December 02, 2024.

[4] You Only Look Once is a series of neural network models for the real-time object detection.

models, such as YOLOv4, YOLOv7, YOLOv7-tiny, RetinaNet, Cascade R-CNN, SSD, and OE-YOLO, were described in quantitative terms. In [10], neural networks for object detection and recognition from moving and stationary target acquisition and recognition (MSTAR)[5] databases were analyzed. Different neural network models and their performance characteristics were evaluated using the following metrics: Recall, Precision, mAP50, and mAP50-95.

In this paper, we compare the speed and recognition quality of YOLO neural network models of the 5th, 8th, and 11th generation with different numbers of trained parameters and evaluate the feasibility of their application in an MC with a neural processor.

CREATING A RADAR IMAGE DATABASE

Radar image databases are conventionally created using three main approaches, including:

- experimental imaging of objects of interest on the Earth's surface by means of onboard SAR, taking into account various factors affecting the formation of radar images;
- simulation of the propagation processes of radio waves reflected from the Earth's surface and further processing of the received signals in accordance with the algorithms of SAR operation;
- search of SAR-obtained radar images in open sources.

The former approach provides the most accurate radar image database, although requiring extensive computational and time budgets. Radar image simulation is a complex process whose efficiency depends on numerous factors, such as the complexity of simulating reflections from terrain and extended objects, as well as the formation of a large flow of radar information from SAR receivers, etc. [12, 13].

In this research, we apply the latter approach, which relies on open-source radar image databases to solve the problem. To that end, the open part of the MSTAR database was used. The radar images in this database are formed according to the characteristics of a radar system and the conditions of image formation (see Table 1).

The MSTAR database comprises two datasets, namely:

- MSTAR target, where each image has a plain background and a vehicle in its middle; radar images are taken from different angles of a scene;
- MSTAR clutter, where radar images of rural areas with roads and forests are taken without vehicle images.

[5] https://www.mathworks.com/help/radar/ug/sar-target-classification-using-deep-learning.html. Accessed December 02, 2024.

Table 1. Radar system characteristics and imaging conditions

Characteristics	Value
Frequency range	X band
Center frequency of the sounding signal	9.6 GHz
Bandwidth of the sounding signal	591 MHz
Radiation and reception polarization	Horizontal
Angle and azimuth resolution	1 foot (~30.5 cm)
Shooting mode	Spotlight
Carrier	Aircraft (Twin Otter)
Carrier speed	140–170 km/h
Inclined range	~5 km
Angles of shooting location from ground plane	15°–45°
Shooting angles in azimuth plane	0°–360°
Weather conditions	Clear, dry
Terrain	Plain
Vegetation	Grassy, low
Season	Autumn (September, November)
Shooting location	US Army installation, Redstone Arsenal, Huntsville

The MSTAR database includes 8890 images of vehicles, 2539 images of radar reflectors, and 100 images of rural areas. The complete list of radar images in the database is presented in Table 2.

Examples of radar images from the MSTAR target database are shown in Fig. 1.

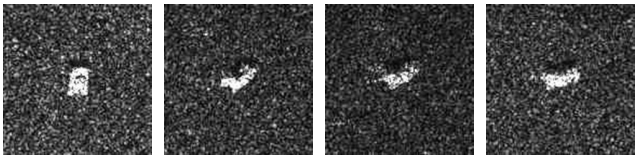

Fig. 1. Examples of radar images from the MSTAR target database

Table 2. List of radar images in the MSTAR database

Target	Description	Angles of site, °	Remarks
T-72	T-72 tank	15	3 sets of 195 images 8 sets of 274 images
		17	3 sets of 230 images 8 sets of 248 images
		30	1 set of 288 images 1 set of 133 images
		45	1 set of 303 images 1 set of 120 images
BMP2	BMP 2 is a tracked infantry fighting vehicle	15 17	3 sets of 196 images 3 sets of 235 images
BTR-60	BTR-60 is an armored personnel carrier (APC)	15 17	1 set of 195 images 1 set of 256 images
BTR-70	BTR-70 is APC	15 17	1 set of 196 images 1 set of 233 images
2S1	2S1 Gvozdika (“Carnation”) is a self-propelled howitzer	15 17 30 45	1 set of 274 images 1 set of 299 images 1 set of 288 images 1 set of 303 images
BRDM-2	BRDM-2 (GAZ-41) is an armored reconnaissance scout vehicle	15	1 set of 274 images
		17	1 set of 298 images
		30	1 set of 287 images 1 set of 133 images
		45	1 set of 303 images 1 set of 120 images
T-62	T-62 tank	15 17	1 set of 273 images 1 set of 299 images
ZSU_23_4	ZSU-23-4 “Shilka” is a self-propelled anti-aircraft gun (SPAAG)	15	1 set of 274 images
		17	1 set of 299 images
		30	1 set of 288 images 1 set of 118 images
		45	1 set of 303 images 1 set of 119 images
ZIL131	ZIL-131 is an expanded mobility truck	15 17	1 set of 274 images 1 set of 299 images
D7	D7 is a tractor-mounted dozer	15 17	1 set of 274 images 1 set of 299 images
SLICY	Construction of geometric figures including basic radar reflector shapes such as flat plate, dihedral, trihedral, and cylinder	15 16 17 29 30 31 43 44 45	1 set of 274 images 1 set of 286 images 1 set of 288 images 1 set of 210 images 1 set of 288 images 1 set of 323 images 1 set of 255 images 1 set of 312 images 1 set of 303 images
CLUTTER	Radar images of Huntsville city and surroundings	15	1 set of 100 images

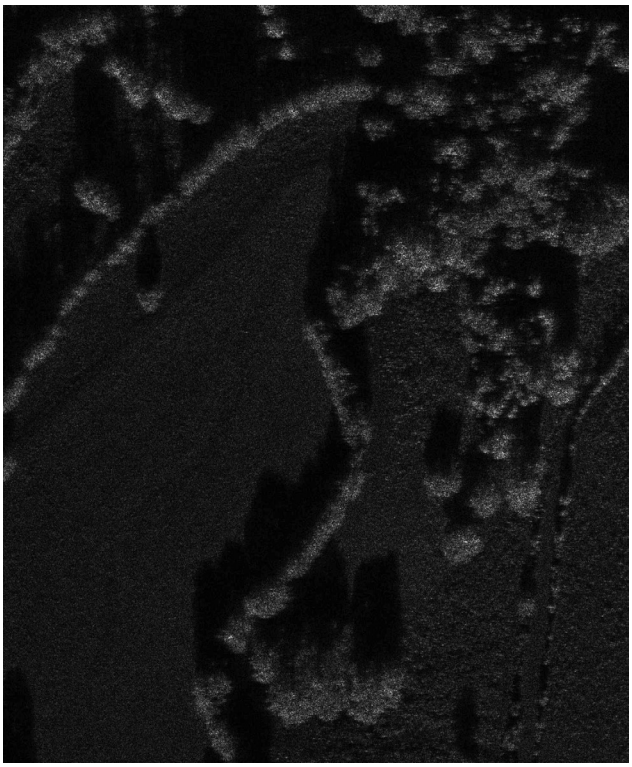

Fig. 2. Rural image from MSTAR cluttered sample

Fig. 3. Example of an image from the created database

A sample image from the MSTAR clutter sample is shown in Fig. 2.

The radar images of the ground surface (MSTAR clutter) and of the vehicles (MSTAR target) are produced under the same conditions. This allows the technique of placing the objects on the background of the rural area to be applied, similar to that reported in [10].

The process of image fusion and generation is performed in three steps [10]:

- selection of the object radar image (MSTAR target) locations on the rural radar image (MSTAR clutter);
- correction of the pixel brightness of the object radar image (MSTAR target) and the selected section of the rural radar image (MSTAR clutter);
- fusion of the object radar image (MSTAR target) and the selected rural radar image (MSTAR clutter).

The MSTAR target angle is equal to the MSTAR clutter angle.

The objects placed in the radar image correspond to the following classes: Class 0 is a radar reflector (SLICY), Class 1 is an armored personnel carrier (APC), Class 2 is an armored reconnaissance scout vehicle, Class 3 is a self-propelled anti-aircraft gun (SPAAG), and Class 4 is a tank. The image from the created database is shown in Fig. 3.

Following the above steps, a database for solving the problem of detecting and recognizing objects on the Earth's surface is created. The sample consists of 350 images with five objects placed on each image. In total, 300 and 50 images are used for training and for validation and testing, respectively. For each image, a text file containing the object coordinates and information about their class is provided.

The speed and recognition quality of the 5th, 8th, and 11th generation YOLO neural network models [14] from the Ultralytics[6] library with different numbers of trained parameters (nano-, small-, medium-, large-, and extra-large-sized models) with the following neural network training parameters were investigated:

- the number of training epochs for all algorithms is 40;
- the optimizer is AdamW with a convergence step of 0.001111, with a momentum equal to 0.9.

TRAINING RESULTS AND PERFORMANCE EVALUATION OF NEURAL NETWORKS

The metrics [9] was used to monitor the training process of the model and to evaluate its performance in the training and validation datasets:

1. Precision is the share of objects that are labelled as positive by the classifier and that are actually positive:

[6] Ultralytics | Revolutionizing the World of Vision AI. https://www.ultralytics.com/. Accessed December 02, 2024.

$$\text{Precision} = \frac{\text{TP}}{\text{TP} + \text{FP}}, \quad (1)$$

where TP (True Positive) is the share of correct classifications belonging to a positive class and FP (False Positive) is the share of incorrect classifications belonging to a positive class (type II error, false alarm). This metric evaluates the model for type II errors.

2. Recall is the share of objects of a given class out of all objects of a given class found by the algorithm:

$$\text{Recall} = \frac{\text{TP}}{\text{TP} + \text{FN}}, \quad (2)$$

where FN (False Negative) is the share of misclassifications not belonging to a positive class (type I error, target omission). This metric evaluates the model for type I errors.

The precision and recall values are obtained for different model confidence thresholds (confidence levels). These thresholds are set manually and the prediction of the bounding box and the prediction of the model class are estimated simultaneously. At higher thresholds, there are fewer detector responses. However, this will reduce the type II error (FP), thus increasing the accuracy but decreasing the completeness value. It is therefore possible to plot Precision against Recall. The average precision (AP) is the area under the Precision–Recall curve:

$$\text{AP} = \int_0^1 P(R)dR. \quad (3)$$

The mean average precision (mAP) is the area under the Precision–Recall curve weighted across all classes:

$$\text{mAP} = \frac{1}{N}\sum_{i=1}^{N} \text{AP}(i). \quad (4)$$

For example, the mAP50-95 metric is a weighted mean accuracy given the values of IoU ∈ [0.5; 0.95], where IoU (intersection over union) is a metric of the degree of intersection between the true bounding box and the predicted bounding box. When the predicted bounding box coincides with the true bounding box, IoU = 1.

An example of object recognition in the test image is shown in Fig. 4.

At the end of training, the best model is considered to be the one with the highest mAP50-95 metric on the validation data.

The numerical values of the metrics obtained during the training of the neural networks of the YOLO family are given in Table 3.

Comparing different YOLO models showed the following: the top three models by precision

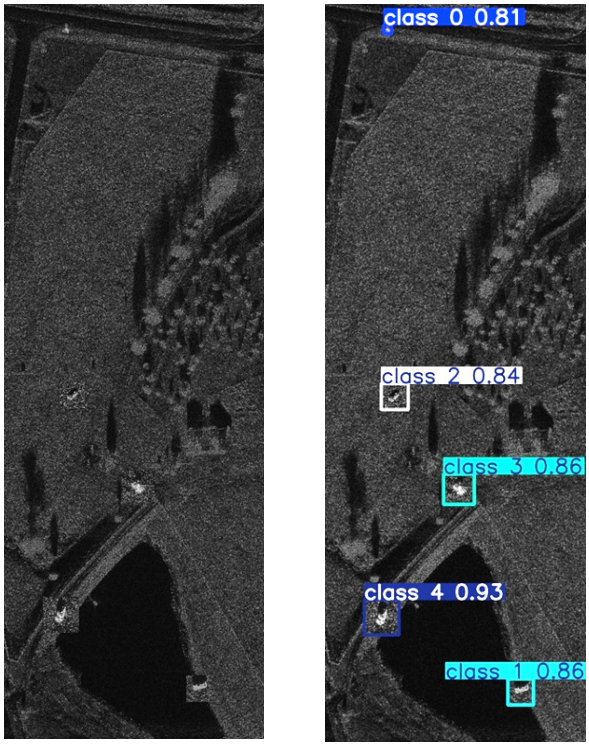

(a) (b)

Fig. 4. Results of object recognition in a radar image using the YOLOv11s model: (a) radar image before recognition; (b) radar image after recognition

are YOLOv11n (0.925), YOLOv5l (0.889), and YOLOv11s (0.883). YOLOv5n (0.932), YOLOv11n (0.928), and YOLOv11s (0.914) show the highest recall metric; YOLOv11s (0.961), YOLOv5n (0.954), and YOLOv11n (0.953) show the highest mAP50 metric; and YOLOv5n (0.756), YOLOv11s (0.74), and YOLOv5l (0.727) show the highest mAP50-95 metric.

The analysis of the number of floating-point operations are represented by a histogram in Fig. 5.

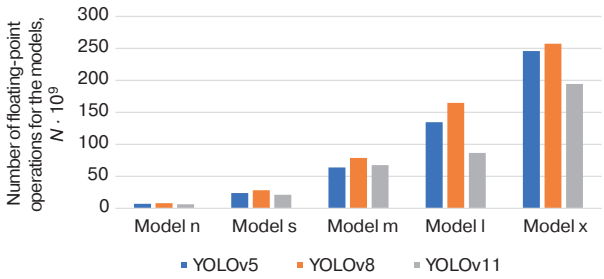

Fig. 5. Comparison of the number of floating-point operations for the models under study

The results obtained allow us to conclude that models l and x with more floating-point operations outperform models n, s, and m in terms of all parameters, largely due to undertraining of models l and x.

Table 3. YOLO neural network model metrics

Neural network model	Precision	Recall	mAP50	mAP50-95	Number of floating-point operations
YOLOv5n	0.844	**0.932**	0.954	**0.756**	7.1e9
YOLOv5s	0.76	0.808	0.871	0.649	23.8e9
YOLOv5m	0.789	0.801	0.889	0.695	64e9
YOLOv5l	0.889	0.881	0.933	0.727	134.7e9
YOLOv5x	0.725	0.802	0.844	0.678	246e9
YOLOv8n	0.748	0.84	0.897	0.65	8.1e9
YOLOv8s	0.643	0.79	0.828	0.617	28.4e9
YOLOv8m	0.739	0.832	0.871	0.678	78.7e9
YOLOv8l	0.694	0.806	0.843	0.648	164.8e9
YOLOv8x	0.772	0.821	0.895	0.697	257.4e9
YOLOv11n	**0.925**	0.928	0.953	0.725	6.3e9
YOLOv11s	0.883	0.914	**0.961**	0.74	21.3e9
YOLOv11m	0.804	0.893	0.91	0.726	67.7e9
YOLOv11l	0.566	0.7	0.761	0.573	86.6e9
YOLOv11x	0.63	0.772	0.82	0.627	194.4e9

For the mAP50 and mAP50-95 metrics, the highest results are achieved using the YOLOv5n, YOLOv11n, and YOLOv11s models. In [10], FasterRCNN (mAP50 = 0.8786), RetinaNet (mAP50 = 0.916), and different modifications of YOLOv5 such as YOLOv5 basic (mAP50 = 0.9169) and YOLOv5 modified (mAP50 = 0.9555) were used to investigate recognition accuracy. For comparison, the YOLO neural network models and the values of the mAP50 metric are shown in Table 4.

Table 4. The mAP50 metric of neural network models

Neural network model	mAP50
YOLOv5n	0.954
YOLOv11n	0.953
YOLOv11s	**0.961**

The data presented in Table 4 indicate that the 11th generation YOLO models perform sufficiently well in solving the problem of ground object detection and recognition in radar images.

The error matrix for the YOLO neural network is shown in Fig. 6, which indicates the number of misclassifications made by the model. The classes as predicted by the model are labelled on the left, and the true classes are labelled at the bottom. In addition to the five classes of recognized objects, there is also a background class representing the background classification errors.

It can be assumed that images of radar reflectors were classified as background more often than others, due to their small effective scattering area compared to the other classes.

When predicting Class 1, the YOLOv11s model has the maximum type I error with 5 out of 50 classified as Class 2 and 6 out of 50 classified as Class 4. Class 4 has the maximum type II error with 6 objects of Class 1, 3 objects of Class 3, and 3 snippets with background classified as Class 4.

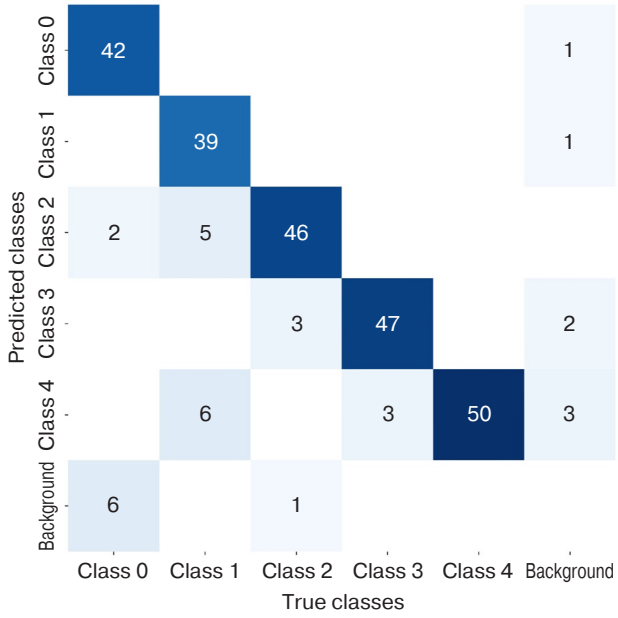

Fig. 6. Error matrix for the YOLOv11s neural network

In [15], in order to evaluate the feasibility of using neural networks on MCs, the number of operations required by the YOLO model was compared to the number of operations per second that can be provided by the MC. The Firefly ROC-RK3588S-PC (Firefly Technology Co., China) was used as a basis, equipped with an onboard RK3588 neural processor capable of up to 6 Tera operations per second (TOPS)[7].

The computational resources consumed by a neural network model on a single input image can be expressed in terms of Giga float operations (GFLOPs). For a relevant evaluation, it is necessary to convert TOPS into a floating-point format, since TOPS defines the number of operations per second[8] and GFLOPs defines the number of floating-point operations with the input image. The performance of 4 TOPS is approximately equal to the performance of 1 TFLOPS[9]; hence, converting 6 TOPS results in 1.5 TFLOPS. Therefore, the performance of the ROC-RK3588S-PC MC allows the installation of YOLOv5n (7.1 GFLOPs), YOLOv11n (6.3 GFLOPs), and YOLOv11s (21.3 GFLOPs), providing a performance of more than 10 frames per second, which is a positive result.

CONCLUSIONS

Our research demonstrates that, out of the neural network models considered, the YOLOv5n, YOLOv5l, YOLOv11n, and YOLOv11s models produce the highest results in terms of the following metrics. The difference in the mAP50-95 metrics between the YOLOv5l and YOLOv11n models is ~0.003. The difference in the Precision metric values between YOLOv5l and YOLOv11s models is ~0.006. The difference in the computational cost is ~102 floating point operations, which has a significant impact on performance. The selected models are therefore YOLOv5n, YOLOv11n, and YOLOv11s. According to their computational costs and the performance of the ROC-RK3588S-PC MC, the selected models can be recommended for installation on the MC for real-time operation.

Authors' contributions

A.S. Krasnoperova—conducting research, interpreting and summarizing results, writing the text of the article.

A.S. Tverdokhlebov—interpreting research results, preparing conclusions.

A.A. Kartashov—defining the research topic and discussing the final text of the article.

V.I. Weber—planning the research, interpreting results, scientific editing of the article.

V.Y. Kuprits—setting the aims and objectives of the research, methods of machine learning.

[7] ROC-RK3588S-PC 8-Core 8K AI Mainboard. https://www.rock-chips.com/a/cn/product/RK35xilie/2022/0926/1656.html. Accessed December 02, 2024.

[8] What is TOPS and TeraFLOPS in AI? https://www.candtsolution.com/news_events-detail/tops-and-teraflops-in-AI/#:~:text=What%20is%20TOPS%20in%20AI,peak%20performance%20of%20AI%20hardware. Accessed December 02, 2024.

[9] What Is the Relationship Between the Units of Tops and Flops? https://premioinc.com/blogs/blog/what-is-tops-and-teraflops-in-ai. Accessed December 02, 2024.

REFERENCES

1. Malmgren-Hansen D., Engholm R., Østergaard Pedersen M. Training Convolutional Neural Networks for Translational Invariance on SAR ATR. In: *Proceedings of EUSAR 2016: 11th European Conference on Synthetic Aperture Radar*. IEEE; 2016. P. 459–462.
2. Cruz H., Véstias M.P., Monteiro J., et al. A Review of Synthetic-Aperture Radar Image Formation Algorithms and Implementations: A Computational Perspective. *Remote Sens.* 2022;14(5):1258. https://doi.org/10.3390/rs14051258
3. Il'in E.M., Polubekhin A.I., Savostyanov V.Yu., Samarin O.F., Cherevko A.G. Airborne multi-functional radar complex for shot-range UAVs. *Vestnik SibGUTI = The Herald of the Siberian State University of Telecommunications and Information Science*. 2017;4:104–109 (in Russ.). https://www.elibrary.ru/item.asp?id=30793295
4. Paul V.G., Simonov A.V. Space radar terrain survey and the joint flight of a spacecraft pair. *Inzhenernyi zhurnal: nauka i innovatsii = Engineering Journal: Science and Innovation.* 2020;7:1–21 (in Russ.). https://doi.org/10.18698/2308-6033-2020-7-1999, https://www.elibrary.ru/item.asp?id=43566045
5. Khakhulina N.B. *Sistemy sbora i obrabotki informatsii rezul'tatov geodezicheskikh izyskanii i distantsionnogo zondirovaniya* (*Systems of Information Collection and Processing of Geodetic Surveys and Remote Sensing Results*). Voronezh: Voronezh State Technical University; 2022. 78 p. (in Russ.).
6. Kondratenkov G.S. (Ed.). *Radiolokatsionnye stantsii vozdushnoi razvedki* (*Airborne Reconnaissance Radar Stations*). Moscow: Voenizdat; 1983. 154 p. (in Russ.).
7. Kanaschenkov A.I., Merkulov V.I. (Eds.). *Radiolokatsionnye sistemy mnogofunktsional'nykh samoletov:* V 3 t. T. 1. *RLS – informatsionnaya osnova boevykh deistvii mnogofunktsional'nykh samoletov. Sistemy i algoritmy pervichnoi obrabotki radiolokatsionnykh signalov* (*Radar Systems of Multi-Functional Aircraft:* in 3 v. V. 1. *Radar Systems – Information Basis for Combat Operations of Multi-Functional Aircraft. Systems and Algorithms for Primary Processing of Radar Signals*). Moscow: Radiotekhnika; 2006. 656 p. (in Russ.).
8. Kupryashkin I.F., Mazin A.S. Classification of military equipment targets on radar images generated in noise interference conditions using a convolutional neural network. *Vestnik Kontserna VKO Almaz-Antey.* 2022;1:71–81 (in Russ.). https://www.elibrary.ru/item.asp?id=48138675
9. Chen D., Ju R., Tu C., Long G., Liu X., Liu J. GDB-YOLOv5s: Improved YOLO-based Model for Ship Detection in SAR Images. *IET Image Process*. 2024;18(11):2869–2883. https://doi.org/10.1049/ipr2.13140
10. Song Y., Wang S., Li Q., Mu H., Feng R., Tian T., Tian J. Vehicle Target Detection Method for Wide-Area SAR Images Based on Coarse-Grained Judgment and Fine-Grained Detection. *Remote Sens*. 2023;15(13):3242. https://doi.org/10.3390/rs15133242
11. Zhang T., Zhang X., Li J., Xu X., Wang B., Zhan X., Xu Y., Ke X., Zeng T., Su H., et al. SAR Ship Detection Dataset (SSDD): Official Release and Comprehensive Data Analysis. *Remote Sens*. 2021;13(18):3690. https://doi.org/10.3390/rs13183690
12. Karmanova N.A., Karmanov A.G., Petrov A.A. Development of a synthetic aperture radar model for unmanned aerial vehicles for remote sensing of woodlands. *Informatsiya i Kosmos = Information and Space*. 2021;4:114–122 (in Russ.). https://www.elibrary.ru/item.asp?edn=esiivj
13. Bryzgalov A.P., Koval'chuk I.V., Khnykin A.V., Shevela I.A., Yusupov R.G. Simulation of Synthetic Aperture Radar Assigned to Solving the Problems of Its Internal and External Design. *Trudy MAI.* 2011;43:25 (in Russ.). https://www.elibrary.ru/item.asp?id=15632049
14. Terven J., Córdova-Esparza D.-M., Romero-González J.-A. A comprehensive review of YOLO architectures in computer vision: from YOLOv1 to YOLOv8 and YOLO-NAS. *Mach. Learn. Knowl. Extr*. 2023;5(4):1680–1716. https://doi.org/10.3390/make5040083
15. Baller S., Jindal A., Chadha M., Gerndt M. DeepEdgeBench: benchmarking deep neural networks on edge devices. In: *Proceedings of the 2021 IEEE International Conference on Cloud Engineering* (*IC2E*). IEEE; 2021. P. 20–30. https://doi.org/10.1109/IC2E52221.2021.00016

СПИСОК ЛИТЕРАТУРЫ

1. Malmgren-Hansen D., Engholm R., Østergaard Pedersen M. Training Convolutional Neural Networks for Translational Invariance on SAR ATR. In: *Proceedings of EUSAR 2016: 11th European Conference on Synthetic Aperture Radar*. IEEE; 2016. P. 459–462.
2. Cruz H., Véstias M.P., Monteiro J., et al. A Review of Synthetic-Aperture Radar Image Formation Algorithms and Implementations: A Computational Perspective. *Remote Sens.* 2022;14(5):1258. https://doi.org/10.3390/rs14051258
3. Ильин Е.М., Полубехин А.И., Савостьянов В.Ю., Самарин О.Ф., Черевко А.Г. Малогабаритный многофункциональный бортовой РЛК для беспилотных летательных аппаратов малой дальности. *Вестник СибГУТИ*. 2017;4:104–109. https://www.elibrary.ru/item.asp?id=30793295
4. Поль В.Г., Симонов А.В. Космическая радиолокационная съемка рельефа и совместный полет пары космических аппаратов. *Инженерный журнал: наука и инновации*. 2020;7:1–21. https://doi.org/10.18698/2308-6033-2020-7-1999, https://www.elibrary.ru/item.asp?id=43566045
5. Хахулина Н.Б. *Системы сбора и обработки информации результатов геодезических изысканий и дистанционного зондирования*. Воронеж: Воронежский государственный технический университет; 2022. 78 с.

6. *Радиолокационные станции воздушной разведки*; под ред. Г.С. Кондратенкова. М.: Воениздат; 1983. 154 с.
7. *Радиолокационные системы многофункциональных самолетов:* в 3 т. Т. 1. *РЛС – информационная основа боевых действий многофункциональных самолетов. Системы и алгоритмы первичной обработки радиолокационных сигналов*; под ред. А.И. Канащенкова, В.И. Меркулова. М.: Радиотехника; 2006. 656 с.
8. Купряшкин И.Ф., Мазин А.С. Классификация объектов военной техники с использованием сверточной нейронной сети на радиолокационных изображениях, сформированных в условиях шумовых помех. *Вестник Концерна ВКО «Алмаз – Антей».* 2022;1:71–81. https://www.elibrary.ru/item.asp?id=48138675
9. Chen D., Ju R., Tu C., Long G., Liu X., Liu J. GDB-YOLOv5s: Improved YOLO-based Model for Ship Detection in SAR Images. *IET Image Process*. 2024;18(11):2869–2883. https://doi.org/10.1049/ipr2.13140
10. Song Y., Wang S., Li Q., Mu H., Feng R., Tian T., Tian J. Vehicle Target Detection Method for Wide-Area SAR Images Based on Coarse-Grained Judgment and Fine-Grained Detection. *Remote Sens*. 2023;15(13):3242. https://doi.org/10.3390/rs15133242
11. Zhang T., Zhang X., Li J., Xu X., Wang B., Zhan X., Xu Y., Ke X., Zeng T., Su H., et al. SAR Ship Detection Dataset (SSDD): Official Release and Comprehensive Data Analysis. *Remote Sens*. 2021;13(18):3690. https://doi.org/10.3390/rs13183690
12. Карманова Н.А., Карманов А.Г., Петров А.А. Разработка модели радара с синтезированной апертурой беспилотного летательного аппарата для дистанционного зондирования лесных массивов. *Информация и Космос*. 2021;4:114–122. https://www.elibrary.ru/item.asp?edn=esiivj
13. Брызгалов А.П., Ковальчук И.В., Хныкин А.В., Шевела И.А., Юсупов Р.Г. Моделирование радиолокатора с синтезированной апертурой при решении задач его внутреннего и внешнего проектирования. *Труды МАИ*. 2011;43:25. https://www.elibrary.ru/item.asp?id=15632049
14. Terven J., Córdova-Esparza D.-M., Romero-González J.-A. A comprehensive review of YOLO architectures in computer vision: from YOLOv1 to YOLOv8 and YOLO-NAS. *Mach. Learn. Knowl. Extr*. 2023;5(4):1680–1716. https://doi.org/10.3390/make5040083
15. Baller S., Jindal A., Chadha M., Gerndt M. DeepEdgeBench: benchmarking deep neural networks on edge devices. In: *Proceedings of the 2021 IEEE International Conference on Cloud Engineering* (*IC2E*). IEEE; 2021. P. 20–30. https://doi.org/10.1109/IC2E52221.2021.00016

About the Authors

Alena S. Krasnoperova, Engineer of the Student Design Bureau of Intelligent Radio Engineering Systems, Department of Radio Engineering Systems, Tomsk State University of Control Systems and Radioelectronics (40, Lenina pr., Tomsk, 634050 Russia). E-mail: alenacergeevna2@icloud.com. RSCI SPIN-code 9055-6959, https://orcid.org/0009-0001-5568-8290

Alexander S. Tverdokhlebov, Engineer of the Student Design Bureau of Intelligent Radio Engineering Systems, Department of Radio Engineering Systems, Tomsk State University of Control Systems and Radioelectronics (40, Lenina pr., Tomsk, 634050 Russia). E-mail: tverdohlebov.a.923-@e.tusur.ru. https://orcid.org/0009-0008-2250-6375

Alexey A. Kartashov, Engineer of the Student Design Bureau of Intelligent Radio Engineering Systems, Department of Radio Engineering Systems, Tomsk State University of Control Systems and Radioelectronics (40, Lenina pr., Tomsk, 634050 Russia). E-mail: kartashov.a.923-m@e.tusur.ru. https://orcid.org/0009-0009-6005-7539

Vladislav I. Weber, Postgraduate Student, Assistant, Department of Radio Engineering Systems, Tomsk State University of Control Systems and Radioelectronics (40, Lenina pr., Tomsk, 634050 Russia). E-mail: vladweber00@gmail.com. RSCI SPIN-code 3880-2107, https://orcid.org/0000-0002-0275-4127

Vladimir Y. Kuprits, Cand. Sci. (Eng.), Associate Professor, Head of the Student Design Bureau of Intelligent Radio Engineering Systems, Department of Radio Engineering Systems, Tomsk State University of Control Systems and Radioelectronics (40, Lenina pr., Tomsk, 634050 Russia). E-mail: vladimir.y.kuprits@tusur.ru. RSCI SPIN-code 4855-3318, https://orcid.org/0000-0001-7190-3213

Об авторах

Красноперова Алена Сергеевна, инженер студенческого конструкторского бюро «Интеллектуальные радиотехнические системы», кафедра радиотехнических систем, ФГАОУ ВО «Томский государственный университет систем управления и радиоэлектроники» (634050, Россия, Томск, пр. Ленина, д. 40). E-mail: alenacergeevna2@icloud.com. SPIN-код РИНЦ 9055-6959, https://orcid.org/0009-0001-5568-8290

Твердохлебов Александр Сергеевич, инженер студенческого конструкторского бюро «Интеллектуальные радиотехнические системы», кафедра радиотехнических систем, ФГАОУ ВО «Томский государственный университет систем управления и радиоэлектроники» (634050, Россия, Томск, пр. Ленина, д. 40). E-mail: tverdohlebov.a.923-@e.tusur.ru. https://orcid.org/0009-0008-2250-6375

Карташов Алексей Андреевич, инженер студенческого конструкторского бюро «Интеллектуальные радиотехнические системы», кафедра радиотехнических систем, ФГАОУ ВО «Томский государственный университет систем управления и радиоэлектроники» (634050, Россия, Томск, пр. Ленина, д. 40). E-mail: kartashov.a.923-m@e.tusur.ru. https://orcid.org/0009-0009-6005-7539

Вебер Владислав Игоревич, аспирант, ассистент кафедры радиотехнических систем, ФГАОУ ВО «Томский государственный университет систем управления и радиоэлектроники» (634050, Россия, Томск, пр. Ленина, д. 40). E-mail: vladweber00@gmail.com. SPIN-код РИНЦ 3880-2107, https://orcid.org/0000-0002-0275-4127

Куприц Владимир Юрьевич, к.т.н., доцент, руководитель студенческого конструкторского бюро «Интеллектуальные радиотехнические системы», кафедра радиотехнических систем, ФГАОУ ВО «Томский государственный университет систем управления и радиоэлектроники» (634050, Россия, Томск, пр. Ленина, д. 40). E-mail: vladimir.y.kuprits@tusur.ru. SPIN-код РИНЦ 4855-3318, https://orcid.org/0000-0001-7190-3213

Translated from Russian into English by K. Nazarov
Edited for English language and spelling by Thomas A. Beavitt

Micro- and nanoelectronics. Condensed matter physics

Микро- и наноэлектроника. Физика конденсированного состояния

UDC 538.955
https://doi.org/10.32362/2500-316X-2025-13-4-37-46
EDN WYJGOZ

RESEARCH ARTICLE

Measurement of magnetostriction using a strain gauge bridge with alternating excitation

Dmitry A. Burdin @

MIREA – Russian Technological University, Moscow, 119454 Russia
@ *Corresponding author, e-mail: phantastic@mail.ru*

• **Submitted:** 21.11.2024 • **Revised:** 15.01.2025 • **Accepted:** 20.05.2025

Abstract

Objectives. Knowledge of the dependence of magnetostriction of various ferromagnetic materials on the magnetic field is important for studying the magnetoelectric effect in composite structures, in particular for calculating the shape of the field dependence of piezomagnetic moduli and for calculating magnetoelastic characteristics. However, the typical resolution level of known strain gauge setups for measuring magnetostriction is about 10^{-6}, which is insufficient to obtain detailed information on the piezomagnetic coefficients of the materials under study. The paper describes the development of an automated setup for the precision measurement of the dependence of magnetostriction of ferromagnetic plates on a magnetic field in the range of ±5 kOe providing an improved strain resolution order of magnitude.

Methods. The setup uses film strain gauges included in a Wheatstone bridge excited by alternating current. Thanks to the applied method of signal frequency shift, as well as the use of a low-noise preamplifier and temperature stabilization of the measuring cell, it was possible to reduce the level of noise referred to the input and zero drift of the measuring circuit.

Results. The developed setup provides an accuracy of the magnetostriction measurement of ferromagnetic plates up to 10^{-7} in the range of magnetic fields of ±5 kOe, which is an order of magnitude higher than known methods. The setup also allows measuring the electric and piezoelectric deformation of materials depending on the applied electrical voltage in the range of ±500 V. The measurement results can be used to more accurately calculate the field dependencies of the piezomagnetic and piezoelectric coefficients of materials, including materials with low magnetostriction, such as various ferrites, hematite, yttrium iron garnet, etc.

Conclusions. The method of alternating excitation of the measuring bridge in combination with other measures can be used to increase the deformation resolution to about 10^{-7}.

Keywords: magnetostriction, strain gauge, deformation, magnetoelectric effect, composite structure

For citation: Burdin D.A. Measurement of magnetostriction using a strain gauge bridge with alternating excitation. *Russian Technological Journal.* 2025;13(4):37–46. https://doi.org/10.32362/2500-316X-2025-13-4-37-46, https://www.elibrary.ru/WYJGOZ

Financial disclosure: The author has no financial or proprietary interest in any material or method mentioned.

The author declares no conflicts of interest.

НАУЧНАЯ СТАТЬЯ

Измерение магнитострикции тензометрическим мостом с переменным возбуждением

Д.А. Бурдин @

МИРЭА – Российский технологический университет, Москва, 119454 Россия
@ *Автор для переписки, e-mail: phantastic@mail.ru*

• **Поступила:** 21.11.2024 • **Доработана:** 15.01.2025 • **Принята к опубликованию:** 20.05.2025

Резюме

Цели. Знание зависимости магнитострикции различных ферромагнитных материалов от магнитного поля важно для исследования магнитоэлектрического эффекта в композитных структурах, в частности для расчета формы полевой зависимости пьезомагнитных модулей и расчета магнитоупругих характеристик. Наиболее распространенным методом измерения магнитострикционного удлинения является использование тензорезистивных датчиков. Однако типичный уровень разрешения известных тензорезистивных установок для измерения магнитострикции составляет около 10^{-6}, что недостаточно для получения детальной информации о пьезомагнитных коэффициентах исследуемых материалов. Цель работы – разработка автоматизированной установки для прецизионного измерения зависимости магнитострикции ферромагнитных пластин от магнитного поля в диапазоне ±5 кЭ с улучшенным на порядок разрешением по деформации.

Методы. В установке использованы пленочные тензорезистивные датчики, включенные в мост Уитстона, возбуждаемый переменным током. Благодаря примененному методу переноса частоты сигнала, а также применению малошумящего предусилителя и температурной стабилизации измерительной ячейки, удалось уменьшить уровень приведенных ко входу шумов и дрейфа нуля измерительной схемы.

Результаты. Созданная установка обеспечивает на порядок более высокую точность измерения магнитострикции ферромагнитных пластин, чем известные, до 10^{-7} в диапазоне магнитных полей ±5 кЭ. Установка позволяет измерять также электро- и пьезодеформацию материалов в зависимости от приложенного электрического напряжения в диапазоне ±500 В. Результаты измерений дают возможность более точно рассчитать полевые зависимости пьезомагнитных и пьезоэлектрических коэффициентов материалов, в т.ч. материалов с малой величиной магнитострикции, таких как различные ферриты, гематит, железо-иттриевый гранат и др.

Выводы. Применение метода переменного возбуждения измерительного моста в совокупности с другими мерами позволило повысить разрешение по деформации, которое составило около 10^{-7}.

Ключевые слова: магнитострикция, тензометр, деформация, магнитоэлектрический эффект, композитная структура

Для цитирования: Бурдин Д.А. Измерение магнитострикции тензометрическим мостом с переменным возбуждением. *Russian Technological Journal*. 2025;13(4):37–46. https://doi.org/10.32362/2500-316X-2025-13-4-37-46, https://www.elibrary.ru/WYJGOZ

Прозрачность финансовой деятельности: Автор не имеет финансовой заинтересованности в представленных материалах или методах.

Автор заявляет об отсутствии конфликта интересов.

INTRODUCTION

Magnetostriction describes the change in the linear dimensions of a ferromagnet when its magnetization is changed. One of the main features of magnetostriction is the saturation magnetostriction λ_{sat}, which is equal to the relative elongation of the sample in the magnetic saturation field H_s. However, the dependence of the relative elongation on the magnetic field $\lambda(H)$ provides a more thorough description of the magnetostriction properties. The ability to measure the dependence of magnetostriction of different ferromagnetic materials on the magnetic field is important for studies of magnetoelectric (ME) effects in composite structures containing ferromagnetic (FM) and piezoelectric (PE) layers, as well as for the development of new smart devices [1–3]. ME effects in such structures arise from the interaction of mechanically bound FM and PE layers under the influence of external electric and magnetic fields.

Typical ME structures and their constituent layers are plates with in-plane dimensions of ~5 × 20 mm and thicknesses of tens and hundreds of micrometers. Ni ($\lambda_{sat} = -30 \cdot 10^{-6}$), Terfenol-D ($\lambda_{sat} = 2000 \cdot 10^{-6}$), amorphous alloys FeBSiC ($\lambda_{sat} = 20–30 \cdot 10^{-6}$), FeCoV ($\lambda_{sat} = 70 \cdot 10^{-6}$), and galfenol ($\lambda_{sat} = 30–90 \cdot 10^{-6}$) are used as materials for FM layers. Recently, the possibility of creating ME structures with single crystal layers of ferro- and antiferromagnetic materials with lower magnetostriction ($\lambda_{sat} < 10^{-5}$) has attracted the interest of researchers. The main methods for direct measurement of magnetostriction are strain gauges [4–8] and dilatometers [9]. Dilatometers are divided into capacitive [10, 11] and optical [12–14] according to the principle of operation. The most convenient method for studying the magnetostriction of planar FM samples and composite structures is the strain gauge method, where a strain gauge resistor is bonded to the sample and included in the measuring bridge. This method is widely used for magnetostriction measurements due to its low cost and the ease of sample preparation. However, disadvantages include its limited applicability for measuring the magnetostriction of films.

In such systems, the measuring bridge is typically powered by a constant voltage (current) source, which imposes restrictions on the minimum resolvable strain magnitude. Such strain gauges have a typical input noise spread of $(2–5) \cdot 10^{-6}$ [15–17], which is acceptable for the study of materials with large saturation magnetostriction $\lambda_{sat} > 10^{-5}$, but cannot be used to study materials having low magnetostriction. In order to solve this problem, it will be necessary to create a setup offering a higher resolution.

The aim of this work is to develop a setup for measuring magnetostriction by the strain gauge method with a higher resolution (better than 10^{-6}). The first part of the paper describes the design of the setup, followed by a description of the operating principle and an analysis of the noise determining the resolution. The final part of the paper deals with the practical verification of the achieved level of input noise and the demonstration of magnetostriction and electrostriction measurements on real samples.

SETUP DESIGN

The external view of the proposed magnetostriction measurement setup is shown in Fig. 1. It consists of three main parts (Fig. 2): magnetic system, measuring cell, and control and measuring unit (CMU). The magnetic system used to generate a constant magnetic field of 0 to 5 kOe represents a laboratory electromagnet with a measuring cell on a movable base and a probe with a Hall sensor installed in the magnetic gap. The movable base of the cell is used for positioning the cell in the gap of the electromagnet and operative removal of the sample (board with the sample). The cell is moved by means of a carriage moving on a rail guide installed between the poles of the electromagnet.

In order to power the electromagnet, a standard laboratory power supply fitted with a switching device for switching the magnetic field polarity is used. The magnetic field is measured using a Lake Shore 421 laboratory gaussmeter (Lake Shore, USA).

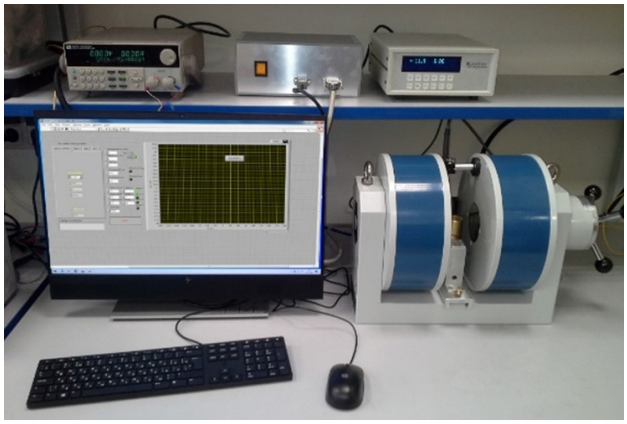

Fig. 1. External view of the magnetostriction measurement setup

The sample to be tested is placed on the removable board of the measuring cell with a strain gauge glued to its surface. The leads of the strain gauge are soldered to the contact pads to form a Wheatstone bridge together with the resistors on this board. Balancing circuits (based on a wire potentiometer) and a preamplifier are implemented on the same board.

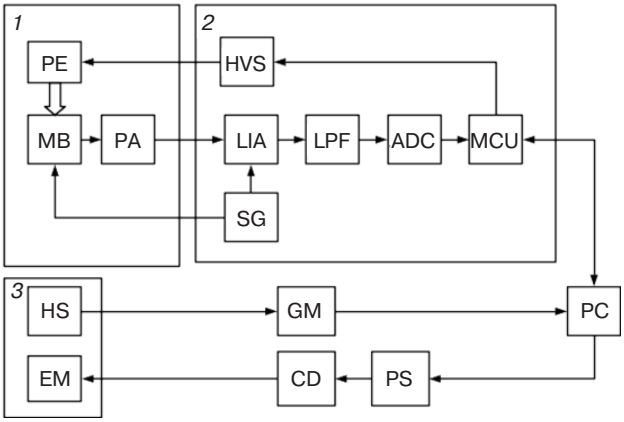

Fig. 2. Schematic diagram of the magnetostriction measurement setup: *1* is a measuring cell, *2* is a CMU, and *3* is a magnetic system; PE is a PE element, MB is a measuring bridge, PA is a preamplifier, LIA is a lock-in amplifier, HVS is a high voltage power supply, SG is a signal generator, LPF is a low pass filter, ADC is an analogue-to-digital converter, MCU is a microcontroller unit, HS is a Hall sensor, EM is an electromagnet, GM is a gaussmeter, CD is a commutation device, PS is a power supply for an electromagnet, and PC is a personal computer

The cell on the base (the electromagnet is shown in cross-section) is shown in Fig. 3. The cell body, which has a cylindrical shape, can be rotated 180° around the vertical axis using a removable handle, allowing orientation-dependent measurements. The angle of the cell orientation is measured on a scale on the side (cylindrical) surface of its body.

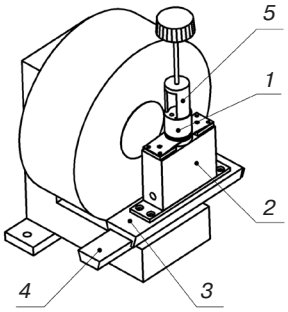

Fig. 3. Cell on the base (construction and external view): (*1*) cell, (*2*) base radiator, (*3*) cell carriage, (*4*) base rail, and (*5*) removable handle

The removable amplifier board is as shown in Fig. 4a. The board with the sample is mounted on top of the Peltier module and connected to the base board by two small six pin connectors. A thermoelectric component is used to stabilize the temperature of the sample plate with an accuracy of 0.01°C. The electrical cable connecting the cell to the CMU is connected to the base board and the thermoelectric cell via pins on the underside of the cell body. The preamplifier is based on a low noise integrated instrument amplifier INA849 (Texas Instruments, USA).

The CMU is used to acquire and digitize the measuring signal, to stabilize the temperature of the sample plate, to supply the bridge with alternating voltage at a frequency of 410 Hz and an amplitude of up to 4 V, and to generate a constant voltage from −500 to 500 V for the study of electrostriction and PE samples. The CMU is housed in a table-top case with dimensions of 300 × 150 × 100 mm. The CMU and the cell are connected by a 15-pin signal cable.

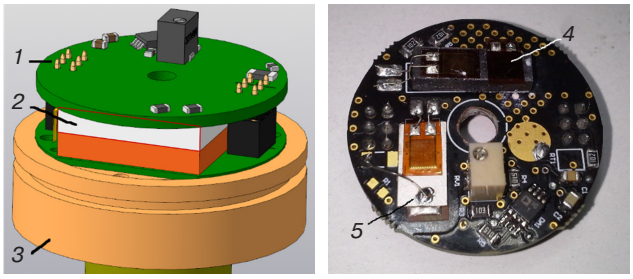

(a) (b)

Fig. 4. Cell design (a) and external view of removable amplifier board (b): (*1*) amplifier board; (*2*) Peltier module; (*3*) cell base; (*4*) FM sample with strain gauge; (*5*) piezoelectric element with strain gauge

STRAIN GAUGE OPERATING PRINCIPLE

The elongation of the sample is measured using standard strain gauges. A foil strain gauge is a meandering grid of thin metal foil on a paper or polyimide substrate. The sensor is bonded to the sample surface taking into account the direction of sensitivity. The two basic sensor configurations are shown in Fig. 5.

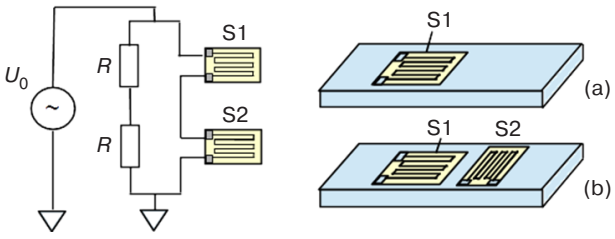

Fig. 5. Strain gauge half-bridge: (a) with one active sensor; (b) with two active sensors

Here, one arm of the bridge is made up of two resistors of the same resistance *R* and the other arm is made up of two strain gauges S1 and S2. In the first case, only one sensor (S1) is bonded to the sample, while the second sensor (S2) only complements the arm of the measuring bridge. This configuration is used when it is necessary to selectively measure elongation in one direction. If the deformation is along the side

of the sample, the second configuration can be used, in which the reference sensor S2 is bonded to the sample (on the same or opposite surface) at an angle of 90° to the first.

Figure 6 depicts the functional diagram of the analogue part of the strain gauge signal path, consisting of the preamplifier K_{amp}, the demodulator on the AD630 chip (Analog Devices, Inc., USA), and the low-pass filter. We consider the conversion of the signal from the measuring bridge to the ADC input. The bridge is fed by the harmonic voltage u_b with amplitude U_0 and frequency ω_0: $u_b = U_0\cos(\omega_0 t)$, where t is time. It can be shown that the unbalanced voltage of the bridge under signal modulated $u_{s.m.} \approx u_b \delta R/4$, where δR is the change in resistance of the strain gauge.

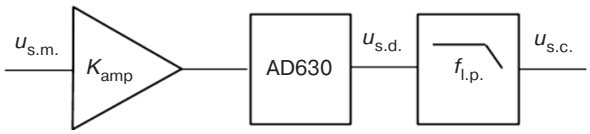

Fig. 6. Analogue part of the input measurement path: $u_{s.m.}$ is the bridge imbalance voltage; $u_{s.d.}$ is the signal at the demodulator output; $f_{l.p.}$ is the low pass filter cut-off frequency; $u_{s.c.}$ is the signal at the ADC input

Let the periodic deformation $\varepsilon = \varepsilon_0\cos(\omega t)$ occur at the frequency $\omega < \omega_0$, with $\delta R = G\varepsilon_0\cos(\omega t)$, where ε_0 is the strain amplitude, and $G \approx 2$ is the strain sensitivity coefficient of the sensor. Then the bridge imbalance voltage is as follows:

$$u_{s.m.} \approx \frac{u_b \delta R}{4} = \frac{U_0\cos(\omega_0 t) G\varepsilon_0 \cos(\omega t)}{4} = \\ = \frac{\frac{1}{2}U_0 G\varepsilon_0 (\cos((\omega_0 - \omega)t) + \cos((\omega_0 + \omega)t))}{4}. \quad (1)$$

Thus, the useful signal, which is proportional to the change in resistance of the strain gauge on the sample, modulates the voltage amplitude. As a result, the signal spectrum is shifted to the frequencies $(\omega_0 + \omega)$ and $(\omega_0 - \omega)$ at the right and left sidebands. In the case of constant strain ($\omega \approx 0$), equation (1) is simplified as follows:

$$u_{s.m.} \approx \frac{u_b \delta R}{4} = \frac{U_0\cos(\omega_0 t) G\varepsilon_0}{4}. \quad (2)$$

The signal $u_{s.m.}$ is amplified by the preamplifier with a gain $K_{amp} \approx 1000$ and is fed to the input of a lock-in amplifier, which is realized with AD630 chip. The signal at the output of lock-in amplifier is as follows:

$$u_{s.d.}(\omega) = K_{amp} u_{s.m.}(\omega)\cos(\omega_0 t) = \\ = \frac{K_{amp} U_0 \cos(\omega t) G\varepsilon_0 \cos^2(\omega_0 t)}{4} = \\ = \left[\frac{K_{amp} U_0 G\varepsilon_0}{8}(1 + 2\cos(\omega_0 t))\right]_{\omega=0}. \quad (3)$$

This means that the original signal is restored and there is an additional component with a frequency of $2\omega_0$. The third-order low-pass filter (LPF), which is located after the detector and has a bandwidth of $\omega_{l.p.} << \omega_0$ ($\omega_{l.p.} \approx 14$ Hz), cuts off the high-frequency components of the signal before the analogue-to-digital conversion. The filter has the following transfer characteristic:

$$K_{l.p.} = \frac{1}{\left(\sqrt{1 + \left(\frac{\omega}{\omega_{l.p.}}\right)}\right)^3}. \quad (4)$$

As a result, the signal at the ADC input is as follows:

$$u_{s.c.}(\omega) = \frac{K_{amp} K_{l.p.} U_0 G\varepsilon_0 \cos(\omega t)}{8} = \\ = \left[\frac{K_{amp} K_{l.p.} U_0 G\varepsilon_0}{8}\right]_{\omega=0}. \quad (5)$$

Following digitization, the signal is smoothed using the simple moving average algorithm. The window size is set within 1–250 samples, and the sample frequency is 250 s^{-1}.

STRAIN GAUGE AMPLIFIER NOISE ANALYSIS

In the analysis of the electrical noise in the strain gauge circuit, only the input noise is considered, since the preamplifier has a high gain (about 1000) and the influence of the noise in the subsequent stages is negligible. The possible sources of this noise are considered.

Thermal noise. Thermal noise (Nyquist noise) is caused by thermal oscillations of charge carriers in conductors, and it is generated constantly, regardless of the current flowing. The spectrum of thermal noise is broadband and uniform, and the power spectral density of a resistor with resistance R is given by the following expression [18]:

$$S_n = 4kTR, \quad (6)$$

where S_n is the spectral voltage density of the thermal noise $\left(V/\sqrt{Hz}\right)$, k = 1.38 · 10^{-23} J/K is

the Boltzmann constant, and T is the absolute temperature. The thermal noise is characteristic of all resistors and is marked as the source of S_n in the diagram (Fig. 7).

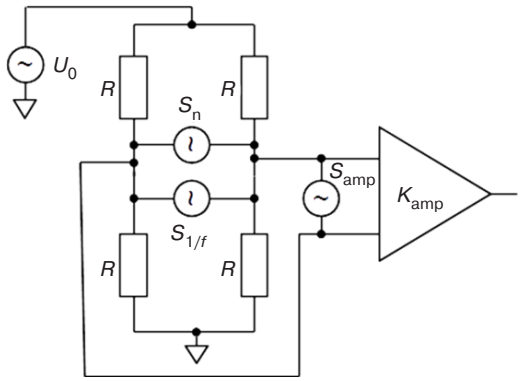

Fig. 7. Main sources of noise in the input circuits. S_{amp} is the amplifier noise

Flicker noise (1/*f*). Flicker noise is characterized by a specific frequency dependence of the spectral density, generally described by the following equation [19]:

$$S_{1/f} = \sqrt{\frac{CR^{\beta}I^{\beta}}{f^{\gamma}}}, \tag{7}$$

where $S_{1/f}$ is the spectral density of the flicker noise voltage $\left(\mathrm{V}/\sqrt{\mathrm{Hz}}\right)$, while C, β and γ are coefficients, I is the intensity of the current flowing, and f is the frequency. For metallic films at relatively low values of current density, β = 2 and γ = 1 can be accepted. The flicker noise of the conductor is assumed to be equivalent to the change in its resistance due to fluctuations in the mobility of the charge carriers during scattering on the lattice or fluctuations in the equilibrium temperature [20]. The flicker noise is denoted by the source $S_{1/f}$ in Fig. 7.

Amplifier noise. Amplifier noise is the combined noise of all sources in an instrument amplifier, represented as an equivalent noise voltage source at the amplifier input (S_{amp} in Fig. 7). Since the current noise density for this chip is approximately $1.1\,\mathrm{pA}/\sqrt{\mathrm{Hz}}$, it can be neglected given the low impedance of the input circuits.

The sources of electrical noise in the circuit in Fig. 7 can therefore be divided into 2 types: additive and multiplicative. Additive noise is voltage and current noise; as such, it does not modulate the pump signal and its spectrum does not change. Multiplicative noise, which comprises fluctuations in the resistances of the bridge resistors, causes a change in the balance of the bridge; as a result of amplitude modulation (AM), its spectral density function is transformed in the same way as a useful signal. Let S_{in} be the spectral density of the noise voltage at the amplifier input at a constant bridge supply voltage; when the bridge is supplied with an alternating voltage of frequency ω, it is transformed into modulated $S_{in.mod.}$:

$$\begin{gathered} S_{in}^2 = S_n^2(\omega) + S_{amp}^2(\omega) + \\ + S_{1/f}^2(\omega) \overset{AM}{\rightarrow} S_{in.mod.}^2(\omega) = \\ = S_n^2(\omega) + S_{amp}^2(\omega) + \frac{1}{4}S_{1/f}^2(\omega_0 - \omega) + \\ + \frac{1}{4}S_{1/f}^2(\omega_0 + \omega). \end{gathered} \tag{8}$$

The fact that for a balanced bridge the output noise is equivalent to the noise of one of the resistors is used here. It can be shown that the spectral density of the noise at the demodulator output S_d is described by the following expression:

$$\begin{gathered} S_d^2(\omega) = K_{amp}^2 \times \\ \times \left(\frac{1}{2}S_n^2(\omega + \omega_0) + \frac{1}{2}S_{amp}^2(\omega + \omega_0) + \frac{1}{4}S_{1/f}^2(\omega) \right). \end{gathered} \tag{9}$$

The spectral density $S_{in.conv.}$ of the noise at the ADC input is as follows:

$$\begin{gathered} S_{in.conv.}^2(\omega) = K_{amp}^2 K_{l.p.}^2 \times \\ \times \left(\frac{1}{2}S_n^2(\omega + \omega_0) + \frac{1}{2}S_{amp}^2(\omega + \omega_0) + \frac{1}{4}S_{1/f}^2(\omega) \right). \end{gathered} \tag{10}$$

The resolution of the strain gauge can be estimated by the total noise level. The value of the noise voltage u_Σ referred to the input (RTI) is obtained by integrating equation (10) and dividing by the gain, as follows:

$$u_\Sigma = \frac{\int_{\omega_l}^{\omega_h} S_{in.conv.}^2(\omega)d\omega}{K_{amp}} = \sqrt{\int_{\omega_l}^{\omega_h} \left(K_{l.p.}^2 \frac{1}{4}S_{1/f}^2(\omega) + K_{l.p.}^2 \frac{1}{2}S_n^2(\omega + \omega_0) + K_{l.p.}^2 \frac{1}{2}S_{amp}^2(\omega + \omega_0) \right) d\omega}. \tag{11}$$

The flicker-noise voltage spectral density $S_{1/f}$ of the 1-XY33-6 standard constantan strain gauges measured in [21] is used in the calculations. Substituting the data into expression (11) and taking into account (6) and (7), the level of the mean square noise voltage referred to the input is $u_\Sigma = 6.7 \cdot 10^{-9}$ V. Knowing the input noise level and taking into account expression (1), the mean square value of the apparent elongation can be expressed as follows:

$$\sigma_\varepsilon = \frac{4u_\Sigma}{u_b G} = \frac{4 \cdot 1.1 \cdot 10^{-8}}{1.5 \cdot 2} = \\ = 1.46 \cdot 10^{-8} = 0.015 \cdot 10^{-6}. \quad (12)$$

The following equation can be used to estimate the noise amplitude value (noise trace width) $\Delta\varepsilon_{pp}$ (peak-to-peak):

$$\Delta\varepsilon_{pp} \approx 6\sigma_\varepsilon = 0.888 \cdot 10^{-6}. \quad (13)$$

By the described means, the limits of the electrical noise on the resolution of the strain gauge are determined. According to calculations, the main contribution to the electrical noise level is made by the flicker noise of the measuring bridge resistor. However, in addition to the electrical noise, there are a number of other factors that affect the elongation measurement result.

Selecting the modulation frequency. From the above analysis, it is clear that the modulation frequency of the strain bridge should be selected to provide sufficient detuning from the low frequency portion of the noise spectrum of the instrument amplifier. On the other hand, increasing the modulation frequency will increase the influence of parasitic reactive elements. Detuning from the industrial frequency (50 Hz) and its harmonics is also required. Taking these factors into account, a frequency of 410 Hz is selected.

Temperature fluctuations and drift. The temperature of the bridge elements can only be regarded as approximately uniform and constant. In reality, there are temperature fluctuations and drifts due to the processes of power dissipation generated by the strain gauges and the instrument amplifier, as well as the instability of the laboratory temperature.

A typical value for the temperature resistance coefficient (TRC) of a constantan strain gauge is TRC = $10 \cdot 10^{-6}$ 1/K. The temperature change causing the false response to the noise trace width is estimated as follows:

$$\Delta T = \frac{\Delta\varepsilon_{pp}}{TRC} = 0.009 \text{ K}. \quad (14)$$

It can be seen that the strain gauge circuit is extremely sensitive to nonuniform temperature changes. However, equation (14) does not take into account the effect of the difference between the thermal expansion coefficients (TEC) of the sample plate and the gauge [15] $\Delta TEC = TEC_{sam.pl.} - TEC_{gauge}$, which can increase the thermal sensitivity several times:

$$\Delta T = \frac{\Delta\varepsilon_{pp}}{TRC \pm \Delta TEC \cdot G}. \quad (15)$$

In standard strain gauge applications, the temperature compensation technique is often used, in which the TRC of the strain gauges is matched to the TEC of the material, so that the sum in the denominator of expression (15) tends to zero. Unfortunately, in the case of a universal strain gauge, this method is practically inapplicable due to the sample material may be different and TEC is generally unknown. In addition, the situation is complicated by the uncertainty in the value of the thermal conductivity and thermal mass of the sample, which affects the process of heat dissipation generated by the strain gauge. The following methods were used in the design of the measurement cell to overcome the parasitic influence of thermal processes. Firstly, the cell is designed to be closed to eliminate the influence of convective air currents. After mounting the sample and balancing the bridge, a period of time is required for the temperature inside the cell to equalize. Secondly, there is active precision temperature stabilization of the amplifier board using a Peltier module. The design of the cell also allows for the balanced configuration of the active arm strain gauges of the bridge, where both resistors are bonded to the sample, thus compensating to some extent for the temperature sensitivity.

MEASUREMENT RESULTS

In order to evaluate the strain resolution of the setup, the time dependence of the strain gauge output signal in the absence of a magnetic field, $H = 0$, is recorded. The sample contains 1000 points and the recording time is 10 min. The resulting noise trace is shown in Fig. 8. The value of the standard deviation in the plot is $\sigma_\varepsilon \approx 0.016 \cdot 10^{-6}$, which corresponds to the amplitude value of the noise, $\Delta\varepsilon_{pp} = 0.096 \cdot 10^{-6}$. This result is in good agreement with the calculation according to (13).

To demonstrate the advantages of the created setup, magnetostriction curves of a magnesium ferrite sample $MgFe_2O_4$ are measured on an alternating

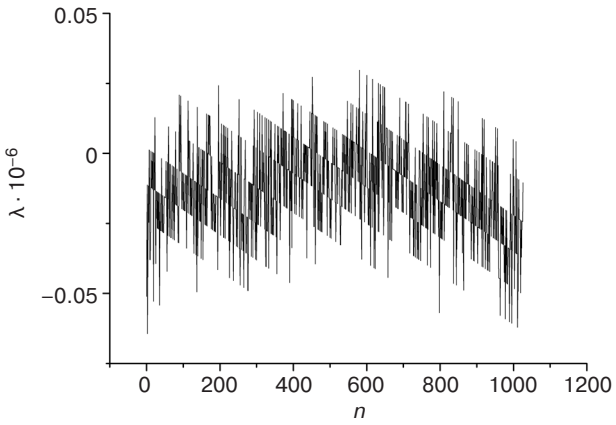

Fig. 8. Noise trace of the strain gauge setup (here, *n* is the sample number)

excitation strain gauge and on a DC strain gauge [18]. The sample is remagnetized by a limit cycle with a magnetic field step of 0.3 Oe. The difference in the noise level of the two setups is as depicted in Fig. 9. Curve *1* is much cleaner and shows the hysteresis during the remagnetization, while curve *2* only gives a qualitative view of the field dependence of the sample magnetostriction.

In order to calculate the field characteristics of ME effects, it is important to know the dependencies of the piezomagnetic coefficient $q = d\lambda/dH$ on the magnetic field. The dependencies $q(H)$ as calculated by numerical differentiation of the $\lambda(H)$ curves (Fig. 9) are shown in Fig. 10. Curve *1* is obtained using data from a strain gauge with alternating excitation, while curve *2* is obtained using data from a conventional DC strain gauge. From the curves, it can be seen that the use of an alternating excitation of the Wheatstone bridge for magnetostriction measurements allows for a much more accurate prediction of the shape of the field dependence of the linear ME effect.

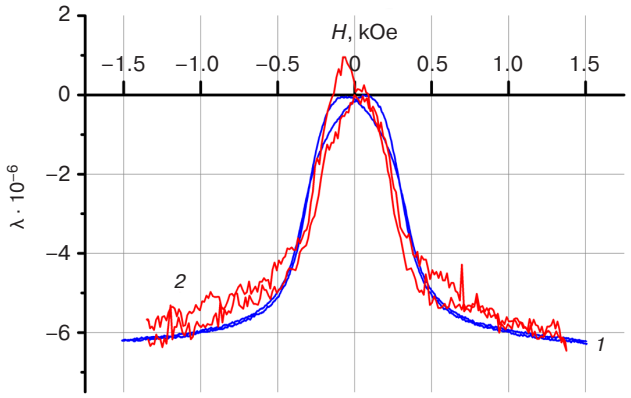

Fig. 9. Dependence of the magnetostriction λ of the $MgFe_2O_4$ plate on the magnetic field strength *H* measured by strain gauge with alternating current (AC) excitation (*1*) and strain gauge with direct current (DC) (*2*)

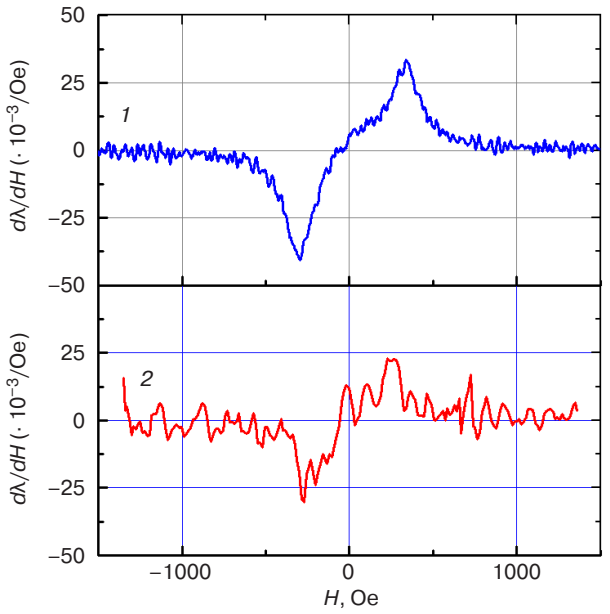

Fig. 10. Calculated dependence of the piezomagnetic coefficient *q* on the magnetic field strength *H* for the $MgFe_2O_4$ sample according to the strain gauge data: (*1*) AC, (*2*) DC

Due to the presence of a controlled bipolar high voltage source (HVS in Fig. 2), the described setup also allows the measurement of the PE effect and the investigation of electro- and magneto-acoustic interactions in composite structures. A constant voltage *U* of up to 500 V is applied to the electrodes of the PE sample to measure the deformation of the sample. The typically measured dependence of the elongation of the 5 × 10 × 0.2 mm thick polarized PZT-5 plate (Research Institute "Elpa," Russia) on the electrical voltage applied to the electrodes on its surface is shown in Fig. 11. The value of the piezoelectric module d_{31} calculated from the data in Fig. 11 at the point of zero displacement is approximately 130 pC/N, which is close to the manufacturer's specification (d_{31} = 155 pC/N).

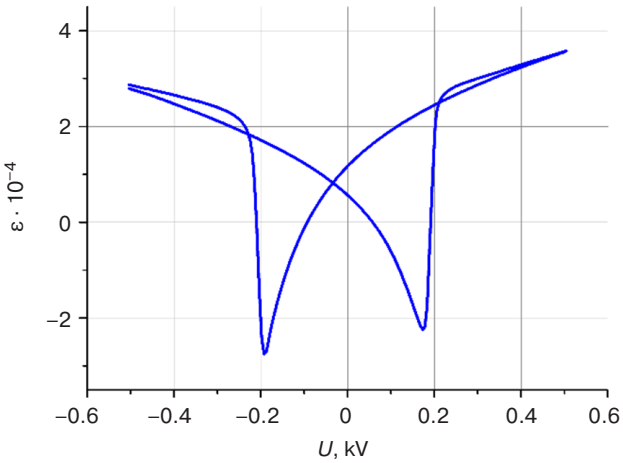

Fig. 11. Measured dependence of the PE deformation ε of the PZT-5 plate on the electrical voltage *U*

The table shows the main characteristics of the created setup (with AC excitation) in comparison to a strain gauge on a DC bridge [18]. With respect to the value of the noise referred to the input, it can be seen that the AC setup significantly outperforms the DC setup, as well as the standard strain gauge amplifier DPM911B[1] (Kyowa Electronic Instruments Co., Japan) used in [6] (RTI = 2).

Table. The setup main properties

Parameter	AC	DC [16]
Measured elongation range, μm/m	0–2000	0–2000
Noise referred to the input, μm/m	0.096	2
Maximum sample dimensions, mm × mm	20 × 10	20 × 10
Maximum magnetic field, G	5000	1500

CONCLUSIONS

The setup is developed for measuring the dependence of the magnetostrictive elongation of plate-shaped samples on the magnetic field and that of the electrostrictive/piezoelectric elongation on the electric field. It is shown that the AC excitation of the Wheatstone bridge, the use of synchronous detection, and the thermostabilization of the sample and the components of the measuring circuit allow the noise level to be reduced by almost an order of magnitude in comparison with conventional devices using DC excited Wheatstone bridge. The strain resolution of the setup is ~10^{-7}. It is determined that the main source of noise in the measurement circuit is the $1/f$ noise of the strain gauges, which, due to its nature, is indistinguishable from the useful signal in terms of signal processing methods. The measured noise level is in agreement with the calculated noise level based on published noise characteristics of film strain gauges. A further improvement of the resolution of the measurement setup can be achieved by improving the ratio between the strain sensitivity coefficient and the flicker noise level of the strain gauges.

ACKNOWLEDGMENTS

The study is supported by the Ministry of Science and Higher Education of the Russian Federation within a State Assignment for Universities (project No. FSFZ-2023-0005).

The calculation data can be provided upon request.

REFERENCES

1. Chu Z., Pourhosseini Asl M., Dong S. Review of multi-layered magnetoelectric composite materials and devices applications. *J. Phys. D: App. Phys.* 2018;51(24):243001. https://doi.org/10.1088/1361-6463/aac29b
2. Serov V.N., Fetisov L.Y., Fetisov Y.K., Shestakov E.I. High-sensitivity magnetometer based on a magnetoelectric sensor. *Rossiiskii tekhnologicheskii zhurnal.* 2016;4(5):24–37 (in Russ.). https://doi.org/10.32362/2500-316X-2016-4-5-24-37
3. Fedulov F.A., Saveliev D.V., Chashin D.V., Shishkin V.I., Fetisov Yu.K. Magnetoelectric effects in stripe- and periodic heterostructures based on nickel–lead zirconate titanate bilayers. *Russian Technological Journal*. 2022;10(3):64–73. https://doi.org/10.32362/2500-316X-2022-10-3-64-73
4. Kuczynski K., Bienkowski A., Szewczyk R. New Measuring System for Testing of the Magnetostrictive Properties of the Soft Magnetic Materials. In: *10th IMIKO TC4 Int. Workshop on ADC Modeling and testing* – IWADC. 2005. P. 434–439. Available from URL: https://www.imeko.info/publications/tc4-2005/IMEKO-TC4-2005-078.pdf
5. Linhares C.C., Santo J.E., Teixeira R.R., Coutinho C.P., Tavares S.M.O., Pinto M., Costa J.S., Mendes H., Monteiro C.S., Rodrigues A.V., Frazao O. Magnetostriction Assessment with strain gauges and fiber bragg gratings. *EAI Endorsed Trans. on Energy Web*. 2020;7(25):e4. https://doi.org/10.4108/eai.13-7-2018.161420
6. Wang Z., Fan Z., Li X., Xu K., Yu R. Measurement of magnetic and magnetostrictive characteristics of transformer core based on triaxial strain gauge and B-H vector sensor. *Sensors.* 2023;23(13):5926. http://doi.org/10.3390/s23135926
7. Pszcaola J., Cetnar T. Measurements of huge magnetostriction of the heavy rare earth – iron intermetallics. *Physics for Economy*. 2021;4:65–74.
8. Wang W., Liu H., Huang R., Zhao Y., Huang C., Guo S., Shan Y., Li L. Thermal expansion and magnetostriction measurements using the Strain Gauge Method. *Front. Chem.* 2018;6:72. https://doi.org/10.3389/fchem.2018.00072
9. Iwakami O., Kawata N., Takeshita M., Yao Y., Abe S., Matsumoto K. Thermal expansion and magnetostriction measurements using a Quantum Design Physical Property Measurement System. *J. Phys.: Conf. Ser*. 2014;568(3):032002. https://doi.org/10.1088/1742-6596/568/3/032002

[1] DPM-911B strain guage amplifer datasheet. https://product.kyowa-ei.com/en/products/amplifiers/type-s_dpm-900_series?tab=specification. Accessed May 19, 2025.

10. Kundys B., Bukhantsev Y., Vasiliev S., Kundys D., Berkowski M., Dyakonov V.P. Three terminal capacitance technique for magnetostriction and thermal expansion measurements. *Rev. Sci. Instrum.* 2004;75(6):2192–2196. https://doi.org/10.1063/1.1753088
11. Miyake A., Mitamura H., Kawachi S., Kimura K., Kimura T., Kihara T., Tachibana M., Tokunaga M. Capacitive detection of magnetostriction, dielectric constant, and magneto-caloric effects in pulsed magnetic fields. *Rev. Sci. Instrum*. 2020;91:105103. https://doi.org/10.1063/5.0010753
12. Tam A.C., Schroeder H. A new high-precision optical technique to measure magnetostriction of a thin magnetic film deposited on a substrate. *IEEE Trans. Magnetic*. 1989;25(3):2629–2638. https://doi.org/10.1109/20.24502
13. Samata H., Nagata Y., Uchida T., Abe S. New optical technique for bulk magnetostriction measurement. *J. Magn. Magn. Mater*. 2000;212(3):355–360. https://doi.org/10.1016/S0304-8853(99)00832-X
14. Hrabovska K., Zivotsky O., Rojicek J., Fusek M., Mares V., Jirakova Y. Surface magnetostriction of FeCoB amorphous ribbons analyzed using magneto-optical Kerr microscopy. *Materials*. 2020;13(2):257. https://doi.org/10.3390/ma13020257
15. Poore M., Kesterson K. Measuring the thermal expansion of solids with strain gauges. *J. Test. Eval*. 1978;6(2):98–102. https://doi.org/10.1520/JTE10926J
16. Khan M.A., Dumstorff G., Winkilmann C., Lang W. Investigation on noise level in AC- and DC-bridge circuits for sensor measurement systems. In: *18th GMA / ITG Conf. Sensors and Meas. Systems*. 2016. P. 601–605. http://doi.org/10.5162/sensoren2016/P4.4
17. Chashin D.V., Burdin D.A., Fetisov L.Y., Economov N.A., Fetisov Y.K. Precise measurement of magnetostriction of ferromagnetic plates. *J. Sib. Fed. Univ. Math. Phys*. 2018;11(1):30–34. https://doi.org/10.17516/1997-1397-2018-11-1-30-34
18. Nyquist H. Thermal Agitation of Electric Charge in Conductors. *Phys. Rev.* 1928;32:110–113. https://doi.org/10.1103/PhysRev.32.110
19. Hooge F.N. 1/f noise is no surface effect. *Phys. Lett. A.* 1969;29(3):139–140. https://doi.org/10.1016/0375-9601(69)90076-0
20. Voss R.F., Clarke J. Flicker (1/f) noise: equilibrium temperature and resistance fluctuations. *Phys. Rev. B*. 1976;13(2):556–573. https://doi.org/10.1103/PhysRevB.13.556
21. Walter D., Bulau A., Zimmermann A. Review on excess noise measurements of resistors. *Sensors*. 2023;23(3):1107. https://doi.org/10.3390/s23031107

About the Author

Dmitry A. Burdin, Cand. Sci. (Phys.-Math.), Senior Researcher, Scientific and Educational Center "Magnetoelectric Materials and Devices," MIREA – Russian Technological University (78, Vernadskogo pr., Moscow, 119454 Russia). E-mail: phantastic@mail.ru. ResearcherID N-9597-2016, RSCI SPIN-code 8152-3011, https://orcid.org/0000-0002-2648-0511

Об авторе

Бурдин Дмитрий Алексеевич, к.ф.-м.н., старший научный сотрудник, НОЦ «Магнитоэлектрические материалы и устройства», ФГБОУ ВО «МИРЭА – Российский технологический университет» (119454, Россия, Москва, пр-т Вернадского, д. 78). E-mail: phantastic@mail.ru. ResearcherID N-9597-2016, SPIN-код РИНЦ 8152-3011, https://orcid.org/0000-0002-2648-0511

Translated from Russian into English by K. Nazarov
Edited for English language and spelling by Thomas A. Beavitt

Micro- and nanoelectronics. Condensed matter physics

Микро- и наноэлектроника. Физика конденсированного состояния

UDC 544.225
https://doi.org/10.32362/2500-316X-2025-13-4-47-54
EDN STUTJW

RESEARCH ARTICLE

Ab initio calculations of the electronic structure of CeI_3 monolayer

Elizaveta T. Mirzoeva,
Andrey V. Kudryavtsev @

MIREA – Russian Technological University, Moscow, 119454 Russia
@ *Corresponding author, e-mail: kudryavcev_a@mirea.ru*

• **Submitted:** 15.01.2025 • **Revised:** 14.02.2025 • **Accepted:** 15.05.2025

Abstract

Objectives. In comparison with three-dimensional structures, two-dimensional (2D) magnetic materials are promising for use in spintronics and magnetic storage devices due to their exceptional characteristics and qualitatively different physical properties. Theoretical studies into 2D magnetic structures pave the way for the development of new compounds based on experimental data. In this work, we carry out a theoretical calculation of the electronic structure of a CeI_3 2D-magnetic material, taking into account the Hubbard repulsion at the site, the partial density of electronic states (DOS), and the distribution of spin and charge densities.

Methods. Calculations of the electronic structure of the CeI_3 monolayer were performed using density functional theory (DFT) and the Hubbard U scheme in the VASP software environment. The Dudarev method was used to account for the Hubbard correction.

Results. The calculated densities of the electronic states and the bandgap values for the ferro- and antiferromagnetic configurations of the material were found to be 1.98 and 2.08 eV, respectively. To assess the influence of correlation effects, the DOS was calculated both with and without the Hubbard correction. It was determined that the system in the ground magnetic state exhibits an antiferromagnetic ordering of the spin subsystem. The difference in the total energies of the antiferro- and ferromagnetic configurations was 2.8 meV per formula unit.

Conclusions. The calculations based on the Hubbard correction clearly demonstrated the presence of a bandgap, which is typical of semiconductor materials. The obtained bandgaps for the ferromagnetic and antiferromagnetic configurations of the system belong to the visible light range, which offers the opportunity of using 2D CeI_3 as a luminescent material in devices with a magnetically controlled emission. To assess the influence of correlation effects, the DOS was calculated both with and without the Hubbard correction. The obtained results agree with those obtained in experimental studies of cerium compounds. The consideration of correlation effects and spin polarization in the presented calculations forms the basis for further research into the magnetic properties of the CeI_3 monolayer for technological applications in the field of 2D magnetism.

Keywords: two-dimensional magnetism, 2D magnetism, density functional theory, DFT, Hubbard correction, rare-earth metals, density of electronic states, luminescence

For citation: Mirzoeva E.T., Kudryavtsev A.V. *Ab initio* calculations of the electronic structure of CeI_3 monolayer. *Russian Technological Journal.* 2025;13(4):47–54. https://doi.org/10.32362/2500-316X-2025-13-4-47-54, https://www.elibrary.ru/STUTJW

Financial disclosure: The authors have no financial or proprietary interest in any material or method mentioned.

The authors declare no conflicts of interest.

НАУЧНАЯ СТАТЬЯ

Первопринципный расчет электронной структуры монослоя CeI_3

Е.Т. Мирзоева,
А.В. Кудрявцев @

МИРЭА – Российский технологический университет, Москва, 119454 Россия
@ *Автор для переписки, e-mail: kudryavcev_a@mirea.ru*

• **Поступила:** 15.01.2025 • **Доработана:** 14.02.2025 • **Принята к опубликованию:** 15.05.2025

Резюме

Цели. Двумерные магнетики, благодаря своим уникальным характеристикам и качественно новым физическим свойствам по сравнению с объемными структурами, обладают значительным потенциалом для применения в спинтронике и магнитных запоминающих устройствах. Теоретические исследования двумерных магнитных структур позволяют сузить область поиска новых соединений и дополнить экспериментальные данные. Целью данной работы является теоретический расчет электронной структуры двумерного магнетика CeI_3, включающий учет хаббардовского отталкивания на узле, расчет парциальной плотности электронных состояний и расчет распределения спиновых и зарядовых плотностей.

Методы. Расчеты электронной структуры монослоя CeI_3 выполнены с использованием программного пакета *VASP* в рамках теории функционала плотности, а также в рамках теории функционала плотности с учетом поправки Хаббарда. Для учета поправки Хаббарда использовался метод Дударева.

Результаты. Рассчитаны энергетические плотности электронных состояний и величины запрещенных зон для ферро- и антиферромагнитной конфигураций материала, равные соответственно 1.98 и 2.08 эВ. Для оценки влияния корреляционных эффектов проведен расчет плотностей состояний как с учетом поправки Хаббарда, так и без него. Определено, что в основном магнитном состоянии система проявляет антиферромагнитное упорядочение спиновой подсистемы. Разница полных энергий с ферромагнитной конфигурацией составила 2.8 мэВ на формульную единицу.

Выводы. Учет поправки Хаббарда наглядно продемонстрировал наличие характерной для полупроводниковых материалов запрещенной зоны. Полученные ширины запрещенной зоны для ферромагнитной и антиферромагнитной конфигураций системы относятся к диапазону видимого света, что открывает возможности использования двумерного CeI_3 в качестве люминесцентного материала в устройствах с магнитным управлением излучения. Представленные результаты согласуются с обобщенными результатами экспериментальных исследований соединений на основе церия. Учет корреляционных эффектов и поляризации по спину в представленных расчетах открывает горизонт для дальнейшего изучения магнитных свойств монослоя CeI_3 для технологических применений в области двумерного магнетизма.

Ключевые слова: двумерный магнетизм, теория функционала плотности, поправка Хаббарда, редкоземельные металлы, плотность электронных состояний, люминесценция

Для цитирования: Мирзоева Е.Т., Кудрявцев А.В. Первопринципный расчет электронной структуры монослоя CeI_3. *Russian Technological Journal*. 2025;13(4):47–54. https://doi.org/10.32362/2500-316X-2025-13-4-47-54, https://www.elibrary.ru/STUTJW

Прозрачность финансовой деятельности: Авторы не имеют финансовой заинтересованности в представленных материалах или методах.

Авторы заявляют об отсутствии конфликта интересов.

INTRODUCTION

Two-dimensional (2D) magnets represent a new class of low-dimensional materials. These materials exhibit a number of unique properties that are promising from the practical point of view. Thus, the magnetic anisotropy of such materials makes it possible to control the properties of a system by changing the direction of an external magnetic field [1]. Magnetic anisotropy is of great importance for 2D ferromagnetism in the sense of avoiding a random redistribution of spin states due to thermal fluctuations. Other important properties of systems based on 2D magnets include the magnetic proximity effect [2], the formation of skyrmions [3], the quantum anomalous Hall effect [4], giant magnetoresistance [5], etc.

In this regard, 2D magnets are promising materials for use in spintronics and magnetic memory devices [6–8]. Experimental studies have confirmed the presence of a long-range magnetic ordering in these materials [9, 10], although the Mermin–Wagner theorem states the impossibility of magnetic ordering in two-dimensional systems at temperatures above zero [11].

At present, the search for materials and compounds with a set of practically important properties is a pressing task. Bulk compounds can be studied both experimentally and theoretically; however, their 2D analogs may exhibit qualitatively different physical properties, which makes their experimental study challenging. In this regard, first-principles (*ab initio*) calculations of material structures are of particular interest. Another powerful theoretical tool comprises calculations using density functional theory (DFT).

In this paper, we carry out an *ab initio* calculation of the physical properties of 2D CeI_3 with orthorhombic symmetry. Along with such 2D materials as transition metal dichalcogenides that have been sufficiently studied [12], new 2D compounds promising in terms of their luminescent properties are increasingly attracting attention. These include 2D materials based on rare-earth elements [13, 14]. The 5*d*–4*f* transitions in the Ce atom have a short lifetime of about 17 ns, which ensures a high luminescence efficiency [15]. The magnetic properties of 2D magnets are due to partially filled *d* and *f* electron shells. Thus, information on the magnetic properties of 2D CeI_3 may pave the way not only for its potential use in spintronics, but also for the creation of optical devices with the magnetic control of emission.

CALCULATION PROCEDURE

The calculations were performed using Vienna *Ab initio* Simulation Package (*VASP*), a commercially available *ab initio* simulation package. *VASP* is a widely used package designed for calculations using DFT [16] to determine the properties of materials in the ground state (total energy, band structure, density of electronic states (DOS), phonon spectra, etc.) by solving the Kohn–Sham equations.

In the presented calculations, the exchange–correlation energy of electrons was approximated by the generalized gradient approximation using the Perdew–Burke–Ernzerhof functional [17]. Electron–ion interactions were described by the project augmented wave method [18]. To define the 2D structure under the three-dimensional (3D) boundary conditions, a 25 Å pseudovacuum space was added to eliminate the interaction between layers during unit cell translation. The plane wave basis cutoff energy was set to 320 eV. For integration over the Brillouin zone, a gamma-centered *k*-point grid of 16 × 16 × 1 was used for structure relaxation; 20 × 20 × 1, for self-consistent calculation; and 26 × 26 × 1, for DOS calculation. The crystal structure was relaxed until the total forces acting on each atom were less than 0.001 eV/Å. The relaxation of the electronic degrees of freedom was discontinued when the energy difference between two calculation iterations was less than 10^{-6} eV. To account for the van der Waals forces, a semiclassical dispersion correction known as DFT-D3 with the Becke–Johnson damping function was used [19].

For rare-earth metals, account should be taken of the repulsion of localized (strongly correlated) electron shells *d* and *f*. To increase the accuracy of the sought parameters, the Hubbard repulsion (DFT+U) was taken into account. The DFT+U calculation implies the separation of localized *d* and *f* electrons, for which the Hubbard correction is considered, and delocalized *s* and *p* electrons. The Hubbard correction was taken into account using the Dudarev approach described in [20]:

$$E_{DFT+U} = E_{DFT} + \frac{U-J}{2} \times \times \sum_{\sigma} \left[\left(\sum_{m_1} n^{\sigma}_{m_1,m_2} \right) - \left(\sum_{m_1,m_2} n^{\sigma}_{m_1,m_2} n^{\sigma}_{m_2,m_1} \right) \right], \quad (1)$$

where m_1 and m_2 are magnetic quantum numbers (m_1, m_2 = −3, −2, …, 3 in the case of *f*-shell electrons); $n^{\sigma}_{m_1,m_2}$ is the matrix element of the density matrix with spin σ; U is the parameter characterizing the Coulomb repulsion at the site, which was taken to be 5.1 eV for the Ce 4*f* level; and J is the parameter characterizing the interstitial repulsion of *d* and *f* electrons [21, 22].

The first term of E_{DFT} is the energy of delocalized *s* and *p* electrons, which is conventionally calculated using DFT in the generalized gradient approximation. The second term takes into account the electron–electron interaction (Hubbard correction) for localized *d* and *f* electrons.

The crystal structure and the spin and charge densities were visualized using the *VESTA* software [23]. The data obtained by the DFT calculation were processed using the *VASPKIT* software [24].

RESULTS AND DISCUSSION

In this paper, we calculated the energy densities of electronic states and the bandgap values for ferromagnetic (FM) and antiferromagnetic (AFM) configurations of the material, along with determination of the configuration with the minimum total energy. The unit cell of the CeI_3 monolayer contains two cerium atoms and six iodine atoms. The crystal structure is an orthorhombic with unit cell parameters of 4.32 × 9.98 Å and a pseudovacuum space of 25 Å (Fig. 1). Cerium atoms are marked in yellow; iodine atoms are marked in violet. The model cell is outlined by a solid black line.

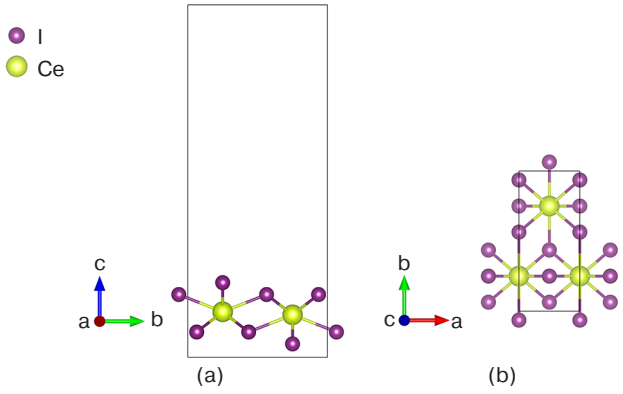

Fig. 1. CeI_3 monolayer: (a) side view; (b) top view

Figure 2 presents the dependencies of the partial densities and total DOS on energy for the FM configuration that were obtained using DFT without taking into account the Hubbard correction (DFT calculation).

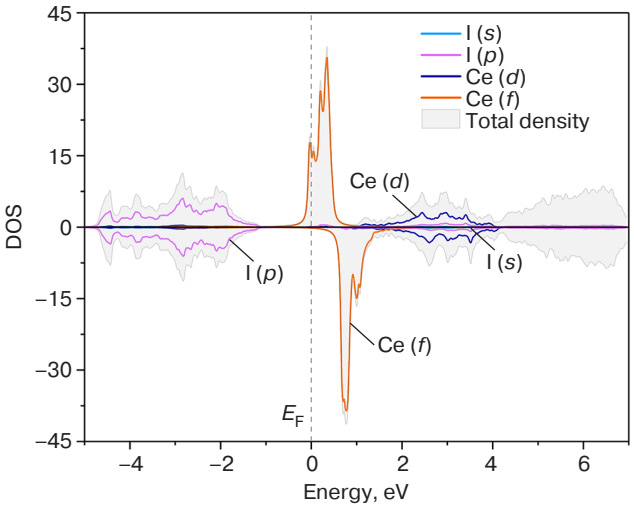

Fig. 2. DOS of the CeI_3 monolayer for the FM configuration (DFT calculation): total DOS (full pattern) and contributions of *s* states of iodine (blue), *p* states of iodine (purple), *d* states of cerium (deep blue), and *f* states of cerium (orange), E_F is the Fermi energy

The presented dependence of the DOS does not show a bandgap, which is characteristic of semiconductors, although 2D CeI_3 is presumably a semiconductor material. This discrepancy is due to incorrect consideration of the correlation effects for localized electrons of the outer shells of cerium using standard DFT. To solve this problem, Hubbard corrections were introduced by the Dudarev method. This method appears optimal for calculations.

It should be noted that the general structure of these dependencies is similar to that of the dependence of the DOS for a 3D CeI_3 crystal [25]. In that work, the valence band was formed by *p* states of iodine, the conduction band was formed by *d* states of cerium, and 4*f* states of cerium were located in the bandgap. However, the calculations [25] were carried out, as indicated above, for a 3D material, without taking correlation effects and spin polarization into account. These considerations impede further studies of magnetic properties, in contrast to the calculations presented in this article.

Figure 3 presents the dependencies of the densities of electronic states of the CeI_3 monolayer that were obtained using DFT and taking the Hubbard correction (DFT+U) into account. As expected, the material is a semiconductor with a bandgap of ~1.9 eV between the *p* shells of iodine and the *f* shells of cerium. The obtained bandgap value agrees with that obtained in experimental studies of compounds of rare-earth elements, including cerium [26, 27].

Cerium is the first element in which occupied states appear on the *f* shell. This is confirmed by the presence of a corresponding peak in the valence band region. The general form of the DOS is characteristic of a ferri- or ferromagnetic structure with two spin subsystems that do not compensate each other completely.

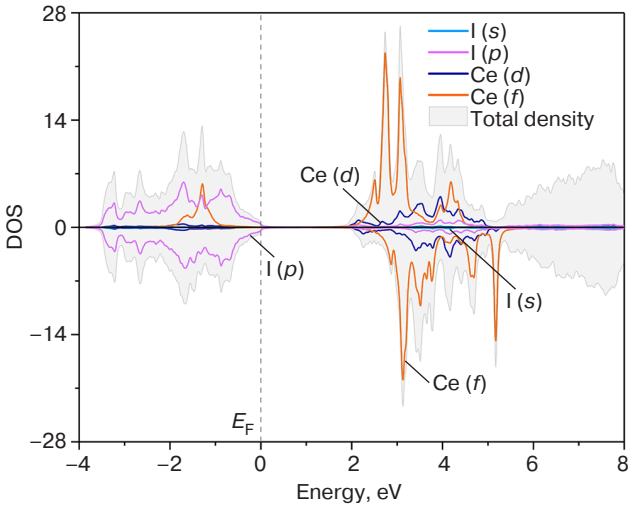

Fig. 3. DOS of the CeI_3 monolayer taking the Hubbard correction into account (DFT+U calculation): total DOS (full pattern) and contributions of *s* states of iodine (blue), *p* states of iodine (purple), *d* states of cerium (deep blue), and *f* states of cerium (orange)

To calculate the AFM configuration, a structural supercell of 2 × 2 unit cells was generated, which comprised 8 cerium atoms and 24 iodine atoms. In addition, the FM supercell was calculated for a comparative analysis and further determination of the type of magnetic ordering corresponding to the minimum total energy.

The DFT+U calculations gave the densities of electronic states (Fig. 4), the spin density distributions (Fig. 5) for the FM and AFM configurations, as well as the general form of the charge density distribution (Fig. 6).

The presented dependencies of the DOS indicate that the energy bandgap width is about 2.08 and 1.98 eV for the AFM and FM configurations, respectively. The obtained values of the bandgap width correspond to the visible light range.

To determine the ground magnetic state, the difference between the total energies of the AFM and FM configurations should be found:

$$\Delta E = E_{AFM} - E_{FM} = -2.8 \text{ meV}. \quad (2)$$

The negative value indicates that, energetically, AFM is the most favorable configuration for the structure under study due to its lower energy. Different values of the total energy are explained by different contributions of the Coulomb repulsion between parallel and antiparallel spins of the outer shells of the system.

The spin density distributions for both configurations (Fig. 5) have the form of a dumbbell concentrated around the cerium atom with a nonzero magnetic moment in accordance with the assumed

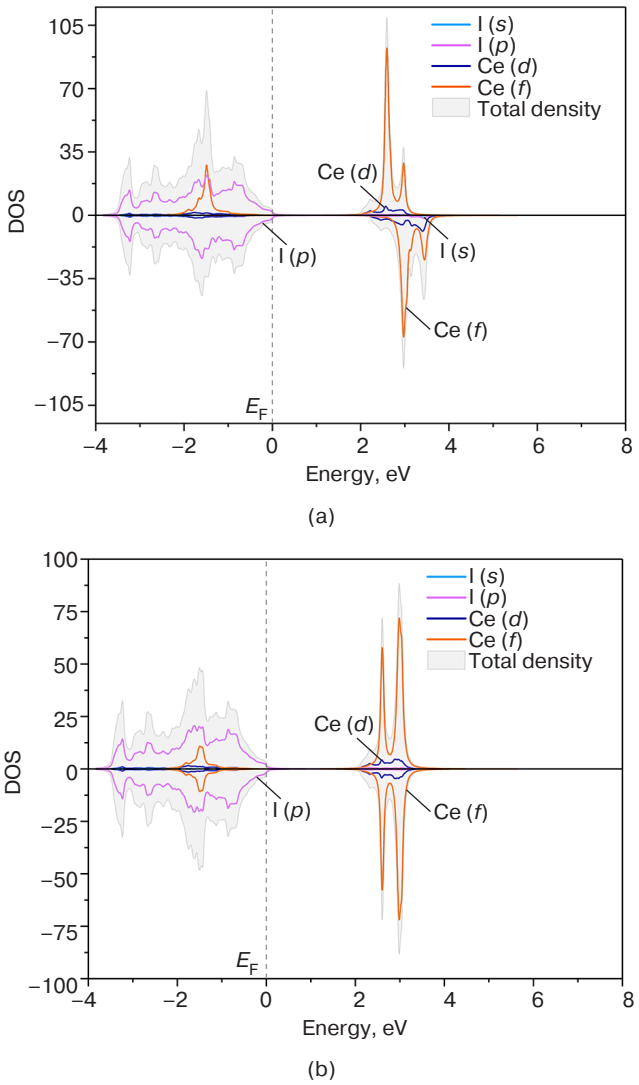

Fig. 4. DOS of the CeI_3 monolayer in the (a) FM and (b) AFM configurations: total DOS (full pattern) and contributions of *s* states of iodine (blue), *p* states of iodine (purple), *d* states of cerium (deep blue), and *f* states of cerium (orange)

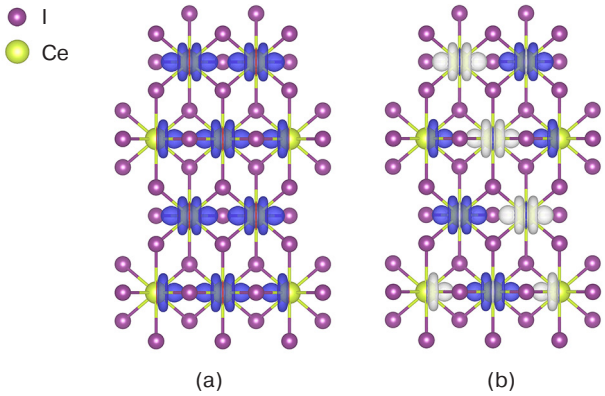

Fig. 5. Spin density distributions in the CeI_3 supercell for the (a) FM and (b) AFM configurations on isosurfaces of ±0.0009 e/Å^3 in the spin-up (blue) and spin-down (white) polarizations

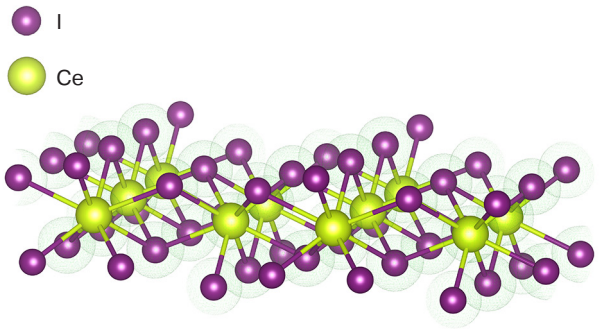

Fig. 6. Charge density distribution in the CeI_3 supercell on the 0.066 e/Å$_3$ isosurface. Isosurfaces are shown in light green

form of the *f* shell orbitals. The charge density distribution (Fig. 6) indicates the concentration of the negative charge around the iodine atoms, which is due to the greater electronegativity of the halogen atoms. Such a shift in the charge density confirms a large contribution of covalence to the metal–halogen chemical bonds. The formation of covalent bonds between Ce–I pairs creates the possibility of superexchange interaction between neighboring Ce atoms.

CONCLUSIONS

In this work, the *ab initio* calculation of the electronic structure of a new two-dimensional compound—CeI_3—was performed using density functional theory. The calculation of the densities of electronic states taking the Hubbard correction into account clearly demonstrated the presence of a bandgap, which is characteristic of semiconductor materials. The bandgap values for the FM and AFM configurations of the material were 1.98 and 2.08 eV, respectively. Such energy values belong to the visible light range, which offers the opportunity of using two-dimensional CeI_3 as a luminescent material in devices with the magnetic control of emission. According to the calculations, the AFM configuration has a lower total energy, i.e., being the ground magnetic state of the structure. The difference between the total energies of the FM and AFM configurations (2.8 meV) is due to different contributions of the Coulomb repulsion between the parallel and antiparallel spins of the outer shells of the system. The presence of covalent polar bonds, which is clearly demonstrated by the charge density distribution, creates the possibility of superexchange interaction between neighboring cerium atoms. The obtained results form a basis for further research and technological applications of the CeI_3 monolayer in the field of two-dimensional magnetism.

ACKNOWLEDGMENTS

The calculations were performed using the equipment of the Center for the Collective Use of Computing Resources of the National Research Center "Kurchatov Institute."

Authors' contributions

E.T. Mirzoeva—performing calculations, processing results, writing the manuscript.

A.V. Kudryavtsev—performing calculations, discussing the results, writing the manuscript.

REFERENCES

1. Tan H., Shan G., Zhang J. Prediction of novel two-dimensional room-temperature ferromagnetic rare-earth material – GdB_2N_2 with large perpendicular magnetic anisotropy. *Mater. Today Phys.* 2022;24:100700. https://doi.org/10.1016/j.mtphys.2022.100700
2. Vobornik I., Manju U., Fujii J., Borgatti F., Torelli P., Krizmancic D., Hor Y.S., Cava R.J., Panaccione G. Magnetic proximity effect as a pathway to spintronic applications of topological insulators. *Nano Lett*. 2011;11(10):4079–4082. https://doi.org/10.1021/nl201275q
3. Heinze S., Von Bergmann K., Menzel M., et al. Spontaneous atomic-scale magnetic skyrmion lattice in two dimensions. *Nature Phys.* 2011;7(9):713–718. https://doi.org/10.1038/nphys2045
4. Zhang J., Zhao B., Yao Y., Yang Z. Robust quantum anomalous Hall effect in graphene-based van der Waals heterostructures. *Phys. Rev. B*. 2015;92(16):165418. https://doi.org/10.1103/PhysRevB.92.165418
5. Song T., Cai X., Tu M.W.Y., Zhang X., Huang B., Wilson N.P., Seyler K.L., Zhu L., Taniguchi T., Watanabe K., McGuire M.A., Cobden D.H., Xiao D., Yao W., Xu X. Giant tunneling magnetoresistance in spin-filter van der Waals heterostructures. *Science*. 2018;360(6394):1214–1218. https://doi.org/10.1126/science.aar4851
6. Wang Z., Sapkota D., Taniguchi T., Watanabe K., Mandrus D., Morpurgo A.F. Tunneling spin valves based on Fe_3GeTe_2/hBN/Fe_3GeTe_2 van der Waals heterostructures. *Nano Lett.* 2018;18(7):4303–4308. https://doi.org/10.1021/acs.nanolett.8b01278
7. Ashton M., Gluhovic D., Sinnott S.B., Guo J., Stewart D.A., Hennig R.G. Two-dimensional intrinsic half metals with large spin gaps. *Nano Lett.* 2017;17(9):5251–5257. https://doi.org/10.1021/acs.nanolett.7b01367
8. Johansen Ø., Risinggård V., Sudbø A., Linder J., Brataas A. Current control of magnetism in two-dimensional Fe_3GeTe_2. *Phys. Rev. Lett.* 2019;122(21):217203. https://doi.org/10.1103/PhysRevLett.122.217203

9. Jiang X., Liu Q., Xing J., Liu N., Guo Y., Liu Z., Zhao J. Recent progress on 2D magnets: Fundamental mechanism, structural design and modification. *Appl. Phys. Rev*. 2021;8(3):031305. https://doi.org/10.1063/5.0039979
10. Tian S., Zhang J.-F., Li C., Ying T., Li S., Zhang X., Liu K., Lei H. Ferromagnetic van der Waals crystal VI_3. *Am. Chem. Soc*. 2019;141(13):5326–5333. https://doi.org/10.1021/jacs.8b13584
11. Mermin N.D., Wagner H. Absence of Ferromagnetism or Antiferromagnetism in One- or Two-Dimensional Isotropic Heisenberg Models. *Phys. Rev. Lett*. 1966;17(22):1133–1136. https://doi.org/10.1103/PhysRevLett.17.1133
12. Pimenov N.Yu., Lavrov S.D., Kudryavtsev A.V., Avdizhiyan A.Yu. Modeling of two-dimensional $MoxW_{1-x}S_{2y}Se_{2(1-y)}$ alloy band structure. *Russian Technological Journal*. 2022;10(3):56–63. https://doi.org/10.32362/2500-316X-2022-10-3-56-63
13. Guo Q., Wang L., Yang L., et al. Spectra stable deep-blue light-emitting diodes based on cryolite-like cerium(III) halides with nanosecond d-f emission. *Sci. Adv*. 2022;8(50):eabq2148. https://doi.org/10.1126/sciadv.abq2148
14. Wang C., Liu X., She C., Li Y. Luminescence of CeI_3 in organic solvents and its application in water detection. *Polyhedron*. 2021;196:115013. https://doi.org/10.1016/j.poly.2020.115013
15. Xie W., Hu F., Gong S., Peng L. Study the optical properties of Cs_3CeI_6: First-principles calculations. *AIP Advances.* 2024;14:015062. https://doi.org/10.1063/5.0187100
16. Kresse G., Furthmüller J. Efficiency of *ab initio* total energy calculations for metals and semiconductors using a plane-wave basis set. *Phys. Rev. B*. 1996;54(16):11169–11186. https://doi.org/10.1103/PhysRevB.54.11169
17. Constantin L.A., Perdew J.P., Pitarke J.M. Exchange–correlation hole of a generalized gradient approximation for solids and surfaces. *Phys. Rev. B*. 2009;79(7):075126. https://doi.org/10.1103/PhysRevB.79.075126
18. Kresse G., Joubert D. From ultrasoft pseudopotentials to the projector augmented-wave method, *Phys. Rev. B*. 1999;59(3): 1758–1775. https://doi.org/10.1103/PhysRevB.59.1758
19. Grimme S., Ehrlich S., Goerigk L. Effect of the damping function in dispersion corrected density functional theory. *J. Comput. Chem*. 2011;32(7):1456–1465. https://doi.org/10.1002/jcc.21759
20. Dudarev S.L., Botton G.A., Savrasov S.Y., Humphreys C.J., Sutton A.P. Electron-energy-loss spectra and the structural stability of nickel oxide: An LSDA+*U* study. *Phys. Rev. B*. 1998;57(3):1505–1509. https://doi.org/10.1103/PhysRevB.57.1505
21. Sheng K., Chen Q., Yuan H., Wang Z. Monolayer CeI_2: An intrinsic room-temperature ferrovalley semiconductor. *Phys. Rev. B*. 2022;105(7):075304. https://doi.org/10.1103/PhysRevB.105.075304
22. Larson P., Lambrecht W.R.L., Chantis A., van Schilfgaarde M. Electronic structure of rare-earth nitrides using the LSDA+*U* approach: Importance of allowing 4*f* orbitals to break the cubic crystal symmetry. *Phys. Rev. B*. 2007;75(4):045114. https://doi.org/10.1103/PhysRevB.75.045114
23. Momma K., Izumi F. *VESTA*: a three-dimensional visualization system for electronic and structural analysis. *J. Appl. Cryst.* 2008;41:653–658. https://doi.org/10.1107/S0021889808012016
24. Wang V., Xu N., Liu J., Tang G., Geng W. VASPKIT: A user-friendly interface facilitating high-throughput computing and analysis using VASP code. *Comput. Phys. Commun*. 2021;267:108033. https://doi.org/10.1016/j.cpc.2021.108033
25. Chornodolskyy Ya.M., Karnaushenko V.O., Vistovskyy V.V., Syrotyuk S.V., Gektin A.V., Voloshinovskii A.S. Energy band structure peculiarities and luminescent parameters of CeX_3 (X = Cl, Br, I) crystals. *J. Lumin*. 2021;237:118147. https://doi.org/10.1016/j.jlumin.2021.118147
26. Birowosuto M.D., Dorenbos P. Novel γ- and X-ray scintillator research: on the emission wavelength, light yield and time response of Ce^{3+} doped halide scintillators. *Phys. Status Solidi A-Appl. Mater. Sci.* 2009;206(1):9–20. https://doi.org/10.1002/pssa.200723669
27. Dorenbos P. Lanthanide 4f-electron binding energies and the nephelauxetic effect in wide band gap compounds. *J. Lumin*. 2013;136:122–129. https://doi.org/10.1016/j.jlumin.2012.11.030

About the Authors

Elizaveta T. Mirzoeva, Master Student, Institute for Advanced Technologies and Industrial Programming, MIREA – Russian Technological University (78, Vernadskogo pr., Moscow, 119454 Russia). E-mail: mirzoeva.elizaveta@gmail.ru. https://orcid.org/0009-0003-4874-7015

Andrey V. Kudryavtsev, Cand. Sci. (Phys.-Math.), Associate Professor, Researcher, Department of Nanoelectronics, Institute for Advanced Technologies and Industrial Programming, MIREA – Russian Technological University (78, Vernadskogo pr., Moscow, 119454 Russia). E-mail: kudryavcev_a@mirea.ru. Scopus Author ID 55219889700, ResearcherID O-1457-2016, https://orcid.org/0000-0002-2126-7404

Об авторах

Мирзоева Елизавета Теофиловна, магистрант, Институт перспективных технологий и индустриального программирования, ФГБОУ ВО «МИРЭА – Российский технологический университет» (119454, Россия, Москва, пр-т Вернадского, д. 78). E-mail: mirzoeva.elizaveta@gmail.ru. https://orcid.org/0009-0003-4874-7015

Кудрявцев Андрей Владимирович, к.ф.-м.н., доцент, научный сотрудник, кафедра наноэлектроники, Институт перспективных технологий и индустриального программирования, ФГБОУ ВО «МИРЭА – Российский технологический университет» (119454, Россия, Москва, пр-т Вернадского, д. 78). E-mail: kudryavcev_a@mirea.ru. Scopus Author ID 55219889700, ResearcherID O-1457-2016, https://orcid.org/0000-0002-2126-7404

Translated from Russian into English by V. Glyanchenko
Edited for English language and spelling by Thomas A. Beavitt

Analytical instrument engineering and technology

Аналитическое приборостроение и технологии

UDC 550.380.8; 621.317.412
https://doi.org/10.32362/2500-316X-2025-13-4-55-68
EDN PEJBLG

RESEARCH ARTICLE

Expanding the capabilities of new magnetometers of ponderomotive and magnetic-rheological types with hemispherical poles

Maria N. Polismakova [1], Daria A. Sandulyak [1, @], Alexey S. Kharin [1], Daria A. Golovchenko [1], Anna A. Sandulyak [1], Alexander V. Sandulyak [1], Haci M. Baskonus [2]

[1] *MIREA – Russian Technological University, Moscow, 119454 Russia*
[2] *Harran University, Sanliurfa, 63190 Turkey*
[@] *Corresponding author, e-mail: d.sandulyak@mail.ru*

• **Submitted:** 25.01.2025 • **Revised:** 07.03.2025 • **Accepted:** 16.05.2025

Abstract

Objectives. The work sets out to explain the expanded capabilities of new magnetometers by conducting appropriate studies. In order to determine the magnetic susceptibility of small-volume objects, ponderomotive and magnetic-rheological magnetometers with hemispherical pole pieces are used to create the magnetic field required for a limited working zone.

Methods. The research is carried out using an original method, which includes finding the coordinate characteristic of the induction of the field B through direct step-by-step measurements by the Hall sensor in the interpolar space along the line of action of the ponderomotive force to provide a basis for obtaining the coordinate characteristic of the gradient.

Results. In magnetometers using hemispherical poles of increased diameter D: 157 and 184 mm, mutually disconnected from one or another by the distance b, the desired key dependencies of magnetic induction B were experimentally obtained (with a step-by-step distance x from the center of symmetry of the interpolar space along the line of action of the ponderomotive force) to provide the dependence of the gradient grad$B = dB/dx$. The characteristic inflection of each of the curves B from x and corresponding individual extremum of the following curves dB/dx from x, in the vicinity of which the values of dB/dx are practically stable, meets the requirement of determining the dislocation of the executive (working) zone such that the inhomogeneity of the field is almost constant.

Conclusions. Coordinates of executive zone dislocation are obtained from established and generalized dependencies B from x and dB/dx from x. To calculate these coordinates, which depend on D and b but do not depend on the magnetizing force of the winding, the corresponding analytical (phenomenological) expressions of power and logarithmic form are obtained. The possibility of using these expressions to identify the executive zone of magnetometers without resorting to additional series of experiments is shown. The expediency of using hemispherical pole pieces of increased diameter is also demonstrated. On this basis, the length of the executive zone can be increased to conduct studies with samples of a wider range of sizes.

Keywords: ponderomotive principle, magnetometer, magnetic susceptibility of the sample, executive zone, coordinate characteristics of induction and gradient, power dependence, logarithmic dependence

For citation: Polismakova M.N., Sandulyak D.A., Kharin A.S., Golovchenko D.A., Sandulyak A.A., Sandulyak A.V., Baskonus H.M. Expanding the capabilities of new magnetometers of ponderomotive and magnetic-rheological types with hemispherical poles. *Russian Technological Journal.* 2025;13(4):55–68. https://doi.org/10.32362/2500-316X-2025-13-4-55-68, https://www.elibrary.ru/PEJBLG

Financial disclosure: The authors have no financial or proprietary interest in any material or method mentioned.

The authors declare no conflicts of interest.

НАУЧНАЯ СТАТЬЯ

Расширение возможностей новых магнитометров пондеромоторного и магнитно-реологического типов с полюсами-полусферами

М.Н. Полисмакова [1], Д.А. Сандуляк [1, @], А.С. Харин [1], Д.А. Головченко [1], А.А. Сандуляк [1], А.В. Сандуляк [1], H.M. Baskonus [2]

[1] *МИРЭА – Российский технологический университет, Москва, 119454 Россия*
[2] *Harran University, Sanliurfa, 63190 Turkey*
[@] *Автор для переписки, e-mail: d.sandulyak@mail.ru*

• **Поступила:** 25.01.2025 • **Доработана:** 07.03.2025 • **Принята к опубликованию:** 16.05.2025

Резюме

Цели. Для определения магнитной восприимчивости малообъемных объектов применяются магнитометры пондеромоторного и магнитно-реологического типов с полюсами-полусферами, позволяющими создавать требуемое для лимитированной рабочей зоны магнитное поле. Цель работы – проведением соответствующих исследований показать, что возможности новых созданных магнитометров могут быть расширены.

Методы. Исследование проводится согласно оригинальному методу, включающему получение координатной характеристики индукции поля B (посредством прямых пошаговых измерений датчиком Холла) в межполюсном пространстве по линии действия пондеромоторной силы с последующим нахождением координатной характеристики градиента.

Результаты. В магнитометрах с применением полюсов-полусфер повышенного диаметра D: 157 и 184 мм, взаимно разобщаемых на то или иное расстояние b, экспериментально получены ключевые зависимости магнитной индукции B при пошаговом удалении x от центра симметрии межполюсной области по линии действия пондеромоторной силы, а по ним – зависимости градиента grad$B = dB/dx$. Характерный перегиб каждой из кривых зависимостей B от x и индивидуальный экстремум последовавших из них кривых зависимостей dB/dx от x, в окрестности которого значения dB/dx практически одинаковы, отвечает требованию выбора дислокации исполнительной (рабочей) зоны, где неоднородность поля практически постоянна.

Выводы. По установленным и обобщенным зависимостям B от x и dB/dx от x найдены координаты дислокации исполнительной зоны. Для вычисления этих координат, зависящих от величин D и b и не зависящих от намагничивающей силы обмотки, получены аналитические (феноменологические) выражения степенного и логарифмического вида. Показана возможность использования этих выражений для идентификации исполнительной зоны магнитометров, не прибегая к проведению дополнительных серий экспериментов. Показана целесообразность применения полюсов-полусфер повышенного диаметра, что позволяет увеличить протяженность исполнительной зоны и проводить исследования с образцами более широкого спектра размеров.

Ключевые слова: пондеромоторный принцип, магнитометр, магнитная восприимчивость образца, исполнительная зона, координатные характеристики индукции и градиента, степенная связь, логарифмическая связь

Для цитирования: Полисмакова М.Н., Сандуляк Д.А., Харин А.С., Головченко Д.А., Сандуляк А.А., Сандуляк А.В., Baskonus H.M. Расширение возможностей новых магнитометров пондеромоторного и магнитно-реологического типов с полюсами-полусферами. *Russian Technological Journal*. 2025;13(4):55–68. https://doi.org/10.32362/2500-316X-2025-13-4-55-68, https://www.elibrary.ru/PEJBLG

Прозрачность финансовой деятельности: Авторы не имеют финансовой заинтересованности в представленных материалах или методах.

Авторы заявляют об отсутствии конфликта интересов.

INTRODUCTION

In various areas of science and technology, it is necessary to obtain data on the magnetic properties of dispersed materials, in particular, composites, powders, suspensions [1–13]. This issue becomes particularly relevant when a relatively small volume of the material under study is available, for example, small samples of ferroimpurities isolated from technological bulk and liquid media for laboratory purposes.

In this regard, it is highly important to have appropriate means of monitoring the magnetic properties of small-volume samples, for which magnetometers based on the ponderomotive principle are generally preferable [14–25]. A contemporary direction in the creation of means for controlling the magnetic characteristics—in particular, in terms of their magnetic susceptibility—of small-sized bodies when using this kind of magnetometer, including small-volume dispersed samples and their individual particles involves the use of pole tip-hemispheres [26–32] (Fig. 1). Such a solution can be used to obtain the necessary working zone, i.e., the zone of stable (along a certain coordinate, generally according to the action of the ponderomotive force) inhomogeneity in terms of gradient and/or magnetic force factor without the difficulties that usually arise in such cases. An indication of the dislocation of this zone is shown in Fig. 1 in the form of a thickening on the x-axis as the axis along which the sample under study is suspended or the particle under study is forced to move in the liquid.

To identify this zone in the interpole region of the magnetometer, it is necessary to obtain the coordinate characteristics of the intensity H (or induction B) of the created inhomogeneous magnetic field [26–32]. Since the relative magnetic permeability of the air medium in the interpole region is close to unity, the values of H and B are related by means of a constant: $H = B/\mu_0$, where $\mu_0 = 4\pi \cdot 10^{-7}$ H/m is the magnetic constant.

At the same time, the condition for the presence within the working zone of the created inhomogeneous field of some stable (practically constant) value—for example, the gradient of intensity grad$H$ (or the gradient of induction grad$B$)—is unambiguous. The values of the field intensity H (induction B) within such a zone, in particular, in the direction x in which the ponderomotive force F (Fig. 1), measured in the magnetometer, acts, must conform to a linear relationship. Only in this case, the corresponding differentiation of such dependence—i.e., the transition to the desired relation dH/dx or dB/dx—will demonstrate the constancy (here, stability along the x coordinate) of the parameter of interest $dH/dx \cong \text{grad}H = \text{const}$ or $dB/dx \cong \text{grad}B = \text{const}$.

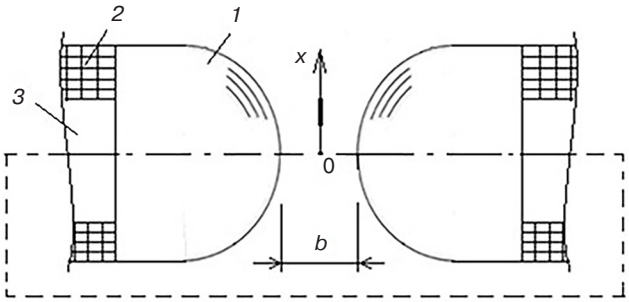

Fig. 1. On the application of pole tips-hemispheres (*1*) in the electromagnetic system with winding (*2*) on the magnetocoupler (*3*) in magnetometers based on the ponderomotive principle

At the same time, already well-proven magnetometers suitable for realization of these methods comprise poles–hemispheres of comparatively small diameter D = 100 mm and 135 mm [26, 27, 29–32]. This somewhat limits the necessary executive zone considering its dislocation and extent in the objectively somewhat constricted interpole space.

The capabilities of such magnetometers can be extended by using poles–hemispheres of larger diameter D. Of course, this requires a set of studies for obtaining the coordinate (along the x-direction of the ponderomotive, i.e., magnetic, force) characteristics of induction B (intensity H), gradient grad$B \cong dB/dx$ (grad$H \cong dH/dx$), force factor Bgrad$B$ (Hgrad$H$) and consequential generalized analytical dependencies, which are necessary for operative prediction and control of the location of the desired working zone (i.e., the zone of relatively stable

field inhomogeneity). At the same time, it is important to establish to what extent such dependencies agree with the previously established dependencies obtained in [26–32] for poles–hemispheres of a smaller diameter.

RESULTS AND DISCUSSION

It was mentioned earlier that the key characteristic for identifying the executive zone of magnetometers of the stipulated ponderomotive principle based on the manifestation of the ponderomotive (i.e., magnetic force) is the coordinate characteristic of the induction B (intensity H) of the magnetic field between the poles, represented here by poles–hemispheres.

As in [26–32], step-by-step values of B along the chosen direction x (Fig. 1) were measured using a milliteslameter fitted with a Hall sensor placed on a coordinate table. The direction x of the sensor movement, which should lie in the plane of symmetry of the area between the pole tips-hemispheres, can be selected by the experimenter by moving the sensor in one of the variants of such direction most convenient for making measurements. Here, specific values of x correspond to the distance from the centerline of the poles to the current location of the sensor. In Fig. 1 this direction is shown upwards; however, in the real design it was more convenient to move in the direction perpendicular to the drawing, i.e., towards oneself.

The experiments were performed alternately using two pairs of pole tips-hemispheres with diameters of D = 157 mm and of D = 184 mm, mutually removed by one or another distance b: for D = 157 mm—from b = 9.5 mm to b = 24 mm; for D = 184 mm—from b = 6.5 mm to b = 28 mm. The magnetizing force $I\omega$ of the winding of the electromagnetic system (Fig. 1) was varied by the value of the supply current I in the range $I\omega$ = 3000–22500 A. In this case, the number of winding coils ω = 3000.

The results of step-by-step measurements of the magnetic induction B in the accepted direction x (Fig. 1) between the poles–hemispheres with the diameter D = 157 mm are shown in Fig. 2 (points) for different values of $I\omega$ and b. This allowed us to obtain the corresponding coordinate characteristics (lines) of B and $dB/dx \cong \text{grad}B$. For this purpose, the experimental data B (Fig. 2, points) were subjected to approximation (Fig. 2, lines) by a fourth degree polynomial using the *Advanced Grapher*[1] software environment.

When their inflection is traced as described in [26–32], the rather meandering appearance of the coordinate characteristics B from x in Fig. 2 indicates the possibility of artificial linear (simplified) approximation of the dependencies of induction B on the x coordinate precisely in the vicinity of the inflection point of each of these dependencies. So, here (i.e., where the section of the curve B from x can be linearly approximated), the gradient of induction $\text{grad}B = dB/dx$ is an almost constant value.

This can be verified in the extreme form of the gradient coordinate characteristics (Fig. 2) according to the very close values of the gradient (bounded area) in the vicinity of the extremum.

From the obtained coordinate characteristics of the gradient (Fig. 2) directly follows the information about the coordinate (abscissa) of the extremum of each of these characteristics, i.e., the value $x = x_{extr}$ (Table 1), and thus on the coordinate of the dislocation of the corresponding executive, namely, the working zone between the poles–hemispheres with diameter D = 157 mm.

[1] https://www.alentum.com/agrapher/. Accessed May 12, 2025.

Table 1. Coordinates of the extremum x_{extr} (dislocation of the stable gradient zone) between poles–hemispheres with the diameter D = 157 mm at different values of magnetizing force $I\omega$ of the winding and different distances b between poles–hemispheres

$I\omega$, A	x_{extr}, mm					
	b = 9.5 mm	b = 13 mm	b = 15.5 mm	b = 18 mm	b = 21 mm	b = 24 mm
3000	17.60	22.26	21.90	22.34	22.17	27.70
6000	18.15	20.86	22.73	22.41	26.21	26.01
12000	17.50	20.54	21.17	22.76	29.49	27.46
22500	17.65	19.58	21.61	22.75	24.12	26.58
Average	**17.73**	**20.81**	**21.85**	**22.57**	**25.5**	**26.94**

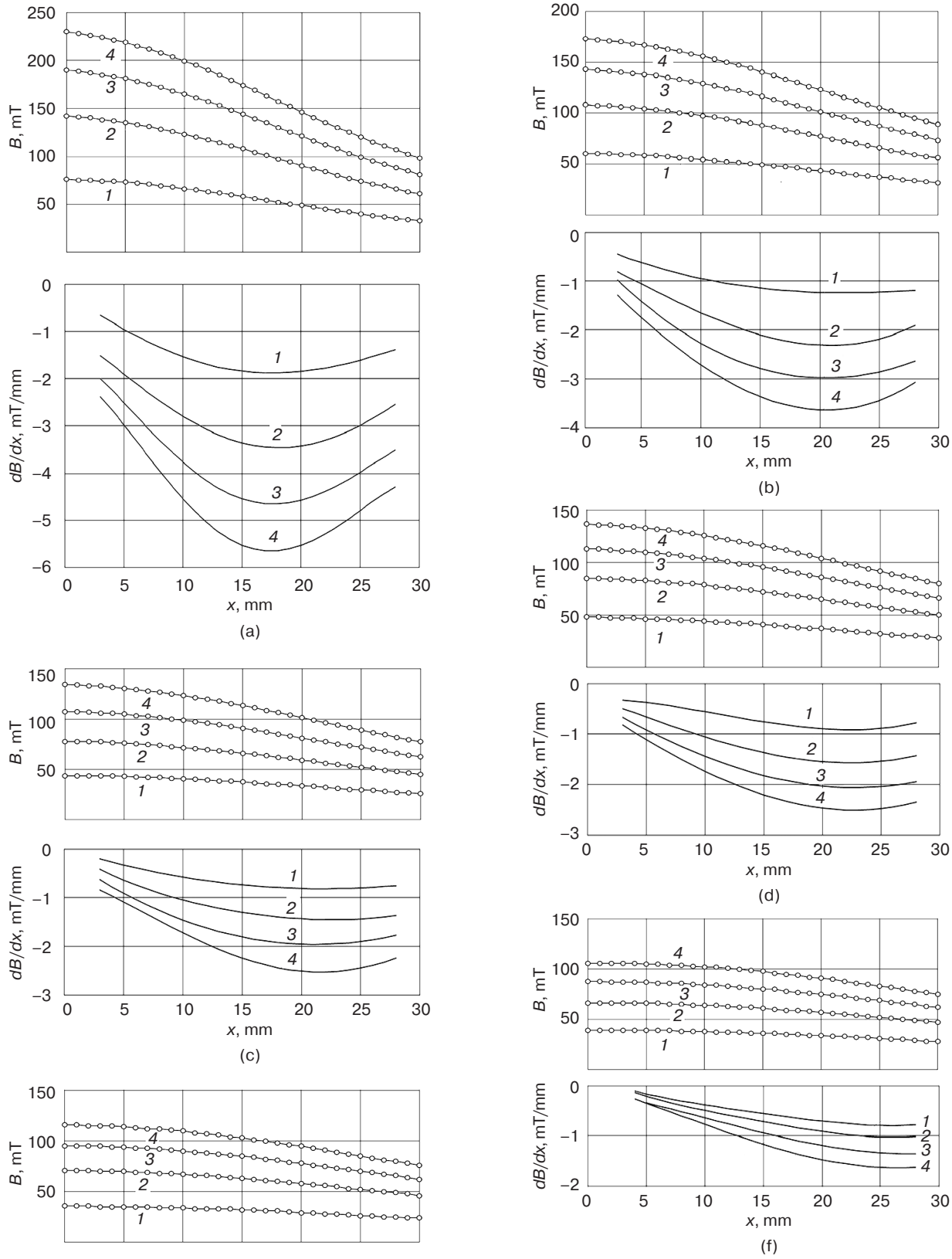

Fig. 2. Coordinate characteristics of induction and field gradient between poles–hemispheres of the diameter D = 157 mm at their mutual distance b:
(a) 9.5 mm; (b) 13 mm; (c) 15.5 mm;
(d) 18 mm; (e) 21 mm; (f) 24 mm;
for the values of the magnetizing force $I\omega$:
(*1*) 3000 A, (*2*) 6000 A, (*3*) 12000 A, (*4*) 22500 A

The obtained data x_{extr} indicate an important fact noted earlier: despite the different values of the magnetizing force $I\omega$ of the winding of the electromagnetic system of the magnetometer, the values of the coordinates of the extrema of the field induction gradient characteristics (Fig. 2) at the same value of b (i.e., the coordinates of the dislocation of the working zones) are very close to each other.

This fact, already found earlier for poles–hemispheres of smaller diameter [26–32], is all the more relevant if we present the ordinates of the initial characteristics available in Fig. 2 in relative quantities, namely, as the ratio of the current (by x) values of the induction B to the individual "starting" value of the induction B_0 obtained at $x = 0$, i.e., to B/B_0, for the corresponding value of the magnetizing force $I\omega$.

Figure 3 shows as an example such characteristics obtained from the data borrowed from Fig. 2a. It can be seen that irrespective of the value $I\omega$ the data B/B_0 are generalized by a single dependence; here, in contrast to Fig. 2a, the point designations have been intentionally changed with a corresponding inflection of this dependence. This also indicates a single dislocation of the working zones at the same mutual distance b of the poles–hemispheres. The dependencies of B/B_0 on x for other values of b are equally revealing (Fig. 4).

The above arguments are methodologically important for the experimenter: when performing experiments to determine the effect of field magnitude on the magnetic susceptibility of a sample, its dislocation between the poles should not be changed.

The extent of the zone (along the x coordinate) of almost constant values of the grad$B$ parameter, i.e., the extent of the working zone of the magnetometer,

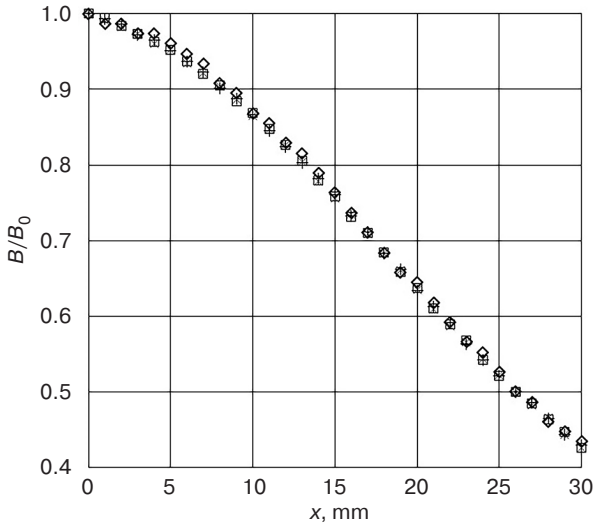

Fig. 3. Generalized (from the data on Fig. 2a) coordinate characteristics of the induction B in relative values B/B_0, b = 9.5 mm, for values of the magnetizing force $I\omega$: ◊ 3000 A, + 6000 A, □ 12000 A, × 22500 A

is indicated by the data of Figs. 2–4, namely, those parts of the dependencies of induction B and relative induction B/B_0 on x that are amenable to linear approximation (areas in the vicinity of the inflection point of such dependencies).

The extent of the working zone of the magnetometer is even more clearly indicated by the coordinate characteristics of the parameter grad$B$ (Fig. 2): this zone is localized in the vicinity of the extremum of one or another dependence of the parameter dB/dx = grad$B$ on x.

The obtained data (Table 1) on the coordinate x_{extr} of the dislocation of the working zone of the magnetometer

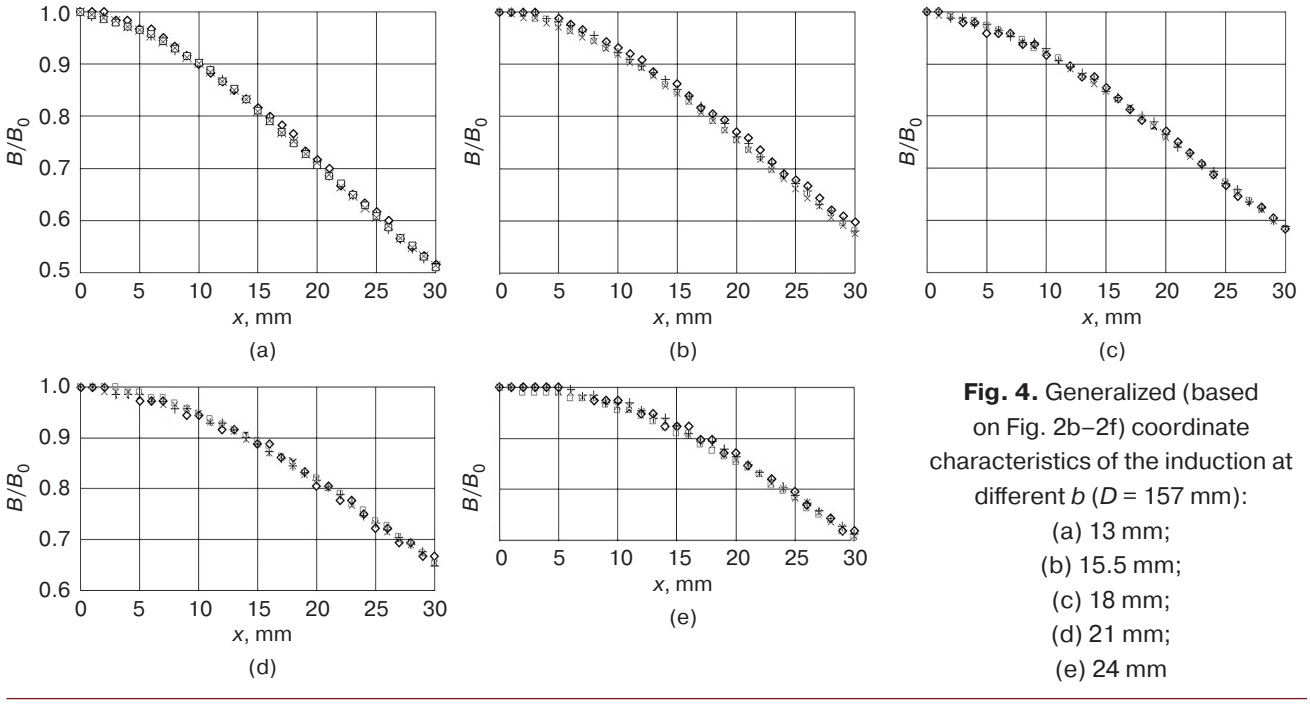

Fig. 4. Generalized (based on Fig. 2b–2f) coordinate characteristics of the induction at different b (D = 157 mm):
(a) 13 mm;
(b) 15.5 mm;
(c) 18 mm;
(d) 21 mm;
(e) 24 mm

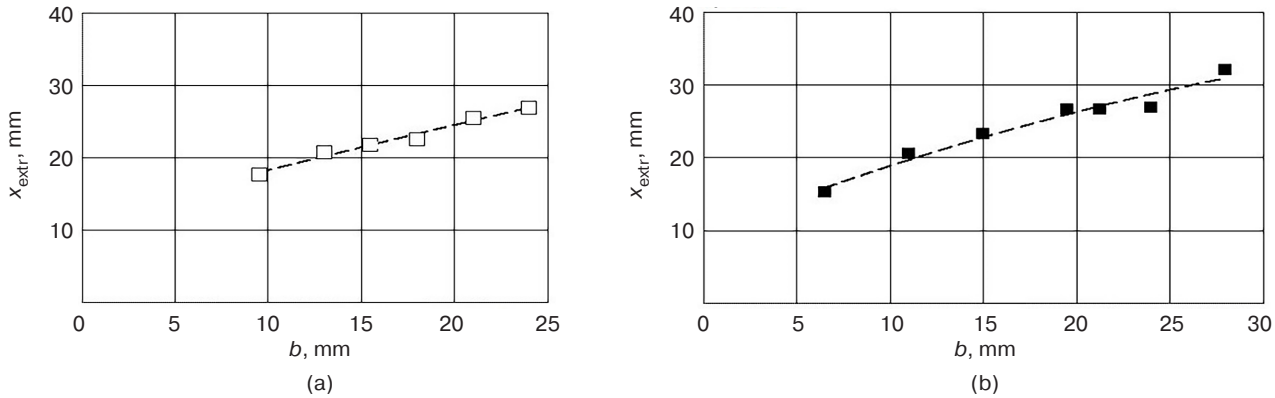

Fig. 5. Dependence of the dislocation coordinate of the working area of the magnetometer on the distance between its poles–hemispheres with the diameters D = 157 mm (a) and D = 184 mm (b)

depending on the mutual distance b of the poles-hemispheres with the diameter D = 157 mm are shown in Fig. 5a (points □). Figure 5b (points ■) shows similar data obtained using poles–hemispheres with the diameter D = 184 mm. Information similar to that previously shown in Figs. 2–4 and Table 1 for D = 184 mm is shown in Figs. 6, 7 and in the Table 2.

It is important to note that if the data obtained for both pairs of poles–hemispheres (Table 1, Table 2, Fig. 5), i.e., for D = 157 mm and D = 184 mm, are presented in a more universal, dimensionless form, namely, as x_{extr}/D on b/D (Fig. 8), the expected (similar to [31]) result follows—they are generalized by a single dependence.

The representation of these data in semi–logarithmic coordinates (Fig. 8b) shows the possibility of their quasi-linearization in these coordinates in the investigated range b/D = 0.035 … 0.153 with obtaining the calculation formula of the logarithmic form:

$$\frac{x_{extr}}{D} = A \ln \frac{b/D}{k} \qquad (1)$$

at values of phenomenological parameters A = 0.061 and k = 0.0096.

The possibility of quasi-linearization of the same data is also observed in logarithmic coordinates (Fig. 8c) by obtaining an alternative calculation formula of the degree type:

$$\frac{x_{extr}}{D} = G\left(\frac{b}{D}\right)^z \qquad (2)$$

at the values of the phenomenological parameters G = 0.43 and z = 0.48.

It is interesting to compare the found expressions (1) and (2) with the corresponding expressions obtained earlier for poles–hemispheres of smaller diameter: D = 100 mm and D = 135 mm [31]. It is important to note that, remaining functionally similar, the compared expressions differ slightly only in the values of the phenomenological parameters A, k, G and z: A = 0.061 instead of A = 0.063, k = 0.0096 instead of k = 0.0095, G = 0.43 instead of G = 0.45, z = 0.48 instead of z = 0.5.

Table 2. Coordinates of the extremum x_{extr} between poles–hemispheres of the diameter D = 184 mm at different values of the magnetizing force $I\omega$ of the winding and different distances b between poles–hemispheres

$I\omega$, A	x_{extr}, mm						
	b = 6.5 mm	b = 11 mm	b = 15 mm	b = 19.5 mm	b = 21.2 mm	b = 24 mm	b = 28 mm
3000	15.65	20.75	23.71	–	26.3	25.58	32.20
6000	15.59	20.67	23.44	26.77	26.965	28.2	32.17
12000	14.89	20.55	22.97	26.71	27.25	28.025	32.32
22500	14.81	20.27	22.81	–	25.85	25.66	31.86
Average	**15.24**	**20.56**	**23.23**	**26.74**	**26.59**	**26.87**	**32.14**

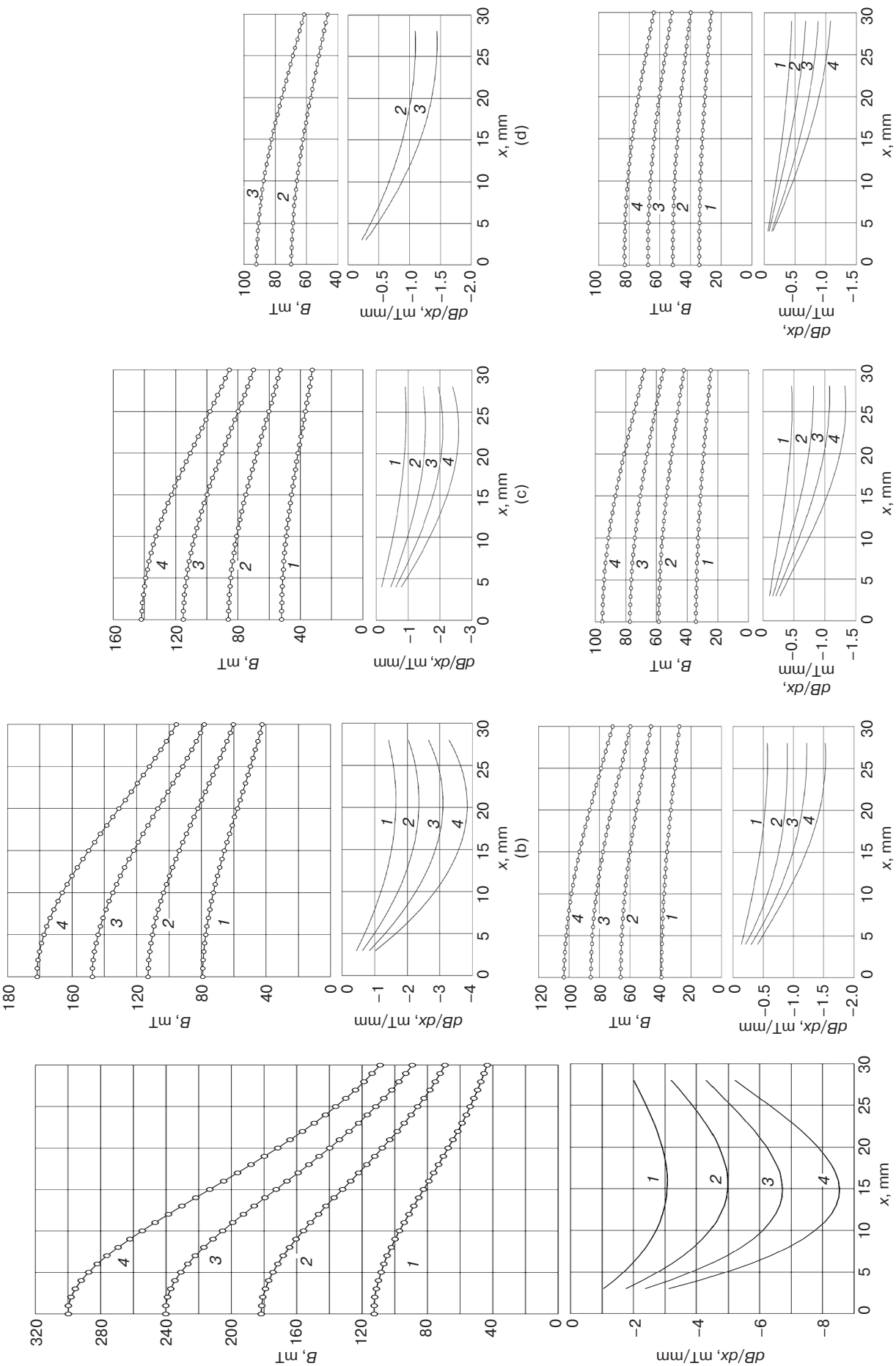

Fig. 6. Coordinate characteristics of induction and field gradient between poles–hemispheres of the diameter D = 184 mm at their mutual distance b: (a) 6.5 mm; (b) 11 mm; (c) 15 mm; (d) 19.5 mm; (e) 21.2 mm; (f) 24 mm; (g) 28 mm; for the values of magnetizing force $I\omega$: (*1*) 3000 A, (*2*) 6000 A, (*3*) 12000 A, (*4*) 22500 A

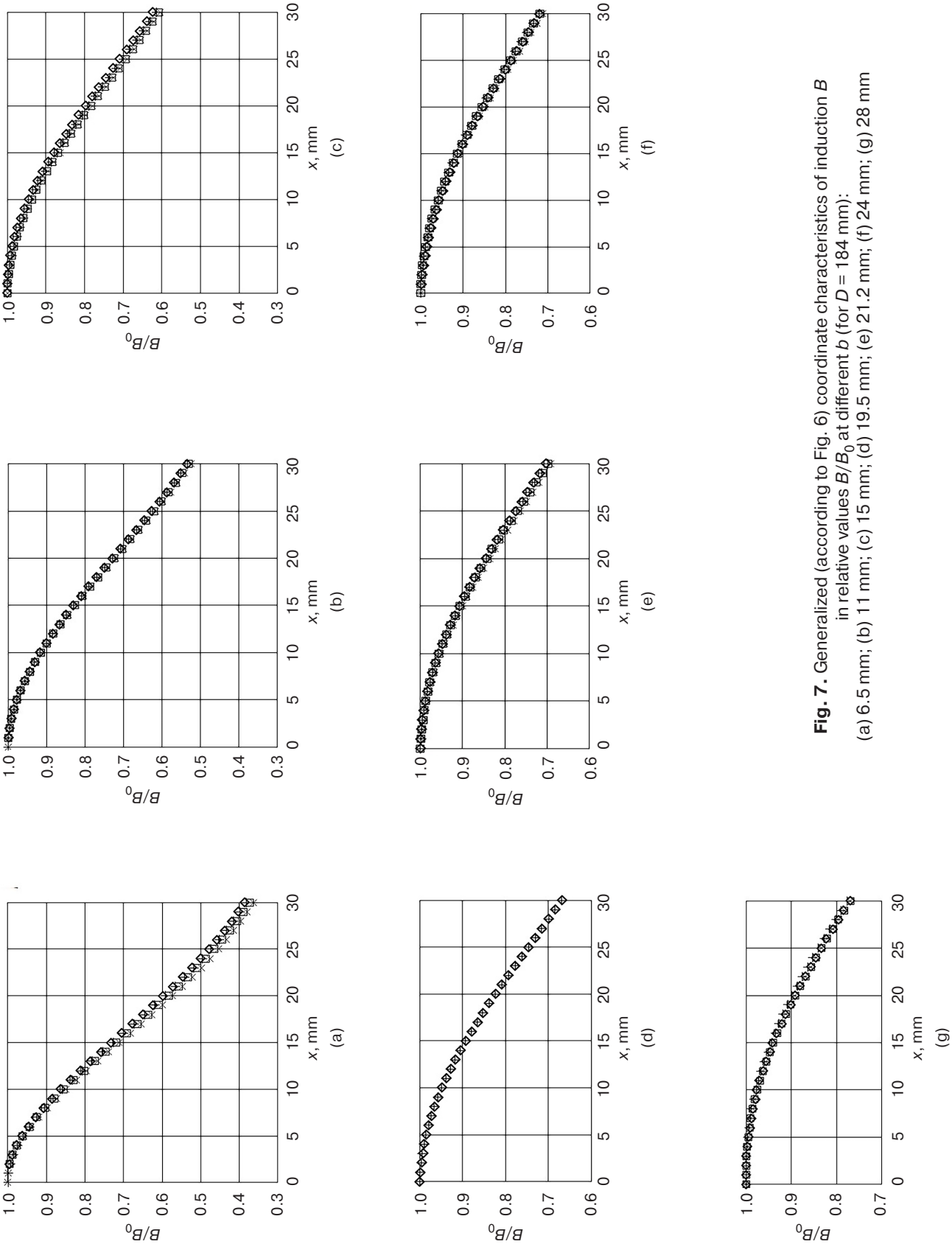

Fig. 7. Generalized (according to Fig. 6) coordinate characteristics of induction B in relative values B/B_0 at different b (for D = 184 mm): (a) 6.5 mm; (b) 11 mm; (c) 15 mm; (d) 19.5 mm; (e) 21.2 mm; (f) 24 mm; (g) 28 mm

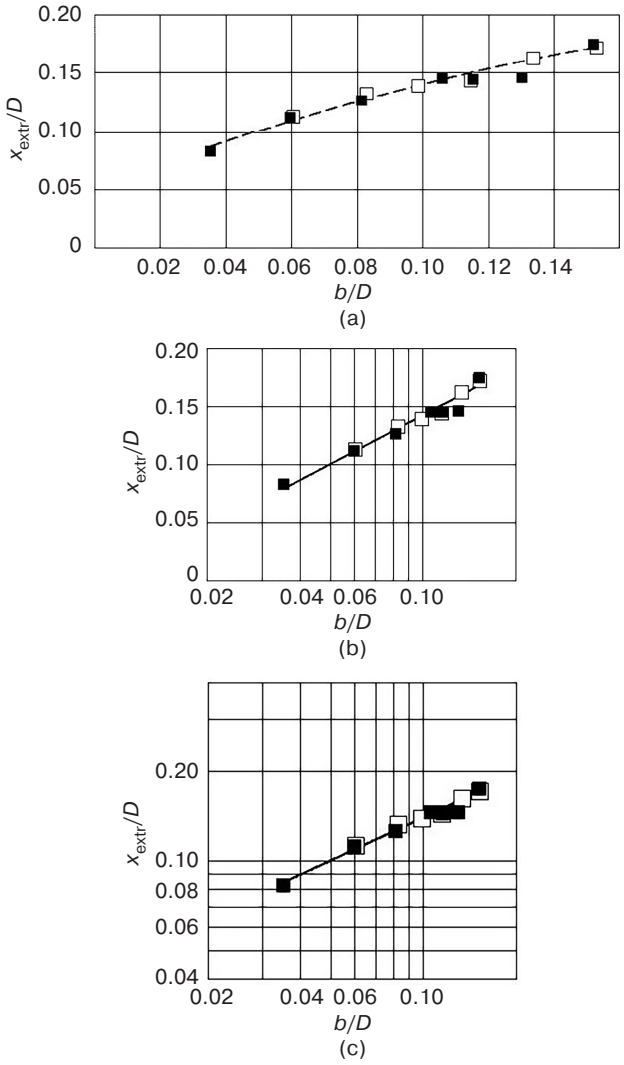

Fig. 8. Dependence of the relative coordinate of the dislocation of the working area of the magnetometer on the relative distance between its poles–hemispheres of the diameter D (□ 157 mm, ■ 184 mm) in ordinary (a), semi–logarithmic (b) and logarithmic (c) coordinates

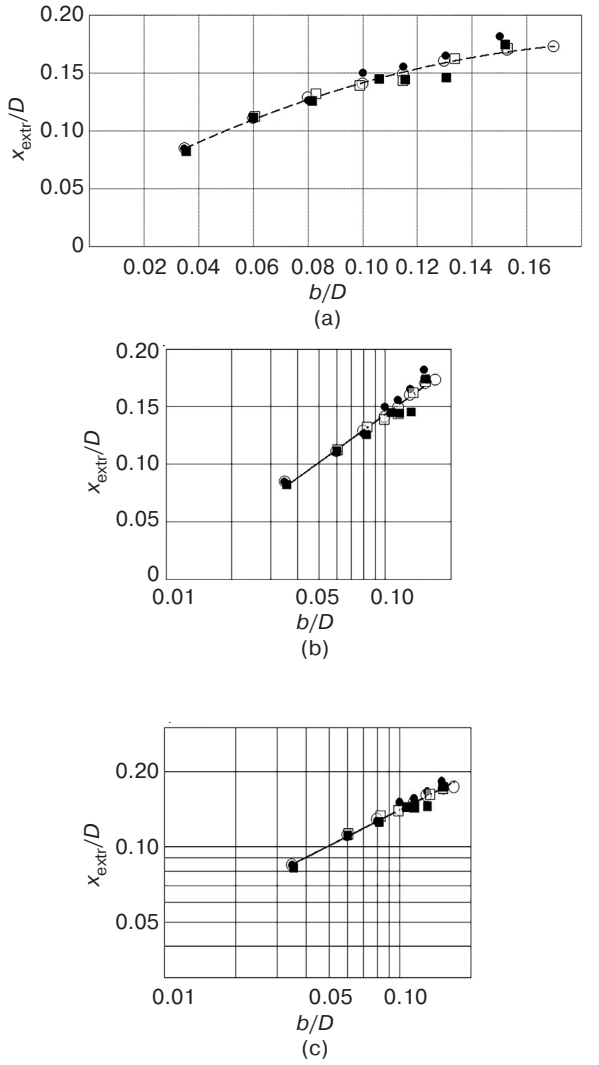

Fig. 9. Generalized dependence of the relative coordinate of the dislocation of the magnetometer working area on the relative distance between its poles–hemispheres with the diameter D (○ 100 mm, ● 135 mm, □ 157 mm, ■ 184 mm) in ordinary (a), semi–logarithmic (b) and logarithmic (c) coordinates

If to carry out joint processing of the data received for poles–hemispheres of the increased diameter, namely D = 157 mm and D = 184 mm, with the data received earlier for poles–hemispheres of the smaller diameter, namely D = 100 mm and D = 135 mm, the generalized dependence presented in Fig. 9, in semi–logarithmic (Fig. 9b) and logarithmic (Fig. 9c) coordinates, will take the form similar to (1) and (2), with the values of phenomenological parameters A = 0.061, k = 0.0094, G = 0.43, and z = 0.48.

CONCLUSIONS

The problem of expanding the capabilities of magnetometers of ponderomotor and magneto-rheological types designed to control the magnetic susceptibility of objects of small sizes, including both dispersed and individual particles, is considered.

In addition to the previously obtained data established using pole–hemisphere pairs of the diameters D = 100 mm and 135 mm, data are obtained for hemispheres of increased diameters D = 157 mm and 184 mm, mutually disconnected by one or another distance b.

The key dependencies of the magnetic induction B at the stepwise distance x from the center of symmetry of the interpole region (i.e., along the line of action of the ponderomotive force) have been experimentally determined to calculate the dependencies of the gradient grad$B \cong dB/dx$. This allows us to establish a characteristic inflection of each of the curves of dependencies of B on x and an extremum of each of the curves of dependencies of dB/dx on x, in the vicinity of which the values of dB/dx

are almost the same, which meets the requirement of constancy of the field inhomogeneity at the choice of the dislocation of the operating zone.

The coordinates of the dislocation of the operating zone are obtained from the determined and generalized dependencies of B on x and dB/dx on x. In order to calculate these coordinates, which depend on the values of D and b but not on the magnetizing force $I\omega$ of the winding of the electromagnetic system, analytical expressions of the power and logarithmic form are obtained.

ACKNOWLEDGMENTS

The study was financially supported by the Ministry of Science and Higher Education of the Russian Federation within the framework of the State Assignment in the field of science (project No. FSFZ-2024-0005).

Authors' contributions

M.N. Polismakova—conceptualization, conducting a research and investigation process, writing and editing the text of the manuscript.

D.A. Sandulyak—methodology, data verification, applying mathematical methods to analyze data, preparation, writing and editing the text of the manuscript.

A.S. Kharin—conducting the study, collecting materials for the study.

D.A. Golovchenko—collecting and analyzing materials for the study, writing the original draft.

A.A. Sandulyak—methodology, editing the manuscript.

A.V. Sandulyak—data verification, formal analysis, supervision.

H.M. Basconus—data verification, collecting materials for the study.

REFERENCES

1. Mosleh N., Insinga A.R., Bahl C.R.H., Bjørk R. The magnetic properties of packings of cylinders. *J. Magn. Magn. Mater*. 2024;607(3):172391. https://doi.org/10.1016/j.jmmm.2024.172391
2. Uestuener K., Katter M., Rodewald W. Dependence of the mean grain size and coercivity of sintered Nd–Fe–B magnets on the initial powder particle size. *IEEE Trans. Magn*. 2006;42(10):2897–2899. https://doi.org/10.1109/TMAG.2006.879889
3. Anhalt M., Weidenfeller B. Magnetic properties of polymer bonded soft magnetic particles for various filler fractions. *J. App. Phys*. 2007;101(2):023907. https://doi.org/10.1063/1.2424395
4. Schäfer K., Braun T., Riegg S., Musekamp J., Gutfleisch O. Polymer-bonded magnets produced by laser powder bed fusion: Influence of powder morphology, filler fraction and energy input on the magnetic and mechanical properties. *Mater. Res. Bull*. 2023;158(3):112051. https://doi.org/10.1016/j.materresbull.2022.112051
5. McFarlane J., Weber C., Wiechert A., Yiacoumi S., Tsouris C. High-gradient magnetic separation of colloidal uranium oxide particles from soil components in aqueous suspensions. *Colloids and Surfaces C: Environmental Aspects*. 2024;2:100023. https://doi.org/10.1016/j.colsuc.2023.100023
6. Zhivulko A.M., Yanushkevich K.I., Danilenko E.G., Zelenov F.V., Bandurina O.N. Magnetic properties of $Mn_{1-x}Gd_xSe$ solid solutions. *Sibirskii aerokosmicheskii zhurnal = Siberian Aerospace Journal.* 2022;23(4):748–755 (in Russ.). https://doi.org/10.31772/2712-8970-2022-23-4-748-755
7. Normile P.S., Andersson M.S., Mathieu R., Lee S.S., Singh G., De Toro J.A. Demagnetization effects in dense nanoparticle assemblies. *Appl. Phys. Lett*. 2016;109(15):152404. https://doi.org/10.1063/1.4964517
8. Bjørk R., Zhou Z. The demagnetization factor for randomly packed spheroidal particles. *J. Magn. Magn. Mater*. 2019;476:417–422. https://doi.org/10.1016/j.jmmm.2019.01.005
9. Walmsley N.S., Chantrell R.W., Gore J.G., Maylin M. Experimental and computational investigation of the magnetic susceptibility of composite soft materials. *J. Phys. D: App. Phys*. 2000;33(7):784–790. http://doi.org/10.1088/0022-3727/33/7/306
10. Gao Y., Fujiki T., Dozono H., Muramatsu K., Guan W., Yuan J., Tian C., Chen B. Modeling of Magnetic Characteristics of Soft Magnetic Composite Using Magnetic Field Analysis. *IEEE Trans. Magn*. 2018;54(3):7401504. https://doi.org/10.1109/TMAG.2017.2772293
11. Tortarolo M., Zysler R.D., Romero H. Magnetic order in amorphous $(Fe_{0.25}Nd_{0.75})_{0.6}B_{0.4}$ nanoparticles. *J. Appl. Phys*. 2009;105(11):113918. https://doi.org/10.1063/1.3140607
12. Zysler R.D., De Biasi E., Ramos C.A., Fiorani D., Romero H. Surface and Interparticle Effects in Amorphous Magnetic Nanoparticles. In: Fiorani D. (Ed.). *Surface Effects in Magnetic Nanoparticles.* Springer; 2005. P. 239–261. https://doi.org/10.1007/0-387-26018-8_8
13. Maciaszek R., Kollár P., Birčáková Z., Tkáč M., Füzer J., Olekšáková D., Volavka D., Samuely T., Kováč J., Bureš R., Fáberová M. Effects of particle surface modifcation on magnetic behavior of soft magnetic $Fe@SiO_2$ composites and Fe compacts. *J. Mater. Sci*. 2024;59:11781–11798. https://doi.org/10.1007/s10853-024-09881-1
14. Baskar D., Adler S.B. High temperature Faraday balance for *in situ* measurement of magnetization in transition metal oxides. *Rev. Sci. Instrum*. 2007;78(2):023908. https://doi.org/10.1063/1.2432476
15. Moze O., Giovanelli L., Kockelmann W., de Groot C.H., de Boer F.R., Buschow K.H.J. Structure and magnetic properties of $Nd_2Co_{17-x}Ga_x$ compounds studied by magnetic measurements and neutron diffraction. *J. Magn. Magn. Mater*. 1998;189:329–334. https://doi.org/10.1016/s0304-8853(98)00291-1
16. Gaucherand F., Beaugnon E. Magnetic texturing in ferromagnetic cobalt alloys. *Physica B: Cond. Matt.* 2004;346–347:262–266. https://doi.org/10.1016/j.physb.2004.01.062

17. Caignaert V., Maignan A., Pralong V., Hébert S., Pelloquin D. A cobaltite with a room temperature electrical and magnetic transition: $YBaCo_4O_7$. *Solid State Sci*. 2006;8(10):1160–1163. https://doi.org/10.1016/j.solidstatesciences.2006.05.004
18. Zhang C.P., Chaud X., Beaugnon E., Zhou L. Crystalline phase transition information induced by high temperature susceptibility transformations in bulk PMP-YBCO superconductor growth *in-situ*. *Physica C.* 2015;508:25–30. https://doi.org/10.1016/j.physc.2014.11.002
19. Bombik A., Leśniewska B., Pacyna A.W. Magnetic susceptibility of powder and single-crystal $TmFeO_3$ orthoferrite. *J. Magn. Magn. Mater*. 2000;214(3):243–250. https://doi.org/10.1016/S0304-8853(00)00049-4
20. Kobayashi H., Tabuchi M., Shikano M., Kageyama H., Kanno R. Structure, and magnetic and electrochemical properties of layered oxides, Li_2IrO_3. *J. Mater. Chem*. 2003;13(4):957–962. https://doi.org/10.1039/b207282c
21. Seidov Z., Krug von Nidda H.-A., Hemberger J., Loidl A., Sultanov G., Kerimova E., Panfilov A. Magnetic susceptibility and ESR study of the covalent-chain antiferromagnets $TlFeS_2$ and $TlFeSe_2$. *Phys. Rev. B*. 2001;65:014433. https://doi.org/10.1103/PhysRevB.65.014433
22. Slobinsky D., Borzi R.A., Mackenzie A.P., Grigera S.A. Fast sweep-rate plastic Faraday force magnetometer with simultaneous sample temperature measurement. *Rev. Sci. Instrum*. 2012;83(12):125104. https://doi.org/10.1063/1.4769049
23. Gopalakrishnan R., Barathan S., Govindarajan D. Magnetic susceptibility measurements on fly ash admixtured cement hydrated with groundwater and seawater. *Am. J. Mater. Sci*. 2012;2(1):32–36. https://doi.org/10.5923/j.materials.20120201.06
24. Mexner W., Heinemann K. An improved method for relaxation measurements using a Faraday balance. *Rev. Sci. Instrum*. 1993;64(11):3336–3337. https://doi.org/10.1063/1.1144303
25. Riminucci A., Uhlarz M., De Santis R., Herrmannsdörfer T. Analytical balance-based Faraday magnetometer. *J. App. Phys*. 2017;121(9):094701. https://doi.org/10.1063/1.4977719
26. Sandulyak A.A., Sandulyak A.V., Polismakova M.N., Kiselev D.O., Sandulyak D.A. An approach for choosing positioning of small volume sample at instantiation ponderomotive Faraday method in determining its magnetic susceptibility. *Russ. Technol. J*. 2017;5(2):57–69 (in Russ.). https://doi.org/10.32362/2500-316X-2017-5-2-57-69
27. Sandulyak A.A., Sandulyak A.V., Polismakova M.N., Sandulyak D.A., Kiselev D.O. *Device for Creation and Diagnostics of Stable Magnetic Field Inhomogeneity Zone*: Pat. RU 2737609 Publ. 01.12.2020 (in Russ.).
28. Sandulyak A.A., Sandulyak A.V., Ershova V.A., Sandulyak D.A. *Method for Magnetic-Reological Control of Magnetic Susceptibility of Particle*: Pat. RU 2753159. Publ. 12.08.2021 (in Russ.).
29. Sandulyak A.V., Sandulyak A.A., Polismakova M.N., Kiselev D.O., Sandulyak D.A. Faraday magnetometer with spheric pole pieces: identification zone with a stable force factor. *Russ. Technol. J*. 2017;5(6):43–54 (in Russ.). https://doi.org/10.32362/2500-316X-2017-5-6-43-54
30. Sandulyak A.V., Sandulyak A.A., Polismakova M.N., Sandulyak D.A., Ershova V.A. The approach to the creation and identification of the positioning zone of the sample in the Faraday magnetometer. *J. Magn. Magn. Mater*. 2019;469:665–673. https://doi.org/10.1016/j.jmmm.2018.06.068
31. Sandulyak A.A., Polismakova M.N., Sandulyak D.A., Dwivedi A.P., Doumanidis C.C., Sandulyak A.V., Ershova V.A. Magnetic Field Between Polar Hemispheres: Remarks on the Dislocation of Zones of a Constant Gradient and Force Factor. *Nanotechnol. Percept*. 2023;19(3):67–79.
32. Sandulyak A.A., Sandulyak A.V., Polismakova M.N., Sandulyak D.A., Ershova V.A., Pamme N. Faraday Magnetometer with Polar Hemispheres: Stability Zones for Measuring of Magnetic Susceptibility of Particles. *Mater. Today: Proc*. 2022;59(3):933–940. https://doi.org/10.1016/j.matpr.2022.02.015

СПИСОК ЛИТЕРАТУРЫ

1. Mosleh N., Insinga A.R., Bahl C.R.H., Bjørk R. The magnetic properties of packings of cylinders. *J. Magn. Magn. Mater*. 2024;607(3):172391. https://doi.org/10.1016/j.jmmm.2024.172391
2. Uestuener K., Katter M., Rodewald W. Dependence of the mean grain size and coercivity of sintered Nd–Fe–B magnets on the initial powder particle size. *IEEE Trans. Magn*. 2006;42(10):2897–2899. https://doi.org/10.1109/TMAG.2006.879889
3. Anhalt M., Weidenfeller B. Magnetic properties of polymer bonded soft magnetic particles for various filler fractions. *J. App. Phys*. 2007;101(2):023907. https://doi.org/10.1063/1.2424395
4. Schäfer K., Braun T., Riegg S., Musekamp J., Gutfleisch O. Polymer-bonded magnets produced by laser powder bed fusion: Influence of powder morphology, filler fraction and energy input on the magnetic and mechanical properties. *Mater. Res. Bull*. 2023;158(3):112051. https://doi.org/10.1016/j.materresbull.2022.112051
5. McFarlane J., Weber C., Wiechert A., Yiacoumi S., Tsouris C. High-gradient magnetic separation of colloidal uranium oxide particles from soil components in aqueous suspensions. *Colloids and Surfaces C: Environmental Aspects*. 2024;2:100023. https://doi.org/10.1016/j.colsuc.2023.100023
6. Живулько А.М., Янушкевич К.И., Даниленко Е.Г., Зеленов Ф.В., Бандурина О.Н. Магнитные свойства твердых растворов $Mn_{1-x}Gd_xSe$. *Сибирский аэрокосмический журнал*. 2022;23(4):748–755. https://doi.org/10.31772/2712-8970-2022-23-4-748-755
7. Normile P.S., Andersson M.S., Mathieu R., Lee S.S., Singh G., De Toro J.A. Demagnetization effects in dense nanoparticle assemblies. *Appl. Phys. Lett*. 2016;109(15):152404. https://doi.org/10.1063/1.4964517
8. Bjørk R., Zhou Z. The demagnetization factor for randomly packed spheroidal particles. *J. Magn. Magn. Mater*. 2019;476:417–422. https://doi.org/10.1016/j.jmmm.2019.01.005
9. Walmsley N.S., Chantrell R.W., Gore J.G., Maylin M. Experimental and computational investigation of the magnetic susceptibility of composite soft materials. *J. Phys. D: App. Phys*. 2000;33(7):784–790. http://doi.org/10.1088/0022-3727/33/7/306

10. Gao Y., Fujiki T., Dozono H., Muramatsu K., Guan W., Yuan J., Tian C., Chen B. Modeling of Magnetic Characteristics of Soft Magnetic Composite Using Magnetic Field Analysis. *IEEE Trans. Magn*. 2018;54(3):7401504. https://doi.org/10.1109/TMAG.2017.2772293
11. Tortarolo M., Zysler R.D., Romero H. Magnetic order in amorphous $(Fe_{0.25}Nd_{0.75})_{0.6}B_{0.4}$ nanoparticles. *J. Appl. Phys*. 2009;105(11):113918. https://doi.org/10.1063/1.3140607
12. Zysler R.D., De Biasi E., Ramos C.A., Fiorani D., Romero H. Surface and Interparticle Effects in Amorphous Magnetic Nanoparticles. In: Fiorani D. (Ed.). *Surface Effects in Magnetic Nanoparticles.* Springer; 2005. P. 239–261. https://doi.org/10.1007/0-387-26018-8_8
13. Maciaszek R., Kollár P., Birčáková Z., Tkáč M., Füzer J., Olekšáková D., Volavka D., Samuely T., Kováč J., Bureš R., Fáberová M. Effects of particle surface modifcation on magnetic behavior of soft magnetic $Fe@SiO_2$ composites and Fe compacts. *J. Mater. Sci*. 2024;59:11781–11798. https://doi.org/10.1007/s10853-024-09881-1
14. Baskar D., Adler S.B. High temperature Faraday balance for *in situ* measurement of magnetization in transition metal oxides. *Rev. Sci. Instrum*. 2007;78(2):023908. https://doi.org/10.1063/1.2432476
15. Moze O., Giovanelli L., Kockelmann W., de Groot C.H., de Boer F.R., Buschow K.H.J. Structure and magnetic properties of $Nd_2Co_{17-x}Ga_x$ compounds studied by magnetic measurements and neutron diffraction. *J. Magn. Magn. Mater*. 1998;189:329–334. https://doi.org/10.1016/s0304-8853(98)00291-1
16. Gaucherand F., Beaugnon E. Magnetic texturing in ferromagnetic cobalt alloys. *Physica B: Cond. Matt.* 2004;346–347:262–266. https://doi.org/10.1016/j.physb.2004.01.062
17. Caignaert V., Maignan A., Pralong V., Hébert S., Pelloquin D. A cobaltite with a room temperature electrical and magnetic transition: $YBaCo_4O_7$. *Solid State Sci*. 2006;8(10):1160–1163. https://doi.org/10.1016/j.solidstatesciences.2006.05.004
18. Zhang C.P., Chaud X., Beaugnon E., Zhou L. Crystalline phase transition information induced by high temperature susceptibility transformations in bulk PMP-YBCO superconductor growth *in-situ*. *Physica C.* 2015;508:25–30. https://doi.org/10.1016/j.physc.2014.11.002
19. Bombik A., Leśniewska B., Pacyna A.W. Magnetic susceptibility of powder and single-crystal $TmFeO_3$ orthoferrite. *J. Magn. Magn. Mater*. 2000;214(3):243–250. https://doi.org/10.1016/S0304-8853(00)00049-4
20. Kobayashi H., Tabuchi M., Shikano M., Kageyama H., Kanno R. Structure, and magnetic and electrochemical properties of layered oxides, Li_2IrO_3. *J. Mater. Chem*. 2003;13(4):957–962. https://doi.org/10.1039/b207282c
21. Seidov Z., Krug von Nidda H.-A., Hemberger J., Loidl A., Sultanov G., Kerimova E., Panfilov A. Magnetic susceptibility and ESR study of the covalent-chain antiferromagnets $TlFeS_2$ and $TlFeSe_2$. *Phys. Rev. B*. 2001;65:014433. https://doi.org/10.1103/PhysRevB.65.014433
22. Slobinsky D., Borzi R.A., Mackenzie A.P., Grigera S.A. Fast sweep-rate plastic Faraday force magnetometer with simultaneous sample temperature measurement. *Rev. Sci. Instrum*. 2012;83(12):125104. https://doi.org/10.1063/1.4769049
23. Gopalakrishnan R., Barathan S., Govindarajan D. Magnetic susceptibility measurements on fly ash admixtured cement hydrated with groundwater and seawater. *Am. J. Mater. Sci*. 2012;2(1):32–36. https://doi.org/10.5923/j.materials.20120201.06
24. Mexner W., Heinemann K. An improved method for relaxation measurements using a Faraday balance. *Rev. Sci. Instrum*. 1993;64(11):3336–3337. https://doi.org/10.1063/1.1144303
25. Riminucci A., Uhlarz M., De Santis R., Herrmannsdörfer T. Analytical balance-based Faraday magnetometer. *J. App. Phys*. 2017;121(9):094701. https://doi.org/10.1063/1.4977719
26. Сандуляк А.А., Сандуляк А.В., Полисмакова М.Н., Киселев Д.О., Сандуляк Д.А. Подход к координации малообъемного образца при реализации пондеромоторного метода определения его магнитной восприимчивости. *Russ. Technol. J*. 2017;5(2):57–69. https://doi.org/10.32362/2500-316X-2017-5-2-57-69
27. Сандуляк А.А., Сандуляк А.В., Полисмакова М.Н., Сандуляк Д.А., Киселев Д.О. *Устройство для создания и диагностики зоны стабильной неоднородности магнитного поля*: пат. 2737609 РФ. Заявка № 2020121691; заявл. 30.06.2020; опубл. 01.12.2020. Бюл. 34.
28. Сандуляк А.А., Сандуляк А.В., Ершова В.А., Сандуляк Д.А. *Способ магнитно-реологического контроля магнитной восприимчивости частицы*: пат. 2753159 РФ. Заявка № 2020143220; заявл. 27.12.2020; опубл. 12.08.2021. Бюл. 23.
29. Сандуляк А.В., Сандуляк А.А., Полисмакова М.Н., Киселев Д.О., Сандуляк Д.А. Магнетометр Фарадея с полюсными наконечниками-полусферами: идентификация зоны стабильного силового фактора. *Russ. Technol. J*. 2017;5(6):43–54. https://doi.org/10.32362/2500-316X-2017-5-6-43-54
30. Sandulyak A.V., Sandulyak A.A., Polismakova M.N., Sandulyak D.A., Ershova V.A. The approach to the creation and identification of the positioning zone of the sample in the Faraday magnetometer. *J. Magn. Magn. Mater*. 2019;469:665–673. https://doi.org/10.1016/j.jmmm.2018.06.068
31. Sandulyak A.A., Polismakova M.N., Sandulyak D.A., Dwivedi A.P., Doumanidis C.C., Sandulyak A.V., Ershova V.A. Magnetic Field Between Polar Hemispheres: Remarks on the Dislocation of Zones of a Constant Gradient and Force Factor. *Nanotechnol. Percept*. 2023;19(3):67–79.
32. Sandulyak A.A., Sandulyak A.V., Polismakova M.N., Sandulyak D.A., Ershova V.A., Pamme N. Faraday Magnetometer with Polar Hemispheres: Stability Zones for Measuring of Magnetic Susceptibility of Particles. *Mater. Today: Proc*. 2022;59(3):933–940. https://doi.org/10.1016/j.matpr.2022.02.015

About the Authors

Maria N. Polismakova, Cand. Sci. (Eng.), Associate Professor, Department of Devices and Information-Measuring Systems, Institute for Cybersecurity and Digital Technologies, MIREA – Russian Technological University (78, Vernadskogo pr., Moscow, 119454 Russia). E-mail: polismakova@mirea.ru. Scopus Author ID 36621096600, ResearcherID O-8796-2017, RSCI SPIN-code 3845-8391, https://orcid.org/0000-0002-4564-6206

Daria A. Sandulyak, Cand. Sci. (Eng.), Associate Professor, Department of Devices and Information-Measuring Systems, Institute for Cybersecurity and Digital Technologies, MIREA – Russian Technological University (78, Vernadskogo pr., Moscow, 119454 Russia). E-mail: sandulyak_d@mirea.ru. Scopus Author ID 36621369400, ResearcherID L-9814-2016, RSCI SPIN-code 8114-8109, https://orcid.org/0000-0003-4269-6133

Alexey S. Kharin, Engineer, Laboratory of Magnetic Control and Material's Separation, MIREA – Russian Technological University (78, Vernadskogo pr., Moscow, 119454 Russia). E-mail: linnetdar@mail.ru. RSCI SPIN-code 8435-3232, https://orcid.org/0000-0002-0922-1366

Daria A. Golovchenko, Researcher Intern, Laboratory of Magnetic Control and Material's Separation, MIREA – Russian Technological University (78, Vernadskogo pr., Moscow, 119454 Russia). E-mail: golovchenko@mirea.ru. RSCI SPIN-code 4303-1093, https://orcid.org/0000-0002-6227-6884

Anna A. Sandulyak, Dr. Sci. (Eng.), Professor, Department of Devices and Information-Measuring Systems, Institute for Cybersecurity and Digital Technologies, MIREA – Russian Technological University (78, Vernadskogo pr., Moscow, 119454 Russia). E-mail: sandulyak_a@mirea.ru. Scopus Author ID 7004032043, ResearcherID S-5187-2017, RSCI SPIN-code 8858-1720, https://orcid.org/0000-0002-5111-6092

Alexander V. Sandulyak, Dr. Sci. (Eng.), Professor, Department of Devices and Information-Measuring Systems, Institute for Cybersecurity and Digital Technologies, MIREA – Russian Technological University (78, Vernadskogo pr., Moscow, 119454 Russia). E-mail: sandulyak@mirea.ru. Scopus Author ID 57194504434, ResearcherID V-6094-2018, RSCI SPIN-code 3795-5374, https://orcid.org/0000-0001-7605-2702

Haci Mehmet Baskonus, Professor, Department of Mathematics and Science Education, Faculty of Education, Harran University (Sanliurfa, 63190 Turkey). E-mail: hmbaskonus@gmail.com. Scopus Author ID 36835781300, ResearcherID H-4335-2019, https://orcid.org/0000-0003-4085-3625

Об авторах

Полисмакова Мария Николаевна, к.т.н., доцент, кафедра «Приборы и информационно-измерительные системы», Институт кибербезопасности и цифровых технологий, ФГБОУ ВО «МИРЭА – Российский технологический университет» (119454, Россия, Москва, пр-т Вернадского, д. 78). E-mail: polismakova@mirea.ru. Scopus Author ID 36621096600, ResearcherID O-8796-2017, SPIN-код РИНЦ 3845-8391, https://orcid.org/0000-0002-4564-6206

Сандуляк Дарья Александровна, к.т.н., доцент, кафедра «Приборы и информационно-измерительные системы», Институт кибербезопасности и цифровых технологий, ФГБОУ ВО «МИРЭА – Российский технологический университет» (119454, Россия, Москва, пр-т Вернадского, д. 78). E-mail: sandulyak_d@mirea.ru. Scopus Author ID 36621369400, ResearcherID L-9814-2016, SPIN-код РИНЦ 8114-8109, https://orcid.org/0000-0003-4269-6133

Харин Алексей Сергеевич, преподаватель-исследователь, инженер лаборатории магнитного контроля и разделения материалов, ФГБОУ ВО «МИРЭА – Российский технологический университет» (119454, Россия, Москва, пр-т Вернадского, д. 78). E-mail: linnetdar@mail.ru. SPIN-код РИНЦ 8435-3232, https://orcid.org/0000-0002-0922-1366

Головченко Дарья Андреевна, преподаватель-исследователь, стажер-исследователь лаборатории магнитного контроля и разделения материалов, ФГБОУ ВО «МИРЭА – Российский технологический университет» (119454, Россия, Москва, пр-т Вернадского, д. 78). E-mail: golovchenko@mirea.ru. SPIN-код РИНЦ 4303-1093, https://orcid.org/0000-0002-6227-6884

Сандуляк Анна Александровна, д.т.н., профессор, кафедра «Приборы и информационно-измерительные системы», Институт кибербезопасности и цифровых технологий, ФГБОУ ВО «МИРЭА – Российский технологический университет» (119454, Россия, Москва, пр-т Вернадского, д. 78). E-mail: sandulyak_a@mirea.ru. Scopus Author ID 7004032043, ResearcherID S-5187-2017, SPIN-код РИНЦ 8858-1720, https://orcid.org/0000-0002-5111-6092

Сандуляк Александр Васильевич, д.т.н., профессор, кафедра «Приборы и информационно-измерительные системы», Институт кибербезопасности и цифровых технологий, ФГБОУ ВО «МИРЭА – Российский технологический университет» (119454, Россия, Москва, пр-т Вернадского, д. 78). E-mail: sandulyak@mirea.ru. Scopus Author ID 57194504434, ResearcherID V-6094-2018, SPIN-код РИНЦ 3795-5374, https://orcid.org/0000-0001-7605-2702

Haci Mehmet Baskonus, Professor, Department of Mathematics and Science Education, Faculty of Education, Harran University (Sanliurfa, 63190 Turkey). E-mail: hmbaskonus@gmail.com. Scopus Author ID 36835781300, ResearcherID H-4335-2019, https://orcid.org/0000-0003-4085-3625

Translated from Russian into English by L. Bychkova
Edited for English language and spelling by Thomas A. Beavitt

Analytical instrument engineering and technology

Аналитическое приборостроение и технологии

UDC 621.313.8
https://doi.org/10.32362/2500-316X-2025-13-4-69-77
EDN AVHESX

RESEARCH ARTICLE

Effect of winding and power supply parameters on the starting characteristics of an upgraded brushless DC motor

Alexandra S. Krivoguzova [@], Sergey N. Tkachenko, Andrey A. Shpilevoy

Immanuel Kant Baltic Federal University, Kaliningrad, 236041 Russia
[@] Corresponding author, e-mail: krivoguzova99@bk.ru

• **Submitted:** 14.11.2024 • **Revised:** 11.02.2025 • **Accepted:** 27.05.2025

Abstract

Objectives. This work is aimed at determining the optimum number of turns in each winding and the effect of winding and power supply parameters on the starting characteristics of an upgraded brushless direct current motor (BLDC motor).

Methods. A full-scale experiment on a test bench consisting of an upgraded BLDC motor, a power supply source, and a speed controller was conducted. Methods of mathematical simulation, linear programming, and approximation were also applied.

Results. During the experiments, the dependencies of inrush current and starting speed on the number of turns in each winding of the upgraded BLDC motor were obtained. It was experimentally established that the number of turns in the windings has a limiting value, which is confirmed by either the intersection of the curves of inrush current and starting speed, or the disappearance of the functional dependence between the inrush current and motor speed. A mathematical model for the upgraded BLDC motor was developed, which showed good agreement with the experimental results. Using this mathematical model, the optimum number of turns in each of the motor windings and the efficiency of a BLDC motor can be determined. A parametric model for determining the motor starting speed by the values of inrush current and battery voltage at the number of turns in the winding from 8 to 14 was proposed. The developed models make it possible to determine the motor characteristics at the design stage.

Conclusions. There exists an interval of the number of turns in each of the windings of a BLDC motor, where the motor demonstrates its optimum efficiency. Inrush current and supply voltage were found to be the parameters that are easily measurable in practice and sufficient for determining the basic starting characteristics of a BLDC motor.

Keywords: brushless direct current motor, BLDC motor, motor starting characteristics, motor windings, number of motor winding turns, mathematical simulation

For citation: Krivoguzova A.S., Tkachenko S.N., Shpilevoy A.A. Effect of winding and power supply parameters on the starting characteristics of an upgraded brushless DC motor. *Russian Technological Journal.* 2025;13(4):69–77. https://doi.org/10.32362/2500-316X-2025-13-4-69-77, https://www.elibrary.ru/AVHESX

Financial disclosure: The authors have no financial or proprietary interest in any material or method mentioned.

The authors declare no conflicts of interest.

НАУЧНАЯ СТАТЬЯ

Влияние параметров обмоток и источника питания на пусковые характеристики модернизированного бесщеточного двигателя постоянного тока

А.С. Кривогузова [@],
С.Н. Ткаченко,
А.А. Шпилевой

Балтийский федеральный университет имени Иммануила Канта, Калининград, 236041 Россия
[@] Автор для переписки, e-mail: krivoguzova99@bk.ru

• **Поступила:** 14.11.2024 • **Доработана:** 11.02.2025 • **Принята к опубликованию:** 27.05.2025

Резюме

Цели. Цель работы – определение оптимального количества витков в каждой из обмоток и влияния параметров обмоток и источника питания на пусковые характеристики модернизированного бесщеточного двигателя постоянного тока (brushless direct current electric motor, BLDC-двигателя).

Методы. Использованы методы натурного эксперимента на испытательном стенде, состоящем из модернизированного BLDC-двигателя, источника питания и регулятора скорости. Также использовались методы математического моделирования, решения задачи линейного программирования и аппроксимации.

Результаты. В ходе экспериментов получены зависимости пускового тока и числа оборотов на старте от числа витков в каждой из обмоток для модернизированного BLDC-двигателя. Экспериментально установлено, что количество витков в обмотках имеет предельное значение, признаками чего является пересечение кривых пускового тока и стартовых оборотов или исчезновение функциональной зависимости между пусковым током и оборотами двигателя. Разработана математическая модель модернизированного BLDC-двигателя, которая хорошо согласуется с экспериментальными результатами. Используя математическую модель, можно определить оптимальное количество витков в каждой из обмоток двигателя, а также уровень коэффициента полезного действия BLDC-двигателя. Предложена параметрическая модель, которая позволяет определить значение стартовых оборотов двигателя по значению пускового тока и напряжению батареи для диапазона витков в обмотке от 8 до 14. Данные модели позволяют определять характеристики двигателя на стадии его проектирования.

Выводы. Выявлено, что существует интервал для количества витков в каждой из обмоток BLDC-двигателя, в котором будет наблюдаться оптимум коэффициента полезного действия двигателя. Также выявлено, что для определения базовых пусковых характеристик BLDC-двигателя достаточно двух параметров, которые легко измерить на практике: пусковой ток и уровень напряжения источника питания.

Ключевые слова: BLDC-двигатель, пусковые характеристики двигателя, обмотки двигателя, количество витков в обмотках двигателя, математическая модель

Для цитирования: Кривогузова А.С., Ткаченко С.Н., Шпилевой А.А. Влияние параметров обмоток и источника питания на пусковые характеристики модернизированного бесщеточного двигателя постоянного тока. *Russian Technological Journal*. 2025;13(4):69–77. https://doi.org/10.32362/2500-316X-2025-13-4-69-77, https://www.elibrary.ru/AVHESX

Прозрачность финансовой деятельности: Авторы не имеют финансовой заинтересованности в представленных материалах или методах.

Авторы заявляют об отсутствии конфликта интересов.

INTRODUCTION

Brushless direct current (BLDC) motors find application in various industries and domains [1, 2]. At present, this type of motor can achieve efficiencies around 94%, provided that losses in the speed controller are minimized [3, 4] and battery operation is optimized [5]. The minimum set of equipment required to operate a BLDC motor involves an electronic speed controller (ESC) and a power battery to supply the speed controller, the converted voltage from which is fed to each of the three phases of the motor.

Structurally, a BLDC motor consists of a stator with windings and permanent magnets, and a rotor that rotates within the stator. 12N14P is one of the most common BLDC motor designs with 12 stator windings and 14 rotor magnetic poles. However, this is a three-phase motor comprising in reality only three, rather than 12, windings. One wire is wound around four magnets. Three-phase speed controllers are used to control such a motor. These devices are sensitive to voltage ripple, which in turn leads to sudden changes in torque and reduces efficiency [6].

The torque fluctuations can be reduced by improving the control of each individual winding [7], which enhances the stability of the system and reduces the power consumption. In this connection, one path for upgrading BLDC motors consists in increasing the number of individual windings. Thus, the researchers in [8] increased the number of windings in a five-phase motor. Such a change in the number of phases resulted in an increased stability and reliability of the motor.

Similar examples [9] demonstrate the feasibility of upgrading BLDC motor by both introducing a modified speed controller and improving the entire motor design. Instead of the conventional scheme based on three windings, 12 separate windings can be used. This allows the current in each winding to be controlled individually, providing for a more precise control of the magnetic field and torque. Such an upgrading approach improves the dynamic characteristics of the motor, reduces pulsation, ensures a more flexible adaptation to different operating modes, and increases reliability [10, 11]. This is particularly important when the motor is operated under severe conditions.

The first stage of the above work consists in upgrading a conventional BLDC motor. This requires modification of all motor windings and creating of separate leads for each of them. Consequently, the effect of the number of windings on the operating parameters of the BLDC motor, particularly on its starting characteristics, should be assessed.

The optimum number of turns in a winding is conventionally determined based on the following parameters [12]: required torque, operating frequency, resistance, and winding inductance. When shifting to 12 separate windings, it is important to consider the increase in resistance due to the increase in the number of turns, as well as the effect of their mutual inductance.

In this work, we aim to determine the optimum number of turns in each winding and the effect of winding parameters and power supply on the starting characteristics of a modernized BLDC motor.

MATERIALS AND METHODS

The BrotherHobby Avenger 2806.5 1300kV motor (BrotherHobby, China) was selected as the research object due to its similarity with the conventional 12N14P BLDC configuration. In this motor, N52H arc magnets are mounted on the rotor, the stator is made of Kawasaki 0.2 mm silicon steel, the housing material is Al 7075 aluminum alloy, and the shaft is hollow and made of titanium alloy. The motor uses a 0.75 mm copper winding.

The two motors were disassembled and rewound with copper wire of the same cross section to create 12 separate windings, each with its own separate lead. Each of the 12 windings was placed into a separate slot according to the stator layout. The original BLDC motor (left) and the upgraded motor (right) are shown in Fig. 1, where three wires coming from the original motor and 12 wires coming from the modernized motor can be seen.

In order to ensure the reproducibility of the values obtained, measurements were carried out for two engines. No differences in the performance of the first and second upgraded engines were noted.

Fig. 1. BLDC motor 2806 + 1350kV before rewinding (left) and after rewinding with the rotor removed (right)

The GW INSTEK GPD-73303S constant current source (GOOD WILL INSTRUMENT, China with a voltage error of ±(0.03% + 10 LSD) and a current error of ±(0.3% + 10 LSD)) was used as a battery power source to control the applied voltage level and to limit the maximum current at the ESC controller. A standard three-phase ESC controller was also used. The speed controller was connected to the upgraded motor by applying voltage to each of the windings, with each phase of the ESC controller applying voltage to four motor windings.

The ESC controller was characterized by an input voltage of DC 5-36 V (specific voltage equal to the nominal motor voltage), an output current of within 15 A, and a protection current of 15 A.

Measurements were conducted under different numbers of turns (from 8 to 16) in each of the motor windings with a step of 1 turn. The supply voltage was varied in the range of 5–7 V with a step of 1 V. The current limit of the power supply was set to 1 A. The selected relatively narrow voltage range is explained by the possibility of large overvoltages during the startup process and the random character of the measured inrush current values at supply voltages higher than 7 V.

The current from the source was supplied to the ESC controller, which supplies the BLDC motor via a special decoupler. The inrush current was measured at the motor input using a Tektronix DMM4020 digital universal meter (Tektronix Corporation, China) with the instrumental error of 0.015%.

A screw with a reflective strip attached to the motor shaft was used to measure the rotational speed. A DT2234A laser type digital tachometer (Shenzhen Sanpo Instrument, China) with a resolution of 1 revolution per minute (rpm) over the entire measuring range and an accuracy of ±0.05% was used.

EXPERIMENTAL RESULTS

In order to determine the optimum number of turns, the relationships between the number of turns in each of the 12 motor windings, the inrush current, and the initial rotational speed at a fixed battery voltage supplied to the motor via the speed controller were obtained (Figs. 2–4).

The inrush current is the minimum value of the current on each phase of the motor (as well as at the ESC controller output) at which the motor starts. The motor starting speed is the number of motor revolutions per minute at a current equal to the inrush value.

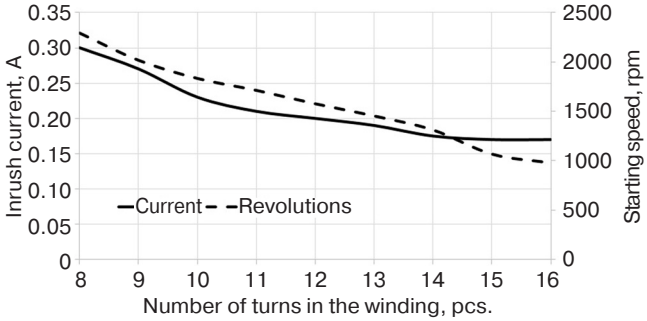

Fig. 2. Inrush current and starting speed as a function of the number of turns in each winding at 5 V battery voltage

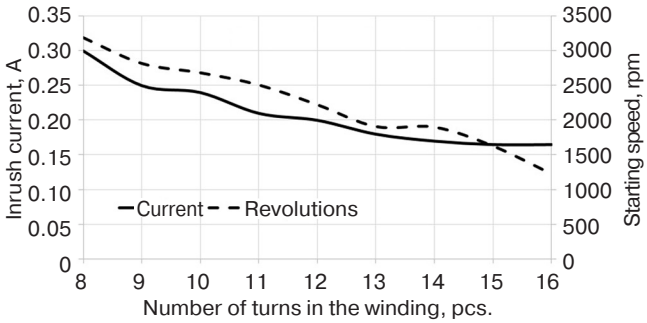

Fig. 3. Inrush current and starting speed as a function of the number of turns in each winding at 6 V battery voltage

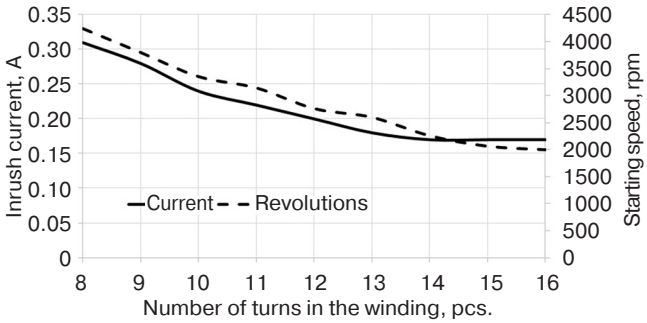

Fig. 4. Inrush current and starting speed as a function of the number of turns in each winding at 7 V battery voltage

It can be seen from Figs. 2–4 that, following 14 turns, the inrush current stabilizes and the speed decreases. This number of revolutions is the maximum permissible value. At this value, the functional dependence between inrush current and motor speed disappears. The characteristic relationship between these values is shown in Fig. 5. Under an increase in the number of turns, the inrush current ceases to change and the starting speed continues to decrease.

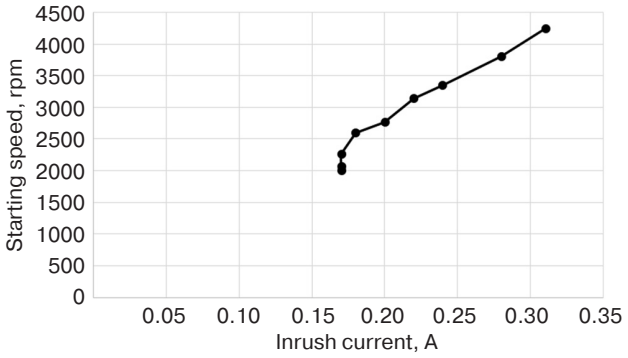

Fig. 5. Relationship between inrush current and motor starting speed at 7 V battery voltage

Figure 5 shows the presence of three points with the same value of inrush current under a decrease in the motor speed. Similar dependencies were obtained at other levels of the battery voltage studied. This fact indicates that the number of turns in each of the windings, whose number exceeds 14, is inappropriate as only increasing the losses and not improving the speed characteristics of the motor (its starting speed in particular).

Thus, it was experimentally established that the number of turns in the windings has a limiting value, the sign of which is the disappearance of a functional dependence between inrush current and motor speed (see Fig. 5). Exceeding a certain limit number of turns in each winding (14 turns in the case studied) leads to a deterioration in the performance of the BLDC motor.

SIMULATION AND DISCUSSION

In order to elucidate the dependencies obtained in the previous section, a BLDC motor model was built in the *MATLAB*[1] environment with respect to the deviations introduced by the motor elements and the ESC controller [13, 14].

In order to describe the relationships between inrush current, motor starting speed, and the number of turns, taking into account the deviations introduced by the motor elements and the ESC controller, a mathematical model that takes into account the characteristics of the system elements and the interrelationship of these parameters was developed. The model is based on the characteristics of the BLDC motor, taking the parameters of electromagnetic resistance and inductance into account.

The electrical parameters are as follows:

1. The winding resistance per phase R_{phase} and its inductance L_{phase}, which depend on the number of turns N.
2. The internal resistance R_{ESC} and inductance L_{ESC} of the controller.
3. Battery parameters: voltage V_{bat} and internal resistance R_{bat}.

The starting parameters are as follows:

1. Inrush current I_{start}.
2. Starting angular velocity ω_{start}.

The dependence of the following parameters on the number of turns was plotted:

1. Winding inductance:

$$L_{phase}(N) = k_L N^2, \quad (1)$$

where k_L is the inductance coefficient per turn, depending on the material and geometry of the winding.

2. Winding resistance:

$$R_{phase}(N) = k_R N, \quad (2)$$

where k_R is the resistance coefficient per turn.

3. Total resistance R_{total} and inductance L_{total} of the circuit:

$$R_{total} = R_{phase} + R_{ESC} + R_{bat}, \quad (3)$$

$$L_{total} = L_{phase} + L_{ESC}. \quad (4)$$

When the motor starts, the inrush current is determined by the total resistance and inductance, as well as the battery voltage. At the moment of starting, no counter electromotive force (EMF) due to zero angular velocity is observed:

$$I_{start} = \frac{V_{bat}}{R_{total}}. \quad (5)$$

Modeling the inrush current as a function of the number of turns.

Since R_{total} and L_{total} depend on the number of turns N, I_{start} can be expressed as follows:

$$I_{start}(N) = \frac{V_{bat}}{k_R N + R_{ESC} + R_{bat}}. \quad (6)$$

Modeling the starting angular velocity as a function of inrush current.

The starting angular velocity ω_{start} depends on the starting torque T_{start} generated by the inrush current. In this case, the torque is defined as follows:

$$T_{start} = K_t I_{start}, \quad (7)$$

where K_t is the motor torque constant.

Accordingly, the starting angular velocity ω_{start} is determined by the equation of motion, where the resisting forces at the starting moment do not affect its value:

$$\omega_{start} = \frac{K_t I_{start}}{J}. \quad (8)$$

[1] https://www.mathworks.com/products/matlab.html. Accessed May 19, 2025.

An increase in inertia J leads to a decrease in the starting angular velocity ω_{start}; therefore, the motor requires more time to accelerate to the initial revolutions.

It is now possible to express the dependence of I_{start} and ω_{start} by the number of turns:

$$I_{start}(N) = \frac{V_{bat}}{k_R N + R_{ESC} + R_{bat}}. \quad (9)$$

$$\omega_{start}(N) = \frac{K_t V_{bat}}{J(k_R N + R_{ESC} + R_{bat})}. \quad (10)$$

To account for variations in the system, random disturbances may be added to the resistance and inductance values:

- winding resistance $R_{phase} = (1 + \delta_R)k_R N$, where δ_R is the random variation of the winding resistance;
- winding inductance $L_{phase} = (1 + \delta_L)k_L N^2$, where δ_L is the random variation of the winding inductance.

Subsequently, taking possible variations into account:

- inrush current

$$I_{start}(N) = \frac{V_{bat}}{(1+\delta_R)k_R N + R_{ESC} + R_{bat}}, \quad (11)$$

- starting angular velocity

$$\omega_{start}(N) = \frac{K_t V_{bat}}{J((1+\delta_R)k_R N + R_{ESC} + R_{bat})}. \quad (12)$$

Angular velocity is converted to revolutions per minute (rpm) as follows:

$$RPM_{start} = \omega_{start}\frac{60}{2\pi}. \quad (13)$$

The starting speed, taking variations into account, has the following form:

$$RPM_{start}(N) = \omega_{start}(N)\frac{60}{2\pi} = \frac{K_t V_{bat} 60}{2\pi J((1+\delta_R)k_R N + R_{ESC} + R_{bat})}. \quad (14)$$

This model expresses the dependence of the motor starting speed RPM_{start} on various factors such as number of turns N, supply voltage V_{bat}, resistance R, winding inductance, and moments of inertia of the system. The motor torque T is proportional to the current flowing through the windings, taking into account the coefficient K_t which reflects the design of the motor. On starting, the motor encounters a resistive torque that is determined by the resistance of the windings and external circuits (controller R_{ESC} and battery R_{bat}), as well as by the internal friction.

The equation takes into account variations in winding resistance δ_R that may occur due to heating or other external factors. The resistance of the entire system is expressed as the sum of $(1 + \delta_R)k_R N + R_{ESC} + R_{bat}$.

Winding inductance affects the response time of the motor; however, the presented model takes the inductance into account indirectly by changing the electrical parameters (resistance and voltage drop). An increase in the number of turns N results in a decrease in the starting speed due to an increase in the total resistance of the system. An increase in the supply voltage V_{bat} increases the starting speed. Variations in the winding resistance δ_R and other system elements can significantly reduce the starting efficiency of the motor.

Therefore, the presented model shows the dependence of the starting speed on the electrical and mechanical parameters of the system. It takes the actual state of the components into account, thereby allowing the motor design to be optimized and the desired performance to be achieved.

The simulation results of the inrush current corresponding to Figs. 2–4 are shown in Fig. 6. Here, the experimental and calculated dependence of the inrush current on the number of turns at 6 V battery voltage is shown. At other battery voltages, a similar good agreement of the calculated and experimental values was observed. Thus, the constructed model is capable of describing the actual dependencies of the inrush current.

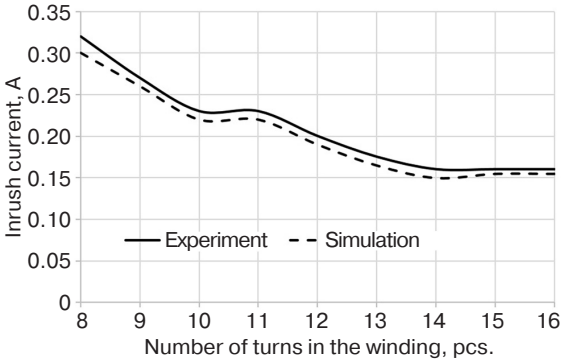

Fig. 6. Experimental and calculated dependence of the inrush current of the upgraded motor on the number of turns in each winding at 6 V battery voltage

Of particular interest are the results obtained when simulating the motor efficiency shown in Fig. 7. It can be seen that, at the number of turns less than 8 and more than 14, the efficiency values are minimal, particularly compared to the range of turns from 12 to 14. In other words, when the number of turns in the winding is low, the efficiency of the motor is also low due to the insufficient intensity of the magnetic field. When the number of turns

exceeds 14, low torque is observed due to high power losses at the winding resistance.

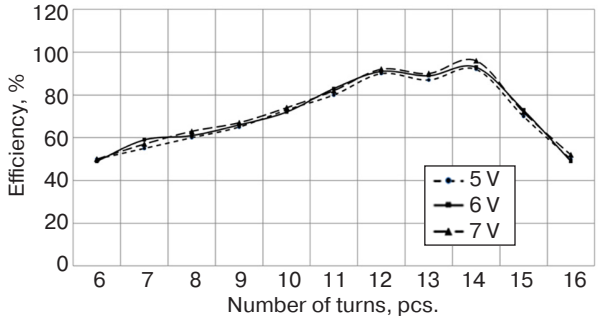

Fig. 7. Motor efficiency as a function of the number of turns in each winding at battery voltages of 5–7 V

The above results allow us to conclude that the values corresponding to 15 and 16 turns should be removed from the data series for inrush current and starting speed of the motor. At the same time, it is also unreasonable to add the values for 6 and 7 turns, since the corresponding efficiencies are too low. In this case, the full functional dependencies between starting speed and inrush current can be obtained. The dependencies of the number of turns on the inrush current and their approximations at three levels of battery voltage are shown in Fig. 8.

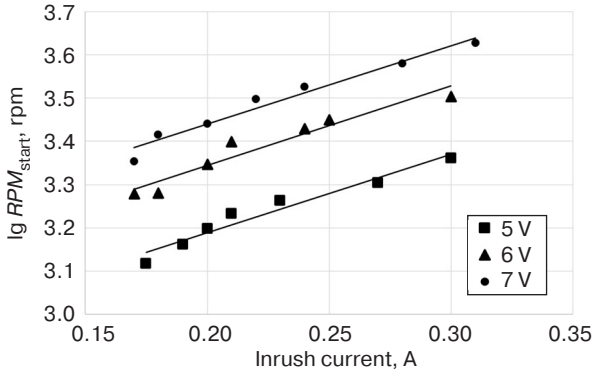

Fig. 8. Number of turns as a function of inrush current at different battery voltage levels

It can be seen that all three curves can be approximated by linear relationships [15], with the angle of inclination of these lines being the same.

In addition to the mathematical model proposed above, a parametric model allowing sufficiently simple and fast engineering calculations was developed. This model predicts the value of the starting speed RPM_{start} from the value of the inrush current I_{start} and the battery voltage V_{bat} for the range of turns in the winding from 8 to 14. As a result, the following analytical relationship was obtained:

$$\lg RPM_{start} = 1.817 I_{start} + \frac{1}{8} V_{bat} + 2.2. \qquad (15)$$

Thus, it becomes possible to calculate the starting speed from the easily measured characteristics of the inrush current and battery voltage for different numbers of turns. This facilitates the process of motor design with predetermined characteristics.

The table shows the motor revolutions calculated using formula (15) compared with the values measured experimentally for a 5 V battery.

The table shows that the relative deviation between the calculated and experimental values did not exceed 6%. For other battery voltages, the relative deviation did not exceed 9%.

Therefore, it can be concluded that the equation proposed in this work can be used to determine the motor starting speed at the design stage with sufficient accuracy for engineering calculations.

CONCLUSIONS

In this work, we propose a mathematical model for an upgraded BLDC motor, which showed good agreement with the actual prototype. This model can be used to determine the optimal number of turns in each winding by calculating the motor efficiency.

Table. Comparison of the values of the motor starting speed obtained experimentally and based on calculations according to Eq. (15) at a battery voltage of 5 V

Number of turns in each motor winding, pcs.	Inrush current, A	Motor starting speed, experiment	Motor starting speed, calculation	Relative deviation
8	0.30	2293	2345	2%
9	0.27	2017	2068	3%
10	0.23	1833	1749	5%
11	0.21	1712	1609	6%
12	0.20	1576	1543	2%
13	0.19	1452	1480	2%
14	0.175	1310	1390	6%

A parametric model to calculate the starting speed of a BLDC motor based on the values of inrush current and battery voltage was developed. The relationship between the starting speed of the upgraded motor and the basic characteristics of power supply and ESC controller, which can be easily measured, is presented. The equation obtained allows engineering calculations to be carried out at the motor design stage.

In order to obtain similar dependencies for motors of other configurations, further research and construction of appropriate mathematical models is required. In addition, the presence of the constant summand "2.2" in formula (15) assumes that not all fundamental dependencies have been discovered and that the engine revolutions might be determined by three, rather than two, physical quantities. Further research should verify this hypothesis.

Authors' contributions

A.S. Krivoguzova—literature review, deriving the calculation formulas, writing the computer programs, conducting the model calculations, plotting, and discussing the results.

S.N. Tkachenko—formulating the problem, verifying the mathematical correctness of the calculation formulas, proofreading the text of the article, and discussing the results.

A.A. Shpilevoy—formulating the problem, the idea of deriving the calculation formulas, and discussing the results.

REFERENCES

1. Moosavi S.S., Djerdir A., Amirat Y.A., Khaburi D.A. Demagnetization fault diagnosis in permanent magnet synchronous motors: A review of the state-of-the-art. *J. Magn. Magn. Mater*. 2015;391:203–212. https://doi.org/10.1016/j.jmmm.2015.04.062
2. Mohanraj D., Aruldavid R., Verma R., Sathyasekar K., Barnawi A., Chokkalingam B., Mihet-Popa L. A Review of BLDC Motor: State of Art, Advanced Control Techniques, and Applications. *IEEE Access*. 2022;10:54833–54869. https://doi.org/10.1109/ACCESS.2022.3175011
3. Nguyen Q., Tran V., Pham Q.D., Giap V.N., Trinh M. Design brushless DC motor control by using proportional-integral strategy for a smart storage cabinet system. *Int. J. Power Electron. Drive Syst*. 2023;14:708–718. https://doi.org/10.11591/ijpeds.v14.i2.pp708-718
4. Carev V., Roháč J., Tkachenko S., Alloyarov K. The Electronic Switch of Windings of a Standard BLDC Motor. *Appl. Sci*. 2022;12(21):11096. https://doi.org/10.3390/app122111096
5. Conradt R., Heidinger F., Birke K. Methodology for Determining Time-Dependent Lead Battery Failure Rates from Field Data. *Batteries*. 2021;7(2):39. https://doi.org/10.3390/batteries7020039
6. Zhu Z., Leong J. Analysis and mitigation of torsional vibration of PM brushless AC/DC drives with direct torque controller. *IEEE Trans. Ind. Appl*. 2012;48(4):1296–1306. https://doi.org/10.1109/TIA.2012.2199452
7. Premkumar K., Manikandan B.V. Adaptive Neuro-Fuzzy Inference System based speed controller for brushless DC motor. *Neurocomputing*. 2014;138:260–270. https://doi.org/10.1016/j.neucom.2014.01.038
8. Assoun I., Idkhajine L., Nahid-Mobarakeh B., Meibody-Tabar F., Monmasson E., Pacault N. Wide-Speed Range Sensorless Control of Five-Phase PMSM Drive under Healthy and Open Phase Fault Conditions for Aerospace Applications. *Energies*. 2023;16(1):279. https://doi.org/10.3390/en16010279
9. Tapre M., Karampuri R. Design and Comparison of Five-Phase Induction Motors with Different Dimensions for Heavy Duty Electric Vehicles. In: *IEEE 3rd International Conference on Sustainable Energy and Future Electric Transportation* (*SEFET*). IEEE; 2023. P. 1–6. https://doi.org/10.1109/SeFeT57834.2023.10245615
10. Xia K., Li Z., Lu J., Dong B., Bi C. Acoustic noise of brushless DC motors induced by electromagnetic torque ripple. *J. Power Electron*. 2018;17(4):963–971. https://doi.org/10.6113/JPE.2017.17.4.963
11. Viswanathan V., Seenithangom J. Commutation torque ripple reduction in the BLDC motor using modified SEPIC and three-level NPC inverter. *IEEE Trans. Power Electron*. 2018;33(1):535–546. https://doi.org/10.1109/TPEL.2017.2671400
12. Varshney A., Gupta D., Dwivedi B. Speed response of brushless DC motor using fuzzy PID controller under varying load condition. *J. Electr. Syst. Inf. Technol*. 2017;4(2):310–321. https://doi.org/10.1016/j.jesit.2016.12.014
13. Manda P., Veeramalla S.K. Brushless DC motor modeling and simulation in the MATLAB/SIMULINK software environment. *Adv. Modelling Anal. B*. 2021;64(1–4):27–33. https://doi.org/10.18280/ama_b.641-404
14. Sial M., Sahoo N. Torque ripple minimization and speed control of switched reluctance motor drives using extremum-seeking PI controller. *Electr. Eng*. 2024;106(6):7301–7322. https://doi.org/10.1007/s00202-024-02427-3
15. Harris F.E. *Mathematics for Physical Science and Engineering*. Academic Press; 2014. 944 p.

About the Authors

Alexandra S. Krivoguzova, Postgraduate Student, Higher School of Computer Science and Artificial Intelligence, Immanuel Kant Baltic Federal University (14, A. Nevskogo ul., Kaliningrad, 236041 Russia). E-mail: krivoguzova99@bk.ru. RSCI SPIN-code 6326-2294, https://orcid.org/0000-0002-4090-662X

Sergey N. Tkachenko, Cand. Sci. (Eng.), Associate Professor, Institute of High Technologies, Head of the Digital Department, Immanuel Kant Baltic Federal University (14, A. Nevskogo ul., Kaliningrad, 236041 Russia). E-mail: sntkachenko@kantiana.ru. Scopus Author ID 35750902000, RSCI SPIN-code 3717-6698, https://orcid.org/0000-0002-4708-6556

Andrey A. Shpilevoy, Cand. Sci. (Phys.-Math.), Associate Professor, Deputy Head, Institute of High Technologies, Immanuel Kant Baltic Federal University (14, A. Nevskogo ul., Kaliningrad, 236041 Russia). E-mail: ashpilevoi@kantiana.ru. Scopus Author ID 6602332593, https://orcid.org/0000-0003-2610-6551

Об авторах

Кривогузова Александра Сергеевна, аспирант, Высшая школа компьютерных наук и искусственного интеллекта, ФГАОУ ВО «Балтийский федеральный университет имени Иммануила Канта» (236041, Россия, Калининград, ул. А. Невского, д. 14). E-mail: krivoguzova99@bk.ru. SPIN-код РИНЦ 6326-2294, https://orcid.org/0000-0002-4090-662X

Ткаченко Сергей Николаевич, к.т.н., доцент ОНК «Институт высоких технологий», руководитель Цифровой кафедры, ФГАОУ ВО «Балтийский федеральный университет имени Иммануила Канта» (236041, Россия, Калининград, ул. А. Невского, д. 14). E-mail: sntkachenko@kantiana.ru. Scopus Author ID 35750902000, SPIN-код РИНЦ 3717-6698, https://orcid.org/0000-0002-4708-6556

Шпилевой Андрей Алексеевич, к.ф.-м.н., доцент, заместитель руководителя ОНК «Институт высоких технологий», ФГАОУ ВО «Балтийский федеральный университет имени Иммануила Канта» (236041, Россия, Калининград, ул. А. Невского, д. 14). E-mail: ashpilevoi@kantiana.ru. Scopus Author ID 6602332593, https://orcid.org/0000-0003-2610-6551

Translated from Russian into English by K. Nazarov
Edited for English language and spelling by Thomas A. Beavitt

Mathematical modeling

Математическое моделирование

UDC 004.02
https://doi.org/10.32362/2500-316X-2025-13-4-78-94
EDN CVZOXD

REVIEW ARTICLE

Modern optimization methods and their application features

Salbek M. Beketov [@], Daria A. Zubkova, Aleksei M. Gintciak, Zhanna V. Burlutskaya, Sergey G. Redko

Peter the Great St. Petersburg Polytechnic University, St. Petersburg, 195251 Russia
[@] Corresponding author, e-mail: salbek.beketov@spbpu.com

• **Submitted:** 29.10.2024 • **Revised:** 13.01.2025 • **Accepted:** 13.05.2025

Abstract

Objectives. The authors conduct an analytical review of available optimization methods and simulation tools to identify their key features, effectiveness, and possible applications. The aim was to form an integrated picture of modern approaches, which may facilitate decision making when selecting the most appropriate method for a particular task. The key objective was to review and classify various optimization tools, which of theoretical and practical value for developers of new models.

Methods. Scientific publications and analytical materials were retrieved from specialized databases and technical documentation libraries.

Results. The analysis and classification of existing optimization methods allowed the authors to identify their advantages, disadvantages, and application features, as well as to determine the relationship between theoretical concepts and their practical implementation. During the analysis, various optimization approaches were considered, covering both classical and modern simulation methods.

Conclusions. The importance of informed selection of optimization methods, which raise the efficiency and accuracy of simulation procedures, is highlighted. The results obtained indicate the need for further study and comparative analysis of the methods used in practice in order to establish their efficiency and applicability in various scenarios. Future research directions include experimental testing of the effectiveness of various approaches based on several models in order to determine their advantages and disadvantages for a more informed selection of the method suitable for a particular task.

Keywords: optimization methods, application features, multi-criteria optimization methods, optimization algorithms, evolutionary algorithms, optimization of digital models, optimization problem, optimization software tools

For citation: Beketov S.M., Zubkova D.A., Gintciak A.M., Burlutskaya Zh.V., Redko S.G. Modern optimization methods and their application features. *Russian Technological Journal.* 2025;13(4):78–94. https://doi.org/10.32362/2500-316X-2025-13-4-78-94, https://www.elibrary.ru/CVZOXD

Financial disclosure: The authors have no financial or proprietary interest in any material or method mentioned.

The authors declare no conflicts of interest.

ОБЗОРНАЯ СТАТЬЯ

Современные методы оптимизации и особенности их применения

С.М. Бекетов [@], **Д.А. Зубкова**, **А.М. Гинцяк**, **Ж.В. Бурлуцкая**, **С.Г. Редько**

Санкт-Петербургский политехнический университет Петра Великого, Санкт-Петербург, 195251 Россия
[@] *Автор для переписки, e-mail: salbek.beketov@spbpu.com*

• **Поступила:** 29.10.2024 • **Доработана:** 13.01.2025 • **Принята к опубликованию:** 13.05.2025

Резюме

Цели. Цель статьи – провести аналитический обзор методов и инструментов оптимизации, используемых в моделировании, для выявления их ключевых особенностей, эффективности и областей возможного применения. Исследование направлено на формирование целостной картины современных подходов, что позволит специалистам выбирать наиболее удобные методы для решения разнообразных задач. Ключевая задача – составить систематизированное представление об инструментах оптимизации, охватывающее различные методики и подходы, которые обеспечат как теоретическую, так и практическую ценность для разработки более эффективных моделей.

Методы. Для достижения поставленных целей исследование основывалось на обширной выборке научных публикаций и аналитических материалов, отобранных из специализированных баз данных и технической документации.

Результаты. Проведены анализ и классификация существующих методов оптимизации, что позволило выявить их сильные и слабые стороны, особенности применения, а также определить взаимосвязь между теоретическими концепциями и их практической реализацией. В ходе анализа рассмотрены различные подходы к оптимизации, охватывающие как классические, так и современные методы, что обеспечило всесторонний обзор применимых подходов в моделировании.

Выводы. Проведенное исследование подтверждает важность грамотного подбора методов оптимизации, что способствует более эффективному и точному моделированию. Полученные результаты подчеркивают необходимость дальнейшего изучения и сравнительного анализа методов на практике с целью более глубокого понимания их эффективности и применимости в различных условиях. Перспективы будущих исследований включают экспериментальное тестирование эффективности различных подходов на базе нескольких моделей, что позволит определить их преимущества и недостатки для более точного выбора метода в зависимости от специфики задач.

Ключевые слова: методы оптимизации, особенности применения, многокритериальные методы оптимизации, оптимизационные алгоритмы, эволюционные алгоритмы, оптимизация цифровых моделей, оптимизационная задача, программные инструменты оптимизации

Для цитирования: Бекетов С.М., Зубкова Д.А., Гинцяк А.М., Бурлуцкая Ж.В., Редько С.Г. Современные методы оптимизации и особенности их применения. *Russian Technological Journal*. 2025;13(4):78–94. https://doi.org/10.32362/2500-316X-2025-13-4-78-94, https://www.elibrary.ru/CVZOXD

Прозрачность финансовой деятельности: Авторы не имеют финансовой заинтересованности в представленных материалах или методах.

Авторы заявляют об отсутствии конфликта интересов.

INTRODUCTION

Optimization plays an important role in simulation modeling, allowing optimal results to be obtained, resources to be saved, and the quality of developed products to be improved. Optimization is becoming an essential element of modern engineering processes aimed at solving complex problems and achieving high technological standards [1]. However, to ensure the efficiency and accuracy of optimization, unnecessary repetition should be avoided while taking into account the diversity of methods and their complexity in software implementation. This is particularly important in such areas as design activity [2], energy [3], and healthcare [4], where even minor improvements may yield significant consequences.

A bibliometric analysis of optimization techniques conducted in [5, 6] described the evolution of the concept of "optimization" from trial and error to more formalized approaches. Due to the rapid progress in this direction, continued efforts are required to trace new methods for an approximate solution to optimization problems and review their computational aspects, applicability areas, and practical merits. The choice of an optimization method must be tailored to the specific features of the models. This requires consideration of the requirements for suitable methods and tools based on the nature of the models and the characteristics of the systems in order to create more flexible and adaptive conditions for the developer [7, 8].

The relevance of the analysis of optimization methods is explained by a number of factors, including the increasing complexity of sociotechnical and socioeconomic systems, the growth of computing power, and the emergence of more efficient methods [9, 10].

In this article, we carry out an analytical review of optimization methods with the purpose of their classification and assessment of their applicability in simulation modeling. Consideration of a large variety of optimization methods and their further analysis simplifies the research process and makes optimization approaches more accessible to a wider range of specialists.

RESEARCH METHODS

The aim of this literature review was to identify key optimization methods that are used in various research areas. The growing interest in model optimization problems has generated a significant amount of research over the past few years, which highlights the relevance and importance of developing efficient optimization methods.

A literature review was conducted using the databases of Scopus[1], Russian Science Citation Index[2], and the List of the Higher Attestation Commission for Academic Degrees and Titles[3] (VAK) under the Ministry of Science and Higher Education of the Russian Federation. The literature search was conducted using the following keywords: optimization type, multicriteria optimization methods, computational complexity of optimization methods, parallel computing, optimization methods, decision making, optimization algorithms, evolutionary algorithms, statistical methods, mathematical methods, simulation modeling, model optimization, optimization problem, optimization problems. The total number of articles on these queries for the period of five years comprised 434.

The analysis of the retrieved articles was performed to identify the most common optimization methods used in different research areas. Figure 1 presents the results of the conducted analysis, i.e., the ratio of published articles on the topic to the total volume over the past five years.

Model optimization methods determine the conditions of existence of an object or process under which the highest value of some property of this object or process is achieved. They are used to search for optimal solutions to various problems where it is necessary to optimize certain parameters or criteria [11].

[1] https://www.scopus.com/. Accessed October 29, 2024.

[2] Russian Science Citation Index is a database that distinguishes the best Russian journals and places them on the Web of Science platform.

[3] Higher Attestation Commission under the Ministry of Science and Higher Education of the Russian Federation. https://vak.minobrnauki.gov.ru/ (in Russ.). Accessed October 29, 2024.

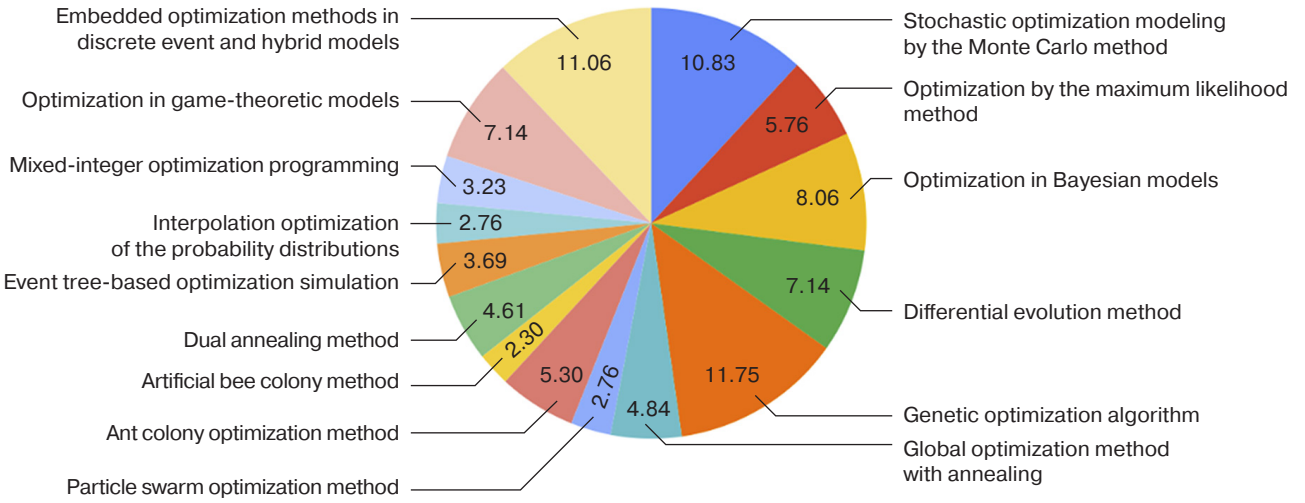

Fig. 1. Share of articles in different research areas over five years

The results offer an integrated picture of optimization methods and their classification, enabling researchers to select a specific model optimization method depending on the objectives, type of optimization, ability to account for complex target functions, and the advantages and disadvantages of the methods.

CLASSIFICATION OF OPTIMIZATION METHODS

Optimization methods can be divided into two categories: those based on the estimation of parameters of the *a posteriori* distribution, and those based on imprecise and approximation estimation. The *a posteriori* estimate is an estimate obtained empirically by performing an experiment, while the approximation estimate is an estimate approximated to real values. Within the latter, two more subgroups can be distinguished: those based on evolutionary algorithms and those based on simulation modeling. The classification of optimization methods developed by the authors is shown in Fig. 2.

Stochastic optimization modeling by Monte Carlo method

The Monte Carlo method is widely used in stochastic modeling, especially in situations where probabilistic parameters need to be taken into account. The popularity of this method is explained by the possibility of predicting different outcomes based on probabilistic factors.

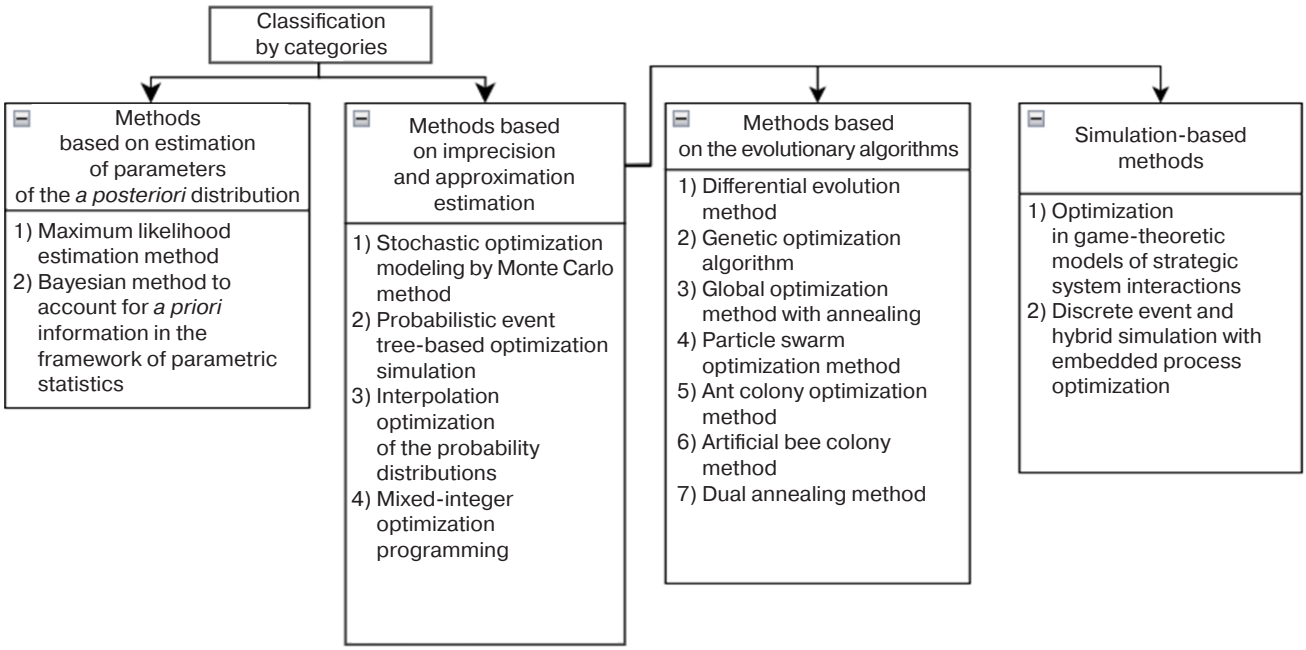

Fig. 2. Classification of optimization methods

The process of stochastic Monte Carlo modeling includes the following steps: generation of random input data, execution of simulation, generalization of results, and evaluation of phenomena, which can be generally described by the formula:

$$mc = \frac{1}{N}\sum_{i=1}^{N} f(i), \quad (1)$$

where mc is the estimation of the phenomenon by the Monte Carlo method, N is the number of the performed simulations, $f(i)$ is the result of the ith model run.

Unlike deterministic approaches that involve strict adherence to fixed algorithms, the Monte Carlo method is based on a multiple repetition of experiments (simulations) using random input data. Each run of the model yields one possible result, and the multitude of such results makes it possible to estimate the statistical distribution of outcomes and, thus, to predict probabilistic phenomena more accurately.

The process of stochastic Monte Carlo modeling includes such stages as generation of random input data, modeling, accumulation of results (the results of each individual modeling are saved), evaluation of phenomena, where statistical processing is performed on the basis of accumulated data and mean values, dispersions, probabilities of occurrence of events, and other characteristics are calculated.

The application of the Monte Carlo method is not limited to one specific area, finding application in various forecasting tasks. For example, the Monte Carlo method was used in combination with an error function in the form of a Gaussian function to predict the spread of the COVID-19 virus in Italy [12]. The authors conducted 150 Monte Carlo simulations to obtain an accurate prediction of the number of deaths in China and Italy.

The Monte Carlo method was also applied to compare the performance of multicriteria prioritization methods for selecting the sites for solar power plants in Iran [13]. The study used two reliability measures to evaluate different prioritization methods, and the Monte Carlo simulation evaluated the reliability values in each of these methods by conducting sensitivity analysis.

Optimization by the maximum likelihood estimation method

The method of maximum likelihood estimation (MLE) is a statistical approach widely used either alone or in combination with other methods to process data in research or problem solving. The method provides an estimation of unknown parameters by maximizing the likelihood function, being used for a variety of purposes [14].

The MLE method searches for the value of θ at which the likelihood function is maximized:

$$\theta_{MLE} = \arg\max_{\theta} L(\theta|X), \quad (2)$$

where X is the data sample, θ is the parametric model; $L(\theta|X)$ is the likelihood function that, for a given model, measures the probability of obtaining the observed data X given the value of the θ parameter.

This algorithm for implementing the method can be interpreted as follows: provided that the observed data can be described by a certain statistical model, MLE selects such model parameters that make the observed data the most probable ones.

The basic steps of the maximum likelihood method include defining the parametric model, formulating the likelihood function, and maximizing the likelihood function.

The maximum likelihood method is widely used in statistics to estimate parameters in various models, such as linear and generalized linear models, factor analysis, structural equation modeling, hypothesis testing, confidence interval formation, and discrete choice models. It is based on maximizing the likelihood function, which reflects the probability of selecting a particular parameter given known events. The MLE method is aimed at finding the parameters at which the results obtained by the model are most consistent with the actual data. The estimation of the parameter correctness is performed using the Akaike information criterion, which balances the model complexity and increases the validity at the optimal ratio with the maximum likelihood. The model with the minimum Akaike information criterion and the maximum likelihood value is considered the best. The following formula for the Akaike information criterion (AIC) is used:

$$AIC = -2\ln L + 2K, \quad (3)$$

where L is the value of the likelihood function of the model (conditional probability of obtaining observed data with given model parameters), K is the number of model parameters.

The AIC can be understood as a measure of the trade-off between model accuracy and its simplicity. In cases where the model is extremely complicated (e.g., contains a large number of parameters), it may produce a good fit of the data, but fail to generalize the data. The AIC criterion avoids this problem by adding a penalty for increasing the number of parameters.

Optimization in Bayesian models

Bayesian models are based on Bayes' theorem, which offers a way of updating probability estimates of model parameters based on new data. These models take

into account *a priori* information about the parameters and adjust this information to the observed data. Bayes' theorem is defined by the formula:

$$P(\boldsymbol{\theta} \mid D) = \frac{P(D \mid \boldsymbol{\theta})P(\boldsymbol{\theta})}{P(D)}, \quad (4)$$

where $\boldsymbol{\theta}$ is the vector of model parameters; D is the data set on which the model is trained; $P(\boldsymbol{\theta}|D)$ is the *a posteriori* probability of the model parameters given the data; $P(D|\boldsymbol{\theta})$ is the probability of the data given the model parameters; $P(\boldsymbol{\theta})$ is the *a priori* probability of the model parameters; $P(D)$ is the marginal probability of the data.

The application of Bayesian models begins with the specification of an *a priori* distribution that reflects the initial assumptions about the model parameters. This distribution can be informative provided the presence of evidence from previous studies, or uninformative provided the minimum initial assumptions. The likelihood ratio is then calculated, which shows the likelihood of the observed data to be observed under different parameter values. In the next step of applying Bayes' theorem, the *a priori* distribution is combined with the likelihood to obtain an *a posteriori* distribution, which reflects the updated knowledge of the model parameters after accounting for the data. The resulting *a posteriori* distribution is interpreted to estimate parameters, determine confidence intervals, and make other statistical inferences. Thus, Bayesian models are a method that enables combining *a priori* knowledge and new data for a more accurate parameter estimation [15].

Such models are used in statistical analysis, machine learning, and other areas where uncertainty must be accounted for and probability estimates updated as new data become available.

For example, [16] proposed a mathematical model for detecting anomalous observations using neural network sensitivity analysis. The use of the Bayesian approach enabled the researchers to take into account the uncertainty parameter and accumulate knowledge about the data behavior. This makes the method effective for anomaly detection in complex multidimensional data spaces, such as medical monitoring or disease prediction systems.

In the economic domain, Bayesian models are helpful in assessing the impact of tax schemes on different social groups [17]. The use of theoretical foundations of planned economy in combination with Bayesian methods enables analysis of the probabilistic effects of changes in tax policy and developing optimal taxation schemes that take into account the uncertainty of initial data and forecasts. Bayesian methods are used in the development and analysis of machine learning algorithms, especially in optimization problems.

For example, the authors [18] proposed a machine learning model for organizing employee performance in remote and hybrid modes. The Bayesian approach is effective in estimating the uncertainty of the data related to employee performance, taking into account the probability distribution of various factors such as work schedule, team interaction, and workflow features. This makes the model more adaptive and flexible.

Interpolation optimization of the probability distributions

Interpolation optimization of the probability distributions is a method that combines interpolation of data with the construction of probability distributions to fill in intermediate values between known discrete points. Splines, i.e., smooth piecewise polynomial functions that can approximate complex relationships with a high degree of accuracy, are used for this purpose.

In this approach, the key problem is to construct a function that not only passes through given points of probability distributions, but also preserves their important characteristics, such as the mathematical expectation. To construct splines, we define the following function [19]:

$$S_i = a_i + b_i(x - x_i) + \frac{c_i}{2}(x - x_i)^2 + \frac{d_i}{6}(x - x_i)^3, \quad (5)$$

where a_i, b_i, c_i, d_i are the coefficients to be determined at each of the segments; $i = \overline{1,n}$, $x_{i-1} \le x \le x_i$.

The method is applied in cases where it is necessary to predict the probability distribution values at intermediate points on the basis of discrete data. For example, in models, splines can be used for interpolation of the probability distributions in time or by the values of the parameters.

Special attention is paid to preserving the mean characteristics of the distribution. To that end, splines are used, which provide coincidence of the mathematical expectation of the approximated function with the mathematical expectation of the original distribution. This approach makes it possible to preserve statistical properties of the data, which is especially important in tasks where correct representation of probabilistic characteristics is required.

One example demonstrating the application of this approach is the study of failures of complex systems under combined loads. The work [20] described an interpolation method that enables the probability of system failure to be estimated from a limited amount of test data under different types of loads. The use of splines to interpolate failure probabilities makes it possible to recover distributions for intermediate values of load parameters while preserving the original statistical characteristics.

Another example is related to solar radiation modeling, where splines with preservation of the mean value are used for interpolation of solar activity data [21]. The author proposed an interpolation method that can correctly reconstruct the distribution of solar radiation at intermediate points of the time series, ensuring the coincidence of the mathematical expectation of the spline function with the initial average value.

Mixed-integer optimization programming

Mixed-integer programming is the following optimization task [22]:

$$\max\{\mathbf{c}^{\mathrm{T}}\mathbf{x} : \mathbf{b}^1 \le \mathbf{A}\mathbf{x} \le \mathbf{b}^2, \mathbf{d}^1 \le \mathbf{x} \le \mathbf{d}^2, x_i \in S\}, \quad (6)$$

where $\mathbf{b}^1$, $\mathbf{b}^2$, $\mathbf{c}$, $\mathbf{d}^1$, $\mathbf{d}^2 \in \mathbb{R}^m$; $\mathbf{A}$ is a real $m \times n$ -matrix; $\mathbf{x}$ is a n-vector of variables (unknowns); $S \subseteq \{1, ..., n\}$ is a set of integer variables, and x_i is a subset of S bounded by integers.

Several approaches are used in practice for solving mixed-integer programming problems.

The branch-and-bound method [23] is based on splitting the original problem into subproblems, each of which is solved separately. The main idea is to build a decision tree, where the search space is partitioned at each level, and binding is used to exclude irrelevant variants based on the solutions of previous nodes of the tree. This method is used in logistics problems where it is necessary to consider both integer and continuous variables, e.g., when optimizing delivery routes.

The method of cutting planes [24] is aimed at improving the approximate solution by adding new constraints that exclude non-integer solutions from the domain of admissible solutions. Such constraints, referred to as “cuts”, gradually refine the search domain and improve the quality of the solution. The cut method is frequently used in inventory management and resource allocation problems.

Decomposition methods [25], such as Benders’ generalized decomposition, involve breaking down a complex problem into simpler subtasks. Each of the subtasks is solved separately followed by combining the results to obtain a solution to the original problem. This approach is effective for large-scale problems, e.g., in network planning or power system modeling problems.

The study presented in [26] carried out a detailed analysis of these methods and their application in linear and nonlinear optimization problems. The specific features of each approach and their effectiveness depending on the specifics of a particular problem were the research focus. The examples include both scheduling and model optimization problems where mixed constraints need to be considered.

Event tree-based optimization simulation

A decision tree is a method for modeling, classification, and regression [27]. It is a hierarchical structure in which each node represents a test of some attribute, each branch represents the result of the test, and the leaves contain the values of the target variable or the decision. Decision trees enable the construction of models capable of making decisions based on the analysis of multiple input attributes, which makes them useful in the tasks of data analysis and forecasting.

Problems that require consideration of the time factor and probabilities of the sequence of events are solved using continuous event trees [28]. Such structures further develop the idea of decision trees and enable modeling of the temporal dependencies and probabilistic nature of events. In such trees, events are described by statistical probabilities or exponentially distributed event rates.

Events in the event tree are associated with statistical probabilities or Poisson-exponentially distributed constant rates. For example, component failures typically occur at some constant failure rate λ (constant hazard function). In the simplest case, the failure probability depends on the rate λ and the exposure time t:

$$P = 1 - \mathrm{e}^{-\lambda t}, \quad (7)$$

where $P \approx \lambda t$, if $\lambda t < 0.001$.

This formula describes the exponential distribution of events characteristic of processes that occur randomly over time, such as failures of equipment or other systems.

Continuous event trees are useful for risk assessment in projects where time-dependent chains of events are possible. For example, in project management, an event tree can model the risks associated with equipment failures or delays in the process, taking into account the probability of problems at each stage [29]. This approach provides an opportunity to predict the probable scenarios of event development and develop strategies for risk minimization.

Optimization in game-theoretic models

Game-theoretic modeling is a method of analyzing strategic interactions between participants in order to optimize their strategies [30]. This method is widely used to study situations of conflict or cooperation, where each participant seeks to maximize their gains or minimize losses depending on the decisions of other participants.

A key concept in game theory is the Nash equilibrium. A Nash equilibrium occurs when no participant has motivation to change their strategy given the selected strategies of other participants. This means that given each player’s strategy, no one has the desire to change their actions, since any deviation from the current strategy will not improve their winnings.

Mathematical formulation: (S, H) is a noncooperative game of n persons in normal form, where S is the set of pure strategies, and H is the set of wins. When each player $i \in \{1, ..., n\}$ chooses a strategy $x\{i\}$ belonging to S in the strategy profile $(x\{1\}, \ldots, (x\{n\})$, player i receives his win $H\{i\}(x)$. A strategy profile $x^*\{i\} \in S$ is a Nash equilibrium if changing one's strategy from $x^*\{i\}$ to $x\{i\}$ is not profitable for any player i, i.e., for any player i: $H_i(x^*) \geq H_i(x_i, x^*_{-i})$.

The work [31] was dedicated to solving optimization problems under uncertainty using game theory, in particular, a move-by-nature model. This model is applied when a participant (player) interacts with an external environment whose behavior cannot be controlled and which is represented as "nature" or an external uncertainty factor. Three classical criteria were used to select the most optimal strategy, including Wald, Bayes, and Hurwitz criteria.

Embedded optimization methods in discrete-event and hybrid models

Discrete-event and hybrid modeling with embedded process optimization represent methods for optimizing system processes in the context of scientific research. Discrete-event modeling enables the representation of a system as a set of entities and resources, emphasizing the changes associated with discrete events. Conversely, hybrid modeling combines discrete and continuous aspects, thus providing a more accurate reflection of the dynamics of systems [32].

Process optimization embedded in the models is an integrated mechanism aimed at automatic parameter adjustment, efficient resource management, and dynamic process adaptation during the simulation process.

This optimization approach is effective for simple variations in the parameters being varied (e.g., different discrete values of resource capacity); however, it becomes significantly more complex with the advent of differently structured process implementations. In addition, some of the existing simulation environments equipped with a built-in process optimization subsystem assume manual configuration of replications. This causes difficulties due to the large number of replications required for the task and the probability of human error; thus, the user may accidentally omit the optimal variant from the list of runs.

Hybrid modeling is being increasingly used to describe complex socioeconomic and sociotechnical systems. This approach includes combinations of basic paradigms of simulation modeling. Hybrid modeling allows the system to be considered from different perspectives, thereby providing a more complete and accurate picture of its behavior [33].

Differential evolution method

The differential evolution method is one of the evolutionary modeling methods designed to solve multidimensional optimization problems. According to the classification of optimization methods, it belongs to the class of stochastic methods due to the use of a random number generator in the process of finding a solution. It also uses some ideas of genetic algorithms; however, unlike such algorithms, it does not require working with variables in binary code.

The algorithm behind this method starts with initialization of the initial population of points (candidates), which is randomly generated in the search space. This population represents potential solutions for the optimization task [34]. The next step involves selecting three random points (vectors) from the current population. These three points will be used to create a new vector that represents a descendant in the mutation process.

Difference vector refinement is the creation of a new vector (descendant) by the difference of two random vectors multiplied by a scaling factor. This step simulates mutation, introducing diversity into the population and providing new candidates for optimization.

The next stage is crossing (crossover), where the elements of the new vector are compared with the elements of the base vector. If an element of the new vector is better (smaller) than the corresponding element of the base vector, it replaces the corresponding element of the base vector. This mechanism ensures preservation of the best characteristics of vectors in the population. Adaptability is assessed by using a target (cost) function. The new vector is evaluated, and if being better (has a lower cost) than the old vector, the new vector is accepted into the population.

The steps are repeated until a stopping criterion is reached, such as the maximum number of iterations or reaching the desired level of fitness. Thus, the differential evolution method effectively and iteratively improves the candidate population in search of an optimal solution to the optimization task.

Genetic optimization algorithm

Genetic algorithms are an evolutionary optimization method based on the mechanisms of natural selection and genetic evolution [35]. This method is aimed at finding an optimal solution to a problem by simulating the evolutionary process. The algorithm starts with initialization, which creates an initial population consisting of a set of possible solutions to the problem represented as chromosomes, where each chromosome encodes a particular solution in the search space. At each step of the algorithm, the fitness of each individual is

evaluated using a target function whose value reflects the quality of the corresponding solution. Individuals with the highest adaptability gain an advantage in the selection process for further stages of evolution.

The evolutionary process is based on the operations of selection, interbreeding, and mutation. Selection is carried out to select the best adapted individuals that form the basis of a new population. Inbreeding combines the genetic data of two parents, producing offspring with combined characteristics, which facilitates the study of new combinations of traits. Mutation introduces random changes to the genotype of individual chromosomes, enabling the exploration of new regions of the solution space and preventing the algorithm from converging prematurely into local extrema. Once these operations are applied, a new population is formed to replace the previous one. The process is repeated until a given number of iterations is reached or a solution with an acceptable level of quality is obtained.

The efficiency of genetic algorithms is largely determined by tuning the key parameters such as population size, mutation and crossing probability, and the number of iterations. These parameters regulate the balance between exploring the solution space and refining the current optimal values, which makes this approach particularly versatile.

For example, the researchers [36] considered the application of a genetic algorithm based on the theory of natural selection to solve optimization problems. The authors demonstrated the effectiveness of the proposed approach using the example of optimizing the load distribution function in resource-constrained systems. A genetic algorithm was used to find the optimal distribution of tasks among the available computational nodes in such a way as to minimize the total execution time and simultaneously balance the load between the nodes.

Global optimization method with annealing

The global optimization method with simulated annealing is a heuristic algorithm that found its inspiration in the physical process of metal annealing [37]. The method has become part of the toolbox for solving complex global optimization problems, particularly in situations where the search space may be complicated, containing many local minima or having uncertain characteristics.

The basic concept of the method simulates the process of material cooling after heating. The initial "temperature" of the algorithm determines the degree of aggressiveness of its steps in the solution space. At the initial stages of the process, the algorithm is more tolerant to random changes, which enables it to avoid getting stuck in local minima. Over time, the temperature gradually decreases, which reduces the probability of making the worst decisions, making the algorithm more focused on finding global optima.

The mechanism of operation of the global optimization method with annealing enables the algorithm to easily overcome local minima, due to random natural wandering through the solution space. This provides a wider coverage of the search for optimal solutions in complex and multidimensional spaces.

Particle swarm optimization method

The method of particle swarm optimization (PSO) is one of the heuristic algorithms inspired by the collective behavior of natural systems, such as flocks of birds or schools of fish [38]. The algorithm is used to solve optimization problems, particularly when the search space is characterized by high dimensionality, nonlinearity, and the presence of multiple local optima.

PSO is based on the idea of simulating the motion of particles, each of which represents a potential solution to the problem. Each particle is characterized by its position and velocity, which are updated at each step of the algorithm. The update is based on two key factors: the personal experience of a particle (the best position it has previously discovered) and the collective experience of the group (the best solution found among all particles). This enables particles to simultaneously explore the search space and focus on the most promising areas [39].

The PSO algorithm has several parameters, such as inertia coefficient, cognitive and social influence parameters, which determine the dynamics of particle movement and their ability to explore and search. Proper tuning of these parameters helps to balance between global exploration of the solution space and its local exploration.

Applications of the PSO method cover a wide range of optimization problems including machine learning and neural network design, finding application in various engineering and scientific fields.

Ant colony optimization method

Ant colony optimization (ACO) is a heuristic method developed based on observations of the collective behavior of ants in nature [40]. It is based on the concept of using pheromones and stigmergy to solve optimization problems. The principle of ACO is based on modeling the behavior of ants that leave a chemical trace—pheromones—when searching for food. These traces serve as a guide for other ants, increasing the probability for them to follow the same route.

One specific feature of this algorithm consists in dynamic updating of pheromone traces. In this case,

shorter and more efficient routes are reinforced by more pheromones left by ants. This mechanism enables the algorithm to gradually concentrate on the most optimal solutions, eliminating less promising routes [41]. The ACO method is effective in problems where it is necessary to explore a large space of possible solutions and select the best of them.

The application of ACO covers a wide range of optimization problems. These include, e.g., solving routing problems and finding optimal paths in networks, such as transportation systems or computer networks. Parallelization of the algorithm, which consists in dividing the work into several independent agents, makes it possible to significantly reduce computation time and make the algorithm applicable to problems with a large number of variables.

Artificial bee colony method

The artificial bee colony (ABC) method is an optimization algorithm that simulates the strategies of bees searching for food sources in nature [42]. The algorithm distinguishes three types of bees: workers, observers, and scouts.

At the initial stage, there is preliminary information about the location of food sources representing admissible solutions to the optimization task. The worker bees head to these sources, search in their vicinity, and memorize new solutions that improve the parameters of the task.

After the search phase is completed, worker bees return to the hive and relay information to observer bees about more attractive sources. The observer bees probabilistically select a source to start their search, conducting it in the same way as the worker bees. New solutions are retained only when the quality improves on the given parameters. The search process continues until a given number of iterations is reached [43].

Dual annealing method

Dual annealing is a stochastic global optimization method that is an extension of the simulated annealing algorithm [44]. The method is designed to improve the efficiency of finding the global optimum by using a local search algorithm in addition to the simulated annealing procedure. This approach improves the accuracy of finding the optimal solution, particularly in problems with a large number of local extrema.

The basic principle of dual annealing implies the initial application of the stochastic global search process based on the principles of thermodynamic annealing. Simulated annealing successfully determines the region of the solution space in which the global optimum is located, although not guaranteeing the exact solution inside this region. To overcome this limitation, the dual annealing algorithm applies a local optimization method to the solution found by simulated annealing in the final step. The local search enables the refinement of the solution found, minimizing the risk of missing the global optimum due to insufficient exploration of a limited region of the solution space.

The dual annealing algorithm is successfully applied in problems where the search space is complex and multidimensional, containing many local extrema. Dual annealing demonstrates high efficiency in engineering when solving design optimization problems, in development of complex technological systems, or in tuning hyperparameters in machine learning models. Its ability to combine the advantages of global and local search makes this method versatile and solvable.

Nevertheless, a detailed study of evolutionary optimization methods is a separate area of scientific research.

A comparative analysis of optimization methods is presented in the table.

Table. Comparison of optimization methods

Method	Type	Field of application	Advantages	Disadvantages
Stochastic optimization modeling by Monte Carlo method	Stochastic	Simulation of random processes, probability estimation, optimization of complex systems	Simple, versatile, high accuracy	Requires a large number of calculations, can be computationally expensive
Optimization by the maximum likelihood method	Deterministic	Estimation of the model parameters based on data	Accuracy, efficiency	Requires knowledge of the target function form, can be sensitive to the choice of initial values
Optimization in Bayesian models	Deterministic	Probability analysis, consideration of *a priori* data, forecasting	Accuracy, flexibility, consideration of *a priori* data	Requires knowledge of the target function form, can be computationally expensive

Table. Continued

Method	Type	Field of application	Advantages	Disadvantages
Differential evolution method	Evolutionary	Global optimization of the multivariate functions	Efficiency, resistance to local minima	Requires knowledge of the target function form, can be sensitive to parameter selection
Genetic optimization algorithm	Evolutionary	Finding optimal solutions in complex problems	Stability to local minima, solving multicriteria tasks	Requires a large number of calculations, can be computationally expensive
Global optimization method with annealing	Evolutionary	Simulation of metal annealing process to find the global minimum	Efficiency, resistance to local minima	Requires a large number of calculations, can be computationally expensive
Particle swarm optimization method	Evolutionary	Collective search for optimal solutions, simulation of the bee swarm behavior	Efficiency, resistance to local minima	Requires a large number of calculations, can be computationally expensive
Ant colony optimization method	Evolutionary	Shortest paths search, route optimization	Efficiency, resistance to local minima	Requires a large number of calculations, can be computationally expensive
Artificial bee colony method	Evolutionary	Simulating the behavior of scout bees and forager bees to find solutions	Efficiency, resistance to local minima	Requires a large number of calculations, can be computationally expensive
Dual annealing method	Evolutionary	Use of two temperature modes	Efficiency, resistance to local minima	Requires a large number of calculations, can be computationally expensive
Event tree-based optimization simulation	Stochastic	Risk analysis, assessment of event occurrence probability	Accuracy, flexibility	Requires knowledge of the target function form, can be computationally expensive
Interpolation optimization of the probability distributions	Stochastic	Modeling of complex probability distributions	Accuracy, flexibility	Requires knowledge of the target function form, can be computationally expensive
Mixed-integer optimization programming	Deterministic	Solving optimization tasks with discrete variables	Accuracy, efficiency	Requires knowledge of the target function form, can be computationally expensive
Optimization in game-theoretic models	Deterministic	Analysis and optimization of strategies in the competitive environment	Accuracy, flexibility	Requires knowledge of the target function form, can be computationally expensive
Discrete event and hybrid models	Stochastic	Optimization of dynamic systems with discrete events	Accuracy, flexibility	Requires knowledge of the target function form, can be computationally expensive

Stochastic methods are used in various fields due to their capacity to estimate model parameters, account for various probabilistic factors, and for model fitting.

In deterministic optimization methods, the process is completely defined and predictable. Deterministic optimization algorithms seek to find a solution by following a strictly defined set of rules or procedure.

Evolutionary algorithms work by creating candidate populations, subjecting them to evolutionary operators such as crossbreeding, mutation, and selection to gradually improve the population toward the optimization of a given function. The methods can also be used for multicriteria optimization when multiple target functions need to be considered.

On the basis of the conducted review, the following algorithm for selecting the necessary optimization method can be proposed:

- first, determine the quality of the input data, completeness of the sample, and the number of attributes to be considered;
- then, select a group of methods based on *a posteriori* or approximation estimation;
- consider the application area, estimate the complexity of the system, and select the optimization object;
- finally, select the method depending on the task and expected results.

CONCLUSIONS

In this article, we carry out an analytical review of optimization methods and provide their classification. The methods under consideration are distinguished into two main groups: those based on the estimation of *a posteriori* distribution parameters, and those based on an inaccurate and approximation estimation. The advantages and disadvantages of each method in terms of its applicability in simulation modeling are discussed.

The results of the study can be used when conducting scientific research in the field of model optimization problems and for the practical tasks of developing models and decision-support systems on their basis.

Future research should be aimed at a detailed study of evolutionary optimization methods and a comparison of the performance and applicability of optimization methods based on various models.

ACKNOWLEDGMENTS

The research was supported by the Ministry of Science and Higher Education of the Russian Federation (State Assignment No. 075-03-2025-256 dated January 16, 2025).

Authors' contribution

All authors equally contributed to the research work.

REFERENCES

1. Kosmacheva I.M., Davidyuk N.V., Sibikina I.V., Kuchin I.Yu. The model for evaluating the effectiveness of an information security system configuration based on genetic algorithms. *Modelirovanie, optimizatsiya i informatsionnye tekhnologii = Modeling, Optimization and Information Technology*. 2020;8(3):40–41 (in Russ.). https://doi.org/10.26102/2310-6018/2020.30.3.022
2. Beketov S.M., Pospelov K.N., Redko S.G. A human capital simulation model in innovation projects. *Control Sci.* 2024;3: 16–25. http://doi.org/10.25728/cs.2024.3.2
   [Original Russian Text: Beketov S.M., Pospelov K.N., Redko S.G. A human capital simulation model in innovation projects. *Problemy upravleniya.* 2024;3:20–31 (in Russ.). http://doi.org/10.25728/pu.2024.3.2]
3. Kenden K.V., Kuznetsov A.V. Particle swarm optimisation for the structure of an autonomous solar energy complex. *Vestnik Irkutskogo gosudarstvennogo tekhnicheskogo universiteta = Proceedings of Irkutsk State Technical University*. 2020;24(3):616–626 (in Russ.). https://doi.org/10.21285/1814-3520-2020-3-616-626
4. Filippova K.A., Redko S.G. The use of the simulation modeling method in a medical institution in order to optimize the movement of patients under the constraints of the COVID-19 pandemic. *Voprosy ustoichivogo razvitiya obshchestva*. 2023:(4 MKVG) (in Russ.). https://doi.org/10.34755/IROK.2022.61.82.009
5. Van Thieu N., Mirjalili S. MEALPY: An open-source library for latest meta-heuristic algorithms in Python. *J. Syst. Architecture.* 2023;139:102871. https://doi.org/10.1016/j.sysarc.2023.102871
6. Dalavi A.M., Gomes A., Husain A.J. Bibliometric analysis of nature inspired optimization techniques. *Comput. Ind. Eng.* 2022;169:108161. https://doi.org/10.1016/j.cie.2022.108161
7. Nagpal A., Gabrani G. Python for data analytics, scientific and technical applications. In: *2019 Amity International Conference on Artificial Intelligence* (*AICAI*). IEEE; 2019. P. 140–145. https://doi.org/10.1109/AICAI.2019.8701341
8. Gintciak A.M., Bolsunovskaya M.V., Burlutskaya Z.V., Petryaeva A.A. Hybrid Simulation as a Key Tool for Socio-economic Systems Modeling. In: Vasiliev Y.S., Pankratova N.D., Volkova V.N., Shipunova O.D., Lyabakh N.N. (Eds.). *System Analysis in Engineering and Control.* Book Series: *Lecture Notes in Networks and Systems*. Springer; 2022. V. 442. P. 262–272. https://doi.org/10.1007/978-3-030-98832-6_23
9. Nikolaev S.V. Multidimensional and systematic digital transformation: sustainable development on the example of the transport industry. *E-Management.* 2023;6(3):39–50 (in Russ.). https://doi.org/10.26425/2658-3445-2023-6-3-39-50
10. Lychkina N. Modelling of Developing Socio-economic Systems Using Multiparadigm Simulation Modelling: Advancing Towards Complexity Theory and Synergetics. In: Perko I., Espejo R., Lepskiy V., Novikov D.A. (Eds.). *World Organization of Systems and Cybernetics 18. Congress-WOSC2021*. Book Series: *Lecture Notes in Networks and Systems*. Springer; 2022. V. 495. P. 191–204. https://doi.org/10.1007/978-3-031-08195-8_19
11. Pevneva A.G., Kalinkina M.E. *Metody optimizatsii* (*Optimization Methods*). St. Petersburg: ITMO University; 2022. 64 p. (in Russ.).

12. Ciufolini I., Paolozzi A. Mathematical prediction of the time evolution of the COVID-19 pandemic in Italy by a Gauss error function and Monte Carlo simulations. *Eur. Phys. J. Plus.* 2020;135(4):355. https://doi.org/10.1140/epjp/s13360-020-00383-y
13. Kannan D., Moazzeni S., Darmian S.M. A hybrid approach based on MCDM methods and Monte Carlo simulation for sustainable evaluation of potential solar sites in east of Iran. *J. Clean. Product.* 2021;279:122368. https://doi.org/10.1016/j.jclepro.2020.122368
14. Xue H., Shen X., Pan W. Constrained maximum likelihood-based Mendelian randomization robust to both correlated and uncorrelated pleiotropic effects. *Am. J. Human Genet.* 2021;108(7):1251–1269. https://doi.org/10.1016/j.ajhg.2021.05.014
15. Lomivorotov R.V. The use of Bayesian methods for the analysis of monetary policy in Russia. *Prikladnaya ekonometrika = Applied Econometrics*. 2015;38(2):41–63 (in Russ.).
16. Scheglevatych R.V., Sysoev A.S. Mathematical model to detect anomalies using Sensitivity Analysis applying to neural network. *Modelirovanie, optimizatsiya i informatsionnye tekhnologii = Modeling, Optimization and Information Technology*. 2022;8(1):14 (in Russ.). https://doi.org/10.26102/2310-6018/2020.28.1.020
17. Manashirov E.S. Theoretical framework of a planned economy and taxation: analysis of the effect on the middle class and optimization of tax schemes. *Innovatsii i investitsii = Innovations and Investments*. 2023;10:272–276 (in Russ.).
18. Vasileva E.V., Gromova A.A., Vishnevskaya N.A. Machine learning model for optimizing the organization of work of office employees in remote and hybrid modes. *Innovatsii i investitsii = Innovations and Investments*. 2023;5:288–295 (in Russ.).
19. Glotov A.F. *Nachala matematicheskogo modelirovaniya v elektronike* (*Beginnings of MAthematical Modeling in Electronics*). Tomsk: Tomsk Polytechnic University; 2017. 363 p. (in Russ.).
20. Goryunov O.V., Kurikov N.N., Egorov K.A. Interpolation method to evaluate the possibility of failure in case of complex load. *Trudy NGTU im. R.E. Alekseeva = Transactions of NNSTU n.a. R.E. Alekseev*. 2023;1(140):42–52 (in Russ.).
21. Ruiz-Arias J.A. Mean-preserving interpolation with splines for solar radiation modeling. *Solar Energy.* 2022;248:121–127. https://doi.org/10.1016/j.solener.2022.10.038
22. Bourguignon S., Ninin J., Carfantan H., Mongeau M. Exact sparse approximation problems via mixed-integer programming: Formulations and computational performance. *IEEE Trans. Signal Process.* 2015;64(6):1405–1419. https://doi.org/10.1109/TSP.2015.2496367
23. Ponz-Tienda J.L., Salcedo-Bernal A., Pellicer E. A parallel branch and bound algorithm for the resource leveling problem with minimal lags. *Comput. Aided Civil Infrastruct. Eng*. 2017;32(6):474–498. https://doi.org/10.1111/mice.12233
24. Bertsimas D., Tsitsiklis J.N. Integer programming methods. In: *Introduction to Linear Optimization*. Belmont, MA: Athena Scientific; 1997. V. 6. P. 479–530.
25. Bolusani S., Ralphs T.K. A framework for generalized Benders' decomposition and its application to multilevel optimization. *Math. Program*. 2022;196(1):389–426. https://doi.org/10.1007/s10107-021-01763-7
26. Kleinert T., Labbé M., Ljubić I., Schmidt M. A survey on mixed-integer programming techniques in bilevel optimization. *EURO J. Computational Opt*. 2021;9(2):100007. https://doi.org/10.1016/j.ejco.2021.100007
27. Kondratov D.V., Volodin D.N. Mathematical modeling of machine learning algorithms. *Matematicheskoe modelirovanie, komp'yuternyi i naturnyi eksperiment v estestvennykh naukakh*. 2023;2:2–7 (in Russ.). https://doi.org/10.24412/2541-9269-2023-2-02-07
28. Sprague C.I., Ögren P. Continuous-time behavior trees as discontinuous dynamical systems. *IEEE Control Syst. Lett.* 2021;6:1891–1896. https://doi.org/10.1109/LCSYS.2021.3134453
29. Phiri D., Simwanda M., Nyirenda V.R., et al. Decision tree algorithms for developing rulesets for object-based land cover classification. *ISPRS Int. J. Geo-Inf*. 2020;9(5):329. https://doi.org/10.3390/ijgi9050329
30. Belozerov S., Sokolovskaya E. The game-theoretic approach to modeling the conflict of interests: The economic sanctions. *Terra Economicus*. 2022;20(1):65–80 (in Russ.). http://doi.org/10.18522/2073-6606-2022-20-1-65-80
31. Petrichenko D.G., Petrichenko G.S. Solving real estate situational problems in conditions of uncertainty. *Vestnik Akademii znanii = Bulletin of the Academy of Knowledge*. 2023;54(1):400–405 (in Russ.).
32. Makarov V.L., Bakhtizin A.R., Beklaryan G.L., Akopov A.S. Digital plant: *methods of discrete-event modeling and optimization of production characteristics. Biznes-informatika = Business Informatics.* 2021;15(2):7–20 (in Russ.). http://doi.org/10.17323/2587-814X.2021.2.7.20
33. Bolsunovskaya M.V., Gintsyak A.M., Burlutskaya Zh.V., Petryaeva A.A., Zubkova D.A., Uspenskii M.B., Seledtsova I.A. The opportunities of using a hybrid approach for modeling socio-economic and sociotechnical systems. *Vestnik VGU. Seriya: Sistemnyi analiz i informatsionnye tekhnologii = Proceedings of Voronezh State University. Series: Systems Analysis and Information Technologies.* 2022.;3:73–86 (in Russ.). https://doi.org/10.17308/sait/1995-5499/2022/3/73-86
34. Ahmad M.F., Isa N.A.M., Lim W.H., Ang K.M. Differential evolution: A recent review based on state-of-the-art works. *Alexandria Eng. J.* 2022;61(5):3831–3872. https://doi.org/10.1016/j.aej.2021.09.013
35. Holodkov D.V. Analysis of features of application of genetic algorithms. *Vestnik nauki.* 2024;4(4–73):678–682 (in Russ.).
36. Albadr M.A., Tiun S., Al-Dhief F.T., Ayob M. Genetic algorithm based on natural selection theory for optimization problems. *Symmetry.* 2020;12(11):1758. https://doi.org/10.3390/sym12111758
37. Kostin A.S., Maiorov N.N. Research of models and methods for routing and practical implementation of autonomous movement by unmanned transport systems for cargo delivery. *Vestnik Gosudarstvennogo universiteta morskogo i rechnogo flota imeni admirala S.O. Makarova*. 2023;15(3):524–536 (in Russ.). https://doi.org/10.21821/2309-5180-2023-15-3-524-536

38. Slovokhotov Yu.L., Novikov D.A. Distributed intelligence of multi-agent systems. Part II: Collective intelligence of social systems. *Control Sci.* 2023;6:2–17. https://doi.org/10.25728/cs.2023.6.1
[Original Russian Text: Slovokhotov Yu.L., Novikov D.A. Distributed intelligence of multi-agent systems. Part II: Collective intelligence of social systems. *Problemy upravleniya.* 2023;6:3–21 (in Russ.). https://doi.org/10.25728/pu.2023.6.1]
39. Gad A.G. Particle swarm optimization algorithm and its applications: a systematic review. *Arch. Computat. Methods Eng*. 2022;29(5):2531–2561. https://doi.org/10.1007/s11831-021-09694-4
40. Kuliev E.V., Zaporozhets D.Yu., Kravchenko Yu.A., Semenova M.M. Solution of the problem of intellectual data analysis based on bioinspired algorithm. *Izvestiya Yuzhnogo federal'nogo universiteta. Tekhnicheskie nauki = Izvestiya SFedU. Engineering sciences*. 2021;6(223):89–99 (in Russ.). https://doi.org/10.18522/2311-3103-2021-6-89-99
41. Dorigo M., Stützle T. Ant colony optimization: overview and recent advances. In book: Gendreau M., Potvin J.Y. (Eds.). *Handbook of Metaheuristics. International Series in Operations Research & Management Science*. Springer; 2019. P. 311–351.https://doi.org/10.1007/978-1-4419-1665-5_8
42. Kureychik V.V., Rodzin S.I. Computational models of evolutionary and swarm bio heuristics (Review). *Informatsionnye tekhnologii = Information Technologies*. 2021;27(1):507–520 (in Russ.). https://doi.org/10.17587/it.27.507-520
43. Almufti S.M., Alkurdi A.A.H., Khoursheed E.A. Artificial Bee Colony Algorithm Performances in Solving Constraint-Based Optimization Problem. *Telematique.* 2022;21(1):6785–6799.
44. Lee J., Perkins D. A simulated annealing algorithm with a dual perturbation method for clustering. *Pattern Recogn.* 2021;112:107713. https://doi.org/10.1016/j.patcog.2020.107713

СПИСОК ЛИТЕРАТУРЫ

1. Космачева И.М., Давидюк Н.В., Сибикина И.В., Кучин И.Ю. Модель оценки эффективности конфигурации системы защиты информации на базе генетических алгоритмов. *Моделирование, оптимизация и информационные технологии*. 2020;8(3):40–41. https://doi.org/10.26102/2310-6018/2020.30.3.022
2. Бекетов С.М., Поспелов К.Н., Редько С.Г. Имитационная модель человеческого капитала в инновационных проектах. *Проблемы управления*. 2024;3:20–31. http://doi.org/10.25728/pu.2024.3.2
3. Кенден К.В., Кузнецов А.В. Оптимизация методом роя частиц структуры автономного энергетического комплекса с использованием солнечной энергии. *Вестник Иркутского государственного технического университета*. 2020;24(3):616–626. https://doi.org/10.21285/1814-3520-2020-3-616-626
4. Филиппова К.А., Редько С.Г. Использование метода имитационного моделирования в медицинском учреждении с целью оптимизации перемещения пациентов в условиях ограничений пандемии COVID-19. *Вопросы устойчивого развития общества*. 2023;(4 МКВГ). https://doi.org/10.34755/IROK.2022.61.82.009
5. Van Thieu N., Mirjalili S. MEALPY: An open-source library for latest meta-heuristic algorithms in Python. *J. Syst. Architecture.* 2023;139:102871. https://doi.org/10.1016/j.sysarc.2023.102871
6. Dalavi A.M., Gomes A., Husain A.J. Bibliometric analysis of nature inspired optimization techniques. *Comput. Ind. Eng.* 2022;169:108161. https://doi.org/10.1016/j.cie.2022.108161
7. Nagpal A., Gabrani G. Python for data analytics, scientific and technical applications. In: *2019 Amity International Conference on Artificial Intelligence* (*AICAI*). IEEE; 2019. P. 140–145. https://doi.org/10.1109/AICAI.2019.8701341
8. Gintciak A.M., Bolsunovskaya M.V., Burlutskaya Z.V., Petryaeva A.A. Hybrid Simulation as a Key Tool for Socio-economic Systems Modeling. In: Vasiliev Y.S., Pankratova N.D., Volkova V.N., Shipunova O.D., Lyabakh N.N. (Eds.). *System Analysis in Engineering and Control.* Book Series: *Lecture Notes in Networks and Systems*. Springer; 2022. V. 442. P. 262–272. https://doi.org/10.1007/978-3-030-98832-6_23
9. Николаев С.В. Многоаспектность и системность цифровой трансформации: устойчивое развитие на примере транспортного комплекса. *E-Management.* 2023;6(3):39–50. https://doi.org/10.26425/2658-3445-2023-6-3-39-50
10. Lychkina N. Modelling of Developing Socio-economic Systems Using Multiparadigm Simulation Modelling: Advancing Towards Complexity Theory and Synergetics. In: Perko I., Espejo R., Lepskiy V., Novikov D.A. (Eds.). *World Organization of Systems and Cybernetics 18*. *Congress-WOSC2021*. Book Series: *Lecture Notes in Networks and Systems*. Springer; 2022. V. 495. P. 191–204. https://doi.org/10.1007/978-3-031-08195-8_19
11. Певнева А.Г., Калинкина М.Е. *Методы оптимизации*. СПб.: Университет ИТМО; 2020. 64 с.
12. Ciufolini I., Paolozzi A. Mathematical prediction of the time evolution of the COVID-19 pandemic in Italy by a Gauss error function and Monte Carlo simulations. *Eur. Phys. J. Plus.* 2020;135(4):355. https://doi.org/10.1140/epjp/s13360-020-00383-y
13. Kannan D., Moazzeni S., Darmian S.M. A hybrid approach based on MCDM methods and Monte Carlo simulation for sustainable evaluation of potential solar sites in east of Iran. *J. Clean. Product.* 2021;279:122368. https://doi.org/10.1016/j.jclepro.2020.122368
14. Xue H., Shen X., Pan W. Constrained maximum likelihood-based Mendelian randomization robust to both correlated and uncorrelated pleiotropic effects. *Am. J. Human Genet.* 2021;108(7):1251–1269. https://doi.org/10.1016/j.ajhg.2021.05.014
15. Ломиворотов Р.В. Использование байесовских методов для анализа денежно-кредитной политики в России. *Прикладная эконометрика*. 2015;38(2):41–63.
16. Щеглеватых Р.В., Сысоев А.С. Математическая модель обнаружения аномальных наблюдений с использованием анализа чувствительности нейронной сети. *Моделирование, оптимизация и информационные технологии*. 2020;8(1):14. https://doi.org/10.26102/2310-6018/2020.28.1.020

17. Манаширов Э.С. Теоретические рамки плановой экономики и налогообложения: анализ эффекта на средний класс и оптимизация налоговых схем. *Инновации и инвестиции.* 2023;10:272–276.
18. Васильева Е.В., Громова А.А., Вишневская Н.А. Модель машинного обучения для оптимизации организации работы сотрудников офиса в удаленном и гибридном режимах. *Инновации и инвестиции.* 2023;5:288–295.
19. Глотов А.Ф. *Начала математического моделирования в электронике*. Томск: Изд-во Томского политехнического университета; 2017. 363 с.
20. Горюнов О.В., Куриков Н.Н., Егоров К.А. Интерполяционный метод оценки вероятности отказа при сложном нагружении. *Труды НГТУ им. Р.Е. Алексеева*. 2023;1(140):42–52.
21. Ruiz-Arias J.A. Mean-preserving interpolation with splines for solar radiation modeling. *Solar Energy.* 2022;248:121–127. https://doi.org/10.1016/j.solener.2022.10.038
22. Bourguignon S., Ninin J., Carfantan H., Mongeau M. Exact sparse approximation problems via mixed-integer programming: Formulations and computational performance. *IEEE Trans. Signal Process.* 2015;64(6):1405–1419. https://doi.org/10.1109/TSP.2015.2496367
23. Ponz-Tienda J.L., Salcedo-Bernal A., Pellicer E. A parallel branch and bound algorithm for the resource leveling problem with minimal lags. *Comput. Aided Civil Infrastruct. Eng*. 2017;32(6):474–498. https://doi.org/10.1111/mice.12233
24. Bertsimas D., Tsitsiklis J.N. Integer programming methods. In: *Introduction to Linear Optimization*. Belmont, MA: Athena Scientific; 1997. V. 6. P. 479–530.
25. Bolusani S., Ralphs T.K. A framework for generalized Benders' decomposition and its application to multilevel optimization. *Math. Program*. 2022;196(1):389–426. https://doi.org/10.1007/s10107-021-01763-7
26. Kleinert T., Labbé M., Ljubić I., Schmidt M. A survey on mixed-integer programming techniques in bilevel optimization. *EURO J. Computational Opt*. 2021;9(2):100007. https://doi.org/10.1016/j.ejco.2021.100007
27. Кондратов Д.В., Володин Д.Н. Математическое моделирование алгоритмов машинного обучения. *Математическое моделирование, компьютерный и натурный эксперимент в естественных науках.* 2023;2:2–7. https://doi.org/10.24412/2541-9269-2023-2-02-07
28. Sprague C.I., Ögren P. Continuous-time behavior trees as discontinuous dynamical systems. *IEEE Control Syst. Lett.* 2021;6:1891–1896. https://doi.org/10.1109/LCSYS.2021.3134453
29. Phiri D., Simwanda M., Nyirenda V.R., et al. Decision tree algorithms for developing rulesets for object-based land cover classification. *ISPRS Int. J. Geo-Inf*. 2020;9(5):329. https://doi.org/10.3390/ijgi9050329
30. Белозёров С.А., Соколовская Е.В. Теоретико-игровой подход к моделированию конфликта интересов: экономические санкции. *Terra Economicus*. 2022;20(1):65–80. http://doi.org/10.18522/2073-6606-2022-20-1-65-80
31. Петриченко Д.Г., Петриченко Г.С. Решение ситуационных задач в сфере недвижимости в условиях неопределенности. *Вестник Академии знаний*. 2023;54(1):400–405.
32. Макаров В.Л., Бахтизин А.Р., Бекларян Г.Л., Акопов А.С. Цифровой завод: методы дискретно-событийного моделирования и оптимизации производственных характеристик. *Бизнес-информатика*. 2021;15(2):7–20. http://doi.org/10.17323/2587-814X.2021.2.7.20
33. Болсуновская М.В., Гинцяк А.М., Бурлуцкая Ж.В., Петряева А.А., Зубкова Д.А., Успенский М.Б., Селедцова И.А. Возможности применения гибридного подхода в моделировании социально-экономических и социотехнических систем. *Вестник ВГУ. Серия: Системный анализ и информационные технологии.* 20224(3):73–86. https://doi.org/10.17308/sait/1995-5499/2022/3/73-86
34. Ahmad M.F., Isa N.A.M., Lim W.H., Ang K.M. Differential evolution: A recent review based on state-of-the-art works. *Alexandria Eng. J.* 2022;61(5):3831–3872. https://doi.org/10.1016/j.aej.2021.09.013
35. Холодков Д.В. Анализ особенностей применения генетических алгоритмов. *Вестник науки*. 2024;4(4–73):678–682.
36. Albadr M.A., Tiun S., Al-Dhief F.T., Ayob M. Genetic algorithm based on natural selection theory for optimization problems. *Symmetry.* 2020;12(11):1758. https://doi.org/10.3390/sym12111758
37. Костин А.С., Майоров Н.Н. Исследование моделей и методов маршрутизации и практического выполнения автономного движения беспилотными транспортными системами для доставки грузов. *Вестник Государственного университета морского и речного флота имени адмирала С.О. Макарова.* 2023;15(3):524–536. https://doi.org/10.21821/2309-5180-2023-15-3-524-536
38. Словохотов Ю.Л., Новиков Д.А. Распределенный интеллект мультиагентных систем. Ч. 2. Коллективный интеллект социальных систем. *Проблемы управления*. 2023;6:3–21. https://doi.org/10.25728/pu.2023.6.1
39. Gad A.G. Particle swarm optimization algorithm and its applications: a systematic review. *Arch. Computat. Methods Eng*. 2022;29(5):2531–2561. https://doi.org/10.1007/s11831-021-09694-4
40. Кулиев Э.В., Запорожец Д.Ю., Кравченко Ю.А., Семенова М.М. Решение задачи интеллектуального анализа данных на основе биоинспирированного алгоритма. *Известия Южного федерального университета. Технические науки.* 2021;6(223):89–99. https://doi.org/10.18522/2311-3103-2021-6-89-99
41. Dorigo M., Stützle T. Ant colony optimization: overview and recent advances. In: Gendreau M., Potvin J.Y. (Eds.). *Handbook of Metaheuristics. International Series in Operations Research & Management Science*. Springer; 2019. P. 311–351. https://doi.org/10.1007/978-1-4419-1665-5_8
42. Курейчик В.В., Родзин С.И. Вычислительные модели эволюционных и роевых биоэвристик (обзор). *Информационные технологии*. 2021;27(10):507–520. https://doi.org/10.17587/it.27.507-520

43. Almufti S.M., Alkurdi A.A.H., Khoursheed E.A. Artificial Bee Colony Algorithm Performances in Solving Constraint-Based Optimization Problem. *Telematique.* 2022;21(1):6785–6799.
44. Lee J., Perkins D. A simulated annealing algorithm with a dual perturbation method for clustering. *Pattern Recogn.* 2021;112:107713. https://doi.org/10.1016/j.patcog.2020.107713

About the Authors

Salbek M. Beketov, Analyst, Laboratory of Digital Modeling of Industrial Systems, Peter the Great St. Petersburg Polytechnic University (29, Politekhnicheskaya ul., St. Petersburg, 195251 Russia). E-mail: salbek.beketov@spbpu.com. ResearcherID KAM-0488-2024, RSCI SPIN-code 6717-9810, https://orcid.org/0009-0009-6448-9486

Daria A. Zubkova, Junior Researcher, Laboratory of Digital Modeling of Industrial Systems, Peter the Great St. Petersburg Polytechnic University (29, Politekhnicheskaya ul., St. Petersburg, 195251 Russia). E-mail: daria.zubkova@spbpu.com. Scopus Author ID 58045650200, RSCI SPIN-code 8130-5458, https://orcid.org/0000-0003-1106-5080

Aleksei M. Gintciak, Cand. Sci. (Eng.), Head of the Laboratory of Digital Modeling of Industrial Systems, Peter the Great St. Petersburg Polytechnic University (29, Politekhnicheskaya ul., St. Petersburg, 195251 Russia). E-mail: aleksei.gintciak@spbpu.com. Scopus Author ID 57203897426, ResearcherID W-8013-2019, RSCI SPIN-code 9339-2635, https://orcid.org/0000-0002-9703-5079

Zhanna V. Burlutskaya, Junior Researcher, Laboratory of Digital Modeling of Industrial Systems, Peter the Great St. Petersburg Polytechnic University (29, Politekhnicheskaya ul., St. Petersburg, 195251 Russia). E-mail: zhanna.burlutskaya@spbpu.com. Scopus Author ID 57645600200, ResearcherID AGC-6277-2022, RSCI SPIN-code 1310-2126, https://orcid.org/0000-0002-5680-1937

Sergey G. Redko, Director of the Higher School of Project Management and Innovation in Industry, Peter the Great St. Petersburg Polytechnic University (29, Politekhnicheskaya ul., St. Petersburg, 195251 Russia). E-mail: redko_sg@spbstu.ru. Scopus Author ID 57211475098, RSCI SPIN-code 3501-2403, https://orcid.org/0000-0002-4343-4154

Об авторах

Бекетов Сальбек Мустафаевич, аналитик, лаборатория «Цифровое моделирование индустриальных систем», ФГАОУ ВО «Санкт-Петербургский политехнический университет Петра Великого» (195251, Россия, Санкт-Петербург, ул. Политехническая, д. 29). E-mail: salbek.beketov@spbpu.com. ResearcherID KAM-0488-2024, SPIN-код РИНЦ 6717-9810, https://orcid.org/0009-0009-6448-9486

Зубкова Дарья Андреевна, младший научный сотрудник, лаборатория «Цифровое моделирование индустриальных систем», ФГАОУ ВО «Санкт-Петербургский политехнический университет Петра Великого» (195251, Россия, Санкт-Петербург, ул. Политехническая, д. 29). E-mail: daria.zubkova@spbpu.com. Scopus Author ID 58045650200, SPIN-код РИНЦ 8130-5458, https://orcid.org/0000-0003-1106-5080

Гинцяк Алексей Михайлович, к.т.н., заведующий лабораторией «Цифровое моделирование индустриальных систем», ФГАОУ ВО «Санкт-Петербургский политехнический университет Петра Великого» (195251, Россия, Санкт-Петербург, ул. Политехническая, д. 29). E-mail: aleksei.gintciak@spbpu.com. Scopus Author ID 57203897426, ResearcherID W-8013-2019, SPIN-код РИНЦ 9339-2635, https://orcid.org/0000-0002-9703-5079

Бурлуцкая Жанна Владиславовна, младший научный сотрудник, лаборатория «Цифровое моделирование индустриальных систем», ФГАОУ ВО «Санкт-Петербургский политехнический университет Петра Великого» (195251, Россия, Санкт-Петербург, ул. Политехническая, д. 29). E-mail: zhanna.burlutskaya@spbpu.com. Scopus Author ID 57645600200, ResearcherID AGC-6277-2022, SPIN-код РИНЦ 1310-2126, https://orcid.org/0000-0002-5680-1937

Редько Сергей Георгиевич, директор Высшей школы проектной деятельности и инноваций в промышленности, ФГАОУ ВО «Санкт-Петербургский политехнический университет Петра Великого» (195251, Россия, Санкт-Петербург, ул. Политехническая, д. 29). E-mail: redko_sg@spbstu.ru. Scopus Author ID 57211475098, SPIN-код РИНЦ 3501-2403, https://orcid.org/0000-0002-4343-4154

Translated from Russian into English by L. Bychkova
Edited for English language and spelling by Thomas A. Beavitt

Mathematical modeling

Математическое моделирование

UDC 681.5.015
https://doi.org/10.32362/2500-316X-2025-13-4-95-106
EDN EFGVQG

RESEARCH ARTICLE

On the identification of decentralized systems

Nikolay N. Karabutov [@], *

MIREA – Russian Technological University, Moscow, 119454 Russia
[@] *Corresponding author, e-mail: karabutov@mirea.ru*

• **Submitted:** 11.11.2024 • **Revised:** 18.01.2025 • **Accepted:** 21.05.2025

Abstract

Objectives. The work set out to consider the problem of identification of decentralized systems (DS). Due to the increasing complexity of systems and *a priori* uncertainty, it becomes necessary to identify appropriate approaches and methods. In particular, this concerns the parametric identifiability (PI) of DSs. This condition can be explained in terms of the complexity of the DS and the presence of internal relationships that complicates the process of parametric estimation. Thus it becomes necessary to propose an approach to PI based on meeting the conditions of the excitation constancy that takes subsystem relationships into account. A class of nonlinear DS is considered whose nonlinearities satisfy the sectoral condition. By taking this condition into account a more rational approach can be taken to the analysis of the DS properties. The work additionally set out to: (1) develop an approach to the analysis of the properties of adaptive identification systems (AIS), taking into account the requirements for the quality of the processes and synthesis of adaptive parametric algorithms; (2) investigate the possibility of using signal adaptation algorithms in DS identification systems and searching for a class of Lyapunov functions for the analysis of AIS with such algorithms; (3) model the proposed methods and algorithms in order to confirm the results obtained.

Methods. The research is based on adaptive identification, implicit identification representation, S-synchronization of a nonlinear system, sector condition, and Lyapunov vector function methods.

Results. The conditions for the parametric identifiability of the DS at the output and in the state space are obtained. A criterion is proposed for estimating the stability of an AIS with signal adaptation. Algorithms for adjusting the parameters of an AIS are synthesized. The exponential dissipativity of the evaluation system is confirmed. The influence of interrelations in the subsystems on the properties of the obtained parameter estimates is considered. An adaptive algorithm can be described by a dynamic matrix system if a functional constraint is imposed on the AIS. The proposed methods and algorithms are modeled to confirm their validity.

Conclusions. Considering the problem of identifying nonlinear DS under uncertainty, estimates have been obtained for the nonlinear part of the system satisfying the quadratic condition. The parametric identifiability of nonlinear DS has been confirmed. Algorithms for parametric and signal adaptive identification have been synthesized. A class of Lyapunov functions is proposed for evaluating the properties of an adaptive system with signal adaptation. The exponential dissipativity of processes in an adaptive system is demonstrated.

Keywords: adaptive identification, identifiability, exponential stability, excitation constancy, Lyapunov vector function, signal adaptation, sector condition

* The Editorial Board expresses its condolences over the death of Nikolay N. Karabutov after the approval of the manuscript for publication.

For citation: Karabutov N.N. On the identification of decentralized systems. *Russian Technological Journal.* 2025;13(4):95–106. https://doi.org/10.32362/2500-316X-2025-13-4-95-106, https://www.elibrary.ru/EFGVQG

Financial disclosure: The author has no financial or proprietary interest in any material or method mentioned.

The author declares no conflicts of interest.

НАУЧНАЯ СТАТЬЯ

Об идентификации децентрализованных систем

Н.Н. Карабутов [@, *]

МИРЭА – Российский технологический университет, Москва, 119454 Россия
[@] *Автор для переписки, e-mail: karabutov@mirea.ru*

• **Поступила:** 11.11.2024 • **Доработана:** 18.01.2025 • **Принята к опубликованию:** 21.05.2025

Резюме

Цели. Рассматривается задача идентификации децентрализованных систем (ДС). Усложнение систем и априорная неопределенность требуют разработки соответствующих подходов и методов. Это касается, прежде всего, параметрической идентифицируемости (ПИ) ДС. Такое состояние можно объяснить сложностью ДС, наличием внутренних взаимосвязей, которые усложняли процесс параметрического оценивания. Необходимо предложить подход к ПИ, основанный на выполнении условия постоянства возбуждения и учете взаимосвязей в подсистемах. Рассматривается класс нелинейных ДС, нелинейности в которых удовлетворяют секторному условию. Учет этого условия позволяет обоснованно подойти к анализу свойств ДС, что является одной из целей данного исследования. Кроме того, целями работы являются: 1) разработка подхода к анализу свойств адаптивных систем идентификации (АСИ) с учетом требований к качеству процессов и синтез адаптивных параметрических алгоритмов; 2) исследование возможности применения алгоритмов сигнальной адаптации в системах идентификации ДС и поиск класса функций Ляпунова для анализа АСИ с такими алгоритмами; 3) моделирование предлагаемых методов и алгоритмов с целью подтверждения полученных результатов.

Методы. Применяются метод адаптивной идентификации, неявное идентификационное представление, S-синхронизация нелинейной системы, секторное условие, метод векторных функций Ляпунова.

Результаты. Получены условия ПИ ДС по выходу и в пространстве состояния. Предложен критерий, позволяющий получить оценки устойчивости АСИ с сигнальной адаптацией. Синтезированы алгоритмы настройки параметров АСИ. Доказана экспоненциальная диссипативность системы оценивания. Рассмотрено влияние взаимосвязей в подсистемах на свойства получаемых оценок параметров. Показано, что адаптивный алгоритм можно описать динамической матричной системой, если на АСИ наложить функциональное ограничение. Выполнено моделирование предлагаемых методов и алгоритмов.

Выводы. Рассмотрена проблема идентификации нелинейных ДС в условиях неопределенности. Получены оценки для нелинейной части системы, удовлетворяющей квадратичному условию. Доказана ПИ нелинейных ДС. Синтезированы алгоритмы параметрической и сигнальной адаптивной идентификации. Предложен класс функций Ляпунова для оценки свойств адаптивной системы с сигнальной адаптацией. Доказана экспоненциальная диссипативность процессов в адаптивной системе.

Ключевые слова: адаптивная идентификация, идентифицируемость, экспоненциальная устойчивость, постоянство возбуждения, векторная функция Ляпунова, сигнальная адаптация, секторное условие

Для цитирования: Карабутов Н.Н. Об идентификации децентрализованных систем. *Russian Technological Journal*. 2025;13(4):95–106. https://doi.org/10.32362/2500-316X-2025-13-4-95-106, https://www.elibrary.ru/EFGVQG

Прозрачность финансовой деятельности: Автор не имеет финансовой заинтересованности в представленных материалах или методах.

Автор заявляет об отсутствии конфликта интересов.

* Редакция приносит свои соболезнования в связи с кончиной Николая Николаевича Карабутова после принятия рукописи к публикации.

INTRODUCTION

Decentralized control systems are widely used to solve various problems. In most cases, the focus is on ensuring the stability and quality of a system. Typically, decentralized systems (DS) operate under conditions of insufficient *a priori* information [1–7]. Various approaches and methods are used for the management of DS. Identification methods based on adaptive observers [2, 5], neural networks [6], frequency methods [7], model-based approaches [8], correlation analysis, and least squares methods [9] are used to recover the missing information. In [10], a two-step identification procedure is implemented. After applying adaptive control regularities, various procedures are used to estimate their parameters [11–13].

The analysis shows that different identification procedures and methods can be applied depending on the subject area for which a DS is being developed. Existing parametric uncertainties are typically compensated by adjusting the parameters of the adaptive control law. However, retrospective identification methods do not always take into account the current state of the system. In addition, the properties of the proposed algorithms and the identifiability of the system itself, as well as the influence of links in the system, are not always taken into account. This is compensated by the use of multistep identification procedures.

The present work considers the problem of adaptive identification of nonlinear DS (NDS) with nonlinearities for which the quadratic condition is satisfied (Section 1). Section 2 analyzes the important problem of parametric identifiability (PI) of an NDS in both the state variable space and the output space. The influence of the properties of the information space of the system on the PI is analyzed. An approach for the synthesis of adaptive algorithms (AA) for identification based on the second Lyapunov method is proposed. Two classes of algorithms, parametric and signaling, are considered. The properties of the identification system are studied. The exponential dissipativity of the adaptive identification system (AIS) is proved.

1. PROBLEM STATEMENT

The system consisting of m interconnected subsystems is considered:

$$S_i: \begin{cases} \dot{\mathbf{X}}_i = \mathbf{A}_i\mathbf{X}_i + \mathbf{B}_i u_i + \sum\limits_{j=1, j\neq i}^{m} \bar{\mathbf{A}}_{ij}\mathbf{X}_j + \mathbf{F}_i\left(\mathbf{X}_i\right), \\ \mathbf{Y}_i = \mathbf{C}_i\mathbf{X}_i, \end{cases} \quad (1)$$

where $\mathbf{X}_i \in \mathbb{R}^{n_i}$, $\mathbf{Y}_i \in \mathbb{R}^{q_i}$ are state and output vectors of S_i subsystem, $u_i \in \mathbb{R}$ is control, $i = \overline{1,m}$, $\sum\limits_{i=1}^{m} n_i = n$.

Elements of matrices $\mathbf{A}_i \in \mathbb{R}^{n_i \times n_i}$, $\mathbf{B}_i \in \mathbb{R}^{n_i}$, $\bar{\mathbf{A}}_{ij} \in \mathbb{R}^{n_i \times n_j}$ are unknown, $\mathbf{C}_i \in \mathbb{R}^{q_i \times n_i}$. The matrix $\bar{\mathbf{A}}_{ij}$ reflects the mutual influence of the S_j subsystem. $\mathbf{F}_i\left(\mathbf{X}_i\right) \in \mathbb{R}^{n_i}$ takes into account the nonlinear state of the S_i subsystem, and the matrix $\mathbf{A}_i \in \mathscr{H}$ is Hurwitz (stable).

Assumption 1. $\mathbf{F}_i(\mathbf{X}_i)$ belongs to class

$$\mathscr{W}_{\mathbf{F}}\left(\pi_1, \pi_2\right) = \\ = \left\{\mathbf{F}(\mathbf{X}) \in \mathbb{R}^n : \pi_1\mathbf{X} \le \mathbf{F}(\mathbf{X}) \le \pi_2\mathbf{X},\ \mathbf{F}(0) = 0\right\} \quad (2)$$

and satisfies the quadratic condition

$$\left(\pi_2\mathbf{X} - \mathbf{F}(\mathbf{X})\right)^{\mathrm{T}}\left(\mathbf{F}(\mathbf{X}) - \pi_1\mathbf{X}\right) \ge 0, \quad (3)$$

where $\pi_1 > 0$, $\pi_2 > 0$ are given numbers.

The mathematical model for system (1) is the following:

$$\dot{\hat{\mathbf{X}}}_i = \mathbf{K}_i\left(\hat{\mathbf{X}}_i - \mathbf{X}_i\right) + \hat{\mathbf{A}}_i\mathbf{X}_i + \hat{\mathbf{B}}_i u_i + \\ + \sum_{j=1, j\neq i}^{m} \hat{\bar{\mathbf{A}}}_{ij}\mathbf{X}_j + \hat{\mathbf{F}}_i\left(\mathbf{X}_i\right), \quad (4)$$

where $\mathbf{K}_i \in \mathscr{H}$ is the Hurwitz matrix with known parameters; $\hat{\mathbf{X}}_i$ is the model state vector; $\hat{\mathbf{A}}_i$, $\hat{\mathbf{B}}_i$, and $\hat{\bar{\mathbf{A}}}_{ij}$ are adjustable matrices of appropriate dimensions and $\hat{\mathbf{F}}_i$ is the *a priori* given nonlinear vector function with known structure. The matrix $\mathbf{K}_i$ is chosen according to control or identification system requirements.

It is necessary to find algorithms for estimating the parameters of model (4) based on the analysis of the set of measurement data $\mathbb{I}_{\mathrm{o},i} = \left\{\mathbf{X}_i(t), u_i(t), \mathbf{X}_j(t), t \in \mathbb{J} = \left[t_0, t_k\right]\right\}$ ($\mathbb{J}$ is the data acquisition interval; t is the time; and t_0, t_e are the beginning and end of the time interval) and satisfying assumption 1, such that

$$\lim_{t\to\infty}\left\|\hat{\mathbf{X}}_i(t) - \mathbf{X}_i(t)\right\| \le \delta_i,$$

where $\delta_i \ge 0$.

2. ON THE IDENTIFICATION OF THE S_i SUBSYSTEM

The possibility of parameter estimation depends on the identifiability of the S_i subsystems. It is known that in adaptive systems, the excitation constancy condition (marginal non-degeneracy) of elements $\mathbb{I}_{\mathrm{o},i}$ should be satisfied when implementing estimation algorithms.

Let the function $u_i(t)$ satisfy the excitation constancy condition:

$$\mathscr{EC}_{\underline{\alpha}_{u_i},\bar{\alpha}_{u_i}}: \underline{\alpha}_{u_i} \le u_i^2(t) \le \bar{\alpha}_{u_i} \ \forall t \in \left[t_0, t_0+T\right], \quad (5)$$

where $\underline{\alpha}_{u_i}, \bar{\alpha}_{u_i}$ are positive numbers, $T > 0$. Further, the condition (5) is written as $u_i(t) \in \mathscr{EC}_{\underline{\alpha}_{u_i},\bar{\alpha}_{u_i}}$. If $u_i(t)$ does not have the excitation constancy property, then it is written as $u_i(t) \notin \mathscr{EC}_{\underline{\alpha}_{u_i},\bar{\alpha}_{u_i}}$ or $u_i(t) \notin \mathscr{EC}$.

Note 1. For the identification (identifiability) of nonlinear systems, condition (5) should be chosen taking into account the S-synchronizability of the nonlinear system [14]. In this case, property (5) is written in the following form:

$$\mathscr{EC}^{\mathrm{S}}_{\underline{\alpha}_{u_i},\bar{\alpha}_{u_i}}: \left(\underline{\alpha}_{u_i} \le u_i^2(t) \le \bar{\alpha}_{u_i}\right) \& \left(\Omega_{u_i}(\omega) \subseteq \Omega_{\mathrm{S}}(\omega)\right),$$

where $\Omega_{u_i}(\omega)$ is the set of frequencies u_i; $\Omega_{\mathrm{S}}(\omega)$ is the set of admissible frequencies of the input u_i, providing S-synchronizability of the system. In the following, the excitation constancy property is denoted by $\mathscr{EC}_{\underline{\alpha}_{u_i},\bar{\alpha}_{u_i}}$, noting that it guarantees $\mathscr{EC}^{\mathrm{S}}_{\underline{\alpha}_{u_i},\bar{\alpha}_{u_i}}$.

The model (4) is considered to obtain the identifiability conditions of S_i. For the error $\mathbf{E}_i = \hat{\mathbf{X}}_i - \mathbf{X}_i$, the following equation is derived:

$$\begin{aligned}\dot{\mathbf{E}}_i &= \mathbf{K}_i\mathbf{E}_i + \Delta\mathbf{A}_i\mathbf{X}_i + \Delta\mathbf{B}_i u_i + \\ &+ \sum_{j=1, j\ne i}^{M} \Delta\bar{\mathbf{A}}_{ij}\mathbf{X}_j + \Delta\mathbf{F}_i\left(\mathbf{X}_i\right),\end{aligned} \quad (6)$$

where $\Delta\mathbf{A}_i = \hat{\mathbf{A}}_i - \mathbf{A}_i$, $\Delta\mathbf{B}_i = \hat{\mathbf{B}}_i - \mathbf{B}_i$, $\Delta\bar{\mathbf{A}}_{ij} = \hat{\bar{\mathbf{A}}}_{ij} - \bar{\mathbf{A}}_{ij}$, $\Delta\mathbf{F}_i = \hat{\mathbf{F}}_i - \mathbf{F}_i$ are parametric discrepancies.

Lemma 1. If the nonlinearity $\mathbf{F}(\mathbf{X}) \in \mathbb{R}^n$ belongs to the class $\mathbf{F}(\mathbf{X}) \in \mathscr{N}_{\mathbf{F}}\left(\pi_1, \pi_2\right)$ and

$$\pi_1\mathbf{X} \le \mathbf{F}\left(\mathbf{X}\right) \le \pi_2\mathbf{X}, \quad (7)$$

then the following estimate holds for $\mathbf{F}(\mathbf{X})$:

$$\left\|\mathbf{F}\left(\mathbf{X}\right)\right\|^2 \le \eta\bar{\alpha}_{\mathbf{X}}, \quad (8)$$

where $\mathbf{X} \in \mathbb{R}^n$, $\pi_1 > 0$, $\pi_2 > 0$, $\eta = \eta\left(\pi_1, \pi_2\right) > 0$, $\bar{\alpha}_{\mathbf{X}} = \bar{\alpha}_{\mathbf{X}}\left(\mathbf{X}\right) > 0$.

Lemma 2. If the conditions of Lemma 1 are satisfied, then the following estimate holds for $\Delta\mathbf{F}(\mathbf{X})$:

$$\Delta\mathbf{F}^{\mathrm{T}}\Delta\mathbf{F} \le 2\eta\bar{\alpha}_{\mathbf{X}} + \delta_{\mathbf{F}},$$

where $\eta = 2\bar{\pi} + \pi^2$, $\bar{\pi} = \pi_1\pi_2$, $\pi = \pi_1 + \pi_2$, $\delta_{\mathbf{F}} > 0$.

Consider the system (6) and the Lyapunov function (LF) $V_i\left(\mathbf{E}_i\right) = 0.5\mathbf{E}_i^{\mathrm{T}}\mathbf{R}_i\mathbf{E}_i$, where $\mathbf{R}_i = \mathbf{R}_i^{\mathrm{T}} > 0$ is a positive definite symmetric matrix. We denote the matrix norm $\Delta\mathbf{A}_i$: $\left\|\Delta\mathbf{A}_i\right\| = \sqrt{\mathrm{Sp}(\Delta\mathbf{A}_i^{\mathrm{T}}\Delta\mathbf{A}_i)}$, $\left\|\Delta\bar{\mathbf{A}}_{ij}\right\| = \sqrt{\mathrm{Sp}(\Delta\mathbf{A}_{ij}^{\mathrm{T}}\Delta\mathbf{A}_{ij})}$, $\mathrm{Sp}(\cdot)$ is the trace of the matrix.

Theorem 1. Let 1) the matrix $\mathbf{A}_i \in \mathscr{H}$; 2) $\mathbf{X}_i(t) \in \mathscr{EC}_{\underline{\alpha}_{\mathbf{X}_i},\bar{\alpha}_{\mathbf{X}_i}}$, $\mathbf{X}_j(t) \in \mathscr{EC}_{\underline{\alpha}_{\mathbf{X}_j},\bar{\alpha}_{\mathbf{X}_j}}$ $u_i(t) \in \mathscr{EC}_{\underline{\alpha}_{u_i},\bar{\alpha}_{u_i}}$; and 3) the conditions of Lemmas 1, 2 are satisfied for $\mathbf{F}_i(\mathbf{X}_i)$. Then the subsystem (1) is identifiable on the set $\mathbb{I}_{\mathrm{o},i}$, provided that

$$\begin{aligned}&2\Bigg(\bar{\alpha}_{\mathbf{X}_i}\left\|\Delta\mathbf{A}_i\right\|^2 + \bar{\alpha}_{u_i}\left\|\Delta\mathbf{B}_i\right\|^2 + \\ &+ \sum_{j=1, j\ne i}^{m} \bar{\alpha}_{\mathbf{X}_j}\left\|\Delta\bar{\mathbf{A}}_{ij}\right\|^2 + 2\eta\bar{\alpha}_{\mathbf{X}_i} + \delta_{\mathbf{F}_i}\Bigg) \le \bar{\lambda}_i V_i,\end{aligned} \quad (9)$$

where $\bar{\lambda}_i = \lambda_i - k_i$, $\lambda_i > 0$ is the minimum eigenvalue of the matrix $\mathbf{Q}_i$, $k_i > 0$, $\mathbf{K}_i\mathbf{R}_i + \mathbf{K}_i^{\mathrm{T}}\mathbf{R}_i = -\mathbf{Q}_i$, $\mathbf{Q}_i$ is a positive symmetric matrix, $\eta = 2\bar{\pi} + \pi^2$, $\pi = \pi_1 + \pi_2$, $\bar{\pi} = \pi_1\pi_2$, $\delta_{\mathbf{F}_i} \ge 0$.

If the conditions of Theorem 1 are satisfied, then the S_i subsystem is called identifiable on the set $\mathbb{I}_{\mathrm{o}}$ or $\mathscr{PI}_{\mathbf{X}_i}$-identifiable.

We consider the identifiability of the subsystem S_i on the set "Input–Output":

$$\mathbb{I}_{\mathrm{o},\mathbf{Y}_i} = \left\{\mathbf{Y}_i(t), u_i(t), \mathbf{Y}_j(t), t \in \mathbb{J} = \left[t_0, t_k\right]\right\}.$$

For the S_i subsystem, the following representation is true:

$$\begin{aligned}\dot{\mathbf{Y}}_i &= \mathbf{A}_{\#,i}\mathbf{Y}_i + \mathbf{B}_{\#,i}u_i + \\ &+ \sum_{j=1, j\ne i}^{m} \bar{\mathbf{A}}_{\#,ij}\mathbf{Y}_j + \tilde{\mathbf{C}}_i^{\#}\mathbf{F}_i\left(\tilde{\mathbf{C}}_i\mathbf{Y}_i\right),\end{aligned} \quad (10)$$

where $\tilde{\mathbf{C}}_i = \left(\mathbf{C}_i^{\mathrm{T}}\mathbf{C}_i\right)^{\#}\mathbf{C}_i^{\mathrm{T}}$, $\mathbf{A}_{\#,i} = \tilde{\mathbf{C}}_i^{\#}\mathbf{A}_i\tilde{\mathbf{C}}_i$, $\mathbf{B}_{\#,i} = \tilde{\mathbf{C}}_i^{\#}\mathbf{B}_i$, $\bar{\mathbf{A}}_{\#,ij} = \tilde{\mathbf{C}}_i^{\#}\bar{\mathbf{A}}_{ij}\tilde{\mathbf{C}}_j$, # is the sign of the matrix pseudoinversion.

Taking into account the specificity of equation (10), the model for (10) has a similar structure to (4). We introduce the error $\mathbf{E}_{\#,i} = \hat{\mathbf{Y}}_i - \mathbf{Y}_i$ and LF $V_{\#,i}\left(\mathbf{E}_{\#,i}\right) = 0.5\mathbf{E}_{\#,i}^{\mathrm{T}}\mathbf{R}_i\mathbf{E}_{\#,i}$.

Theorem 2. Let: 1) the matrix $\mathbf{A}_{\#,i} \in \mathscr{H}$; 2) $\mathbf{Y}_i(t) \in \mathscr{EC}_{\underline{\alpha}_{\mathbf{Y}_i},\bar{\alpha}_{\mathbf{Y}_i}}$, $\mathbf{Y}_j(t) \in \mathscr{EC}_{\underline{\alpha}_{\mathbf{Y}_j},\bar{\alpha}_{\mathbf{Y}_j}}$ $u_i(t) \in \mathscr{EC}_{\underline{\alpha}_{u_i},\bar{\alpha}_{u_i}}$; 3) the conditions of Lemmas 1, 2 are satisfied for $\mathbf{F}_i(\mathbf{X}_i)$;

and 4) the S_i subsystem is observable. Then the subsystem (1) is identifiable on the set $\mathbb{I}_{o,\mathbf{Y}_i}$, provided that

$$2\left(\bar{\alpha}_{\mathbf{Y}_i}\left\|\Delta\mathbf{A}_{\#,i}\right\|^2+\bar{\alpha}_{u_i}\left\|\Delta\mathbf{B}_{\#,i}\right\|^2+\right.$$

$$\left.+\sum_{j=1,j\neq i}^{m}\bar{\alpha}_{\mathbf{Y}_j}\left\|\Delta\bar{\mathbf{A}}_{\#,ij}\right\|^2+2\eta\bar{\alpha}_{\mathbf{Y}_i}+\delta_{\mathbf{F}_i}\right)\leq\bar{\lambda}_{\#,i}V_{\#,i},$$

where $\Delta\mathbf{A}_{\#,i}=\hat{\mathbf{A}}_{\#,i}-\mathbf{A}_{\#,i}$, $\Delta\mathbf{B}_{\#,i}=\hat{\mathbf{B}}_{\#,i}-\mathbf{B}_{\#,i}$, $\Delta\bar{\mathbf{A}}_{\#,ij}=\hat{\bar{\mathbf{A}}}_{\#,ij}-\bar{\mathbf{A}}_{\#,ij}$, $\Delta\mathbf{F}_i=\hat{\mathbf{F}}_i-F_i$, $\bar{\lambda}_{\#,i}>0$.

The proof of Theorems 1 and 2 is reduced to ensuring the non-positivity of the LF derivatives.

3. SYNTHESIS OF ADAPTATION ALGORITHMS

We consider the LF $V_i\left(\mathbf{E}_i\right)=0.5\mathbf{E}_i^{\mathrm{T}}\mathbf{R}_i\mathbf{E}_i$ whose derivative on the motions (6) has the following form:

$$\dot{V}_i=-\mathbf{E}_i^{\mathrm{T}}\mathbf{Q}_i\mathbf{E}_i+\mathbf{E}_i^{\mathrm{T}}\mathbf{R}_i\times$$

$$\times\left(\Delta\mathbf{A}_i\mathbf{X}_i+\Delta\mathbf{B}_iu_i+\sum_{j=1,j\neq i}^{m}\Delta\bar{\mathbf{A}}_{ij}\mathbf{X}_j+\Delta\mathbf{F}_i\left(\mathbf{X}_i\right)\right).$$

We require that in the process of adaptation the following functional constraint is satisfied:

$$\dot{V}_i\leq-\chi_i\left(\Delta\mathbf{A}_i,\Delta\bar{\mathbf{A}}_i,\Delta\mathbf{B}_i,\Delta\mathbf{F}_i\right),$$

where

$$\chi\left(\Delta\mathbf{A}_i,\Delta\bar{\mathbf{A}}_i,\Delta\mathbf{B}_i,\Delta\mathbf{F}_i\right)=0.5\left(\varphi_{\mathbf{A}_i}(t)\left\|\Delta\mathbf{A}_i(t)\right\|^2+\right.$$

$$\left.+\varphi_{\tilde{\mathbf{A}}_i}(t)\left\|\Delta\bar{\mathbf{A}}_i(t)\right\|^2+\varphi_{\mathbf{B}_i}(t)\left\|\Delta\mathbf{B}_i\right\|^2+\varphi_{\mathbf{F}_i}(t)\left\|\Delta\mathbf{F}_i(t)\right\|^2\right),$$

$\varphi_{\mathbf{A}_i}(t)$, $\varphi_{\tilde{\mathbf{A}}_i}(t)$, $\varphi_{\mathbf{B}_i}(t)$, $\varphi_{\mathbf{F}_i}(t)$ are bounded non-negative functions. Then

$$\eta_i=\dot{V}_i+\chi_i=-\mathbf{E}_i^{\mathrm{T}}\mathbf{Q}_i\mathbf{E}_i+\chi\left(\Delta\mathbf{A}_i,\Delta\bar{\mathbf{A}}_i,\Delta\mathbf{F}_i\right)+$$

$$+\mathbf{E}_i^{\mathrm{T}}\mathbf{R}_i\left(\Delta\mathbf{A}_i\mathbf{X}_i+\Delta\mathbf{B}_iu_i+\sum_{j=1,j\neq i}^{m}\Delta\bar{\mathbf{A}}_{ij}\mathbf{X}_j+\Delta\mathbf{F}_i\left(\mathbf{X}_i\right)\right).\quad(11)$$

From the condition $\eta\leq 0$, the AA is derived, as follows:

$$\Delta\dot{\mathbf{A}}_i=-\boldsymbol{\Gamma}_{\mathbf{A}_i}\left(\varphi_{\mathbf{A}_i}\Delta\mathbf{A}_i+\mathbf{E}_i\mathbf{R}_i\mathbf{X}_i^{\mathrm{T}}\right),$$

$$\Delta\dot{\bar{\mathbf{A}}}_{ij}=-\boldsymbol{\Gamma}_{\bar{\mathbf{A}}_{ij}}\left(\varphi_{\tilde{\mathbf{A}}_{ij}}\Delta\bar{\mathbf{A}}_{ij}+\mathbf{E}_i\mathbf{R}_i\mathbf{X}_j^{\mathrm{T}}\right),\quad(12)$$

$$\Delta\dot{\mathbf{B}}_i=-\boldsymbol{\Gamma}_{\mathbf{B}_i}\left(\varphi_{B_{ij}}\Delta\mathbf{B}_i+\mathbf{R}_i\mathbf{E}_iu_i\right),$$

where $\boldsymbol{\Gamma}_{\mathbf{A}_i}$, $\boldsymbol{\Gamma}_{\tilde{\mathbf{A}}_{ij}}$, and $\boldsymbol{\Gamma}_{\mathbf{B}_i}$ are diagonal matrices of corresponding dimensions with positive diagonal elements. This guarantees the stability of the adaptation processes.

3.1. Parametric algorithm for $\mathbf{F}_i$

Parametric and signaling algorithms can be used to estimate $\mathbf{F}_i$. We consider the parametric approach [15].

Assumption 2. The function $\mathbf{F}_i(\mathbf{X}_i)$ is defined on the following set:

$$\mathbf{F}_i\in\mathbb{F}_{\mathbf{F}_i}=\left\{\mathbf{F}_i\in\mathscr{W}_{\mathbf{F}}\left(\pi_1,\pi_2\right):\mathbf{F}_i(\mathbf{X}_i)=\right.$$

$$=\tilde{\mathbf{F}}_i^{\mathrm{T}}\left(\mathbf{X}_i,\mathbf{N}_{i,1}\right)\mathbf{N}_{i,2},\quad(13)$$

$$\left.\mathbf{N}_i=\left[\mathbf{N}_{i,1}^{\mathrm{T}},\mathbf{N}_{i,2}^{\mathrm{T}}\right]^{\mathrm{T}},\ \mathbf{N}_i\in\mathbb{N}_{i,\mathrm{a}}\right\},$$

where $\mathbb{N}_{i,\mathrm{a}}=\left\{\mathbf{N}_{\mathbf{i}}\in\mathbb{R}^n:\underline{\mathbf{N}}_i\leq\mathbf{N}_i\leq\overline{\mathbf{N}}_i\right\}$ is the *a posteriori* formed parametric domain for $\mathbf{F}_i$; $\underline{\mathbf{N}},\overline{\mathbf{N}}$ are the vector bounds for $\mathbf{N}$, understood as $\underline{n}_i\in\underline{\mathbf{N}}_i$, $\overline{n}_i\in\overline{\mathbf{N}}_i$; $\mathbf{N}_{i,1}$ is the *a priori* known vector of nonlinearity parameters, $\mathbf{N}_{i,2}$ is the *a priori* unknown set of parameters, which is further considered as a vector to be estimated. Some elements of $\underline{\mathbf{N}}_i$, $\overline{\mathbf{N}}_i$ may be unknown. The structure $\tilde{\mathbf{F}}_i\left(\mathbf{X}_i,\mathbf{N}_{i,1}\right)$ is formed *a priori* taking into account the known vector $\mathbf{N}_{i,1}$.

It follows from (13) that the estimate of the vector function $\mathbf{F}_i(\mathbf{X}_i)$ in the identification step is sought in the following form:

$$\hat{\mathbf{F}}_i(X_i)=\tilde{\mathbf{F}}_i^{\mathrm{T}}\left(\mathbf{X}_i,\hat{\mathbf{N}}_{i,1}\right)\hat{\mathbf{N}}_{i,2},\quad(14)$$

where $\hat{\mathbf{N}}_{i,1}\in\mathbb{R}^{n_{i,1}}$ is the *a priori* estimate of known parameters, $\hat{\mathbf{N}}_{i,2}\in\mathbb{R}^{n_{i,2}}$ is the vector of adjustable parameters.

We assume $\mathbb{N}_i=\mathbb{N}_{i,1}\cup\mathbb{N}_{i,2}$. The set $\mathbb{N}_{i,1}\subset\mathbb{R}^{n_{i,1}}$ $\left(\mathbf{N}_{i,1}\in\mathbb{N}_{i,1}\right)$ contains elements that are not available for tuning with AA. The elements $\mathbf{N}_{i,2}\in\mathbb{N}_{i,2}\subset\mathbb{R}^{n_{i,2}}$ are estimated in the identification step. The matrix $\tilde{\mathbf{F}}_i\left(y,\hat{\mathbf{N}}_{i,1}\right)$ is formed in the step of structural synthesis (analysis) of the system. The representation (14) is a consequence of the proposed parametric concept for $\mathbf{F}_i(\mathbf{X}_i)$.

Note 2. The vector $\hat{\mathbf{N}}_{i,1}$ can be tuned iteratively based on the forcing algorithm [15].

Since $\Delta\mathbf{F}=\tilde{\mathbf{F}}_i^{\mathrm{T}}\left(y,\hat{\mathbf{N}}_{i,1}\right)\hat{\mathbf{N}}_{i,2}-\mathbf{F}_i(\mathbf{X}_i)$, then from the condition $\dot{V}_i\leq 0$ we obtain AA for $\hat{\mathbf{N}}_{i,2}$, as follows:

$$\dot{\hat{\mathbf{N}}}_{i,2} = -\mathbf{\Gamma}_{\mathbf{F}_i}\left(\varphi_{F_i}\hat{\mathbf{N}}_{i,2} + \tilde{\mathbf{F}}_i^{\mathrm{T}}\mathbf{R}_i\mathbf{E}_i\left(\mathbf{X}_i, \hat{\mathbf{N}}_{i,1}\right)\right), \quad (15)$$

where $\mathbf{\Gamma}_{\mathbf{F}_i}$ is a diagonal matrix with positive diagonal elements.

In the following, the system (6), (11), (15) will be denoted as AS_{AF_i} to simplify the references.

3.2. Signaling algorithm

We consider the following model:

$$\dot{\hat{\mathbf{X}}}_i = \mathbf{K}_i\left(\hat{\mathbf{X}}_i - \mathbf{X}_i\right) + \hat{\mathbf{A}}_i\mathbf{X}_i + \hat{\mathbf{B}}_i u_i + \sum_{j=1, j\neq i}^{m}\hat{\bar{\mathbf{A}}}_{ij}\mathbf{X}_j + \mathbf{U}_i \quad (16)$$

and the error equation:

$$\dot{\mathbf{E}}_i = \mathbf{K}_i\mathbf{E}_i + \Delta\mathbf{A}_i\mathbf{X}_i + \Delta\mathbf{B}_i u_i + \sum_{j=1, j\neq i}^{m}\Delta\bar{\mathbf{A}}_{ij}\mathbf{X}_j + \mathbf{U}_i\left(\mathbf{X}_i\right) - \mathbf{F}_i\left(\mathbf{X}_i\right). \quad (17)$$

The LF derivative has the following form:

$$\dot{V}_i = -\mathbf{E}_i^{\mathrm{T}}\mathbf{Q}_i\mathbf{E}_i + \mathbf{E}_i^{\mathrm{T}}\mathbf{R}_i \times \times\left(\Delta\mathbf{A}_i\mathbf{X}_i + \Delta\mathbf{B}_i u_i + \sum_{j=1, j\neq i}^{m}\Delta\bar{\mathbf{A}}_{ij}\mathbf{X}_j + \mathbf{U}_i - \mathbf{F}_i\right), \quad (18)$$

and the algorithm for $\mathbf{U}_i$ is as follows:

$$\mathbf{U}_i = -\mathbf{D}_i\mathbf{R}_i\mathbf{E}_i, \quad (19)$$

where $\mathbf{D}_i \in \mathbb{R}^{n_i\times n_i}$ is the diagonal matrix with positive elements.

Since $\mathbf{F}_i\left(\mathbf{X}_i\right) \in \mathscr{N}_{\mathbf{F}}\left(\pi_1, \pi_2\right)$, Lemma 1 holds for $\mathbf{F}_i(\mathbf{X}_i)$.

We use the approach described in [16]. Choose the elements of the matrix $\mathbf{D}_i$ from the condition $\left\|\mathbf{D}_i\right\| \geq d_i \geq \eta\bar{\alpha}_{X_i}$. Then we obtain the following for (18):

$$\dot{V}_i = -\mathbf{E}_i^{\mathrm{T}}\mathbf{Q}_i\mathbf{E}_i + \mathbf{E}_i^{\mathrm{T}}\mathbf{R}_i\left(\Delta\mathbf{A}_i\mathbf{X}_i + \Delta\mathbf{B}_i u_i + \sum_{j=1, j\neq i}^{m}\Delta\bar{\mathbf{A}}_{ij}\mathbf{X}_j - \mathbf{D}_i\mathbf{R}_i\mathbf{E}_i - \mathbf{F}_i\right). \quad (20)$$

Since $\mathbf{E}_i^{\mathrm{T}}\mathbf{R}_i\mathbf{D}_i\mathbf{R}_i\mathbf{E}_i \geq 2\eta\underline{\alpha}_{\mathbf{X}_i}\underline{\lambda}_{\mathbf{R}_i}V_i$, where $\underline{\lambda}_{\mathbf{R}_i}$ is the smallest eigenvalue of the matrix $\mathbf{R}_i$, then

$$\dot{V}_i \leq -\sigma V_i + \mathbf{E}_i^{\mathrm{T}}\mathbf{R}_i \times \times\left(\Delta\mathbf{A}_i\mathbf{X}_i + \Delta\mathbf{B}_i u_i + \sum_{j=1, j\neq i}^{m}\Delta\tilde{\mathbf{A}}_{ij}\mathbf{X}_j\right), \quad (21)$$

where $\sigma = \lambda_{\mathbf{Q}_i} + 2\eta\underline{\alpha}_{\mathbf{X}_i}\underline{\lambda}_{\mathbf{R}_i}$.

After simple transformations we obtain the following:

$$\dot{V}_i \leq -\sigma V_i + 2\left(\bar{\alpha}_{X_i}\left\|\Delta\mathbf{A}_i\right\|^2 + \bar{\alpha}_{u_i}\left\|\Delta\mathbf{B}_i\right\|^2 + \sum_{j=1, j\neq i}^{m}\bar{\alpha}_{X_j}\left\|\Delta\bar{\mathbf{A}}_{ij}\right\|^2\right).$$

If the condition

$$2\left(\bar{\alpha}_{\mathbf{X}_i}\left\|\Delta\mathbf{A}_i\right\|^2 + \bar{\alpha}_{u_i}\left\|\Delta\mathbf{B}_i\right\|^2 + \sum_{j=1, j\neq i}^{m}\bar{\alpha}_{\mathbf{X}_j}\left\|\Delta\tilde{\mathbf{A}}_{ij}\right\|^2 + \eta\bar{\alpha}_{i,\mathbf{X}_i}\right) \leq \sigma V_i$$

is satisfied, then the system (16) at $\left(u_i(t), \mathbf{X}_i(t), \mathbf{X}_j(t)\right) \in \mathscr{E}$ is parametrically identifiable on the set $\left\{u_i(t), \mathbf{X}_i(t), \mathbf{X}_j(t)\right\}$ on the class of algorithms (12), (19).

For ease of references, the system (6), (12), (19) is denoted below as AS_{AS_i}.

4. ADAPTIVE ALGORITHM AS A DYNAMIC SYSTEM

The considered approach to AA synthesis is based on meeting stability properties and is typical of AIS. Attempts to obtain more complex AAs involve imposing constraints on the system. This approach requires certain knowledge and does not always lead to workable algorithms. Below, a method is proposed that takes into account a number of requirements for AIS.

Consider the synthesis of AA using the matrix $\mathbf{A}_i$ as an example. We apply LF, as follows:

$$V_i^{\Delta}\left(\mathbf{E}_i, \Delta\mathbf{A}_i, \Delta\dot{\mathbf{A}}_i\right) = 0.5\mathbf{E}_i^{\mathrm{T}}\mathbf{R}_i\mathbf{E}_i + 0.5\mathrm{Sp}\left(\Delta\mathbf{A}_i^{\mathrm{T}}\Delta\dot{\mathbf{A}}_i\right).$$

We require that the functional constraint is satisfied:

$$\dot{V}_i^{\Delta} \leq -\chi_{\Delta} = -\alpha_{\Delta}\mathrm{Sp}\left(\Delta\mathbf{A}_i^{\mathrm{T}}\Delta\mathbf{A}_i\right).$$

Then for $\eta_{\Delta} = \dot{V}_i^{\Delta} + \alpha_{\Delta}\mathrm{Sp}\left(\Delta A_i^{\mathrm{T}}\Delta A_i\right)$ on the motions (6) we obtain the following:

$$\eta_{\Delta} = -\mathbf{E}_i^{\mathrm{T}}\mathbf{Q}_i\mathbf{E}_i + \mathbf{E}_i^{\mathrm{T}}\mathbf{R}_i\Delta\mathbf{A}_i\mathbf{X}_i + \mathrm{Sp}\left(\Delta\dot{\mathbf{A}}_i^{\mathrm{T}}\Delta\dot{\mathbf{A}}_i\right) + \\ + \mathrm{Sp}\left(\Delta\mathbf{A}_i^{\mathrm{T}}\Delta\ddot{\mathbf{A}}_i\right) + \alpha_{\Delta}\mathrm{Sp}\left(\Delta\mathbf{A}_i^{\mathrm{T}}\Delta\mathbf{A}_i\right).$$

Hence AA follows for $\Delta\mathbf{A}_i$:

$$\Delta\ddot{\mathbf{A}}_i = -\Delta\dot{\mathbf{A}}_i - \alpha_{\Delta}\Delta\mathbf{A}_i - \boldsymbol{\Gamma}_{\mathbf{A}_i}\mathbf{E}_i\mathbf{R}_i\mathbf{X}_i^{\mathrm{T}}.$$

Let $\Delta\mathbf{A}_i = \mathbf{Z}_1$. Then

$$S_{\mathrm{AA}}: \begin{cases} \dot{\mathbf{Z}}_1 = \mathbf{Z}_2, \\ \dot{\mathbf{Z}}_2 = -\alpha_{\Delta}\mathbf{Z}_1 - \mathbf{Z}_2 - \boldsymbol{\Gamma}_{\mathbf{A}_i}\mathbf{E}_i\mathbf{R}_i\mathbf{X}_i^{\mathrm{T}}. \end{cases}$$

Thus, we obtain the AA whose state is described by the S_{AA} system, provided that the functional constraint $\chi_{\Delta} \geq 0$ is imposed on the AIS.

Note 3. Theoretically, different classes of algorithms can be obtained from this approach. Their implementation requires further structuring, taking into account the operating conditions of the loop system.

5. ADAPTIVE SYSTEM PROPERTIES

5.1. The AS_{AF_i} system

We consider the AS_{AF_i} and AS_{AF_j} systems along with LF $V_i\left(\mathbf{E}_i\right) = 0.5\mathbf{E}_i^{\mathrm{T}}\mathbf{R}_i\mathbf{E}_i$,

$$V_{\Delta,i} = 0.5\cdot\mathrm{Sp}\left(\Delta\mathbf{A}_i^{\mathrm{T}}\boldsymbol{\Gamma}_i^{-1}\Delta\mathbf{A}_i\right) + \\ + 0.5\sum_{j=1}^{m}\mathrm{Sp}\left(\Delta\bar{\mathbf{A}}_{ij}^{\mathrm{T}}\boldsymbol{\Gamma}_{ij}^{-1}\Delta\bar{\mathbf{A}}_{ij}\right) + \\ + 0.5\Delta\mathbf{B}_i^{\mathrm{T}}\boldsymbol{\Gamma}_i^{-1}\Delta\mathbf{B}_i + 0.5\Delta\mathbf{N}_{i,2}^{\mathrm{T}}\boldsymbol{\Gamma}_{\mathbf{N}_{i,2}}^{-1}\Delta\mathbf{N}_{\mathbf{N}_{i,2}}. \qquad (22)$$

Theorem 3. Let: 1) there exist LFs $V_i(t)$ and $V_{\Delta,i}(t)$ admitting an infinitesimal upper limit; 2) $\mathbf{A}_i \in \mathscr{H}$; 3) $\bar{\mathbf{A}}_{ij}$ guarantee the stability of the S_i subsystem; 4) $\mathbf{X}_i(t) \in \mathscr{C}_{\underline{\alpha}_{\mathbf{X}_i},\bar{\alpha}_{\mathbf{X}_i}}$, $\mathbf{X}_j(t) \in \mathscr{C}_{\underline{\alpha}_{\mathbf{X}_j},\bar{\alpha}_{\mathbf{X}_j}}$, $u_i(t) \in \mathscr{C}_{\underline{\alpha}_{u_i},\bar{\alpha}_{u_i}}$; 5) $\mathbf{F}_i \in \mathbb{F}_{\mathbf{F}_i}$, where $\mathbb{F}_{\mathbf{F}_i}$ is the set of functions belonging to $\mathscr{H}_{\mathbf{F}}$; 6) the system of inequalities is valid for the vector LF $\mathbf{W}_i = \left[V_i, V_{\Delta,i}\right]^{\mathrm{T}}$:

$$\begin{bmatrix} \dot{V}_i \\ \dot{V}_{\Delta,i} \end{bmatrix} \leq \underbrace{\begin{bmatrix} -\mu_i & \dfrac{2}{\mu_i}\kappa_i \\ \vartheta_{\chi\alpha,i}\rho_i & -\beta_{\lambda\chi,i} \end{bmatrix}}_{\mathbf{A}_{\mathbf{W}_i}} \begin{bmatrix} V \\ V_{\Delta,i} \end{bmatrix} + \underbrace{\begin{bmatrix} \dfrac{2}{\mu_i}\bar{\upsilon}_{\tilde{\mathbf{F}}_i} \\ 0.5\delta_{\mathbf{N},i} \end{bmatrix}}_{\mathbf{L}_i}, \qquad (23)$$

where $\mu_i, \kappa_i, \vartheta_{\chi\alpha,i}, \rho_i, \beta_{\lambda\chi,i}, \bar{\upsilon}_{\tilde{F}_i}, \delta_{N,i}$ are positive numbers depending on the parameters of the S_i subsystem and the characteristics of the information set; and 7) the upper solution for $\mathbf{W}_i$ satisfies the system of equations $\dot{\mathbf{S}}_{\mathbf{W}_i} = A_{\mathbf{W}_i}\mathbf{S}_{\mathbf{W}_i} + \mathbf{L}_i$, provided that

$$w_{\rho}(t) \leq s_{\rho}(t) \quad \forall\left(t \geq t_0\right)\&\left(w_{\rho}\left(t_0\right) \leq s_{\rho}\left(t_0\right)\right),$$

$\rho = e,i;\Delta,i$ for elements $\mathbf{W}_i$, $w_{\rho} \in \mathbf{W}_i$, $s_{\rho} \in \mathbf{S}_{\mathbf{W}_i}$. Then the system is exponentially dissipative with the following estimate:

$$\mathbf{W}_i(t) \leq \mathrm{e}^{\mathbf{A}\mathbf{w}_i\left(t-t_0\right)}\mathbf{S}_{\mathbf{W}_i}(t_0) + \int_{t_0}^{t}\mathrm{e}^{\mathbf{A}\mathbf{w}_i\left(t-\tau\right)}\mathbf{L}_i d\tau, \qquad (24)$$

if

$$\mu_i^2\beta_{\lambda\chi,i} \geq 2\kappa_i\vartheta_{\chi\alpha,i}\rho_i. \qquad (25)$$

The limiting properties of $AS_{F,i}$ are determined by the elements of the vector $\mathbf{L}_i$. If the structure and the parameters of the vector $\hat{\mathbf{N}}_{i,1}$ are known, then the subsystem is exponentially stable, provided that $\tilde{\mathbf{F}}_i \in \mathscr{C}$.

We consider the $AS_{F,i,j}$ system consisting of the $AS_{F,i}$ и $AS_{F,j}$ subsystems. For $AS_{F,i,j}$, the following system of inequalities applies:

$$\begin{bmatrix} \dot{\mathbf{W}}_i \\ \dot{\mathbf{W}}_j \end{bmatrix} \leq \begin{bmatrix} \mathbf{A}_{\mathbf{W}_i} & 0 \\ 0 & \mathbf{A}_{\mathbf{W}_j} \end{bmatrix}\begin{bmatrix} \mathbf{W}_i \\ \mathbf{W}_j \end{bmatrix} + \begin{bmatrix} \mathbf{L}_i \\ \mathbf{L}_j \end{bmatrix}, \qquad (26)$$

where $\mathbf{A}_{\mathbf{W}_i}$ and $\mathbf{L}_i$ are of the form (23).

The conditions for exponential stability are as follows:

$$\mu_i^2\beta_{\lambda\chi,i} \geq 2\kappa_i\vartheta_{\chi\alpha,i}\rho_i, \quad \mu_i^2\beta_{\lambda\chi,j} \geq 2\kappa_j\vartheta_{\chi\alpha,j}\rho_j.$$

5.2. The AS_{AS_i} system

We consider the LFs $V_i(t)$ and

$$V_{\Delta_S,i} = 0.5\cdot\mathrm{Sp}\left(\Delta\mathbf{A}_i^{\mathrm{T}}\boldsymbol{\Gamma}_i^{-1}\Delta\mathbf{A}_i\right) + \\ + 0.5\sum_{j=1}^{m}\mathrm{Sp}\left(\Delta\bar{\mathbf{A}}_{ij}^{\mathrm{T}}\boldsymbol{\Gamma}_{ij}^{-1}\Delta\bar{\mathbf{A}}_{ij}\right) + 0.5\Delta\mathbf{B}_i^{\mathrm{T}}\boldsymbol{\Gamma}_i^{-1}\Delta\mathbf{B}_i + \\ + 0.5\int_{t_0}^{t}\Delta_{\mathbf{U}_i}\mathbf{F}_i^{\mathrm{T}}(\tau)\Delta_{\mathbf{U}_i}\mathbf{F}_i(\tau)d\tau,$$

where $\Delta_{\mathbf{U}_i}\mathbf{F}_i = \mathbf{U}_i - \mathbf{F}_i$.

Theorem 4. Let the following conditions be satisfied: 1) there exist LFs $V_i(t)$ and $V_{\Delta_S,i}(t)$ admitting

an infinitesimal upper limit; 2) $\mathbf{A}_i \in \mathscr{H}$; 3) $\bar{\mathbf{A}}_{ij}$ guarantee the stability of the S_i subsystem; 4) $\mathbf{F}_i(\mathbf{X}_i) \in \mathscr{N}_{\mathbf{F}}(\pi_1, \pi_2)$; 5) $u_i(t) \in \mathscr{C}_{\underline{\alpha}_{u_i}, \bar{\alpha}_{u_i}}$, $\mathbf{X}_i(t) \in \mathscr{C}_{\underline{\alpha}_{\mathbf{X}_i}, \bar{\alpha}_{\mathbf{X}_i}}$, $\mathbf{X}_j(t) \in \mathscr{C}_{\underline{\alpha}_{\mathbf{X}_j}, \bar{\alpha}_{\mathbf{X}_j}}$; 6) in some origin region there exist such $\nu_i > 0$ that $\mathbf{F}_i^{\mathrm{T}} \Delta_{\mathbf{U}_i} \mathbf{F}_i = \nu_i \left(\|\mathbf{F}_i\|^2 + \|\Delta_{\mathbf{U}_i} \mathbf{F}_i\|^2 \right)$ is valid at $t >> t_0$; 7) the system of inequalities for the vector LF $\mathbf{W}_{S,i} = \left[V_i, V_{\Delta_S,i} \right]^{\mathrm{T}}$ is satisfied:

$$\underbrace{\begin{bmatrix} \dot{V}_i \\ \dot{V}_{\Delta_{S,i}} \end{bmatrix}}_{\dot{\mathbf{W}}_{S_i}} \le \underbrace{\begin{bmatrix} -\mu_i & \frac{2}{\mu_i} \kappa_{\Delta_{S,i}} \\ \vartheta_{\Delta_{S,i}} \rho_i & -\beta_{\Delta_{S,i}} \end{bmatrix}}_{\mathbf{A}_{\mathbf{W}_{S_i}}} \underbrace{\begin{bmatrix} V_i \\ V_{\Delta_{S,i}} \end{bmatrix}}_{\mathbf{W}_{S_i}} + \underbrace{\begin{bmatrix} 0 \\ \sqrt{0.125} \nu_i \eta_i \bar{\alpha}_{\mathbf{X}_i} \end{bmatrix}}_{\mathbf{L}_{S,i}}, \tag{27}$$

where $\mu_i, \kappa_{\Delta_S,i}, \vartheta_{\Delta.i}, \rho_i, \beta_{\Delta,i}, \nu_i, \eta_i$ are positive numbers depending on the parameters of the AS_{AS_i} subsystem and properties of the information set $\mathbb{I}_{\mathrm{o},i}$; and 8) for the upper solution $\mathbf{W}_{S,i}$, the system of equation $\dot{\mathbf{S}}_{\mathbf{W}_{Si}} = \mathbf{A}_{\mathbf{W}_{S,i}} \mathbf{S}_{\mathbf{W}_{S,i}} + \mathbf{L}_{S,i}$ is valid, provided that

$$w_\rho(t) \le s_\rho(t) \quad \forall \left(t \ge t_0 \right) \& \left(w_\rho(t_0) \le s_\rho(t_0) \right),$$

$\rho = e, i$; $\Delta_{S,i}$ for elements $\mathbf{W}_{S_i}$, $w_\rho \in \mathbf{W}_{S_i}$, $s_\rho \in \mathbf{S}_{\mathbf{W}_{S,i}}$. Then the AS_{AS_i} system is exponentially dissipative with the following estimate:

$$\mathbf{W}_{S_i}(t) \le \mathrm{e}^{\mathbf{A}_{\mathbf{W}_{S_i}}(t-t_0)} \mathbf{S}_{\mathbf{W}_{S_i}}(t_0) + \int_{t_0}^{t} \mathrm{e}^{\mathbf{A}_{\mathbf{W}_{S_i}}(t-\sigma)} \mathbf{L}_{S,i} d\sigma, \tag{28}$$

if $\mu_i^2 \beta_{\Delta,i} \ge 2 \vartheta_{\Delta.i} \rho_i \kappa_{\Delta_S,i}$.

It follows from the results that using the AS_{AS_i} system gives biased estimates of the S_i subsystem parameters.

The scheme used to prove Theorems 3, 4 is given in [17].

Note 4. It should be noted that signaling algorithms are widely used in adaptive control systems. Their use is justified on the basis of ensuring the non-positivity of the LF derivative. This is due to the use of quadratic LFs, which incompletely reflect the specificity of the processes in AS_{AS_i} systems. The LF $V_{\Delta_{S,i}}$ proposed in the paper makes it possible to substantiate the properties of the AS_{AS_i} system and to obtain estimates of the quality of its functioning.

Note 5. Algorithm (19) is a compensation control. Therefore, the term "signal adaptation" (SA) only refers to the choice of the gain matrix in (19). In identification problems, the SA use depends largely on the quality requirements of the identification system.

Note 6. The results obtained in [15] can be used to analyze the properties of the algorithm (12) with $\varphi_i = 0$.

6. EXAMPLE

We consider the following system:

$$S_1 : \begin{cases} \begin{bmatrix} \dot{x}_{11} \\ \dot{x}_{12} \end{bmatrix} = \begin{bmatrix} 0 & 1 \\ -a_{21} & -a_{22} \end{bmatrix} \begin{bmatrix} x_{11} \\ x_{12} \end{bmatrix} + \begin{bmatrix} 0 \\ \bar{a}_1 \end{bmatrix} x_2 + \begin{bmatrix} 0 \\ b_1 \end{bmatrix} u_1 + \begin{bmatrix} 0 \\ c_1 \end{bmatrix} f_1(x_{11}), \\ y_1 = x_{11}, \end{cases}$$
$$S_2 : \begin{cases} \dot{x}_2 = -a_2 x_2 + \bar{a}_2 x_{11} + b_2 u_2 + c_2 f_1(x_{11}), \\ y_2 = x_2, \end{cases} \tag{29}$$

where $\mathbf{X}_1 = \left[x_{11} \; x_{12} \right]^{\mathrm{T}}$; y_1 is the state vector and the output of the S_1 subsystem; u_1 is the input (control); $f_1(x_{11})$ = sat(x_{11}) is the saturation function; $f_2(x_2)$ = sign(x_2) is the sign function; and y_2 is the output of the S_2 subsystem. The parameters of the system (29) are: $b_1 = 1$, $a_{21} = 2$, $a_{22} = 3$, $\bar{a}_1 = 1.5$, $c_1 = 1$, $a_2 = 1.25$, $\bar{a}_2 = 0.2$, $b_2 = 1$, and $c_2 = 0.25$. The inputs $u_i(t)$ are sinusoidal.

Since the variable x_{12} is not measured, the S_1 subsystem is transformed to the form where only the observable variables are used. Applying the approach from [15], the representation in the "Input–Output" space for S_1 is obtained:

$$\dot{y}_1 = -\alpha_1 y_1 + \alpha_2 p_{y_1} + \beta_{12} p_{x_2} + b_1 p_{u_1} + c_1 p_{f_1}, \tag{30}$$

where α_1, α_2, β_{12}, b_1, c_1 are the coefficients to be estimated; $\mu > 0$,

$$\dot{p}_{y_1} = -\mu p_{y_1} + y_1, \; \dot{p}_{x_2} = -\mu p_{x_2} + x_2, \\ \dot{p}_{u_1} = -\mu p_{u_1} + u_1, \; \dot{p}_{f_1} = -\mu p_{f_1} + f_1. \tag{31}$$

The phase portrait for S_1 is shown in Fig. 1. The processes in the subsystem are nonlinear. In addition, there is a relationship $y_2 = y_2(y_1)$ between y_1 and y_2 (coefficient of determination is 75%), which is reflected in the properties of the S_1 subsystem (see Fig. 1). In particular, y_2 affects the S-synchronizability of S_1 and the parameter estimation. Applying the approach from [15],

it can be concluded that the subsystem S_1 is structurally identifiable.

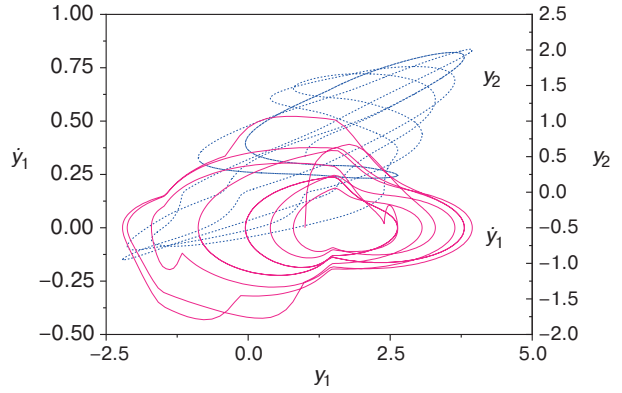

Fig. 1. Phase portrait of the S_1 subsystem

The models for the S_1 and S_2 subsystems are as follows

$$\dot{\hat{y}}_1 = -k_1 e_1 + \hat{a}_{11} y_1 + \hat{a}_{12} p_{y_1} + \\ + \hat{\beta}_{12} p_{x_2} + \hat{b}_1 p_{u_1} + \hat{c}_1 p_{f_1}, \quad (32)$$

$$\dot{\hat{y}}_2 = -k_2 e_2 + \hat{a}_2 y_2 + \hat{\bar{a}}_2 y_1 + \hat{b}_2 u_2 + \hat{c}_1 f_2, \quad (33)$$

where k_1, k_2 are *a priori* positive numbers, $e_1 = \hat{y}_1 - y_1$, $e_2 = \hat{y}_2 - y_2$ are identification errors, and $\hat{a}_i, \hat{\bar{a}}_i, \hat{b}_i, \hat{c}_i$ are adjustable parameters.

The algorithms (12) with $\varphi_i = 0$ are used to adjust the parameters of the models, as follows:

$$\dot{\hat{a}}_{11} = -\gamma_{a_{11}} e_1 y_1, \dot{\hat{a}}_{12} = -\gamma_{a_{12}} e_1 p_{y_1}, \\ \dot{\hat{\beta}}_{12} = -\gamma_{\beta_{12}} e_1 p_{x_2}, \quad (34) \\ \dot{\hat{b}}_1 = -\gamma_{b_1} e_1 p_{u_1}, \dot{\hat{c}}_1 = -\gamma_{c_1} e_1 p_{f_1},$$

$$\dot{\hat{a}}_2 = -\gamma_{a_2} e_2 y_2, \dot{\hat{\bar{a}}}_2 = -\gamma_{\bar{a}_2} e_2 y_1, \\ \dot{\hat{b}}_2 = -\gamma_{b_2} e_2 u_1, \dot{\hat{c}}_2 = -\gamma_{c_2} e_2 f_2, \quad (35)$$

where $\gamma_{a_{ij}} > 0, \gamma_{\bar{a}_{ij}} > 0, \gamma_{\beta_{ij}} > 0, \gamma_{b_i} > 0, \gamma_{c_i} > 0$ are the gain coefficients of the adaptation loop.

The process of adjusting the model (32) parameters for S_1 is shown in Fig. 2.

The results of evaluating the adequacy of models (32) and (33) in the output space are shown in Fig. 3.

In Fig. 4, the dynamics of the adjustment processes of the model (33) parameters depending on e_2 is shown. It can be seen that the processes are nonlinear in the AIS for the S_2 subsystem, while the adjustment process is more regular in the AIS for the S_1 subsystem.

The parameter adjustment processes of models (32) and (33) are multitemporal (Fig. 5).

We consider the AIS with SA for S_2. We apply the model:

$$\dot{\hat{y}}_2 = -k_2 e_2 + \hat{a}_2 y_2 + \hat{\bar{a}}_2 y_1 + \hat{b}_2 u_2 + u_{s,2}, \quad (32a)$$

where $u_{s,2} = -d_2 e_2 x_2$.

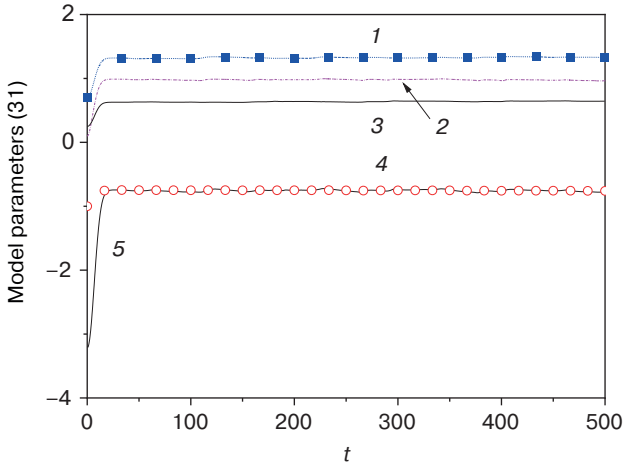

Fig. 2. Tuning of model (32) parameters: (*1*) $\hat{\beta}_{11}$, (*2*) $\hat{c}_{11}$, (*3*) $\hat{a}_{11}$, (*4*) $\hat{a}_{12}$, and (*5*) $\hat{b}_1$

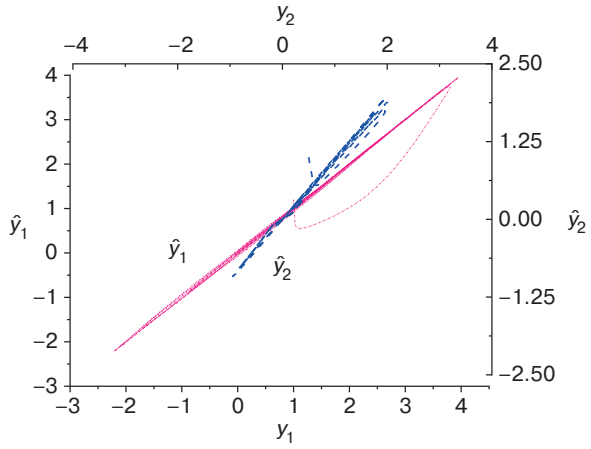

Fig. 3. Adequacy of models (32) and (33)

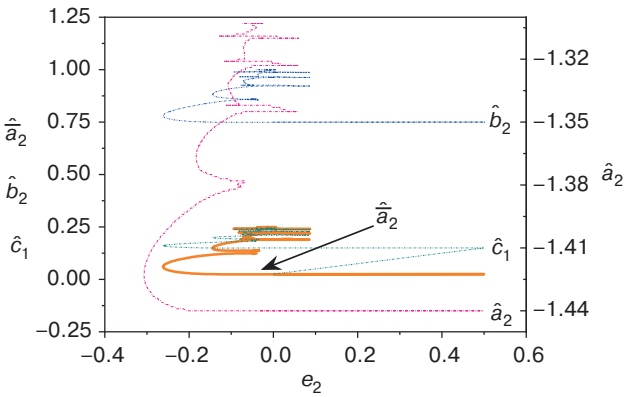

Fig. 4. Tuning of model (33) parameters

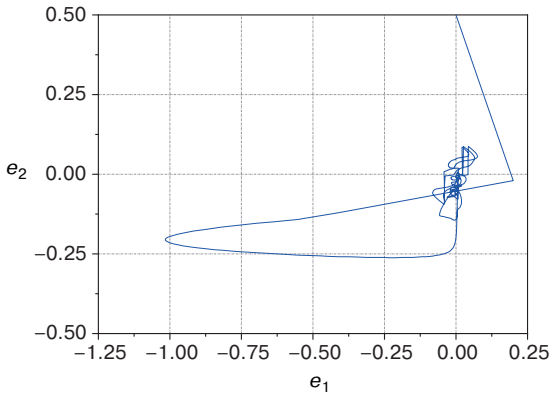

Fig. 5. AIS phase portrait in error space

The results of the AIS with SA are shown in Figs. 6–9. In Figs. 6 and 7, the adjustment processes of the model (32) parameters and the adequacy of the models in the output space are shown. The dynamics of the processes in AIS and the SA signal variation as a function of the identification error for the S_2 subsystem are shown in Fig. 8.

The results of AIS modeling with SA show that the output of the S_2 subsystem influences the AIS parameter adjustment of the S_1 subsystem. Therefore, provided that the requirements for the quality of the adaptation process are met, identification systems with SA should be used. Nevertheless, despite the compensating properties, SA may lead to complication of processes in AIS.

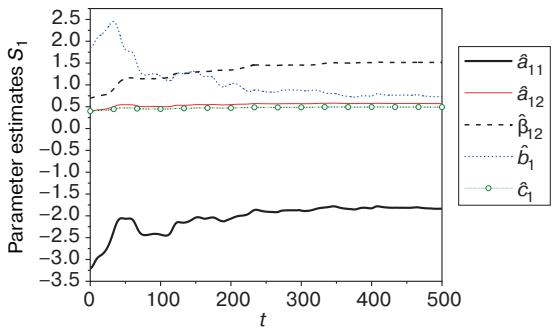

Fig. 6. Tuning of model (32) parameters

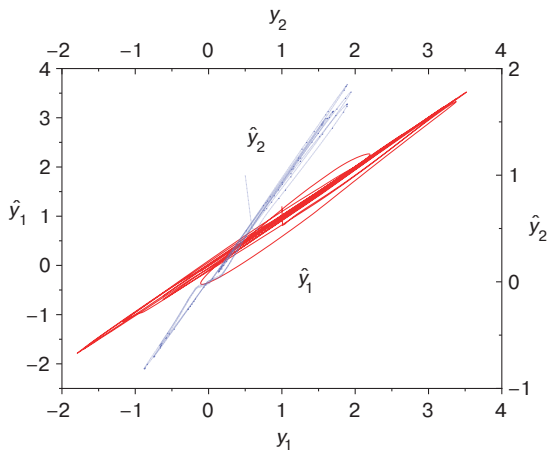

Fig. 7. Adequacy of models (32) and (32a)

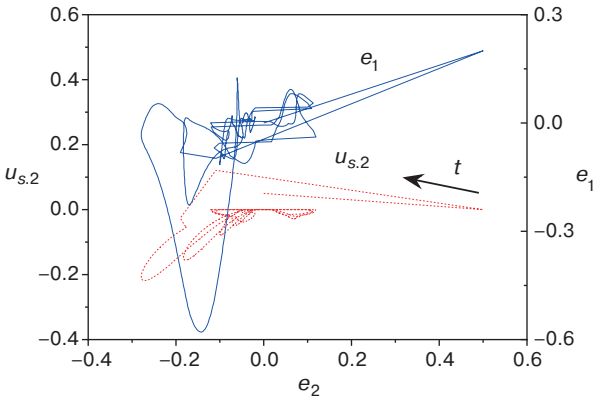

Fig. 8. AIS phase portraits and SA output in error space

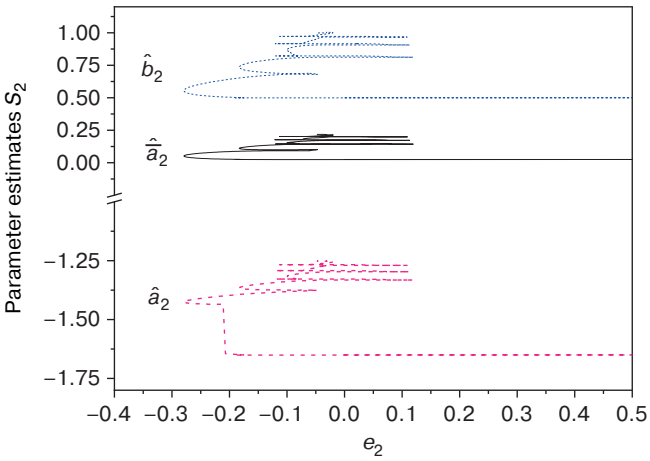

Fig. 9. Tuning of model (32a) parameters

CONCLUSIONS

An approach for the identification of NDS under uncertainty is proposed. The class of NDS is considered where the nonlinearity satisfies the sector condition (quadratic coupling). Estimates of the nonlinearity are obtained. The presence of internal correlations significantly complicates the problem of parametric estimation. Here, the problem of NDS identifiability plays an important role. The PI conditions of the DS are obtained both for the output and in the state space. These are based on the verification of the excitation constancy condition. The PI is shown to be influenced by the interconnections between the subsystems. Algorithms for parametric and signal adaptive identification of DSs are obtained along with the properties of signal-adaptive DS. For the first time, a justification of the stability of AIS with the above class of algorithms is carried out based on a special class of Lyapunov functions used for this purpose. The proposed approach to AA synthesis takes into account the requirements of the identification system.

REFERENCES

1. Hua C., Guan X., Shi P. Decentralized robust model reference adaptive control for interconnected time-delay systems. In: *Proceeding of the 2004 American Control Conference Boston, Massachusetts June 30 – July 2, 2004*. 2004. P. 4285–4289. https://doi.org/10.23919/ACC.2004.1383981
2. Yang Q., Zhu M., Jiang T., He J., Yuan J., Han J. Decentralized Robust Adaptive output feedback stabilization for interconnected nonlinear systems with uncertainties. *J. Control Sci. Eng*. 2016;2016:article ID 3656578. https://doi.org/10.1155/2016/3656578
3. Wu H. Decentralized adaptive robust control of uncertain large-scale non-linear dynamical systems with time-varying delays. *IET Control Theory & Applications*. 2012;6(5):629–640. https://doi.org/10.1049/iet-cta.2011.0015
4. Fan H., Han L., Wen C., Xu L. Decentralized adaptive output-feedback controller design for stochastic nonlinear interconnected systems. *Automatica.* 2012;48(11):2866–2873. https://doi.org/10.1016/j.automatica.2012.08.022
5. Bronnikov A.M., Bukov V.N. Decentralized adaptive control in multivariate system with identification and model coordination. *Mekhatronika, Avtomatizatsiya, Upravlenie.* 2010;1:22–30 (in Russ.).
6. Benitez V.H., Sanchez E.N., Loukianov A.G. Decentralized adaptive recurrent neural control structure. *Eng. Appl. Artif. Intell*. 2007;20(8):1125–1132. https://doi.org/10.1016/j.engappai.2007.02.006
7. Lamara A., Colin G., Lanusse P., Chamaillard Y., Charlet A. Decentralized robust control-system for a non-square MIMO system, the air-path of a turbocharged Diesel engine. *IFAC Proceedings Volumes.* 2012;45(30):130–137. https://doi.org/10.3182/20121023-3-FR-4025.00002
8. Nguyen T., Mukhopadhyay S. Identification and optimal control of large-scale systems using selective decentralization. In: *2016 IEEE International Conference on Systems, Man, and Cybernetics* (*SMC*). IEEE; 2016. P. 000503–000508. https://doi.org/10.1109/SMC.2016.7844289
9. Gudi R.D., Rawlings J.B., Venkat A., Jabbar N. Identification for decentralized MPC. *IFAC Proceedings Volumes.* 2004;37(9):299–304. https://doi.org/10.1016/S1474-6670(17)31827-X
10. Mao X., He J. Decentralized System Identification Method for Large-Scale Networks. In: *2022 American Control Conference* (*ACC*). IEEE; 2022. P. 5173–5178. https://doi.org/10.23919/ACC53348.2022.9867516
11. Ioannou P.A. Decentralized adaptive control of interconnected systems. *IEEE Trans. Automat. Control.* 1986;31(4):291–298. https://doi.org/10.1109/TAC.1986.1104282
12. Jiang Z.-P. Decentralized and adaptive nonlinear tracking of large-scale systems via output feedback. *IEEE Trans. Automat. Control*. 2000;45(11):2122–2128. https://doi.org/10.1109/9.887638
13. Li X.-J., Yan G.-H. Adaptive decentralized control for a class of interconnected nonlinear systems via backstepping approach and graph theory. *Automatica*. 2017;76:87–95. https://doi.org/10.1016/j.automatica.2016.10.019
14. Karabutov N.N. *Vvedenie v strukturnuju identificiruemost' nelinejnyh system* (*Introduction to Structural Identifiability of Nonlinear Systems*). Moscow: URSS/LENAND; 2021. 144 p. (in Russ.). ISBN 978-5-9710-9022-9
15. Karabutov N. Structural-parametrical design method of adaptive observers for nonlinear systems. *International Journal of Intelligent Systems and Applications* (*IJISA*). 2018;10(2):1–16. https://doi.org/10.5815/ijisa.2018.02.01
16. Gromyko V.D., Sankovskii E.A. *Samonastraivayushchiesya sistemy s model'yu* (*Self-Adjusting Systems with a Model*). Moscow: Energiya; 1974. 80 p. (in Russ.).
17. Karabutov N.N. On adaptive identification of systems having multiple nonlinearities. *Russian Technological Journal.* 2023;11(5):94–105. https://doi.org/10.32362/2500-316X-2023-11-5-94-10

СПИСОК ЛИТЕРАТУРЫ

1. Hua C., Guan X., Shi P. Decentralized robust model reference adaptive control for interconnected time-delay systems. In: *Proceeding of the 2004 American Control Conference Boston, Massachusetts June 30 – July 2, 2004*. 2004. P. 4285–4289. https://doi.org/10.23919/ACC.2004.1383981
2. Yang Q., Zhu M., Jiang T., He J., Yuan J., Han J. Decentralized Robust Adaptive output feedback stabilization for interconnected nonlinear systems with uncertainties. *J. Control Sci. Eng*. 2016;2016:article ID 3656578. https://doi.org/10.1155/2016/3656578
3. Wu H. Decentralized adaptive robust control of uncertain large-scale non-linear dynamical systems with time-varying delays. *IET Control Theory & Applications*. 2012;6(5):629–640. https://doi.org/10.1049/iet-cta.2011.0015
4. Fan H., Han L., Wen C., Xu L. Decentralized adaptive output-feedback controller design for stochastic nonlinear interconnected systems. *Automatica.* 2012;48(11):2866–2873. https://doi.org/10.1016/j.automatica.2012.08.022
5. Бронников А.М., Буков В.Н. Децентрализованное адаптивное управление с идентификацией и модельной координацией в многосвязных системах. *Мехатроника, автоматизация, управление*. 2010;1:22–30.
6. Benitez V.H., Sanchez E.N., Loukianov A.G. Decentralized adaptive recurrent neural control structure. *Eng. Appl. Artif. Intell*. 2007;20(8):1125–1132. https://doi.org/10.1016/j.engappai.2007.02.006
7. Lamara A., Colin G., Lanusse P., Chamaillard Y., Charlet A. Decentralized robust control-system for a non-square MIMO system, the air-path of a turbocharged Diesel engine. *IFAC Proceedings Volumes.* 2012;45(30):130–137. https://doi.org/10.3182/20121023-3-FR-4025.00002
8. Nguyen T., Mukhopadhyay S. Identification and optimal control of large-scale systems using selective decentralization. In: *2016 IEEE International Conference on Systems, Man, and Cybernetics* (*SMC*). IEEE; 2016. P. 000503–000508. https://doi.org/10.1109/SMC.2016.7844289

9. Gudi R.D., Rawlings J.B., Venkat A., Jabbar N. Identification for decentralized MPC. *IFAC Proceedings Volumes.* 2004;37(9):299–304. https://doi.org/10.1016/S1474-6670(17)31827-X
10. Mao X., He J. Decentralized System Identification Method for Large-Scale Networks. In: *2022 American Control Conference* (*ACC*). IEEE; 2022. P. 5173–5178. https://doi.org/10.23919/ACC53348.2022.9867516
11. Ioannou P.A. Decentralized adaptive control of interconnected systems. *IEEE Trans. Automat. Control.* 1986;31(4):291–298. https://doi.org/10.1109/TAC.1986.1104282
12. Jiang Z.-P. Decentralized and adaptive nonlinear tracking of large-scale systems via output feedback. *IEEE Trans. Automat. Control*. 2000;45(11):2122–2128. https://doi.org/10.1109/9.887638
13. Li X.-J., Yan G.-H. Adaptive decentralized control for a class of interconnected nonlinear systems via backstepping approach and graph theory. *Automatica*. 2017;76:87–95. https://doi.org/10.1016/j.automatica.2016.10.019
14. Карабутов Н.Н. *Введение в структурную идентифицируемость нелинейных систем*. М.: URSS/ЛЕНАНД; 2021. 144 с. ISBN 978-5-9710-9022-9
15. Karabutov N. Structural-parametrical design method of adaptive observers for nonlinear systems. *International Journal of Intelligent Systems and Applications* (*IJISA*). 2018;10(2):1–16. https://doi.org/10.5815/ijisa.2018.02.01
16. Громыко В.Д., Санковский Е.А. *Самонастраивающиеся системы с моделью*. М.: Энергия; 1974. 80 с.
17. Карабутов Н.Н. Об адаптивной идентификации систем с несколькими нелинейностями. *Russian Technological Journal*. 2023;11(5):94–05. https://doi.org/10.32362/2500-316X-2023-11-5-94-10

About the Author

Nikolay N. Karabutov, Dr. Sci. (Eng.), Professor, Department of Problems Control, Institute of Artificial Intelligence, MIREA – Russian Technological University (78, Vernadskogo pr., Moscow, 119454 Russia). Laureate of the State Prize of the Russian Federation in the field of Science and Technology. E-mail: karabutov@mirea.ru. Scopus Author ID 6603372930, ResearcherID P-5683-2015, RSCI SPIN-code 9646-9721, https://orcid.org/0000-0002-3706-7431

Об авторе

Карабутов Николай Николаевич, д.т.н., профессор, кафедра проблем управления, Институт искусственного интеллекта, ФГБОУ ВО «МИРЭА – Российский технологический университет» (119454, Россия, Москва, пр-т Вернадского, д. 78). Лауреат Государственной премии в области науки и техники. E-mail: karabutov@mirea.ru. Scopus Author ID 6603372930, ResearcherID P-5683-2015, SPIN-код РИНЦ 9646-9721, https://orcid.org/0000-0002-3706-7431

Translated from Russian into English by K. Nazarov
Edited for English language and spelling by Thomas A. Beavitt

Mathematical modeling

Математическое моделирование

UDC 536.715
https://doi.org/10.32362/2500-316X-2025-13-4-107-122
EDN FXQFZG

RESEARCH ARTICLE

Simulation of the detonation regime excited by combustion process turbulence

Evgeny V. Radkevich [1], Mikhail E. Stavrovsky [2, @], Olga A. Vasilyeva [3], Nikolay N. Yakovlev [4], Mikhail I. Sidorov [5]

[1] *M.V. Lomonosov Moscow State University, Moscow, 119991 Russia*
[2] *Bauman Moscow State Technical University, Moscow, 105005 Russia*
[3] *Moscow State University of Civil Engineering, Moscow, 129337 Russia*
[4] *N.N. Semenov Federal Research Center for Chemical Physics of the Russian Academy of Sciences, Moscow, 119991 Russia*
[5] *MIREA – Russian Technological University, Moscow, 119454 Russia*
[@] *Corresponding author, e-mail: stavrovskiyme@bmstu.ru*

• **Submitted:** 12.12.2024 • **Revised:** 14.03.2025 • **Accepted:** 30.05.2025

Abstract

Objectives. The work considers critical processes involving excess energy, which include combustion and explosion, destruction of materials, crystallization, sintering of materials, etc. The results of numerical modeling of the turbulence of the combustion process (laminar–turbulent transition) and the patterns of phenomena associated with the laminar–turbulent transition in critical processes are studied.

Methods. Thermodynamic analysis was used to outline the trajectories of a system's evolution and identify areas of laminar combustion stability during combustion, as well as metastable and labile regions where laminar combustion is unstable. An energy analysis approach was used to solve research problems involving the study of the redistribution of excess energy and the formation of distinctive structural features and parameters of the object and processes.

Results. The results of a numerical experiment of the vibrational turbulence regime of the combustion process are presented as an interaction of the Rauschenbach resonance and laminar–turbulent transition. The resonance occurring during kinetic energy pumping, which implements the discharge of excess energy, is modeled on a variety of local equilibrium. In order to explain the new concepts that arise in this case, the resonance of the adiabatic hydrodynamic process is described. The possibility of avoiding resonance through the mechanism of dumping excess energy by turbulence of the laminar process is confirmed by the results of field experiments.

Conclusions. The possibility of avoiding resonance in vibrational combustion due to disruption of the local equilibrium from the manifold by turbulence of the laminar process (approximation of local equilibrium) during pumping kinetic energy is demonstrated. During the combustion process, areas of laminar combustion stability are identified, along with metastable and labile areas where laminar combustion is unstable. However, this does not mean that signs of turbulence will not be observed in the stability region in its developed state: in these regions the diffusion of perturbations will blur them, whereas in the instability regions the process of negative (Cahn) diffusion will result in their concentration. It can be assumed that the instability regions of a homogeneous system are sources of perturbations, while the stability regions are sinks.

Keywords: laminar-turbulent transition, detonation, combustion, energy, diffusion

For citation: Radkevich E.V., Stavrovsky M.E., Vasilyeva O.A., Yakovlev N.N., Sidorov M.I. Simulation of the detonation regime excited by combustion process turbulence. *Russian Technological Journal.* 2025;13(4):107–122. https://doi.org/10.32362/2500-316X-2025-13-4-107-122, https://www.elibrary.ru/FXQFZG

Financial disclosure: The authors have no financial or proprietary interest in any material or method mentioned.

The authors declare no conflicts of interest.

НАУЧНАЯ СТАТЬЯ

Моделирование детонационного режима, возбуждаемого турбулизацией процесса горения

Е.В. Радкевич [1], М.Е. Ставровский [2, @], О.А. Васильева [3], Н.Н. Яковлев [4], М.И. Сидоров [5]

[1] *Московский государственный университет им. М.В. Ломоносова, Москва, 119991 Россия*
[2] *МГТУ имени Н.Э. Баумана, Москва, 105005 Россия*
[3] *Московский государственный строительный университет, Москва, 129337 Россия*
[4] *Федеральный исследовательский центр химической физики им. Н.Н. Семёнова РАН, Москва, 119991 Россия*
[5] *МИРЭА – Российский технологический университет, Москва, 119454 Россия*
[@] *Автор для переписки, e-mail: stavrovskiyme@bmstu.ru*

• **Поступила:** 12.12.2024 • **Доработана:** 14.03.2025 • **Принята к опубликованию:** 30.05.2025

Резюме

Цели. Объектом исследования являются критические процессы с избыточной энергией, к которым относятся процессы горения и взрыва, разрушения материалов, кристаллизации, спекания материалов и др. Предметом исследования являются результаты численного моделирования турбулизации процесса горения (ламинарно-турбулентного перехода) и закономерностей явлений, связанных с ламинарно-турбулентным переходом в критических процессах.

Методы. Использован термодинамический анализ, обозначивший траектории эволюции системы и показавший, что в процессе горения существуют области устойчивости ламинарного горения, а также метастабильные и лабильные области, где ламинарное горение неустойчиво. Применен энергетический подход к решению задач исследования, при котором основное внимание уделяется вопросам изучения перераспределения избыточной энергии и формирования отличительных признаков структуры и параметров объекта и процессов.

Результаты. Представлены результаты численного эксперимента вибрационного режима турбулизации процесса горения, как взаимодействие резонанса Раушенбаха и ламинарно-турбулентного перехода. На многообразии локального равновесия смоделирован резонанс при накачке кинетической энергии, реализующий сброс избыточной энергии. Для пояснения возникающих при этом новых понятий описан резонанс адиабатического гидродинамического процесса и показана возможность избежать резонанс через механизм сброса избыточной энергии турбулизацией ламинарного процесса, что подтверждается результатами натурных экспериментов.

Выводы. Показано, что в вибрационном горении можно избежать резонанс за счет срыва с многообразия локального равновесия турбулизацией ламинарного процесса (приближения локального равновесия) при накачке кинетической энергии. В процессе горения существуют области устойчивости ламинарного горения, а также метастабильные и лабильные области, где ламинарное горение неустойчиво. Это не означает, что в области устойчивости не будут наблюдаться признаки турбулентности при ее развитом состоянии и в этих областях диффузия возмущений будет их размывать, тогда как в областях неустойчивости процесс «отрицательной» (кановской) диффузии будет их концентрировать. Сделано предположение, что области неустойчивости гомогенной системы являются источниками возмущений, а области устойчивости – «стоками».

Ключевые слова: ламинарно-турбулентный переход, детонация, горение, энергия, диффузия

Для цитирования: Радкевич Е.В., Ставровский М.Е., Васильева О.А., Яковлев Н.Н., Сидоров М.И. Моделирование детонационного режима, возбуждаемого турбулизацией процесса горения. *Russian Technological Journal*. 2025;13(4):107–122. https://doi.org/10.32362/2500-316X-2025-13-4-107-122, https://www.elibrary.ru/FXQFZG

Прозрачность финансовой деятельности: Авторы не имеют финансовой заинтересованности в представленных материалах или методах.

Авторы заявляют об отсутствии конфликта интересов.

INTRODUCTION

According to the logic of the Cahn–Hilliard formulations of the theory of nonequilibrium phase transitions [1, 2] and Debye's theory of critical opalescence [3], critical phenomena are described solely as excess energy processes while omitting the details of chemistry. The degradation of a laminar process by a turbulent process is shown to lead to energy dissipation [4–8]. Turbulence is hypothesized to be "one of the mechanisms of nucleation of a stable detonation zone" [4]. This hypothesis is confirmed experimentally by Shiplyuk[1] et al. [9–11] by applying an adjustable inhomogeneity on a streamlined surface. Of particular interest here is the location and timing of the disruption of the local equilibrium manifold during the release of excess energy by turbulence of the process.

In the present work, energy is conceptualized in different forms:

(a) chemical energy is represented in terms of concentrations;
(b) the nonequilibrium part of the free energy according to Cahn is the concentration gradient;
(c) the mechanical component is in the form of a "gradient" of stresses (structured as a spring), which produces a coherent spinodal [11];
(d) by analogy, the kinetic energy of vortices (as quasi-particles, fluid particles of continuum mechanics) can be added.

The energy method is characterized by its clarity and simplicity for solving a wide range of problems. However, in order to outline the simplest practical methods of acting on an oscillating system and to provide its full theoretical description, it is necessary to take feedback mechanisms into account. A well-known but poorly studied transient process involves switching from laminar to turbulent modes.

PROBLEM STATEMENT FOR THE SIMULATION OF TURBULENCE IN VIBRATING COMBUSTION

The present work sets out to solve the following problems:

- derivation of the model of laminar combustion in the field of gravity with energetic consideration of hydrodynamics;
- vortex energy, degradation measure of laminar combustion, entropy, and free energy of the turbulence process of laminar combustion;
- sign-variable diffusion, an analog of the Cahn–Hilliard operator in the internal energy equation (closure of the disturbance from the manifold of the laminar combustion process);
- numerical experiment of the vibrational mode of combustion turbulence as an interaction of Rauschenbach resonance [5] and laminar–turbulent transition.

TURBULENCE MECHANISM FOR VIBRATIONAL COMBUSTION

In [6–8], a vibrational explosion (resonance when pumping kinetic energy) implementing excess energy discharge is modeled on the local equilibrium manifold (within the laminar process of the local equilibrium approximation). In [8], the resonance of an adiabatic hydrodynamic process is described to explain the new concepts arising in this case. The possibility of avoiding the resonance through the mechanism of excess energy discharge by turbulence of the laminar process is empirically confirmed in [12].

[1] Shiplyuk A.N. *Growth of perturbations and control of boundary layers at hypersonic speeds*. Dr. Sci. Thesis (Phys.-Math.). Novosibirsk, 2005. 320 p. (in Russ.).

According to I.G. Barenblatt, a transformed state occurs in vibrational combustion where the mechanism of excess energy release is either resonance or turbulence of the process. For a single active component, the global inhomogeneity of the system can be characterized as an inhomogeneous enthalpy distribution across the flow (mixture). When pumping kinetic energy in the combustion process in the phase-space field of gravity described by variables (volume V, pressure P, temperature T, reduced amount of active component n, entropy S, internal energy E, velocity of the active component u_1, and velocity of the passive component u_2), the enthalpy increment is a full differential on the local equilibrium manifold [5], on which the laminar process (in the local equilibrium approximation) is described by equations (1)–(4) of the classical two-component model of the combustion process in the gravitational field:

$$\partial_t \rho + \partial_x(\rho U) = \varepsilon_R \Delta\rho, \tag{1}$$

$$\partial_t((1-c_0 n)\rho u_2) + \partial_x((1-c_0 n)\rho u_2^2) + \partial_x P = \\ = \varepsilon_R \Delta u_2 + \varepsilon_g (1-c_0 n),$$

$$\partial_t(c_0 n \rho u_1) + \partial_x(c_0 n \rho u_1^2) + \partial_x P = \\ = \varepsilon_R \Delta u_1 + \varepsilon_g c_0 n \rho,$$

$$\rho \frac{d}{dt} E + P \mathrm{div} U = \varepsilon_R \Delta E,$$

where ρ is density; x is the spatial variable; t is time; c_0 is the concentration of active component; ε_g is the free fall acceleration; ε_R = 1/Re; Re is the Reynolds number; $\varepsilon_R = \varepsilon / (\rho_* U_* L_*)$; ρ_* is the characteristic density of homogeneous mixture; U_* is the characteristic velocity of homogeneous mixture; L_* is the characteristic size of medium; ε is the kinetic viscosity; the average velocity of mixture is $U = c_0 n u_1 + (1-c_0 n)u_2$; $\frac{d}{dt} = \partial_t + U\partial_x$; kinetic equations [13, 14] are:

$$\rho c \frac{d}{dt} T = \partial_x(\lambda \partial_x T) + QW(n,T), \tag{2}$$

where c is the molar concentration and Q is heat.

$$\rho \frac{d}{dt} n = \partial_x(\rho D \partial_x NNn) - W(n,T),$$

where D is the mobility coefficient; NNn is the reduced amount of the active component of the two-component mixture.

$$W = k_0 \rho n^\beta \mathrm{e}^{-\frac{E_*}{RT}}, \tag{3}$$

where k_0 is the reaction rate constant at temperature; β is the reaction order; R is the universal gas constant; E_* is activation energy.

The closing equations in this case are the equations of state:

$$P = (\gamma - 1)\rho E + \frac{P_{\mathrm{ad}}^0}{\rho_0}\rho - \rho g(x, e_1) + \\ + TS\rho + n\rho\mu + RnT\rho, \tag{4}$$

where γ is the adiabatic exponent; P_{ad}^0 is the initial adiabatic pressure; ρ_0 is the density; g is the gravitational constant; e_1 = 1, 0, 0; μ is the chemical potential.

$$S + nS + n\left(\frac{d\mu_0(T)}{dT} + R\ln\left(\frac{nT\rho^2}{n_0 T_0 \rho_0^2}\right)\right) = 0, \tag{5}$$

where μ_0 is the chemical potential at the input T_0 is the temperature; n_0 is the reduced amount of active component.

Here, the primary hypothesis states that the mechanism of the laminar–turbulent transition in the combustion process during the kinetic energy pumping is represented by diffusive stratification. In the one-dimensional case, this is implemented by a striped structure of interleaved layers with large (turbulent layers) and small (laminar layers) gradients of variables. The increased entropy of the system during the transition from the laminar to the turbulent state is represented in the form of the entropy of mixing of specific volumes (layers of an ideal mixture) having different values of the hydrodynamic component of the enthalpy, as well as the work against gravity, the energy component of the combustion process, and the component due to compressibility.

TURBULENCE OF VIBRATIONAL COMBUSTION. PUMPING

For vibrational combustion, it is natural to take the ratio of the vortex energy density H_{M} to the kinetic energy density (a measure of laminar combustion degradation) as a measure of the process degradation due to the laminar–turbulent transition, as follows:

$$h = \frac{\rho H_{\mathrm{M}}}{\frac{1}{2}\rho U^2},$$

where M is the local equilibrium manifold.

At the same time, the energetic influence of gravity on the laminar–turbulent transition in the combustion process is taken into account. To construct the second order phase transition, it is first necessary to construct an analog of the Landau–Ginzburg potential (specific Gibbs free energy). We investigate the possibility of extending the concept of nonequilibrium phase transitions as conceptualized in the Cahn–Hilliard spinodal decomposition theory to include the laminar–turbulent transition of the kinetic energy pumping combustion process. Here, the condition for breaking the local equilibrium manifold is formulated using the degradation measure of the laminar combustion process. We now turn to new variables. We introduce pumping by analogy with the laser terminology of Haken [15]:

$$\xi = \frac{(\gamma-1)\rho E}{\rho \tilde{U}^2}, \tag{6}$$

where $\tilde{U}$ is the internal energy.

We denote the laminar–turbulent transition variable by

$$h = \frac{H_M}{\rho U^2} = \xi + \nu,$$

where the number of vibrational turbulence is:

$$\nu = \frac{-\rho_0 E_0 - \rho^3 g(x,e_1) + \frac{P_{ad}^0}{\rho_0}(\rho-\rho_0) + \left[-T\frac{d\mu_0(T)}{dT} + \mu_0(T) - RT\right]n\rho}{\rho \tilde{U}^2},$$

where E_0 is the initial internal energy.

The vortex energy is as follows:

$$H_M = (\gamma-1)(\rho E - \rho_0 E_0) - \rho g(x,e_1) + \frac{P_{ad}^0}{\rho_0}(\rho-\rho_0) + \left[-T\frac{d\mu_0(T)}{dT} + \mu_0(T) - RT\right]n\rho =$$
$$= P_{ad,g} - P_{comb} + \left[-T\frac{d\mu_0(T)}{dT} + \mu_0(T)\right]n\rho - (\gamma-1)\rho_0 E_0 - P_{ad}^0,$$

where $P_{ad,g} = (\gamma-1)\rho E + \frac{P_{ad}^0}{\rho_0}\rho - \rho^3 \varepsilon_g(x,e_1)$ is the pressure of adiabatic hydrodynamic process in the gravity field and $P_{comb} = RTn\rho$ is the Mendeleev–Clapeyron equation.

The initial partial pressure $P_{ad}^0 = \text{const}$, as well as $\rho_0 = \text{const}$, and the initial internal energy $E_0 = \text{const}$.

As shown below, the condition for the excitation of turbulence has the form of $\nu \ll 1$. It should be noted that, for $\nu \to 0$, a larger U^2 denotes more developed turbulence (ν is an analog of the Reynolds number).

The condition for the nucleation of the laminar–turbulent transition in vibrational combustion (feedback) is that the vibrational turbulence number is sufficiently small ($\nu \to 0$) provided that $U^2 \to \infty$. The latter is true if

$$\frac{Tn}{U^2} \to 0, \tag{7}$$

being verified by a numerical experiment.

LAMINAR–TURBULENT TRANSITION POTENTIAL OF THE COMBUSTION PROCESS, $\tilde{F}(\xi, \nu)$

The laminar–turbulent transition in vibrational combustion occurs when the velocity of the passive component at the input increases. This corresponds to phase transitions in systems of poorly soluble liquids with a lower critical point for stratification (in such systems, stratification occurs when the temperature increases, which corresponds to an increase in enthalpy; in hydrodynamic systems, it corresponds to an increase in the hydrodynamic component of the total enthalpy). It is known from experiments that a mixture of turbulent and laminar layers (sponges in Landau's terminology) can be considered as a perfect mixture for which the entropy of the laminar–turbulent transition process is:

$$s = (h) = -(h^2\ln(h^2) + (1-h^2)\ln(1-h^2)), \tag{8}$$

$$h = \xi + \nu,\ \nu \to 0, \text{ if } |U| \to \infty. \tag{9}$$

The distribution h represents the excess enthalpy of an inhomogeneous thermodynamic system with respect to a homogeneous one. Here, h^2 and s are the dimensionless enthalpy and entropy of the laminar–turbulent transition, respectively. The dimensionless Gibbs free energy G of the laminar–turbulent transition process is given by

$$F(\xi;\alpha,\nu_{comb}) = h_{comb}^2 - \alpha(\nu_{comb})h_{comb}^2 s(h_{comb}^2), \tag{10}$$

which is an analog of the Gibbs–Helmholtz equation $\Delta G = \Delta H - T\Delta S$, where the intensive variable T (temperature) is represented by the parameter $\alpha(\nu_{comb})h_{comb}^2$, reflecting the relationship between temperature and enthalpy H due to the energy intensity of the medium (analog of the heat capacity); α is a parameter on the design interval; ν_{comb} is the number

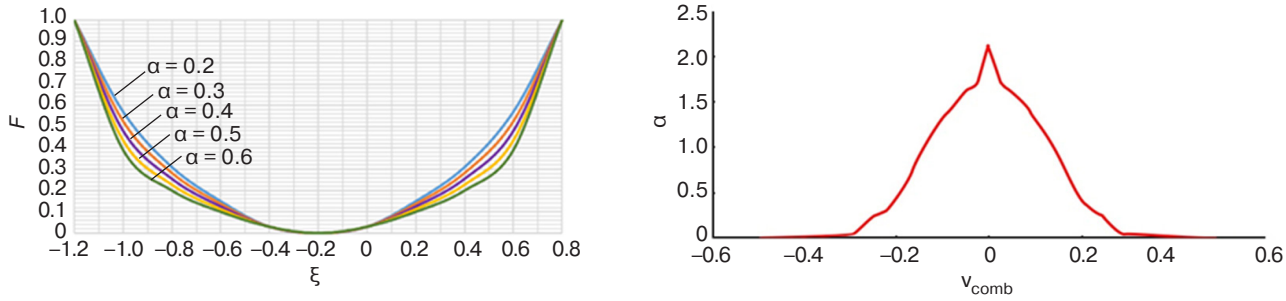

(a) (b)

Fig. 1. (a) Potential $F(\xi; \alpha; v_{comb})$ at $v = 0.2$ and different values of $\alpha = 0.2, 0.3, 0.4, 0.5, 0.6$; (b) dependence $\alpha(v_{comb})$

of turbulence at heat pumping; h_{comb} is the calculated enthalpy. Here, the function $\alpha(v_{comb})$ is defined by the graph shown in Fig. 1b. The plots of the potential $F(\xi;\alpha,v_{comb})$ at $v = 0.2$ and different values of α are shown in Fig. 1a.

We perform the correction of the potential $F(\xi;\alpha,v_{comb})$ according to [13], as follows:

1) for $-1 < v_{comb} \le 0$, $-1 + |v| < \xi < 1 + |v|$ we set:

$$\tilde{F}(\xi,v_{comb}) = \begin{cases} F(\xi,v_{comb}), & 0 \le \xi < 1+|v_{comb}|, \\ \gamma_-(h^2(\xi) - h^2(0) + F(0,v_{comb})), & \xi < 0. \end{cases} \quad (11)$$

The constant γ_- is found from the condition

$$2\gamma_- v = \frac{d}{d\xi}F(0,v) = 2v(1 + 2\alpha v^2 \ln(v^2) + \alpha(1 - 2\alpha v^2)\ln(1 - v^2))$$

or

$$\gamma_- = (1 + 2\alpha v^2 \ln(v^2) + \alpha(1 - 2v^2)\ln(1 - v^2)).$$

2) for $0 < v < 0.5$, $-1 - v < \xi < 1 - v$

$$\tilde{F}(\xi,v_{comb}) = \begin{cases} F(\xi,v_{comb}), & -v_{comb} \le \xi < 1 - v_{comb}, \\ \gamma_+ g_1(\xi), & \xi < 1 - v. \end{cases}$$

The constant γ_+ is found from the condition

$$\gamma_+ g''_1(-v_{comb}) = F''(-v_{comb}, -v_{comb}).$$

Here,

$$g_1(\xi, v) = h^2(1 + \alpha(1 - h^2)^6 \ln(1 - h^2)).$$

The plots of the laminar–turbulent transition potential are shown in Figs. 2a and 2b.

BREAKDOWN EQUATION OF THE LOCAL EQUILIBRIUM MANIFOLD (INSTABILITY OF THE LAMINAR PROCESS OF APPROXIMATION OF LOCAL EQUILIBRIUM)

The work sets out to demonstrate that kinetic energy pumping leads to an excess of energy in the laminar process as the local equilibrium is approached, thus causing its instability. The latter is expressed either by resonance or by breaking out of the local equilibrium manifold, which is characterized by process turbulence. Through the process turbulence, the excess energy generated by the kinetic energy pumping is "dumped." The mathematical model of process turbulence can be described as follows.

In order to simulate the breakdown of the local equilibrium manifold, represented by the breakdown of the laminar combustion process at mixture heating in the

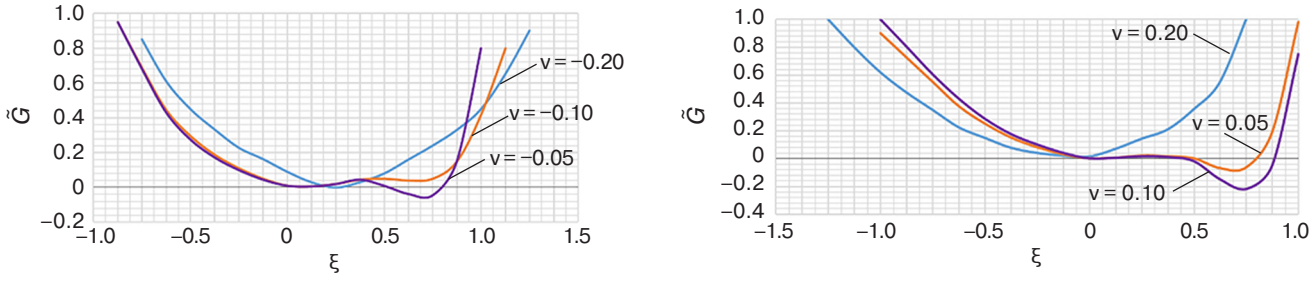

(a) (b)

Fig. 2. Potential $\tilde{F}(\xi; v)$ (a) $v = -0.20, -0.10, -0.05$; (b) $v = 0.05, 0.10, 0.20$

phase space of dimensionless variables $(\tilde{E}, \tilde{u}_1, \tilde{u}_2, \tilde{\rho}, \tilde{T}, \tilde{n})$, it is necessary to move to new variables $(\xi, \tilde{u}_1, \tilde{u}_2, \tilde{\rho}, \tilde{T}, \tilde{n})$, namely, the pumping ξ as a variable of the laminar–turbulent transition. The equations

$$\rho \frac{d}{d\tilde{t}} \tilde{E} + \tilde{P} \widetilde{\operatorname{div}} \tilde{U} = 0; \; (\gamma - 1)\tilde{E} = \xi \tilde{U}^2 \tag{12}$$

allow us to obtain for the pumping:

$$\tilde{\rho}\tilde{U}^2 \frac{d}{d\tilde{t}} \tilde{E} + 2\tilde{\rho}\tilde{U}\xi \frac{d}{d\tilde{t}} \tilde{U} = \tilde{\rho} \frac{d}{d\tilde{t}} (\tilde{U}^2 \xi) = -(\gamma - 1)\tilde{P} \widetilde{\operatorname{div}} \tilde{U},$$

where $\tilde{P}$ is the pressure; $d\tilde{t}$ is the temperature difference.

Hence: $\tilde{\rho} \frac{d}{d\tilde{t}} \xi + \frac{2\tilde{\rho}\xi}{\tilde{U}} \frac{d}{d\tilde{t}} \tilde{U} + \frac{(\gamma - 1)\tilde{P}}{\tilde{U}^2} \widetilde{\operatorname{div}} \tilde{U} = 0.$

Here,

$$\frac{d}{d\tilde{t}} \tilde{U} = \frac{1}{\tilde{\rho}} \frac{d}{d\tilde{t}} (\tilde{\rho}\tilde{U}) - \frac{1}{\tilde{\rho}} \tilde{U} \frac{d}{d\tilde{t}} \tilde{\rho} =$$

$$= \frac{1}{\tilde{\rho}} [-\partial_{\tilde{x}} ((1 - c_0 \tilde{n})\tilde{\rho}\tilde{u}_2^2) - \partial_{\tilde{x}} \tilde{P} + \tilde{\varepsilon}_g (1 - c_0 \tilde{n})\tilde{\rho} -$$

$$- \partial_{\tilde{x}} (c_0 \tilde{n}\tilde{\rho}\tilde{u}_1^2) - \partial_{\tilde{x}} \tilde{P} + \tilde{\varepsilon}_g c_0 \tilde{n}\tilde{\rho}] + \frac{1}{\tilde{\rho}} \tilde{U} \partial_{\tilde{x}} (\tilde{\rho}\tilde{U}).$$

Finally:

$$\tilde{\rho} \frac{d}{dt} \xi - \frac{2\xi}{\tilde{U}} [\partial_{\tilde{x}} ((1 - c_0 \tilde{n})\tilde{\rho}\tilde{u}_2^2) +$$
$$+ \partial_{\tilde{x}} (c_0 \tilde{n}\tilde{\rho}\tilde{u}_1^2) + 2\partial_{\tilde{x}} \tilde{P} - \tilde{\varepsilon}_g \tilde{\rho}] +$$
$$+ 2\xi \partial_{\tilde{x}} (\tilde{\rho}\tilde{U}) + \frac{(\gamma - 1)\tilde{P}}{\tilde{U}^2} \widetilde{\operatorname{div}} \tilde{U} = 0.$$

We now regularize the equations of momentum and the equation of continuity (hydrodynamics) by the viscosity:

$$\partial_{\tilde{t}} \tilde{\rho} + \partial_{\tilde{x}} (\tilde{\rho}\tilde{U}) = \tilde{\varepsilon}_R \tilde{\Delta}\tilde{\rho}, \tag{13}$$

$$\partial_{\tilde{t}} ((1 - c_0 \tilde{n})\tilde{\rho}\tilde{u}_2) + \partial_{\tilde{x}} ((1 - c_0 \tilde{n})\tilde{\rho}\tilde{u}_2^2) + \partial_{\tilde{x}} \tilde{P} =$$
$$= \tilde{\varepsilon}_g (1 - c_0 \tilde{n})\tilde{\rho} + \tilde{\varepsilon}_R \tilde{\Delta}\tilde{u}_2,$$

$$\partial_{\tilde{t}} (c_0 \tilde{n}\tilde{\rho}\tilde{u}_1) + \partial_{\tilde{x}} (c_0 \tilde{n}\tilde{\rho}\tilde{u}_1^2) + \partial_{\tilde{x}} \tilde{P} =$$
$$= \tilde{\varepsilon}_g c_0 \tilde{n}\tilde{\rho} + \tilde{\varepsilon}_R \tilde{\Delta}\tilde{u}_1,$$

where $\tilde{U} = c_0 \tilde{n}\tilde{U}_1 + (1 - c_0 \tilde{n})\tilde{U}_2$ is the average velocity of the mixture; $\mathrm{Re} = 1 / \tilde{\varepsilon}_R$, $\mathrm{Re} = \eta_D / (U_* L_*) = \eta_D / (\rho_* U_* L_*)$ is the Reynolds number of homogeneous state $\rho_*, n_*, T_*, u_1^*, u_2^*$; η_D is the dynamic viscosity in Reynolds number; $U_* = c_* n_* u_1^* + (1 - c_* n_*)U_*$ is the characteristic velocity of homogeneous mixture; L_* is the characteristic size of the medium; $\tilde{\varepsilon}_R$ is the dynamic viscosity.

From the equation for the internal energy, we derive the equation for the pumping, in which a covariant Cahn diffusion (Cahn operator of variable diffusion) is introduced:

$$\tilde{\rho} \frac{d}{d\tilde{t}} \xi - \frac{2\xi}{\tilde{U}} [\partial_{\tilde{x}} ((1 - c_0 \tilde{n})\tilde{\rho}\tilde{u}_2^2) +$$
$$+ \partial_{\tilde{x}} (c_0 \tilde{n}\tilde{\rho}\tilde{u}_1^2) + 2\partial_{\tilde{x}} \tilde{P} + \tilde{\varepsilon}_g \tilde{\rho}] +$$
$$+ 2\xi \partial_{\tilde{x}} (\tilde{\rho}\tilde{U}) + \frac{(\gamma - 1)\tilde{P}}{\tilde{U}^2} \widetilde{\operatorname{div}} \tilde{U} = \tag{14}$$
$$= \partial_{\tilde{x}} \left(\frac{\tilde{D}}{\tilde{T}} \partial_{\tilde{x}} (F(\xi, \nu) - \tilde{\varepsilon}_K^2 \partial_{\tilde{x}}^2 \xi) \right),$$

where ε_K is the Cahn alternating diffusion, $\tilde{D} = D / (\rho_* U_* L_* T_*)$, D is the mobility coefficient, and the potential F in this case is $F(\xi, \nu) = \partial_\xi \tilde{G}(\xi, \nu)$.

We add the kinetic equations for temperature and reduced substance $\tilde{n}$. Finally, we obtain a model of vibrational combustion turbulence in hydrodynamics, kinetics, and pumping:

$$\partial_{\tilde{t}} \tilde{\rho} + \partial_{\tilde{x}} (\tilde{\rho}\tilde{U}) = \tilde{\varepsilon}_R \tilde{\Delta}\tilde{\rho}, \tag{15}$$

$$\partial_{\tilde{t}} ((1 - c_0 \tilde{n})\tilde{\rho}\tilde{u}_2) + \partial_{\tilde{x}} ((1 - c_0 \tilde{n})\tilde{\rho}\tilde{u}_2^2) + \partial_{\tilde{x}} \tilde{P} =$$
$$= \tilde{\varepsilon}_g (1 - c_0 \tilde{n})\tilde{\rho} + \tilde{\varepsilon}_R \tilde{\Delta}\tilde{u}_2,$$

$$\partial_{\tilde{t}} (c_0 \tilde{n}\tilde{\rho}\tilde{u}_1) + \partial_{\tilde{x}} (c_0 \tilde{n}\tilde{\rho}\tilde{u}_1^2) + \partial_{\tilde{x}} \tilde{P} =$$
$$= \tilde{\varepsilon}_g c_0 \tilde{n}\tilde{\rho} + \tilde{\varepsilon}_R \tilde{\Delta}\tilde{u}_1,$$

$$\tilde{\rho}\tilde{c} \frac{d}{d\tilde{t}} \tilde{T} = \partial_{\tilde{x}} (\tilde{\lambda} \partial_{\tilde{x}} \tilde{T}) + \tilde{T}\tilde{S}\tilde{W}(\tilde{n}, \tilde{T}), \tag{16}$$

$$\tilde{\rho} \frac{d}{d\tilde{t}} \tilde{n} = \partial_{\tilde{x}} (\tilde{\rho}\tilde{D} \partial_{\tilde{x}} \tilde{n}) - \tilde{W}(\tilde{n}, \tilde{T}),$$

$$\tilde{W} = \tilde{k}_0 \tilde{\rho}\tilde{n}^\beta \mathrm{e}^{-\frac{\tilde{E}_*}{RT}}, \tag{17}$$

$$\tilde{\rho} \frac{d}{d\tilde{t}} \xi - \frac{2\xi}{\tilde{U}} [\partial_{\tilde{x}} ((1 - c_0 \tilde{n})\tilde{\rho}\tilde{u}_2^2) +$$
$$+ \partial_{\tilde{x}} (c_0 \tilde{n}\tilde{\rho}\tilde{u}_1^2) + 2\partial_{\tilde{x}} \tilde{P} + \tilde{\varepsilon}_g \tilde{\rho}] + 2\xi \partial_{\tilde{x}} (\tilde{\rho}\tilde{U}) + \tag{18}$$
$$+ \frac{(\gamma - 1)\tilde{P}}{\tilde{U}^2} \widetilde{\operatorname{div}} \tilde{U} = \partial_{\tilde{x}} \left(\frac{\tilde{D}}{\tilde{T}} \partial_{\tilde{x}} [\hat{F}(\xi, \nu) - \hat{\varepsilon}_K^2 \partial_{\tilde{x}}^2 \xi] \right),$$

$$\tilde{P} = \tilde{P}_{\text{ad,g}} + \tilde{P}_{\text{comb}} + \left(-\tilde{T}\frac{d\tilde{\mu}_0(\tilde{T})}{d\tilde{T}} + \tilde{\mu}_0(\tilde{T}) \right)\tilde{n}\tilde{\rho}, \quad (19)$$

$$\tilde{S} = -\left(\frac{d}{d\tilde{T}}\tilde{\mu}_0(\tilde{T}) + \ln\left(\frac{\tilde{\rho}^2\tilde{T}\tilde{n}}{\tilde{\rho}_0^2\tilde{T}_0\tilde{n}_0} \right) \right)\tilde{n}.$$

NUMERICAL EXPERIMENT OF THE MODEL (15)–(19)

In order to establish the possibility of combustion turbulence, we perform numerical experiments of model (15)–(19) on a segment $\tilde{x} \in [0,1]$ with boundary conditions to control the kinetic energy pumping rate:

$$\tilde{u}_2|_{\tilde{x}=0} = \tilde{u}_2^0(1+V\tilde{t})\partial_{\tilde{x}}\tilde{\rho}|_{\tilde{x}=0} = \partial_{\tilde{x}}\tilde{\rho}|_{\tilde{x}=1} =$$
$$= \partial_{\tilde{x}}\tilde{u}_1|_{\tilde{x}=0} = \partial_{\tilde{x}}\tilde{u}_1|_{\tilde{x}=1} = \partial_{\tilde{x}}\tilde{T}|_{\tilde{x}=0} = \partial_{\tilde{x}}\tilde{T}|_{\tilde{x}=1} = 0,$$
$$\partial_{\tilde{x}}\tilde{u}_2|_{\tilde{x}=1} = \partial_{\tilde{x}}\tilde{n}|_{\tilde{x}=0} = \partial_{\tilde{x}}\tilde{n}|_{\tilde{x}=1} = 0,$$
$$\partial_x\xi|_{x=0} = \partial_x\xi|_{x=1} = \partial_x\mu|_{x=0} = \partial_x\mu|_{x=1},$$

(where $\mu = \hat{F}_{\text{comb}}(\xi,\nu) - \hat{\varepsilon}_{\text{K}}^2\partial_{\tilde{x}}^2\xi$, $\hat{F}_{\text{comb}}$ is the free energy resulting from the calculation) and initial conditions modeling, in the one-dimensional case, the injection from the nozzle of the combustible component of a two-component mixture:

$$\tilde{\rho}|_{\tilde{t}=0} = \tilde{\rho}_0 = 1,\ \tilde{u}_1|_{\tilde{t}=0} = \tilde{u}_1^0 = 0.2,$$
$$\tilde{u}_2|_{\tilde{t}=0} = \tilde{u}_2^0 = 0.2,\ \tilde{T}|_{\tilde{t}=0} = \tilde{T}_0 = 10,$$

$\tilde{E}_* = 100$. Initial data for pumping ξ_0 = const from the lability zone of the potential $\hat{F}_{\text{comb}}(\xi,\nu_\upsilon)$ (index υ is the velocity turbulence) is:

$$\tilde{\varepsilon}_{\text{K}} = 0.04,\ \tilde{\varepsilon}_{\text{g}} = 0.01.$$

Example 1 (Figs. 3a–3h). The resonance elimination by turbulence (far from resonance), for $j = 1$ in the standard chemical potential formula:

$$\tilde{\mu}_0(\tilde{T}) = \tilde{T}_0\left[B_* - (R + A_*)\frac{\tilde{T}^j}{\tilde{T}_0^j} \right], \quad (20)$$

where $\tilde{\mu}_0(\tilde{T})$ is the chemical potential; $\tilde{T}_0$ is the initial temperature; $\tilde{T}, B_*, A_*$ are constants; and R is the universal gas constant.

The basic turbulence parameters for vibrational combustion are $u_1(0) = u_2(0) = 10$, $\xi(0) = 0.2$, $\rho(0) = 1$. The cross sections in all the plots below are $t = 0.005$, 0.01, 0.025, 0.035, 0.05, 0.065, 0.125; $T(0) = 10$.

As can be seen in Fig. 3a and 3b, the pressure increases and the entropy decreases, i.e., deflagration becomes detonation when turbulence is involved. There is an increase in temperature and density.

Example 2 (Figs. 4a–4j). The resonance elimination by turbulence (for critical values $A_* + R = 3$), for $j = 4$ in (20). We consider the account for the basic turbulence parameters of vibrational combustion: $u_1(0) = u_2(0) = 10$, $\xi(0) = 0.2$, $\rho(0) = 1.5$. For all plots below the cross-section $t = 0$, 0.005, 0.010, 0.025, 0.035, 0.050, 0.065, 0.125. The first case (base case): $T(0) = 5$. The pressure and the entropy increase significantly. There is a wide zone of the detonation mode of the vibrational combustion (in the absence of turbulence, there was a narrow zone of the detonation combustion close to the resonance [3]). The internal energy increases but decreases relative to pumped kinetic energy $\xi \to 0$. A part of the pumped kinetic energy is converted into heat.

Example 3 (Figs. 5a–5j). The resonance elimination for $j = 4$ (20) (far from the critical resonance parameters), at low temperatures, with the basic turbulence parameters $u_1(0) = u_2(0) = 12$, $\xi(0) = 0.2$, $\rho(0) = 1.5$, and the cross-section $\tilde{t} = 0$, 0.005, 0.010, 0.025, 0.035, 0.050, 0.065, 0.125. Here, $T(0) = 0.8$. The pressure and the entropy decrease. The internal energy increases but decreases relative to pumped kinetic energy $\xi \to 0$. A part of the kinetic energy is converted into heat ($\tilde{T}$ and $\tilde{T}\tilde{S}$ increase).

Example 4 (Figs. 6a–6j). The resonance elimination by turbulence (close to the critical resonance parameters) for $j = 4$ in (20), at low temperatures, $u_1(0) = u_2(0) = 8$, $\xi(0) = 0.2$, $\rho(0) = 1.5$, cross-section $\tilde{t} = 0$, 0.005, 0.010, 0.025, 0.035, 0.050, 0.065, 0.125; $T(0) = 0.8$.

The entropy decreases and the pressure increases (the same as before turbulence, but the detonation zone is much wider). The internal energy increases but decreases relative to pumped kinetic energy ($\xi \to 0$). A part of the pumped kinetic energy is converted into heat (the internal energy $\tilde{E}$ and $\tilde{T}$ increase).

Example 5 (Figs. 7a–7j). Mixing. Numerical experiment (20) for $j = 4$, $A_* + R = 0.5$ (base parameters); $\tilde{\text{n}}|_{\tilde{t}=0} = \tilde{\text{n}}_0 = 1$, $\tilde{u}_1|_{\tilde{t}=0} = \tilde{u}_1^0 = 0.2$; $\tilde{u}_2|_{\tilde{t}=0} = \tilde{u}_2^0 = 0.2$; $\tilde{T}|_{\tilde{t}=0} = \tilde{T}_0 = 10$ are constants; $\tilde{n}|_{\tilde{t}=0} = \tilde{n}_1 = 0.5$, $\tilde{x} \in (0;0.3) \cup (0.4;0.5)$, $\tilde{n}|_{\tilde{t}=0} = 0.66$, $\tilde{x} \in (0.3;0.4)$; $E_* = 100$; $\tilde{t} = 0$, 0.005, 0.010, 0.025, 0.035, 0.050, 0.065, 0.125; initial data for internal energy $\tilde{E}_0 = \text{const}$, $\tilde{T}_0 = 8$, $\tilde{u}_2 = 8$.

Resonance elimination for mixing. Modeling the injection of the combustible component of a two-component mixture from three nozzles in the one-dimensional case with initial conditions.

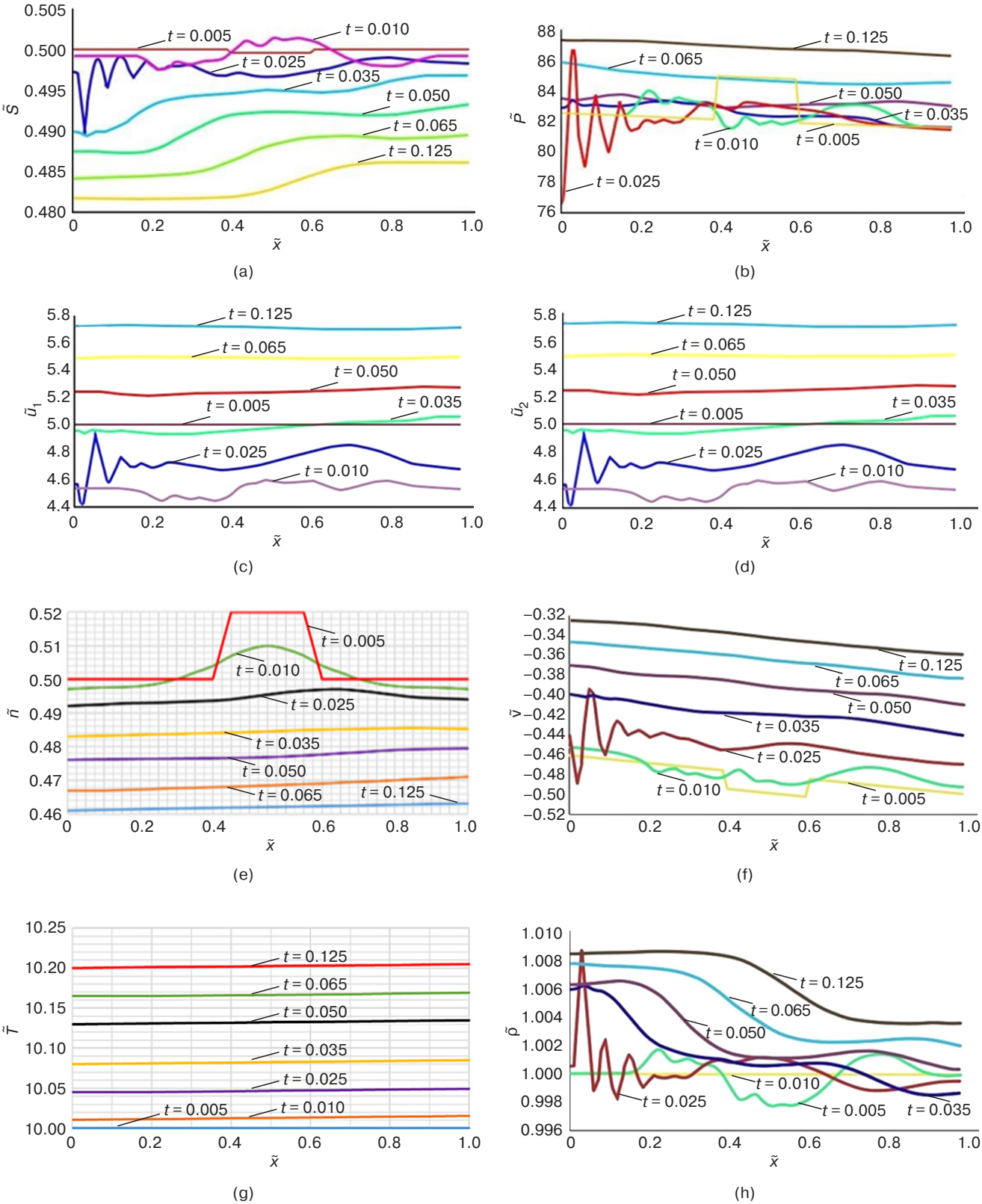

Fig. 3. Numerical experimental results of model (15)–(19) on the segment $\tilde{x} \in [0,1]$ for different t: (a) $\tilde{S}$; (b) $\tilde{P}$; (c) $\tilde{u}_1$; (d) $\tilde{u}_2$; (e) reduced amount of substance $\tilde{n}$; (f) $\tilde{v}$; (g) $\tilde{T}$; (h) $\tilde{\rho}$

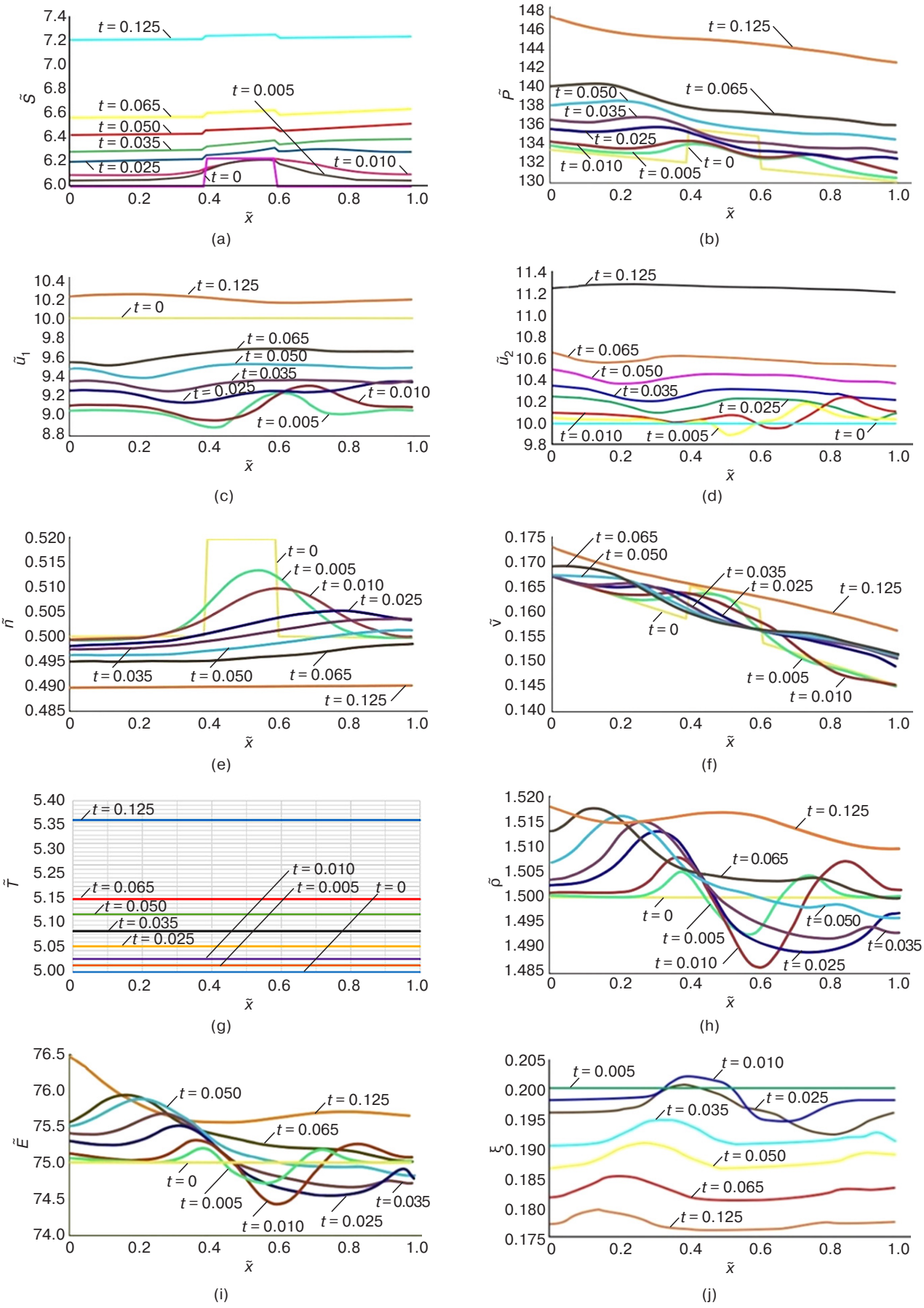

Fig. 4. Calculation results for the basic turbulence parameters of vibrational combustion for different t: (a) $\tilde{S}$; (b) $\tilde{P}$; (c) $\tilde{u}_1$; (d) $\tilde{u}_2$; (e) $\tilde{n}$; (f) $\tilde{v}$; (g) $\tilde{T}$; (h) $\tilde{\rho}$; (i) $\tilde{E}$; (j) ξ

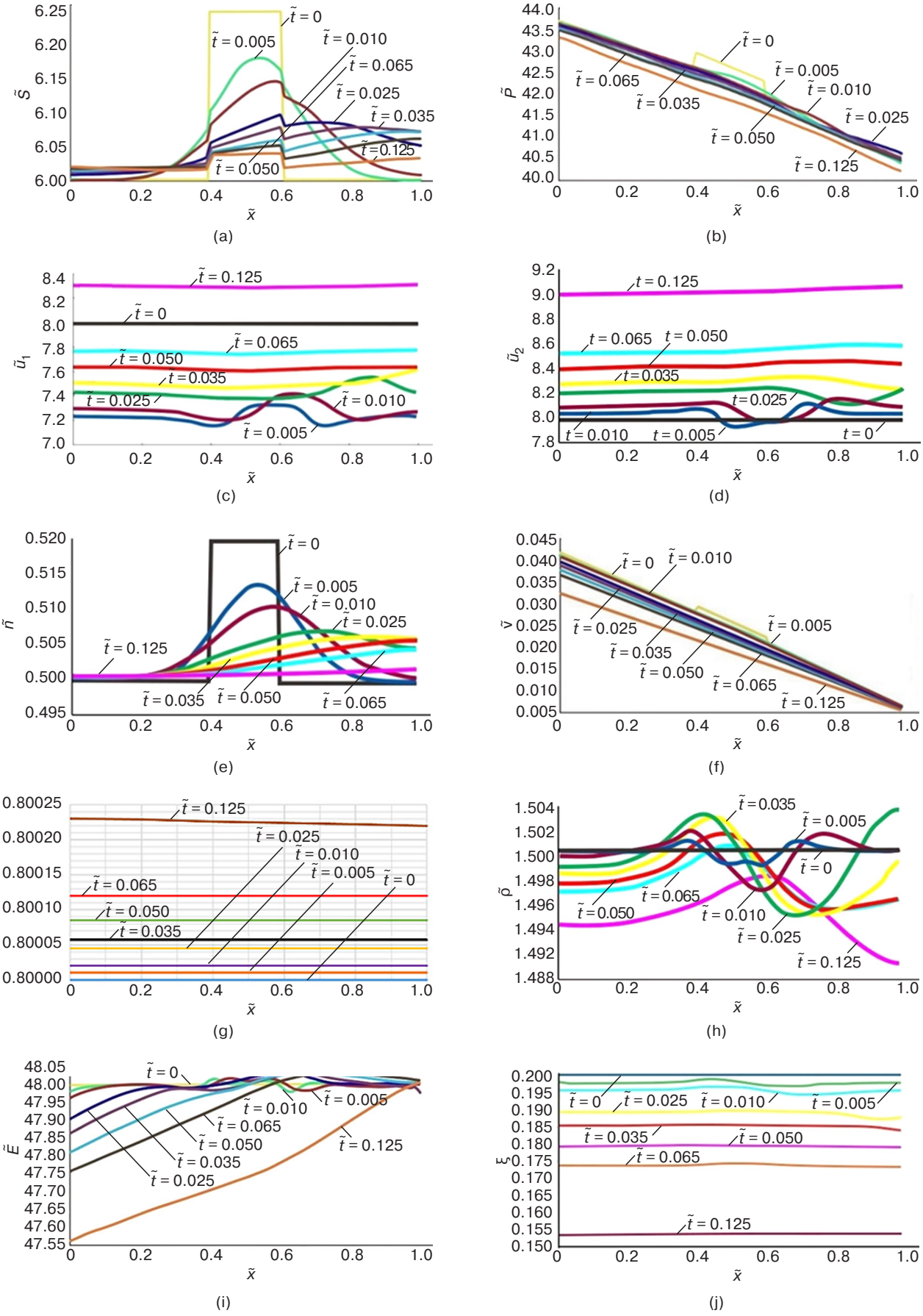

Fig. 5. Calculation results of the resonance elimination for $j = 4$ (20) (far from the critical resonance parameters) at low temperatures for different $\tilde{t}$: (a) $\tilde{S}$; (b) $\tilde{P}$; (c) $\tilde{u}_1$; (d) $\tilde{u}_2$; (e) $\tilde{n}$; (f) $\tilde{v}$; (g) $\tilde{T}$; (h) $\tilde{\rho}$; (i) $\tilde{E}$; (j) ξ

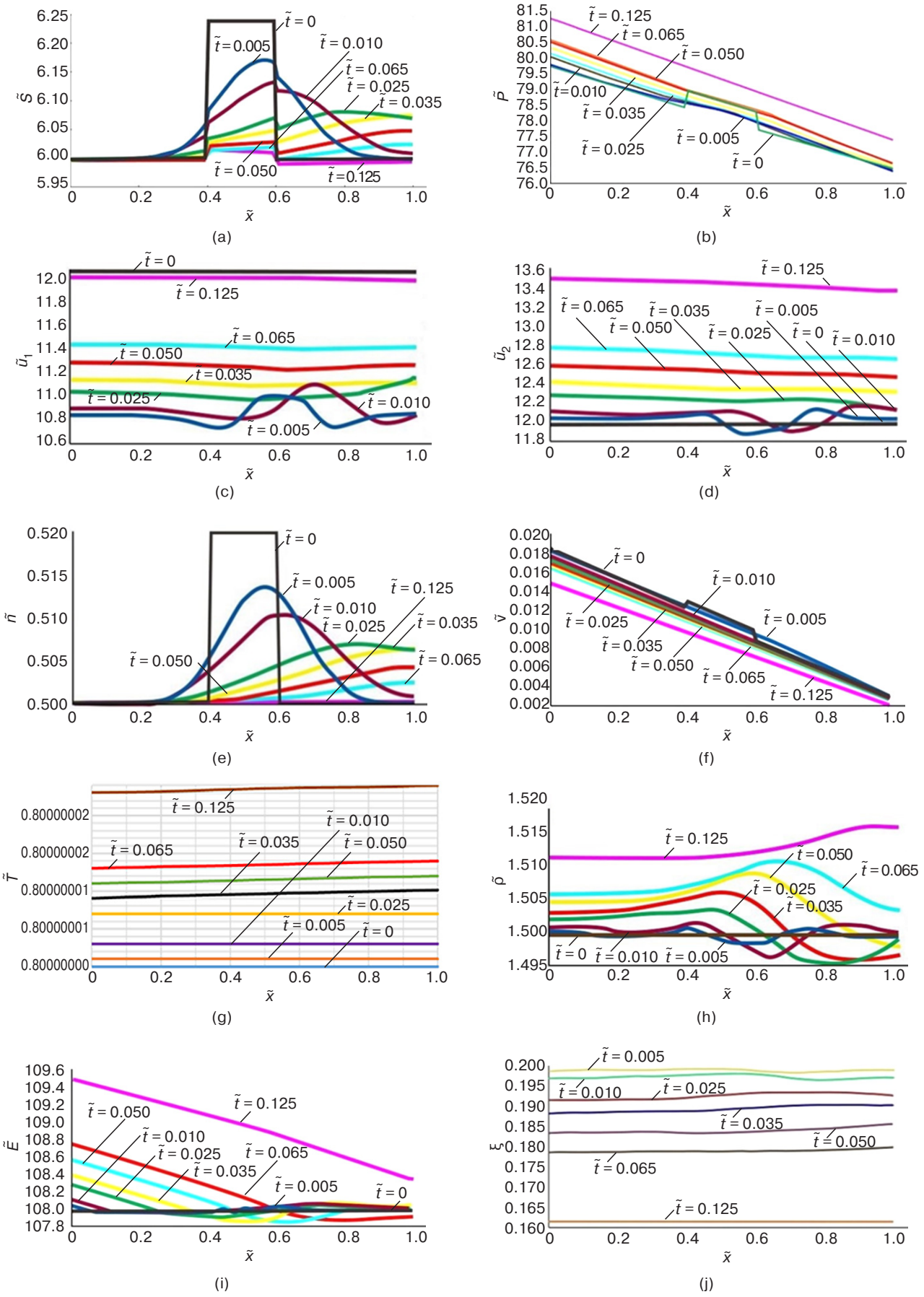

Fig. 6. Calculation results for the resonance elimination by turbulence (close to the critical resonance parameters) for $j = 4$ in (20) at low temperatures for different $\tilde{t}$: (a) $\tilde{S}$; (b) $\tilde{P}$; (c) $\tilde{u}_1$; (d) $\tilde{u}_2$; (e) $\tilde{n}$; (f) $\tilde{v}$; (g) $\tilde{T}$; (h) $\tilde{\rho}$; (i) $\tilde{E}$; (j) ξ

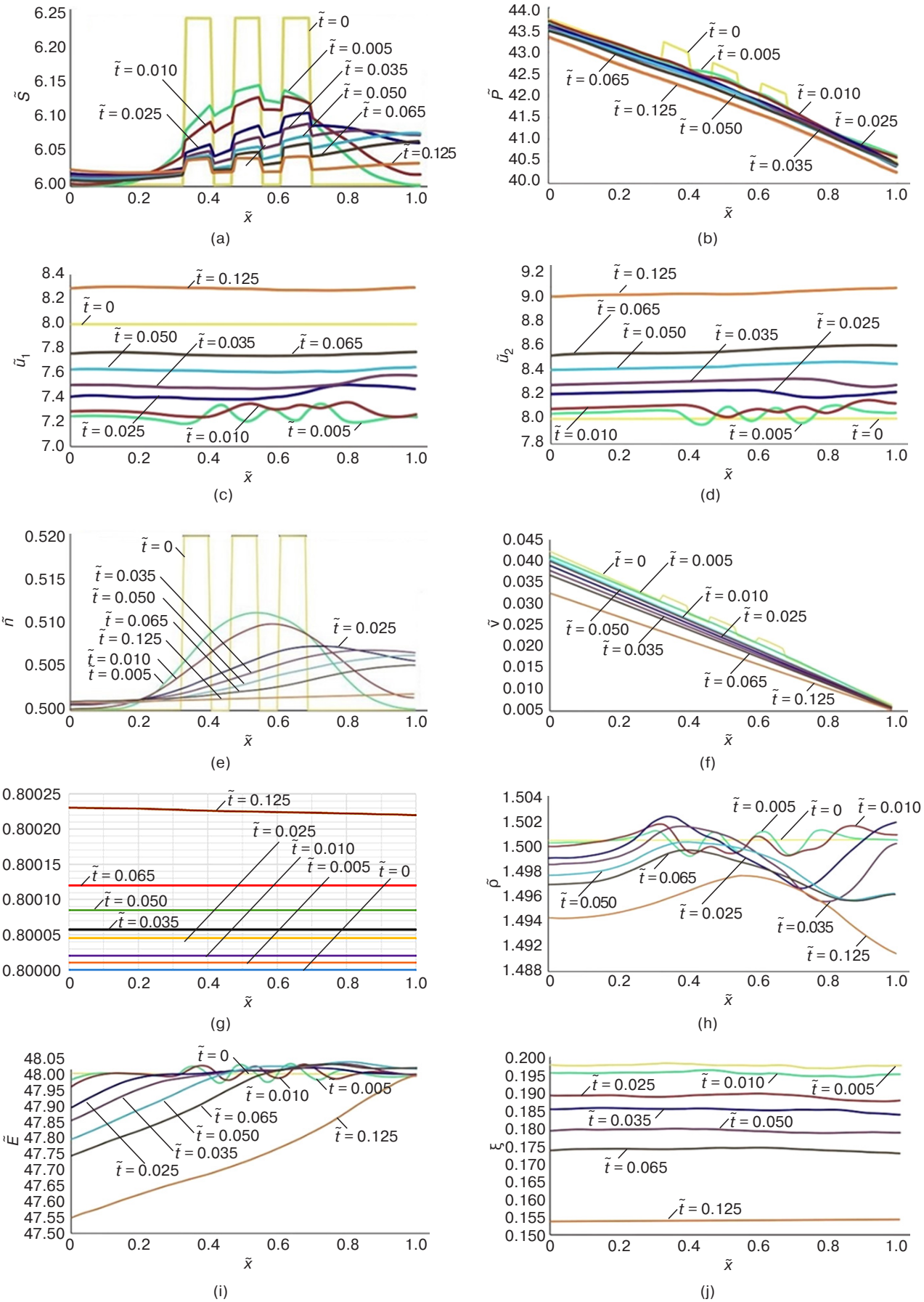

Fig. 7. Numerical results of the experiment (20) for $j = 4$, $A_* + R = 0.5$ for different $\tilde{t}$: (a) $\tilde{S}$; (b) $\tilde{P}$; (c) $\tilde{u}_1$; (d) $\tilde{u}_2$; (e) $\tilde{n}$; (f) $\tilde{v}$; (g) $\tilde{T}$; (h) $\tilde{\rho}$; (g) $\tilde{E}$; (j) ξ

The entropy and the pressure continue to decrease (as before turbulence). However, as the velocity $\tilde{u}^2$ of the neutral component at the input increases, detonation combustion mode occurs. The numerical experiment also predicts a detonation combustion mode. Meanwhile, temperature, density, and internal energy increase. The pattern of the plots reflects the effect of gravity. Similar numerical experimental results are obtained for resonance elimination by turbulence $j = 4$ in (20) under mixing, with an increase in the initial velocity of the passive variable $\tilde{u}_2^0 = 10$. As the velocity of the neutral component $\tilde{u}_2$ at the input increases with mixing, the detonation combustion mode occurs.

CONCLUSIONS

The described studies support the conclusion that the thermodynamic method offers fundamental possibilities for studying the evolution of a system (in this case, the tendency of stratification into "turbulent" and "non-turbulent" combustion). It should be noted that the applied thermodynamic analysis can only indicate process evolution trends (main possibility of implementation) and the choice of system evolution trajectory, but not the speed of this process. The analysis confirms that regions of laminar combustion stability develop during combustion, along with metastable and labile regions where laminar combustion is unstable. However, this does not imply that there will be no signs of turbulence in the developed state of the region of stability. The diffusion of perturbations in these regions will dilute them, while in the regions of instability the process of "negative" (Cahn) diffusion will concentrate them. It can be assumed that regions of instability of the homogeneous system are sources of perturbations, and regions of stability are sinks. These assumptions have been verified by numerical experiments using the mathematical model described above. When starting from the initial thermodynamic model, the mathematical model of the laminar–turbulent transition during the combustion as an analog of the nonequilibrium phase transition can become complicated.

ACKNOWLEDGMENTS

The study was carried out within the framework of the Agreement on Federal Support for Major Scientific Projects in Priority Areas of Scientific and Technological Development No. 075-15-2024-527 dated April 23, 2024.

Authors' contributions

E.V. Radkevich—development and mathematical interpretation of the combustion model.

M.E. Stavrovsky—description of models of critical phenomena.

O.A. Vasilyeva—numerical experiment of models.

N.N. Yakovlev—full-scale experiment, obtaining data for models.

M.I. Sidorov—verification of the adequacy of models and description of processes.

REFERENCES

1. Cahn J.W., Hillard J.E. Free energy of a nonuniform system. 1. Interfacial free energy *J. Chem. Phys*. 1958;28(2):258–271. https://doi.org/10.1063/1.1744102
2. Cahn J.W. Spinodal decomposition. *Acta Metall*. 1961;9(9):795–811. https://doi.org/10.1016/0001-6160(61)90182-1
3. Debye P. *Izbrannye trudy* (*Collected Papers*). Leningrad: Nauka; 1987. 559 p. (in Russ.).
4. Radkevich E.V., Lukashev E.A., Yakovlev N.N., Vasil'eva O.A., Sidorov M.I. *Vvedenie v obobshchennuyu teoriyu neravnovesnykh fazovykh perekhodov i termodinamicheskii analiz zadach mekhaniki sploshnoi sredy* (*Introduction to the Generalized Theory of Nonequilibrium Phase Transitions and Thermodynamic Analysis of Continuum Mechanics Problems*). Moscow: Moscow University Press; 2019. 342 p. (in Russ.).
5. Raushenbakh B.V. *Vibratsionnoe gorenie* (*Vibrational Combustion*). Moscow: Fizmatgiz; 1961. 500 p. (in Russ.).
6. Radkevich E.V., Vasil'eva O.A., Sidorov M.I., et al. On the Raushenbakh Resonance. *Moscow Univ. Mech. Bull*. 2021;76(3):65–77. https://doi.org/10.3103/S0027133021030055
[Original Russian Text: Radkevich E.V., Vasil'eva O.A., Sidorov M.I., Stavrovskii M.E. On the Raushenbakh Resonance. *Vestnik Moskovskogo universiteta. Seriya 1: Matematika, Mekhanika*. 2021;3:54–65 (in Russ.).]
7. Radkevich E.V., Yakovlev N.N., Vasil'eva O.A. Mathematical Modeling of Vibrational-Combustion. *Dokl. Math.* 2020;102(3):505–509. https://doi.org/10.1134/S1064562420060162
[Original Russian Text: Radkevich E.V., Yakovlev N.N., Vasil'eva O.A. Mathematical Modeling of Vibrational-Combustion. *Doklady Rossiiskoi Akademii Nauk. Matematika, Informatika, Protsessy Upravleniya*. 2020;495:69–73 (in Russ.). https://doi.org/10.31857/S2686954320060144]
8. Radkevich E.V., Yakovlev N.N., Vasil'eva O.A. Questions and problems of mathematical modeling qua nonequilibrium of combustion processes. *Eurasian J. Math. Computer Appl*. 2020;8(4):31–68. https://doi.org/10.32523/2306-6172-2020-8-4-31-68

9. Shiplyuk A.N., Buntin D.A., Maslov A.A., et al. Nonlinear Mechanisms of the Initial Stage of the Laminar–Turbulent Transition at Hypersonic Velocities. *J. Appl. Mech. Tech. Phys.* 2003;44(5):654–659. https://doi.org/10.1023/A:1025500219183
[Original Russian Text: Shiplyuk A.N., Buntin D.A., Maslov A.A., Chokani N. Nonlinear Mechanisms of the Initial Stage of the Laminar–Turbulent Transition at Hypersonic Velocities. *Prikladnaya Mekhanika i Tekhnicheskaya Fizika.* 2003;44(5): 64–71 (in Russ.).]
10. Lukashevich S.V., Morozov S.O., Shiplyuk A.N. Investigations of high-speed boundary layer stabilization by using porous coatings (review). *J. Appl. Mech. Tech. Phys*. 2023;64(4):575–590. https://doi.org/10.1134/S002189442304003X
[Original Russian Text: Lukashevich S.V., Morozov S.O., Shiplyuk A.N. Investigations of high-speed boundary layer stabilization by using porous coatings (review). *Prikladnaya Mekhanika i Tekhnicheskaya Fizika.* 2023;64(4):27–45. https://doi.org/10.15372/PMTF202215169]
11. Morozov S.O., Lukashevich S.V., Shiplyuk A.N. Hypersonic Boundary Layer Instability and Control by Passive Porous Coatings. In: Sherwin S., Schmid P., Wu X. (Eds.). *IUTAM Laminar-Turbulent Transition. IUTAM Bookseries*. Springer; 2023. V. 38. P. 613–619. https://doi.org/10.1007/978-3-030-67902-6_53
12. Radkevich E.V., Vasil'eva O.A., Yakovlev N.N., Sidorov M.I., Stavrovskii M.E. *Matematicheskoe modelirovanie detonatsionnogo goreniya* (*Mathematical Modeling of Detonation Combustion*). Moscow: Eco-Press; 2024. 200 p. (in Russ.).
13. Zel'dovich Ya.B., Barenblat G.I., Librovich V.B., Makhviladze G.M. *Matematicheskaya teoriya goreniya i vzryva* (*Mathematical Theory of Combustion and Explosion*). M.: Nauka; 1980. 472 p. (in Russ.).
14. Skripov V.P., Skripov A.V. Spinodal decomposition (phase transition via unstable states). *Phys. Usp.* 1979;22:(6)389–410. https://doi.org/10.1070/PU1979v022n06ABEH005571
[Original Russian Text: Skripov V.P., Skripov A.V. Spinodal decomposition (phase transition via unstable states). *Uspekhi fizicheskikh nauk*. 1979;128(2):193–231 (in Russ.). https://doi.org/10.3367/UFNr.0128.197906a.0193]
15. Haken H. *Sinergetika* (*Synergetics*): transl. from Engl. Moscow: Mir; 1980. 405 p. (in Russ.).
[Haken H. *Synergetics.* Springer; 1978. 355 p.]

СПИСОК ЛИТЕРАТУРЫ

1. Cahn J.W., Hillard J.E. Free energy of a nonuniform system. 1. Interfacial free energy *J. Chem. Phys*. 1958;28(2):258–271. https://doi.org/10.1063/1.1744102
2. Cahn J.W. Spinodal decomposition. *Acta Metall*. 1961;9(9):795–811. https://doi.org/10.1016/0001-6160(61)90182-1
3. Дебай П. *Избранные труды*. Л.: Наука; 1987. 559 с.
4. Радкевич Е.В., Лукашев Е.А., Яковлев Н.Н., Васильева О.А., Сидоров М.И. *Введение в обобщенную теорию неравновесных фазовых переходов и термодинамический анализ задач механики сплошной сред*ы. М.: Изд-во МГУ; 2019. 342 с.
5. Раушенбах Б.В. *Вибрационное горение*. М.: Физматгиз; 1961. 500 с.
6. Радкевич Е.В., Васильева О.А., Сидоров М.И., Ставровский М.Е. О резонансе Раушенбаха. *Вестник Московского университета. Серия 1: Математика, Механика*. 2021;3:54–65.
7. Радкевич Е.В., Яковлев Н.Н., Васильева О.А. Вопросы математического моделирования вибрационного горения. *Доклады Российской академии наук. Математика, информатика, процессы управления*. 2020;495:69–73. https://doi.org/10.31857/S2686954320060144
8. Radkevich E.V., Yakovlev N.N., Vasil'eva O.A. Questions and problems of mathematical modeling qua nonequilibrium of combustion processes. *Eurasian J. Math. Computer Appl*. 2020;8(4):31–68. https://doi.org/10.32523/2306-6172-2020-8-4-31-68
9. Шиплюк А.Н., Бунтин Д.А., Маслов А.А., Чокани Н. Нелинейные механизмы начальной стадии ламинарно-турбулентного перехода при гиперзвуковых скоростях. *Прикладная механика и техническая физика.* 2003;44(5):64–71.
10. Лукашевич С.В., Морозов С.О., Шиплюк А.Н. Исследование стабилизации высокоскоростного пограничного слоя с помощью пористых покрытий (обзор). *Прикладная механика и техническая физика.* 2023;64(4):27–45. https://doi.org/10.15372/PMTF202215169
11. Morozov S.O., Lukashevich S.V., Shiplyuk A.N. Hypersonic Boundary Layer Instability and Control by Passive Porous Coatings. In book: Sherwin S., Schmid P., Wu X. (Eds.). *IUTAM Laminar-Turbulent Transition. IUTAM Bookseries*. Springer; 2023. V. 38. P. 613–619. https://doi.org/10.1007/978-3-030-67902-6_53
12. Радкевич Е.В., Васильева О.А., Яковлев Н.Н., Сидоров М.И., Ставровский М.Е. *Математическое моделирование детонационного горения*. М.: Типография «Эко-Пресс»; 2024. 200 с.
13. Зельдович Я.Б., Баренблат Г.И., Либрович В.Б., Махвиладзе Г.М. *Математическая теория горения и взрыва*. М.: Наука; 1980. 472 с.
14. Скрипов В.П., Скрипов А.В. Спинодальный распад (фазовый переход с учетом неустойчивых состояний). *Успехи физических наук.* 1979;128(2):193–231. https://doi.org/10.3367/UFNr.0128.197906a.0193
15. Хакен Дж. *Синергетика*: пер. с англ. М.: Мир; 1980. 405 с.

About the Authors

Evgeny V. Radkevich, Dr. Sci. (Phys.-Math.), Professor, Department of Differential Equations, Lomonosov Moscow State University (1, Leninskie Gory, Moscow, 119991 Russia). E-mail: evrad07@gmail.com. Scopus Author ID 6603609635, https://orcid.org/0000-0001-7904-4476

Mikhail E. Stavrovsky, Dr. Sci. (Eng.), Professor, Department of Industrial Logistics, Bauman Moscow State Technical University (5, 2-ya Baumanskaya ul., Moscow, 105005 Russia). E-mail: stavrov@list.ru. Scopus Author ID 56766192700, ResearcherID H-6399-2017, RSCI SPIN-code 6166-2296, https://orcid.org/0000-0001-7144-2461

Olga A. Vasilyeva, Cand. Sci. (Phys.-Math.), Associate Professor, Department of Applied Mathematics, Moscow State University of Civil Engineering (National Research University) (26, Yaroslavskoe sh., Moscow, 129337 Russia). E-mail: vasiljeva.ovas@ya.ru. Scopus Author ID 56966381200, RSCI SPIN-code 2411-9316, https://orcid.org/0000-0001-6426-2067

Nikolay N. Yakovlev, Cand. Sci. (Eng.), Scientific Consultant, Detonation Laboratory, N.N. Semenov Federal Research Center for Chemical Physics of the Russian Academy of Sciences (4, Kosygina ul., Moscow, 119991 Russia). E-mail: amntksoyuz@mail.ru. Scopus Author ID 7004647760, RSCI SPIN-code 2067-7668, https://orcid.org/0009-0002-8058-3586

Mikhail I. Sidorov, Dr. Sci. (Eng.), Deputy Head of the Department, MIREA – Russian Technological University (78, Vernadskogo pr., Moscow, 119454 Russia). E-mail: m.sidorov60@mail.ru. Scopus Author ID 57194154324, ResearcherID U-5720-2019, RSCI SPIN-code 6774-8834, https://orcid.org/0009-0005-5607-7589

Об авторах

Радкевич Евгений Владимирович, д.ф.-м.н., профессор, кафедра дифференциальных уравнений, ФГБОУ ВО «Московский государственный университет имени М.В. Ломоносова» (119991, Россия, Москва, Ленинские Горы, д. 1). E-mail: evrad07@gmail.com. Scopus Author ID 6603609635, https://orcid.org/0000-0001-7904-4476

Ставровский Михаил Евгеньевич, д.т.н., профессор, кафедра промышленной логистики, ФГАОУ ВО «Московский государственный технический университет имени Н.Э. Баумана (национальный исследовательский университет)» (МГТУ им. Н.Э. Баумана) (105005, Россия, Москва, 2-я Бауманская ул., д. 5). E-mail: stavrov@list.ru. Scopus Author ID 56766192700, ResearcherID H-6399-2017, SPIN-код РИНЦ 6166-2296, https://orcid.org/0000-0001-7144-2461

Васильева Ольга Александровна, к.ф.-м.н., доцент, кафедра прикладной математики, ФГБОУ ВО «Национальный исследовательский Московский государственный строительный университет» (НИУ МГСУ) (129337, Россия, Москва, Ярославское шоссе, д. 26). E-mail: vasiljeva.ovas@ya.ru. Scopus Author ID 56966381200, SPIN-код РИНЦ 2411-9316, https://orcid.org/0000-0001-6426-2067

Яковлев Николай Николаевич, к.т.н., научный консультант, лаборатория детонации, ФГБУН «Федеральный исследовательский центр химической физики им. Н.Н. Семенова Российской академии наук» (ФИЦ ХФ РАН) (119991, Россия, Москва, ул. Косыгина, д. 4). E-mail: amntksoyuz@mail.ru. Scopus Author ID 7004647760, SPIN-код РИНЦ 2067-7668, https://orcid.org/0009-0002-8058-3586

Сидоров Михаил Игоревич, д.т.н., заместитель начальника отдела, Инжиниринговый центр мобильных решений, ФГБОУ ВО «МИРЭА – Российский технологический университет» (119454, Россия, Москва, пр-т Вернадского, д. 78). E-mail: m.sidorov60@mail.ru. Scopus Author ID 57194154324, ResearcherID U-5720-2019, SPIN-код РИНЦ 6774-8834, https://orcid.org/0009-0005-5607-7589

Translated from Russian into English by K. Nazarov
Edited for English language and spelling by Thomas A. Beavitt

Economics of knowledge-intensive and high-tech enterprises and industries. Management in organizational systems

Экономика наукоемких и высокотехнологичных предприятий и производств. Управление в организационных системах

UDC 330.342.24
https://doi.org/10.32362/2500-316X-2025-13-4-123-134
EDN XXKOTU

RESEARCH ARTICLE

Industrial revolutions: From Industry 3.0 to Industry 5.0 in the context of the Russian economy

Natalia N. Karpukhina [@], **Evgeny S. Mityakov, Aleksey Yu. Pronin**

MIREA – Russian Technological University, Moscow, 119454 Russia
[@] *Corresponding author, e-mail: karpukhina@mirea.ru*

• **Submitted:** 31.07.2024 • **Revised:** 27.01.2025 • **Accepted:** 24.04.2025

Abstract

Objectives. The study set out to substantiate the principles of Industry 5.0 as a necessary development for the classical model of economic growth proposed by Solow. An adapted and expanded Solow model is presented that takes into account technological progress, as well as social and environmental aspects, which influence long-term development and economic growth in the context of the Russian economy.

Methods. The main results of the work are obtained through a comparative analysis of the distinctive features of Industry 3.0, Industry 4.0, and Industry 5.0 in the context of an extended Solow model and an expert survey to assess the factors influencing economic growth.

Results. In order to substantiate the necessity of transition to more promising models of production and development, the main distinguishing features of Industry 3.0, Industry 4.0, and Industry 5.0, are shown to be determined by unique orientations, technologies, objectives, approaches to working with data, and types of interfaces. The Russian economy is shown to be insufficiently prepared for the challenges of Industry 5.0. The principles of Industry 5.0 apply to such factors of the Solow economic growth model as labor, capital, and technological progress, as well as human capital, natural resources, and the current technological level. A survey of experts was conducted to assess the contribution of factors to production processes. The extended Solow model is a convenient tool for developing specific economic policy strategies based on the analysis of the interrelated factors.

Conclusions. The transition to Industry 4.0 technologies and subsequent planning for the implementation of Industry 5.0 technologies are necessary steps prior to the creation of an innovative and competitive economy. The conducted expert survey exemplified the different contributions of various factors to Industry 5.0 production processes, including a decrease in the role of capital and labor, along with a concomitant increase in the importance of human capital, technological development, and natural resources. This transition is evidenced by the presented numerical values for the Solow model coefficients for Industry 3.0, Industry 4.0, and Industry 5.0. Such Industry 5.0 priorities not only do not contradict economic growth, but can be expected to enhance it in the long term.

Keywords: Industry 3.0, Industry 4.0, Industry 5.0, technologies, comparative analysis, Solow model, human capital, digitalization, innovative economy

For citation: Karpukhina N.N., Mityakov E.S., Pronin A.Yu. Industrial revolutions: From Industry 3.0 to Industry 5.0 in the context of the Russian economy. *Russian Technological Journal*. 2025;13(4):123–134. https://doi.org/10.32362/2500-316X-2025-13-4-123-134, https://www.elibrary.ru/XXKOTU

Financial disclosure: The authors have no financial or proprietary interest in any material or method mentioned.

The authors declare no conflicts of interest.

НАУЧНАЯ СТАТЬЯ

Промышленные революции: от Индустрии 3.0 к Индустрии 5.0 в контексте российской экономики

Н.Н. Карпухина [@], Е.С. Митяков, А.Ю. Пронин

МИРЭА – Российский технологический университет, Москва, 119454 Россия
[@] Автор для переписки, e-mail: karpukhina@mirea.ru

• **Поступила:** 31.07.2024 • **Доработана:** 27.01.2025 • **Принята к опубликованию:** 24.04.2025

Резюме

Цели. Цель статьи – доказать, что принципы Индустрии 5.0 являются необходимым развитием для классической модели экономического роста, предложенной Солоу. В статье модель Солоу адаптирована и расширена новыми факторами, которые учитывают технологический прогресс, социальные и экологические аспекты и в контексте российской экономики оказывают влияние на долгосрочное развитие и экономический рост.

Методы. Основные результаты работы получены с помощью сравнительного анализа отличительных особенностей Индустрии 3.0, Индустрии 4.0 и Индустрии 5.0, расширенной модели Солоу и экспертного опроса для оценки факторов, влияющих на экономический рост.

Результаты. Для обоснования необходимости перехода к более перспективным моделям производства и развития выделены основные отличительные особенности Индустрии 3.0, Индустрии 4.0 и Индустрии 5.0, определяемые уникальной ориентацией, технологиями, целями, подходами к работе с данными и типами интерфейсов. Установлено, что российская экономика пока недостаточно готова к вызовам Индустрии 5.0. Доказано, что принципы Индустрии 5.0 расширяют такие факторы модели экономического роста Солоу, как труд, капитал и технологический прогресс, добавляя человеческий капитал, природные ресурсы и уровень технологий. Для оценки вклада факторов в производственные процессы проведен опрос экспертов. Расширенная модель Солоу является инструментом для разработки конкретных стратегий в области экономической политики на основе анализа взаимосвязанных факторов.

Выводы. Переход к технологиям Индустрии 4.0 и последующее планирование внедрения технологий Индустрии 5.0 являются необходимыми шагами для создания инновационной и конкурентоспособной экономики. Проведенный опрос экспертов доказал разный вклад факторов в производственные процессы: уменьшение роли капитала и труда, рост значимости человеческого капитала, технологического развития и природных ресурсов в Индустрии 5.0. Такие приоритеты Индустрии 5.0 не только не противоречат экономическому росту, но и могут его усилить в долгосрочной перспективе.

Ключевые слова: Индустрия 3.0, Индустрия 4.0, Индустрия 5.0, технологии, сравнительный анализ, модель Солоу, человеческий капитал, цифровизация, инновационная экономика

Для цитирования: Карпухина Н.Н., Митяков Е.С., Пронин А.Ю. Промышленные революции: от Индустрии 3.0 к Индустрии 5.0 в контексте российской экономики. *Russian Technological Journal*. 2025;13(4):123–134. https://doi.org/10.32362/2500-316X-2025-13-4-123-134, https://www.elibrary.ru/XXKOTU

Прозрачность финансовой деятельности: Авторы не имеют финансовой заинтересованности в представленных материалах или методах.

Авторы заявляют об отсутствии конфликта интересов.

INTRODUCTION

Contemporary Russia has two distinctly pronounced trends of the economic development that make it unique. The formation of a "knowledge economy" in the first decade of the 21st century was focused on the latest knowledge, innovations, and the development of an information society. The process of universal digitalization that actively unfolded since 2010 has led to the development of digital innovation and increased digital competition [1].

Digitalization in Russia differs significantly by sector. According to the Ministry of Digital Development, by the beginning of 2024, more than 90% of government services were provided electronically via the Gosuslugi services portal.[1] The Russian financial sector has always been a leader in the implementation of digital technologies,[2] while retail companies are also constantly increasing their budget for informatization by implementing integrated solutions.[3] However, the level of digitalization used in industrial enterprises is characterized by the chaotic use of individual digital solutions. According to a study by the Russian consulting company SBS Consulting, the level of digital maturity of large and medium-sized manufacturing companies in Russia is only 26.6%.[4]

The digital transformation of industry involves the use of digital solutions to improve the production efficiency and then apply these solutions to the activities of the enterprise as a whole to enable prompt responses to emerging problems [2]. For this reason, many Russian industrial enterprises remain critically dependent on the implementation of Industry 4.0 technologies. This dependence is exacerbated by labor force shortages and the need to increase labor productivity.[4]

The chaotic implementation of technological solutions in industrial enterprises inherent in Industry 3.0 approaches has revealed a number of key problems in the context of the Industry 4.0, including human factors and emerging environmental hazards. Issues related to mismatches between different aspects of the economy include inefficient production and consumption patterns, significant social differentiation, social instability, etc. [3].

The current emphasis of global economic development and scientific research is changing from the robotization and automation inherent in Industry 4.0 to the development of sociocentric and environmentally sustainable technologies. Here the focus is placed on human–machine interactive systems in which humans act as creative participants in collaboration with robots. Traditional enterprises are giving way to the digital ecosystem, which opens new opportunities for the economy, but also brings risks of digital monopolization in virtual sectors [4]. Given these changes, the need for transition to the Industry 5.0 paradigm becomes obvious.

As a new industrial model, Industry 5.0 naturally emerges from the expansion of Industry 4.0. Industry 5.0 heralds a multiple increase in production efficiency and flexibility through automation, process optimization, and improved cooperation between humans and the technosphere. In response to the threat of job losses resulting from the introduction of Industry 4.0 technologies, Industry 5.0 opens up new opportunities for the creation of specialized jobs related to the management and maintenance of new technologies.

The feasibility of transition from Industry 3.0 to Industries 4.0 and 5.0 is especially relevant for the Russian economy, where technologies become a critical factor of competitiveness and are increasingly necessary to ensure the country's technological sovereignty. Industry 5.0 represents a qualitatively new stage in the development of production processes, characterized by an emphasis on a human-centered approach and the concept of sustainable development. The introduction of innovative technologies in this paradigm significantly increases production efficiency, which becomes especially important in the context of

[1] Digitalization in Russia: New Development Vectors in 2024. https://www.sostav.ru/blogs/277074/50927 (in Russ.). Accessed November 10, 2024.

[2] Digitalization of the financial sector 2024. https://generation-startup.ru/calendar/82432/ (in Russ.). Accessed November 10, 2024.

[3] Three IT trends in eCommerce in 2024. https://www.retail.ru/rbc/pressreleases/tri-trenda-it-v-ecommerce-v-2024-godu/ (in Russ.). Accessed November 10, 2024.

[4] Analysis of the digitalization level of Russian manufacturing enterprises. https://www.tadviser.ru (in Russ.). Accessed November 10, 2024.

demographic changes, shrinking labor resources and the need to improve the living standards of the population. Adaptation of the Russian economy to these challenges requires a comprehensive analysis and development of system solutions, which emphasizes the relevance of this study.

LITERATURE REVIEW

Currently, there is a significant increase in the number of scientific publications devoted to various aspects of the Industry 5.0 [5]. Many contemporary works focus on global problems of sustainable development, health care, education, industry, and technology development. Studies reflect different views on the terminology of the subject area, as well as questions concerning whether Industry 5.0 is a new paradigm or the next stage of Industry 4.0 development.

Nahavandi describes Industry 5.0 in terms of a vision of the future of humanity. According to this perspective, production within Industry 5.0 combines the advantages of advanced technologies with creativity and human problem-solving skills, which are aimed at making production processes more efficient and flexible, as well as reducing the risk of accidents and injuries [6]. The author argues that the fifth industrial revolution will occur when smart devices are fully integrated with the human mind and the physical world. Such cooperation will ensure high efficiency, production flexibility, and waste minimization.

In [7], it is argued that Industry 5.0 is aimed at enhancing the experience of end-users through the application of various available tools, including artificial intelligence and robotics. The article [8] outlines a design approach in which human operators and intelligent machines form collaborative teams.

In [9], Industry 5.0 is presented as a paradigm aimed at overcoming global social problems resulting from previous industrial revolutions. According to the authors, this paradigm is based on the idea of human-centered intellectual environment and its interaction with robotic systems.

In [10], Industry 5.0 is understood as a renewed human-centered industrial archetype that transforms the processes of industrial production. Examples of technologies that contribute to this transformation include artificial intelligence (AI), blockchain, and the Internet of Things.

In [11] an overview of the benefits of human interaction with the technological environment in industrial automation is presented. The authors consider Industry 5.0 as an evolution of Industry 4.0, in which creative humans collaborate with intelligent systems to improve the efficiency, speed, and scalability of manufacturing systems. Industry 5.0 is also seen in [12] as an extension of Industry 4.0 with a greater emphasis on human-centered interaction with computers.

The article [13] focuses on education to develop the necessary skills and competencies that enable employees to adapt to Industry 5.0 and changes in the university landscape.

A number of authors study common aspects of Industry 5.0 and Industry 4.0 in parallel. For example, article [14] describes the technological elements common to Industry 4.0 and 5.0.

Problems arising in connection with Industry 5.0 are also considered by Russian researchers. Thus, review studies are presented in the articles [15] and [16]. The authors of the article [17] argue that Industry 5.0 involves an integration of virtual and real worlds. The authors of the article [18] point out the advantages of the Industry 5.0 technologies for oil and gas companies.

The article [19] considers the problem of diagnostics of meso-economic systems in the process of evolution to the Industry 5.0. The authors put forward and substantiate the hypothesis about the existence of basic factors affecting the development of the economic system in the conditions of this transition, and propose a classification of methods for the study of such systems.

In general, the analysis of scientific literature has shown that the readiness of the Russian economy to respond to the challenges of the Industry 5.0 is insufficiently studied. In conclusion, it should be noted that Industry 5.0 is a relatively new concept. Thus, despite the noticeable increase in the number of works in this area, the formation of strategies for transition to Industry 5.0 technologies is still fragmentary. Examples are presented in the national programs of some countries (here we can highlight the EU program “Industry 5.0”, “Made in China – 2025”, and the Japanese “Society 5.0”) [20].

RESULTS

Analysis of the publications allowed us to identify the main distinguishing features of the Industry 3.0, Industry 4.0, and Industry 5.0 (figure), which are defined by their unique orientation, technologies, objectives, data approaches and types of interfaces.

From the figure it can be seen that each successive industrial revolution represents a significant step in the development of technologies and production methods aimed at increasing efficiency, flexibility, and eliminating human error factors in production processes. In Industry 5.0, the interface between humans and the technological environment has been significantly improved to include advanced technologies such as virtual and augmented reality.

A number of academic economists characterize Industry 5.0 as a “revolution of human participation,” where industrial growth is organically combined with the

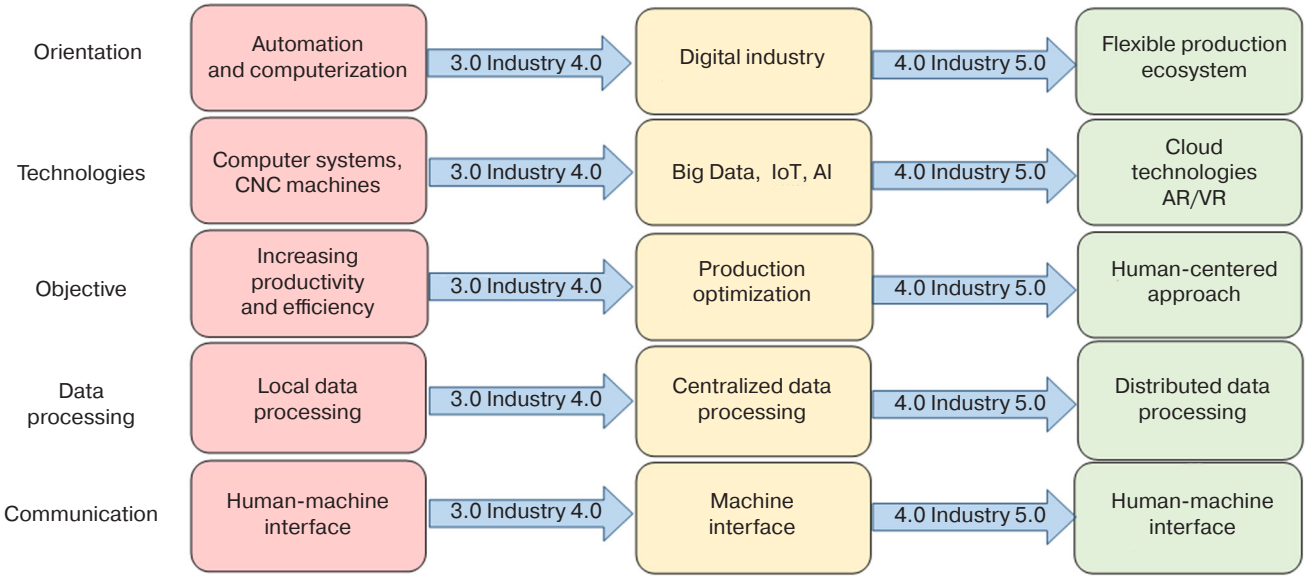

Sources: developed by the authors on the basis of [21, 22]

Figure. Key differentiating features of Industry 3.0, Industry 4.0, and Industry 5.0. CNC—Computer Numerical Control; IoT—Internet of Things; AI—Artificial Intelligence

solution of socioeconomic issues through the synergy of cyber and physical spaces [23]. One of the advantages of such synergy is the integration of intelligent systems with current work processes, resulting in an increase in operational efficiency in general.

The evolution presented in the figure is relevant in the context of the Russian economy. At present, Russia is actively seeking to accelerate the introduction of digital technologies. Thus, in 2017 the Ministry of Industry and Trade of the Russian Federation initiated the national program "4.0 RU"[5] aimed at digital transformation of all stages of the production process in accordance with the concept of Industry 4.0. However, with the launch of the national project "Digital Economy"[6] in 2018, the focus shifted towards the introduction of so-called "end-to-end technologies" aimed primarily at improving the social sphere, including identification systems and digital services for the population. This shift in priorities has led to a slowdown in digitalization processes in the industrial sector, as well as the lack of integrated digital infrastructure at the enterprise level, which makes it difficult to implement a unified digital environment within the national economy.

Regulatory documents testifying to the ongoing digitalization of government structures and the social sphere include the national program "Digital Economy" and the nine federal projects it encompasses, of which "Digital Technologies" and the national project "Data Economy"[7] currently under development are examples. However, the fully-fledged digital transformation of Russian industry requires the restoration of priorities in the field of digitalization of production processes and the development of specialized program documents aimed at supporting enterprises in the real sector of the economy.

In addition, these program documents do not sufficiently take into account the human factor, which plays a central role in Industry 5.0. The accessibility and inclusiveness of new digital solutions for all segments of society should also be taken into account to avoid deepening the digital divide. It becomes increasingly clear that the data economy is not just about simply using new digital technologies in the economy, society and everyday life, but also includes the creation of a country's own scientific, educational, technological, industrial, socioeconomic and cultural base to ensure its technological sovereignty through import substitution and integration into global value chains.

The transition to Industry 5.0 in Russia is accompanied not only by prospects, but also by various challenges. Since the introduction of innovative technologies requires highly qualified specialists, one of the key challenges involves the need to train and retrain labor resources. In particular, the following

[5] https://niieap.com/2017/07/24/minpromtorg-rossii-i-ryad-vysokotehnologichnyh-kompanij-predstavili-tsifrovoj-proekt-v-sfere-aviastroeniya-industriya-4-0/ (in Russ.). Accessed November 10, 2024.

[6] http://government.ru/info/35568/ (in Russ.). Accessed November 10, 2024.

[7] https://национальныепроекты.рф/new-projects/ekonomika-dannykh/ (in Russ.). Accessed November 10, 2024.

challenges can be noted: exponential growth of data volume, increased vulnerability to cyberattacks, job cuts in enterprises, lack of consideration of ethical issues of artificial intelligence. At the same time, Industry 5.0 envisions increased efficiency of production processes through automation and improved interaction between the technological environment and humans. Thus Industry 5.0 opens new perspectives for the creation of jobs related to the maintenance of new technologies.

While the transition to Industry 4.0 and 5.0 does not imply an automatic and immediate transition for all enterprises of the national economy, the introduction of new technologies and management methods at some enterprises may serve as a catalyst for others, creating a snowball effect according to which the number of enterprises involved increases over time. Awareness of the trends and challenges of Industries 4.0 and 5.0 is necessary for Russian enterprises to maximize their resources and capabilities and successfully complete the transition to Industry 4.0.

Despite the significant potential advantages conferred by the transition to Industry 5.0, this process in the Russian economy faces a number of serious barriers. Key among these are insufficient readiness of technological infrastructure and limited investment in research and innovation activities. The introduction of advanced technologies is hindered by the current level of equipment of enterprises, which does not yet meet the requirements of Industry 5.0. Limited investment in research and development also significantly hinders innovative development [24]. The elimination of these barriers requires a comprehensive approach and state support.

Taking into account that Industry 5.0 "represents the next stage of industrial development" [21], when approaches "to business management emphasizing the human factor"[8] are radically changing [21], it is important to be guided by the following principles of Industry 5.0 [4, 21, 22] in order to successfully overcome the listed challenges and barriers:

1. *The principle of human-centeredness* implies production processes that are based on human needs.
2. *The principle of digitalization* requires the full use of advanced digital technologies in the production of goods and the provision of services.
3. *The principle of integration* implies not only the introduction of technologies to automate production, but also the formation of proper conditions for effective interaction between humans and the technological environment, utilizing the best qualities of both parties.
4. *The principle of synergy* implies the use of modern technologies (cloud technologies, artificial intelligence, etc.) to automate production processes while retaining a significant human role in management.
5. *The principle of optimization* implies the search for models of economic activity that minimize the use of resources to achieve maximum efficiency in the interaction between humans and the technological environment.
6. *The principle of virtualization* implies the creation and implementation of digital twins of physical objects and production and management processes to augment analytics and artificial intelligence applications.
7. *The principle of platformization* implies connection to a single information space of various users for interaction, systems and equipment along the entire chain of the production life cycle.
8. *The principle of personalization* implies the creation of systems that will enable mass production of personalized products and services using digital technologies.
9. *The principle of ecosystemness* implies bringing together elements disparate in time, space, and types of industries to create technology and business collaborations.
10. *The principle of environmental friendliness* implies implementation of energy-efficient technologies in order to reduce the negative impact on the environment.

We may note that each industrial revolution forms its own unique principles. For example, at the stage of Industry 3.0 development, the main focus was on automation and the introduction of electronics, which reduced the relevance of human-technology integration that nevertheless became a key principle for Industry 5.0. At the stage of Industry 4.0 development, where digitalization and the spread of the Internet of Things dominate, principles such as environmental friendliness and human interaction with the technological environment also play a secondary role. At the stage of Industry 5.0 development, the focus shifts to the integration of digital technologies and the human factor, which requires the creation of comprehensive program documents, including by the government and the state, which are aimed at stimulating business and industry to implement new digital technologies. Special attention should be paid not only to large state corporations, but also to private small and medium-sized industrial enterprises.

Incorporating the principle of human-centeredness into production processes provides opportunities to increase productivity and create more sustainable business models. This involves not only modernizing

[8] Industry 5.0: The Human-Centered Future of Business and New Growth Strategies. https://pakhotin.org/technologies/industry-5/ (in Russ.). Accessed November 10, 2024.

technologies, but also adapting them to the real needs of society. In Russia, human-centeredness can be a key factor in the successful implementation of new technological solutions due to increased employee satisfaction, which encourages them to learn and develop, resulting in improved customer experience.

MATHEMATICAL MODEL OF THE PRODUCTION FUNCTION

Comparisons between different industrial revolutions can be made using economic growth models. For example, using the Solow model, it is possible to trace what significant changes in production processes each subsequent industrial revolution brings, as well as to conduct studies of growth processes under conditions of continuous technological development. In this case, the so-called production function is analyzed, which defines the relationship between the volume of production Y, the number of workers L, the amount of capital K and technological progress A:

$$Y = AK^{\alpha}L^{1-\alpha}. \quad (1)$$

In formula (1), the value of the parameter α, which falls within the range from 0 to 1, determines how much of the production is provided by capital.

Typically, the three main factors of production, comprising labor, capital, and technological progress, do not provide a complete picture of the production process. In such cases, extended models are used, or additional variables are added for deeper analysis. For example, the extended Solow model [25] can be formalized as follows:

$$Y = AK^{\alpha}L^{\beta}H^{\gamma}N^{\delta}R^{\varepsilon}. \quad (2)$$

In the extended model, in contrast to the original one, new factors are introduced: human capital H, natural resources N and the current level of technology R. The model parameters (α, β, γ, δ, and ε) determine the impact of these factors on the production process (elasticity of output with respect to each production factor). The sum of the values of these parameters should be equal to 1 to ensure the completeness of accounting for all factors. For example, α shows by how many percent output Y will change if the capital K changes by 1 percent provided that the other factors remain unchanged.

For each industrial revolution, the coefficients of the model should take different values. Let us consider considerations on the values of the parameters of the extended Solow model in the context of Industries 3.0, 4.0, and 5.0.

Industry 3.0. Capital K plays a key role in Industry 3.0 as physical inputs (machinery, equipment) remain the basis of production. Labor L also remains important in Industry 3.0, but arguably has less influence compared to machinery and equipment. Human capital, education, and skills H are less important as compared to physical resources and technology. The influence of natural resources N depends largely on the specifics of the industry, but is still significant, especially in the production of raw materials. The level of technology development R is quite important, but not as important as in Industries 4.0 and 5.0.

Industry 4.0. Capital K remains important; however, the main vector of development is focused on innovative technologies and digitalization of production. With automation and the use of robotics, the human factor L is less significant compared to Industry 3.0, and training and skills H become more important as highly skilled professionals are required to work with new technologies. Considering sustainability and eco-efficiency, the impact on natural resources N may be less, while the impact of R technologies, especially digital technologies, may be significant for production.

Industry 5.0. Capital K in the form of intellectual and digital capital becomes the main factor of production. Human resource L is still important, but more attention can be paid to creativity, innovation, and interdisciplinary cooperation. In Industry 5.0, education, creativity, and flexible skills H are key factors. Sustainability priorities and environmental awareness determine the importance of minimizing the use of natural resources N. The influence of advanced R technologies such as artificial intelligence or nanotechnology becomes a major determinant.

The setting of coefficients α, β, γ, δ, ε for each Industry X.0 iteration depends on the specific conditions and objectives of a certain industrial sector. In order to numerically determine the values of the coefficients of model (2), an expert survey was conducted. To ensure the representativeness and reliability of the study, 110 experts were recruited representing various sectors of the economy, including higher educational institutions (RTU MIREA and R.E. Alekseev Nizhny Novgorod State Technical University), academic research centers, industry, and business (Nizhny Novgorod Regional Branch of the All-Russian Public Organization “Free Economic Society of Russia”), which is generally sufficient for such studies [26]. This approach made it possible to cover a wide range of opinions and ensure the diversity of views on the importance of various factors of production. The experts were asked to assess the contribution of five major factors to the total output for three industrial revolutions. In doing so, each expert had to allocate the factors such that their sum for each industrial revolution equaled 1. The data obtained from the survey were averaged to obtain the total coefficients (Table).

Table. Distribution of coefficients of the extended Solow model

Industry	α	β	γ	δ	ε	Explanation
3.0	0.32	0.18	0.16	0.1	0.24	Capital has the largest impact on output, indicating that Industry 3.0 is capital intensive. The contribution of labor is significant, but less than that of capital. Human capital, important, but inferior to capital and labor. The contribution of natural resources is small. The high contribution of the level of technology development emphasizes the importance of technological progress
4.0	0.26	0.16	0.19	0.09	0.3	Capital contribution is high, but less than in Industry 3.0. The contribution of labor is reduced compared to Industry 3.0. Human capital contributes more than in Industry 3.0. The contribution of natural resources remains the same as in Industry 3.0. The highest contribution among all factors is given to the level of technology development, indicating a high dependence on technological innovation
5.0	0.21	0.11	0.24	0.14	0.3	Lowest contribution of capital and labor among all industries. Highest contribution of human capital, emphasizes the importance of knowledge and skills. Higher contribution of natural resources compared to other industries. Contribution of technology remains high

According to the presented comparative analysis of the contribution of each factor to production in the context of Industries 3.0, 4.0, and 5.0, we can state that the relative contribution of capital is decreasing. The role of labor is also decreasing, generally indicating less dependence on the quantity of labor. On the contrary, the contribution of human capital increases, emphasizing its extreme importance. The role of the factor related to natural resources remains relatively stable, with a slight increase in Industry 5.0, while the importance of technological development remains consistently high, indicating the importance of innovation for economic growth.

Thus, each industrial revolution has its own peculiarities and differences regarding the contribution of each factor, which should be taken into account when designing economic policies and investment strategies. Although from a theoretical point of view the distribution of the coefficients α, β, γ, δ, ε seems reasonable, in order to fully confirm the fairness and adequacy of the model in practical application, it is necessary to carry out its empirical verification.

CONCLUSIONS

The present study discusses conceptual differences between Industries 3.0, 4.0, and 5.0, including unique orientation, technologies, and goals, as well as approaches to data handling and communication. Special attention is paid to the justification of the need for accelerated implementation of Industry 5.0 technologies in Russia. It is noted that the Russian economy is insufficiently prepared for the challenges of Industry 5.0. The main obstacles are the lack of a clear government strategy for digital transformation of industry, the low level of digitalization of most industrial enterprises, limited funding and support for small and medium-sized industrial companies in the implementation of advanced technologies, and a lack of qualified personnel. However, the introduction of Industry 4.0 technologies and planned transition to Industry 5.0 technologies are seen as necessary steps for the formation of an innovative and competitive economy.

The following conclusions can be drawn on the basis of the conducted research: although the transition to Industry 5.0 technologies in the Russian economy is at an embryonic stage, the need to accelerate this process is obvious. Recommendations for accelerating the transition include: the development of a clear strategy for the implementation of Industry 5.0 principles at the level of the national economy, strengthening of state support for small and medium-sized industrial enterprises, and the creation of specialized educational programs to train personnel to work with new technologies.

The Solow model can serve as a basis for the development of economic strategies aimed at accelerating the implementation of the principles and technologies of Industry 5.0. The Solow model can be used to analyze the impact of technological change on long-term economic growth, taking into account the importance of

investment in research and development, as well as the impact of human capital and technological progress on the growth of gross domestic product. However, these conclusions are based on theoretical assumptions and expert assessments, which require further empirical confirmation. To fully justify the proposed strategic steps, it is necessary to conduct additional research and test the model on practical data. Here the importance of financial capital and investments in critical infrastructure and human capital development should be emphasized, due to the significant costs and comprehensive analysis required to support the transition to new technologies.

ACKNOWLEDGMENTS

The study was supported by the Russian Science Foundation grant (project No. 23-78-10009).

Authors' contributions

N.N. Karpukhina—the idea of the study, literature analysis, writing and editing the text of the article.

E.S. Mityakov—the idea of the study, literature analysis, substantiation of the mathematical model, interpretation and generalization of the research results, writing and editing the text of the article.

A.Yu. Pronin—the idea of the study, writing the text of the article.

REFERENCES

1. Sitnikova S.E. Digital form of commercialization of innovations in universities and ways to improve its efficiency: international experience and prospects for Russia. *Innovatsionnoe razvitie ekonomiki = Innovative Development of Economy.* 2020;6(60):61–70 (in Russ.).
2. Starozhuk I.N., Komissarov V.D. Digital twin as a mechanism for transition from Industry 4.0 to Industry 5.0. In: *Digital Transformation of Economic Systems: Problems and Prospects: Proceedings of the 6th All-Russian Scientific and Practical Conference with Foreign Participation.* St. Petersburg: POLITEKh-PRESS; 2022. P. 151–154 (in Russ.).
3. Ageev A.I. Managing the digital future. *Mir novoi ekonomiki = The World of New Economy*. 2018;12(3):6–23 (in Russ.). https://doi.org/10.26794/2220-6469-2018-12-3-6-23
4. Rozanova N.M. Industry 5.0: a golden age or a leap into the dark? *Vestnik Instituta ekonomiki Rossiiskoi akademii nauk = Bulletin of the Institute of Economics of the Russian Academy of Sciences.* 2023;6:61–77 (in Russ.).
5. Barata J., Kayser I. Industry 5.0 – Past, Present, and Near Future. *Procedia Comput. Sci*. 2023;219(1):778–788. https://doi.org/10.1016/j.procs.2023.01.351
6. Nahavandi S. Industry 5.0 – A Human-Centric Solution. *Sustainability*. 2019;11(16):4371. https://doi.org/10.3390/su11164371
7. Orea-Giner A., Fuentes-Moraleda L., Villacé-Molinero T., et al. Does the Implementation of Robots in Hotels Influence the Overall TripAdvisor Rating? A Text Mining Analysis from the Industry 5.0 Approach. *Tour. Manag*. 2022;93(2):104586. https://doi.org/10.1016/j.tourman.2022.104586
8. Kaasinen E., Anttila A.H., Heikkilä P., et al. Smooth and Resilient Human–Machine Teamwork as an Industry 5.0 Design Challenge. *Sustainability*. 2022;14(5):2773. https://doi.org/10.3390/su14052773
9. Coronado E., Kiyokawa T., Ricardez G.A.G., et al. Evaluating quality in human-robot interaction: A systematic search and classification of performance and human-centered factors, measures and metrics towards an industry 5.0. *J. Manufactur. Syst*. 2022;63:392–410. https://doi.org/10.1016/j.jmsy.2022.04.007
10. Carayannis E.G., Christodoulou K., Christodoulou P., et al. Known Unknowns in an Era of Technological and Viral Disruptions – Implications for Theory, Policy, and Practice. *J. Knowl. Econ.* 2022;13(1):587–610. https://doi.org/10.1007/s13132-020-00719-0
11. Fatima Z., Tanveer M.H., Waseemullah, et al. Production Plant and Warehouse Automation with IoT and Industry 5.0. *Appl. Sci.* 2022;12(4):2053. https://doi.org/10.3390/app12042053
12. Paul G., Abele N.D., Kluth K. A Review and Qualitative Meta-Analysis of Digital Human Modeling and Cyber-Physical-Systems in Ergonomics 4.0. *IISE Trans. Occup. Ergon. Hum. Factors.* 2021;9(3–4):111–123. https://doi.org/10.1080/24725838.2021.1966130
13. Broo D.G., Kaynak O., Sait S.M. Rethinking engineering education at the age of industry 5.0. *J. Industr. Inform. Integrat*. 2021;25(8):100311. https://doi.org/10.1016/j.jii.2021.100311
14. Alvarez-Aros E.L., Bernal-Torres C.A. Technological competitiveness and emerging technologies in industry 4.0 and industry 5.0. *Anais da Academia Brasileira de Ciências*. 2021;93(1). https://doi.org/10.1590/0001-3765202120191290
15. Gasanov E.A. New form of human-machine connection in the Industry 5.0 production model. *Ekonomika i upravlenie innovatsiyami = Economy and Innovation Management*. 2022;3(22):39–49 (in Russ.). https://doi.org/10.26730/2587-5574-2022-3-39-49
16. Trofimova N.N. Industry 5.0 as a new direction of industrial development. *Ekonomika i Upravlenie: Problemy, Resheniya*. 2023;5(133):24–28 (in Russ.). https://doi.org/10.36871/ek.up.p.r.2023.01.05.003
17. Evgenev G.B. Industry 5.0 as an integration of the Internet of Knowledge and the Internet of Things. *Ontologiya proektirovaniya = Ontology of Designing.* 2019;9(1–31):7–23 (in Russ.).
18. Azieva R.Kh., Taimaskhanov H.E. Modernization of the oil and gas industry in the style of Industry 5.0. *Finansovyi biznes*. 2021;2(212):82–86 (in Russ.).

19. Galimulina F.F., Shinkevich M.V. Diagnostics of mesoeconomic systems in Russia under condition of transition to Industry 5.0. *Ekonomicheskie i sotsial'no-gumanitarnye issledovaniya = Economic and Social Research*. 2023;4(40):23–32 (in Russ.).
20. Tingting Hu. Review of national strategies for transition to Industry 5.0. *Ekonomika i upravlenie innovatsiyami = Economics and Innovation Management.* 2022;3(22):28–38 (in Russ.). https://dx.doi.org/10.26730/2587-5574-2022-3-28-38
21. Makovetskii S.A. Continued evolution: comparison of Industry 4.0 and Industry 5.0 in the context of modern requirements. In: *Business. Education. Economy: Proceedings of the International Scientific and Practical conference*. Minsk; 2023. P. 81–85 (in Russ.).
22. Pronin A.Yu. Tendencies in digital transformation of high-tech enterprises in the transition from Industry 4.0 to Industry 5.0. *Cifra. Ekonomika = Cifra. Economy*. 2024;3(6) (in Russ.). https://doi.org/10.60797/ECNMS.2024.6.1
23. Cherepanov N.V. Principles and approaches of using Industry 5.0 at the enterprise. *Innovatsii i investitsii = Innovation & Investment*. 2019;9:144–147 (in Russ.).
24. Lapaev D.N., Mityakova O.I., Murashova N.A., Mityakov E.S. *Organizatsiya NIOKR* (*Organization R&D*). N. Novgorod: Nizhny Novgorod State Technical University; 2017. 100 p. (in Russ.).
25. Kanametova D.A. Analysis of Models of Dynamic Economic Systems. *Izvestiya Kabardino-Balkarskogo nauchnogo tsentra RAN = News of the Kabardino-Balkarian Scientific Center of the Russian Academy of Sciences.* 2023;4(114):88–97 (in Russ.). https://doi.org/10.35330/1991-6639-2023-4-114-88-97
26. Memon M., Ting H., Hwa C., Ramayah T., Chuah F., Cham T.H. Sample Size for Survey Research: Review and Recommendations. *Journal of Applied Structural Equation Modeling* (*JASEM*). 2020;4(2):i-xx. http://doi.org/10.47263/JASEM.4(2)01

СПИСОК ЛИТЕРАТУРЫ

1. Ситникова С.Е. Цифровая форма коммерциализации инноваций в вузах и пути повышения ее эффективности: международный опыт и перспективы для России. *Инновационное развитие экономики*. 2020;6(60):61–70.
2. Старожук И.Н., Комиссаров В.Д. Цифровой двойник как механизм перехода от Индустрии 4.0 к Индустрии 5.0. В сб.: *Цифровая трансформация экономических систем: проблемы и перспективы* (*ЭКОПРОМ-2022*): *Сборник трудов VI Всероссийской научно-практической конференции с зарубежным участием*. СПб.: ПОЛИТЕХ-ПРЕСС; 2022. С. 151–154.
3. Агеев А.И. Управление цифровым будущим. *Мир новой экономики*. 2018;12(3):6–23. https://doi.org/10.26794/2220-6469-2018-12-3-6-23
4. Розанова Н.М. Индустрия 5.0: золотой век или прыжок в темноту? *Вестник Института экономики Российской академии наук.* 2023;6:61–77.
5. Barata J., Kayser I. Industry 5.0 – Past, Present, and Near Future. *Procedia Comput. Sci*. 2023;219(1):778–788. https://doi.org/10.1016/j.procs.2023.01.351
6. Nahavandi S. Industry 5.0 – A Human-Centric Solution. *Sustainability*. 2019;11(16):4371. https://doi.org/10.3390/su11164371
7. Orea-Giner A., Fuentes-Moraleda L., Villacé-Molinero T., et al. Does the Implementation of Robots in Hotels Influence the Overall TripAdvisor Rating? A Text Mining Analysis from the Industry 5.0 Approach. *Tour. Manag*. 2022;93(2):104586. https://doi.org/10.1016/j.tourman.2022.104586
8. Kaasinen E., Anttila A.H., Heikkilä P., et al. Smooth and Resilient Human–Machine Teamwork as an Industry 5.0 Design Challenge. *Sustainability*. 2022;14(5):2773. https://doi.org/10.3390/su14052773
9. Coronado E., Kiyokawa T., Ricardez G.A.G., et al. Evaluating quality in human-robot interaction: A systematic search and classification of performance and human-centered factors, measures and metrics towards an industry 5.0. *J. Manufactur. Syst*. 2022;63:392–410. https://doi.org/10.1016/j.jmsy.2022.04.007
10. Carayannis E.G., Christodoulou K., Christodoulou P., et al. Known Unknowns in an Era of Technological and Viral Disruptions – Implications for Theory, Policy, and Practice. *J. Knowl. Econ.* 2022;13(1):587–610. https://doi.org/10.1007/s13132-020-00719-0
11. Fatima Z., Tanveer M.H., Waseemullah, et al. Production Plant and Warehouse Automation with IoT and Industry 5.0. *Appl. Sci.* 2022;12(4):2053. https://doi.org/10.3390/app12042053
12. Paul G., Abele N.D., Kluth K. A Review and Qualitative Meta-Analysis of Digital Human Modeling and Cyber-Physical-Systems in Ergonomics 4.0. *IISE Trans. Occup. Ergon. Hum. Factors.* 2021;9(3–4):111–123. https://doi.org/10.1080/24725838.2021.1966130
13. Broo D.G., Kaynak O., Sait S.M. Rethinking engineering education at the age of industry 5.0. *J. Industr. Inform. Integrat*. 2021;25(8):100311. https://doi.org/10.1016/j.jii.2021.100311
14. Alvarez-Aros E.L., Bernal-Torres C.A. Technological competitiveness and emerging technologies in industry 4.0 and industry 5.0. *Anais da Academia Brasileira de Ciências*. 2021;93(1). https://doi.org/10.1590/0001-3765202120191290
15. Гасанов Э.А. Новая форма соединения человека и машины в модели производства Индустрии 5.0. *Экономика и управление инновациями*. 2022;3(22):39–49. https://doi.org/10.26730/2587-5574-2022-3-39-49
16. Трофимова Н.Н. Индустрия 5.0 как новое направление промышленного развития. *Экономика и управление: проблемы, решения*. 2023;5(133):24–28. https://doi.org/10.36871/ek.up.p.r.2023.01.05.003

17. Евгенев Г.Б. Индустрия 5.0 как интеграция интернета знаний и интернета вещей. *Онтология проектирования*. 2019;9(1–31):7–23.
18. Азиева Р.Х., Таймасханов Х.Э. Модернизация нефтегазовой отрасли в стиле Индустрии 5.0. *Финансовый бизнес*. 2021;2(212):82–86.
19. Галимулина Ф.Ф., Шинкевич М.В. Диагностика мезоэкономических систем в России в условиях перехода к Индустрии 5.0. *Экономические и социально-гуманитарные исследования*. 2023;4(40):23–32.
20. Тинтин Ху. Обзор национальных стратегий перехода к Индустрии 5.0. *Экономика и управление инновациями*. 2022;3(22):28–38. https://doi.org/10.26730/2587-5574-2022-3-28-38
21. Маковецкий С.А. Продолжение эволюции: сравнение Индустрии 4.0 и Индустрии 5.0 в контексте современных требований. В сб.: *Бизнес. Образование. Экономика: Материалы Международной научно-практической конференции*. Минск; 2023. С. 81–85.
22. Пронин А.Ю. Тенденции цифровой трансформации высокотехнологичных предприятий в условиях перехода от Индустрии 4.0 к Индустрии 5.0. *Cifra. Экономика*. 2024;3(6). https://doi.org/10.60797/ECNMS.2024.6.1
23. Черепанов Н.В. Принципы и подходы применения Индустрии 5.0 на предприятии. *Инновации и инвестиции*. 2019;9:144–147.
24. Лапаев Д.Н., Митякова О.И., Мурашова Н.А., Митяков Е.С. *Организация НИОКР*. Н. Новгород: Нижегородский государственный технический университет им. Р.Е. Алексеева; 2017. 100 с.
25. Канаметова Д.А. Анализ моделей динамических экономических систем. *Известия Кабардино-Балкарского научного центра РАН*. 2023;4(114):88–97. https://doi.org/10.35330/1991-6639-2023-4-114-88-97
26. Memon M., Ting H., Hwa C., Ramayah T., Chuah F., Cham T.H. Sample Size for Survey Research: Review and Recommendations. *Journal of Applied Structural Equation Modeling* (*JASEM*). 2020;4(2):i-xx. http://doi.org/10.47263/JASEM.4(2)01

About the Authors

Natalia N. Karpukhina, Dr. Sci. (Econ.), Associate Professor, Head of the Department of Innovation Management, Institute of Management Technologies, MIREA – Russian Technological University (78, Vernadskogo pr., Moscow, 119454 Russia). E-mail: karpukhina@mirea.ru. Scopus Author ID 57190409353, RSCI SPIN-code 7442-9985, https://orcid.org/0000-0003-3378-5230

Evgeny S. Mityakov, Dr. Sci. (Econ.), Professor, Head of the Department of Subject-Oriented Information Systems, Institute for Cybersecurity and Digital Technologies, MIREA – Russian Technological University (78, Vernadskogo pr., Moscow, 119454 Russia). E-mail: mityakov@mirea.ru. Scopus Author ID 55960540500, RSCI SPIN-code 5691-8947, https://orcid.org/0000-0001-6579-0988

Aleksey Yu. Pronin, Cand. Sci. (Eng.), Associate Professor, Department of Innovation Management, Institute of Management Technologies, MIREA – Russian Technological University (78, Vernadskogo pr., Moscow, 119454 Russia). E-mail: pronin@mirea.ru. Scopus Author ID 57190872536, RSCI SPIN-code 6833-7914, https://orcid.org/0000-0001-8947-3047

Об авторах

Карпухина Наталия Николаевна, д.э.н., доцент, заведующий кафедрой управления инновациями, Институт технологий управления, ФГБОУ ВО «МИРЭА – Российский технологический университет» (119454, Россия, Москва, пр-т Вернадского, д. 78). E-mail: karpukhina@mirea.ru. Scopus Author ID 57190409353, SPIN-код РИНЦ 7442-9985, https://orcid.org/0000-0003-3378-5230

Митяков Евгений Сергеевич, д.э.н., профессор, заведующий кафедрой КБ-9 «Предметно-ориентированные информационные системы», Институт кибербезопасности и цифровых технологий, ФГБОУ ВО «МИРЭА – Российский технологический университет» (119454, Россия, Москва, пр-т Вернадского, д. 78). E-mail: mityakov@mirea.ru. Scopus Author ID 55960540500, SPIN-код РИНЦ 5691-8947, https://orcid.org/0000-0001-6579-0988

Пронин Алексей Юрьевич, к.т.н., доцент, кафедра управления инновациями, Институт технологий управления, ФГБОУ ВО «МИРЭА – Российский технологический университет» (119454, Россия, Москва, пр-т Вернадского, д. 78). E-mail: pronin@mirea.ru. Scopus Author ID 57190872536, SPIN-код РИНЦ 6833-7914, https://orcid.org/0000-0001-8947-3047

Translated from Russian into English by Lyudmila O. Bychkova
Edited for English language and spelling by Thomas A. Beavitt

Economics of knowledge-intensive and high-tech enterprises and industries. Management in organizational systems

Экономика наукоемких и высокотехнологичных предприятий и производств. Управление в организационных системах

UDC 332.025.13, 332.056.2, 332.055.2, 336.1, 336.13, 351.72
https://doi.org/10.32362/2500-316X-2025-13-4-135-148
EDN YYMNZI

RESEARCH ARTICLE

Electronics inventory as the foundation of a breakthrough into global leadership

Vasily V. Shpak @

MIREA – Russian Technological University, Moscow, 119454 Russia
@ *Corresponding author, e-mail: morser@yandex.ru*

• **Submitted:** 28.04.2025 • **Revised:** 13.05.2025 • **Accepted:** 13.06.2025

Abstract

Objectives. In the context of aggressive sanctions and unfriendly behavior of competitors, the multi-sectoral structure of the Russian economy is undergoing a process of rapidly restructuring to increase its competitiveness and import independence. The locomotive of this process is the electronic industry, whose products influence almost all aspects of the economy and society. This indicates the decisive role of the electronic industry in the lives of Russians. Thus, the inventorization of the productive forces of the electronic industry presented in this article constitutes a necessary step towards an effective and optimal solution to the problems at hand.

Methods. Classical methods of studying the socioeconomic relations of a complex system are used to consider the example of the electronic industry along with its sub-sectors, enterprises, and other organizational forms. The system analysis method is applied to management problems emerging at three levels: macro-, meso- and micro-level. The induction method of inventory management is supplemented by the deduction method representing an analytical movement from the electronic industry as an integral system to individual factors of the reproduction process.

Results. The first step of a practically feasible implementation chain of digital technologies in industry management should consist in an inventory of all reproduction factors. The presented rationale and detailed inventory program are compiled into a management block diagram in the format of digital twins of electronic industry enterprises.

Conclusions. The barriers facing the Russian electronic industry in the form of foreign competitors are not insurmountable. Sanctions and unfriendly actions of foreign competitors represent an opportunity the Russian electronics industry to overcome such barriers to significantly accelerate the scientific and technological, organizational, and managerial development of the industry. The country's leadership and industry actors are aggressively implementing a program for developing the electronic industry as the locomotive of the entire economy. The inventory presented in this article will serve to facilitate a resurgence of the Russian electronics industry with respect to foreign competitors.

Keywords: inventory, electronics, microelectronics, general scheme, GISP, multi-agent model

For citation: Shpak V.V. Electronics inventory as the foundation of a breakthrough into global leadership. *Russian Technological Journal.* 2025;13(4):135–148. https://doi.org/10.32362/2500-316X-2025-13-4-135-148, https://www.elibrary.ru/YYMNZI

Financial disclosure: The author has no financial or proprietary interest in any material or method mentioned.

The author declares no conflicts of interest.

НАУЧНАЯ СТАТЬЯ

Инвентаризация электроники – фундамент прорыва в лидеры

В.В. Шпак [@]

МИРЭА – Российский технологический университет, Москва, 119454 Россия
[@] *Автор для переписки, e-mail: morser@yandex.ru*

• **Поступила:** 28.04.2025 • **Доработана:** 13.05.2025 • **Принята к опубликованию:** 13.06.2025

Резюме

Цели. Многоотраслевая структура российской экономики в условиях агрессивных санкций и недружественного поведения конкурентов приняла этот вызов и ускоренно реструктуризируется, повышая свою конкурентоспособность и импортонезависимость. Локомотивом этого процесса является электронная промышленность, продукция которой определяет и влияет практически на все стороны экономики и общества. Это свидетельствует об определяющей роли электронной промышленности в жизни россиян. Настоящая статья показывает первый шаг на пути к эффективному и оптимальному решению стоящих задач – инвентаризацию производительных сил электронной промышленности.

Методы. Использованы классические методы исследования социально-экономических отношений сложной системы, которой является электронная промышленность с входящими в нее подотраслями, предприятиями и организациями. Применен метод системного анализа проблем управления на макро-, мезо- и микроуровнях. Метод индукции, к которому относится инвентаризация, дополнен в исследовании методом дедукции, т.е. аналитическим движением от электронной промышленности как целостной системы к отдельным факторам воспроизводственного процесса.

Результаты. Выстроена реальная и практически осуществимая цепочка внедрения цифровых технологий в управление отраслью, первым шагом в которой должна стать инвентаризация всех факторов воспроизводства. Представлены обоснование и развернутая программа инвентаризации, которые выводят на реалистичную цель, скомпонованную в блок-схему управления в формате «цифровой двойник электронной промышленности – цифровые двойники предприятий электронной промышленности».

Выводы. Отставание российской электронной промышленности от иностранных конкурентов не является непреодолимым. Санкции и недружественные действия иностранных конкурентов позволили российской электронной промышленности их нивелировать, преодолеть и существенно ускорить как научно-технологическое, так и организационно-управленческое развитие отрасли. Руководство страны и отрасли наступательно реализуют программу развития электронной промышленности как локомотива всей экономики, а проведение инвентаризации позволит направить отрасль в обгон иностранных конкурентов.

Ключевые слова: инвентаризация, электроника, микроэлектроника, электронная промышленности, генеральная схема, ГИСП, мультиагентная модель

Для цитирования: Шпак В.В. Инвентаризация электроники – фундамент прорыва в лидеры. *Russian Technological Journal*. 2025;13(4):135–148. https://doi.org/10.32362/2500-316X-2025-13-4-135-148, https://www.elibrary.ru/YYMNZI

Прозрачность финансовой деятельности: Автор не имеет финансовой заинтересованности в представленных материалах или методах.

Автор заявляет об отсутствии конфликта интересов.

INTRODUCTION

The development of any complex economic system becomes more effective when there is an objective and complete understanding of the actual means for its achievement. The development of the Russian electronics industry in recent years has demonstrated stable positive dynamics in accordance with the goals set by the country's leadership. However, in order to maintain and increase the pace of development, it is necessary to work on increasing the efficiency of interaction between all industry participants. A basis for this consists in constructing a general scheme of development and location of productive forces of electronics. A systemic idea of the available resources for the basis of the general scheme can only be provided by a large-scale and all-encompassing inventory of all production factors available to public and private enterprises.

1. IMPLEMENTATION OF THE STATE POLICY FRAMEWORK IN THE ELECTRONICS SECTOR

Since the approval in January 2020 of the Strategy for the Development of the Electronic Industry of the Russian Federation for the Period until 2030[1], the industry has been demonstrating notable growth in all key indicators (Fig. 1). Despite external restrictions (COVID-19 pandemic, intensifying sanctions, etc.), the volume of Russian electronic products has been growing every year. By the end of 2024, according to preliminary data, Russia will produce electronic products, including components and equipment, worth RUR 3.36 tn.

Over the same period, the number of employees in the industry grew by only 10%. On the one hand, this is insufficient, with estimating showing that the industry workforce will need to be bolstered by at least another 50000 people by 2030. On the other hand, the faster growth of production volume as compared to the number of employees shows that labor productivity in the industry is growing faster with output per employee/year having already reached RUR 6 mln.

An important indicator of the effectiveness of the state policy in the electronics sector is the accelerated growth of the nomenclature of Russian electronic products. By the end of 2024, the register of Russian radioelectronic products[2] contained more than 29000 items, of which at least 20% were electronic components. This applies not only to the industrial sector, but also to consumer goods. In particular, Russian laptops and tablets are no longer rare. Such products have reached the retail market, with many brands demonstrating competitiveness in price and quality with foreign analogs.

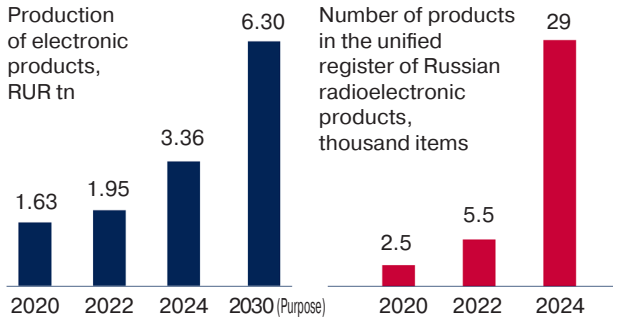

Fig. 1. Dynamics of industry development indicators in 2020–2024

Such dynamics became possible largely due to the launch of a systemic set of support tools and increased sources of industry financing (Fig. 2). Here it is important to note that the range of support measures is designed for all stages of the life cycle from development to production and introduction of electronic products [1]. These are mainly subsidy support measures, where a part of organizational costs for the creation of new technologies and products is compensated in exchange for achieving the indicators for the commercialization of developments. In total, as of the beginning of 2025, more than 500 projects are being implemented in the outline of the Ministry of Industry and Trade of Russia[3], of which more than 100 are at the stage of commercialization. New products have already been sold to a value of about RUR 100 bn. Budget financing in the period of 2020–2024 amounted to over RUR 430 bn, while for the next three-year period, it is planned at the level of RUR 250 bn.

In addition, more than 240 projects in the field of electronics are being implemented by foundations and development institutions, including the Russian Science Foundation[4], Innovation Promotion Fund[5], Advanced Research Foundation[6], Industrial Development Fund[7],

[1] Order of the Government of the Russian Federation No. 20-r dated January 17, 2020 "On Approval of the Strategy for the Development of the Electronic Industry until 2030." http://government.ru/docs/38795/ (in Russ.). Assessed May 07, 2025.
[2] https://gisp.gov.ru/pp719v2/pub/prod/rep/ (in Russ.). Assessed May 07, 2025.
[3] Ministry of Industry and Trade of the Russian Federation. https://minpromtorg.gov.ru/ (in Russ.). Assessed May 07, 2025.
[4] https://rscf.ru/ (in Russ.). Accessed May 07, 2025.
[5] https://fasie.ru/ (in Russ.). Accessed May 07, 2025.
[6] https://fpi.gov.ru/ (in Russ.). Accessed May 07, 2025.
[7] https://frprf.ru/ (in Russ.). Accessed May 07, 2025.

Fig. 2. Measures to support the industry

Skolkovo Fund[8], and the Technological Development Agency[9].

In addition to direct financial measures for stimulating specific projects, one of the most important measures to support enterprises and organizations in the industry is the provision of tax benefits in terms of insurance premiums and income tax[10, 11]. To date, more than 600 companies in the industry have benefited from these incentives. In 2022–2024, electronics companies and organizations will save more than RUR 180 bn as a result, which is comparable to the amount of direct state support.

Although the Russian electronics industry is already demonstrating healthy growth, the country's leadership has set even more ambitious goals. A new impetus to the industry development was given by the decision of the President of the Russian Federation Vladimir Putin, who approved the "Fundamentals of the State Policy of the Russian Federation in the field of development of electronic and radioelectronic industry for the period up to 2030 and further prospect"[12], representing the main strategic document for the development of electronics. The general goal is proclaimed technological sovereignty of the Russian electronics industry. The documents also approved indicators for achieving this goal (Fig. 3), including:

(1) continued growth of industry revenue up to RUR 6.3 tn per year (2.4 times growth by 2023);
(2) meeting domestic demand for electronic products by at least 70%;
(3) ensuring sovereignty over resources and means of production;
(4) further technological development and industrialization of topological standards of 28 nm and lower.

[8] https://sk.ru/ (in Russ.). Accessed May 07, 2025.
[9] https://atr.gov.ru/ (in Russ.). Accessed May 07, 2025.
[10] Resolution of the Government of the Russian Federation No. 1310 dated July 22, 2022 "On Approval of the List of Electronic (Radioelectronic) Products for the Purposes of Application of Reduced Tax Rates for Corporate Profit Tax and Tariffs of Insurance Contributions." http://publication.pravo.gov.ru/Document/View/0001202208010004 (in Russ.). Accessed May 07, 2025.
[11] Resolution of the Government of the Russian Federation No. 1311 dated July 22, 2022 "On Approval of the List of Materials and Technologies for the Production of Electronic Component Base (Electronic Modules) for the Purposes of Applying Reduced Tax Rates for Corporate Profit Tax and Insurance Contributions Tariffs." http://publication.pravo.gov.ru/Document/View/0001202208010009 (in Russ.). Accessed May 07, 2025.
[12] Decree of the President of the Russian Federation No. 344 dated May 12, 2023 (in Russ.).

Fig. 3. Ensuring technological sovereignty in electronics

It is also necessary to ensure the development of new materials, which are especially important for microwave electronics, power electronics, and optoelectronics. To date, in particular, specific plans have been drawn up for the development of technologies for the use of gallium arsenide and gallium nitride, as well as silicon-germanium and silicon carbide [1].

In order to maintain the dynamics of the industry's development and to achieve the target benchmarks, it is necessary to improve the efficiency of work within the industry in order to optimize support measures and obtain a synergetic result. At the micro level, i.e, at the level of the economy of the enterprises of the industry, the main specific goal is to improve production efficiency and labor productivity growth. Here relevant tools include the principles of lean production [2] and scientific organization of labor[13], whose positive effects have been repeatedly confirmed[14].

At a higher level of organization, which can be referred to as the meso-level of management [3], it is the growth of efficiency of interaction of all industry participants both among themselves and with external suppliers and consumers of electronics products in order to achieve the strategic indicators set at the highest macro-level by the President of the Russian Federation and the Government of the Russian Federation (Fig. 4). In this respect, the achievements of the Russian electronics industry in the recent past serve as a foundation [4, 5]. An effective tool consists in the proven technology of sectoral planning and management as set out in the General Scheme of Development and Location of Productive Forces of the Electronics Industry for the strategic depth of planning [6, 7]. Quality planning requires a reliable basis in the form of complete information on the real state of productive forces of the electronics industry. This can only be provided by a complete inventory in the industry carried out irrespective of the various organizational and legal forms of legal entities and their forms of ownership. Such an inventory will present a real picture of the electronics industry economy to enable organizations to identify the optimal application of their competencies and qualifications.

2. SCIENTIFIC APPROACHES OF PROFESSOR V.M. SIMCHERA

Professor V.M. Simchera defined the general inventory of electronics and the entire economy of Russia as a one-time accounting (census, censorship, audit, revaluation) of all available material, labor, financial and intellectual assets of the industry (country), comprehensively characterizing its general condition and wealth, its total national wealth in all forms of ownership, types, and areas of activity in specific conditions of space and time[15].

According to Simchera, the results of the inventory serve as "the most complete source of primary data, the most reliable tool for verification of existing

[13] https://национальныепроекты.рф/news/umnaya-optimizatsiya-chto-takoe-berezhlivoe-proizvodstvo-i-zachem-ego-vnedryat/ (in Russ.). Accessed May 07, 2025.
[14] https://производительность.рф/ (in Russ.). Accessed May 07, 2025.
[15] Manuscript archives of Dr. of Economics, Prof. V.M. Simchera (in Russ.).

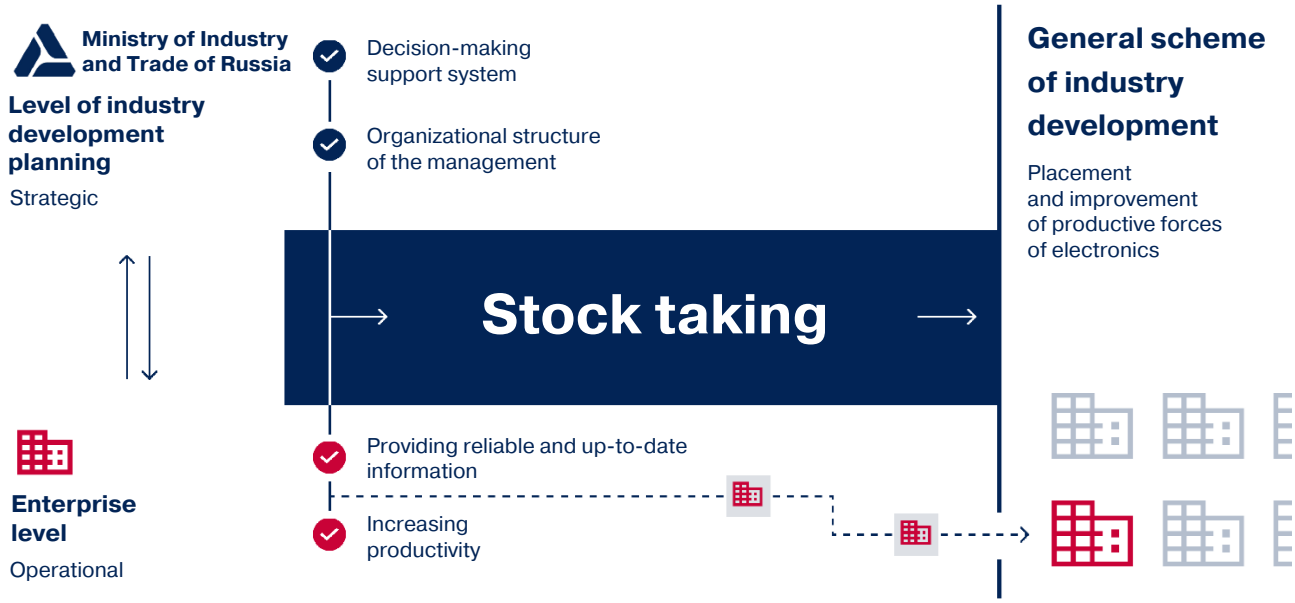

Fig. 4. Strategic planning of industry development

assessment databases of big data and knowledge bases, their basis of foundations, a kind of initial reference point, outside or bypassing which it is impossible to verify and nominate the state of the country even in the crudest form."[16] The development of events since February 2022 demonstrates the acute nature of the issue of inventory management. At that point, the Russian economy began to receive unexpected blows of Western attackers on its most vulnerable points, which until then had seemed quite solid.

Whether at any particular moment or in terms of the dynamics from the past to the future, it is impossible to see the whole without precise knowledge of the state of productive forces of the economy. This involves measuring achievements and failures to objectively assess its state and potential in both favorable and critical situations. Thus a deep knowledge of the entire system of productive forces of the country's economy in all the diversity and integrity of production and economic relations is necessary to avoid gross errors and develop a capable management system.

It still seems astonishing that the Russian privatization was carried out by its executors without scientifically substantiated data on the role of each enterprise in the life of the country, which could be obtained only as a result of a total inventory. This fact alone calls into question the ideas underpinning the irresponsible and inequitable privatization of property that belonged under the Constitution[17] to all citizens of the country in an equal, inheritable, and inalienable share. In the first place, these ill-considered, hasty, and harmful actions affected the most advanced sectors of the national economy in general—and electronics in particular.

Since is very difficult to quantify the damage that was caused to Russia by the leaders of privatization in the 1990s, we will refer to the estimates of V.M. Simchera, who considered the damage to the national economy and population of Soviet Union during the Great Patriotic War at 1.0 tn American dollars of the mid-20th century or USD 17.9 tn, which were circulating in the 1990s. V.M. Simchera estimated privatization and collapse of the USSR no less than 100 tn modern American dollars [8, 9]. The President of the Russian Federation and the Government of the Russian Federation are actively engaged in trying to compensate for this damage.

Taking the form of classical census surveys, inventorization has been conducted on a regular basis every 5–10 years in developed countries since the middle of the nineteenth century. However, in Russia there have never been general regular censuses; as a consequence, there is a lack of reliable cadaster of data and full-fledged statistics of the Russian economy.

[16] Manuscript archives of Dr. of Economics, Prof. V.M. Simchera (in Russ.).

[17] Constitution of the USSR, Chapter 2 "Economic System", Article 10 (adopted at the Extraordinary Seventh Session of the Supreme Soviet of the USSR of the Ninth Convocation on October 7, 1977 (in Russ.).)

3. JUSTIFICATION OF THE NEED FOR INVENTORY

More than 80 different strategic planning documents and development programs have been adopted in Russia (e.g., "Strategy for the Development of the Russian Electronic Industry until 2030,"[18] "Strategy for the Production of Stringed Musical Instruments,"[19] etc.). All of these are based on different worldview platforms, methods of goal-setting, dimensionalities, as well as variations in the scope and coverage of the tasks to be solved. Since each initiator of such documents sees their strategy as the dominant one, mechanisms and technologies are proposed to achieve the set goals. However, due to the lack of even the most general idea of actually available resources and opportunities, one has a holistic view of the structure, capacity, and distribution of productive forces today. It is clear that disparate and unconsolidated strategic planning documents and development programs can be implemented only accidentally—and, as previous experience shows, only fragmentarily. And, if a disruption in the production of stringed musical instruments will be an unpleasant fact, the lack of electronic components, equipment and electronic products will be a disaster for the economy of the whole country.

Clearly, the other extreme of investing all funds in electronics should also be avoided: electronic products must grow proportionally to demand. However, it is remains impossible to metrically determine the existing proportions in the country's economy and dynamically forecast the optimally balanced development of industries and enterprises of both electronics producers and consumers without a total and coherent inventory. Consequently, it already becomes clear at this step of scientific analysis that only multidirectional detailed and reliable knowledge of the structure of productive forces of each industry and the country's economy can ensure the growth of electronic products production in proportion to the growth of productive capacities and solvent demand of electronics consumers.

The necessary total inventory should be based on unified databases and knowledge, as well as on unified functional and instrumental support, which is unfortunately still only being formed in the academic community. In terms of its dimensionality, structure, scale, and coverage, involving a multitude of fixed factor indicators and schemes of their multidimensional functional-cost analysis, technical regulations, standards, registers and other fundamental system characteristics, the Russian electronic industry has no analogs in the world. For this reason, any borrowing of foreign tools will be unsuitable for practical purposes.

Successful management of the country's economy, industry, enterprise, city, family requires reliable information that represents an undistorted image of any managed object or process. Such an adequate virtual model can now be formed digitally. However, since an image cannot be created on the basis of analytical "average ceiling" representation, it will be necessary to obtain first-hand genuine (ontological) primary data, which can be collected and processed only through a total inventory of economic and business objects and processes in which they are involved. Between two related inventories, it is necessary to regularly conduct clarifying continuous or selective, statistical, and non-statistical measurements of changes and dynamics of productive forces. The necessary inventory of intellectual, organizational, material-technological, and financial resources allocated for the development of electronics is currently being formed in the Ministry of Industry and Trade of Russia. This task, which falls within the achievement purview of Russian developers of big data platforms [10], can be easily supported by the current capabilities of Russian supercomputers[20].

The process of adaptation to Western sanctions and planning for the development of the Russian economy can become more effective if reliable data on all elements of the structure of productive forces (production facilities and qualified personnel) are obtained along with the potential for their effective utilization in the current environmental conditions. In order not to assume unfulfilled obligations, it is necessary to carry out a complete inventory and establish specific responsible executors for the efficient use of production funds.

As a result of the lack of reliable information about the country's productive forces, including the lack of strict control over top managers, the Russian economy

[18] Order of the Government of the Russian Federation No. 20-r dated January 17, 2020 "On Approval of the Strategy for the Development of the Electronic Industry until 2030." http://government.ru/docs/38795/ (in Russ.). Accessed May 07, 2025.

[19] Order of the Government of the Russian Federation No. 1582-r dated June 11, 2021 "On Approval of the Strategy for the Development of the Musical Instruments and Sound Equipment Industry for the Period until 2030." http://government.ru/docs/42466/ (in Russ.). Accessed May 07, 2025.

[20] http://top50.supercomputers.ru/newsfeed (in Russ.). Accessed May 07, 2025.

is developing at an insufficient pace to overtake modern leaders in electronics. This applies to electronics, foreign exchange reserves, durable goods, and food. However, without scientifically sound and verified practices, in which total inventory plays a paramount role, it will be extremely difficult to move to the stage of sovereignty. While the task of responding to sanctions and other challenges is undoubtedly urgent, the important business of inventory cannot be neglected, since in the long term this will provide the country and the population a sustainable positive boost in development terms.

For decades already, instead of joint and creative work on the inventory of the economy, "effective managers" have been fighting for some Western ratings, like Moody's[21], Fitch Ratings[22], in order to report about the increase in the rating of the country, or a particular university, bank, etc. What ended their struggle is now clearly visible, despite nothing catastrophic having happened to the Russian economy as a result.

Under the new conditions of the economic war of the West against Russia, it is obvious that it the development and nationwide discussion of an independent inventory strategy-program is required. This should be transferred to the development of organizational structures of industry management and the creation of the general scheme of development and location of productive forces of the country in sectoral, territorial, and generalizing formats [1]. The first step in the form of the General Scheme of Electric Power Industry Development by the Government of the Russian Federation[23] has already been taken.

4. INVENTORY OBJECT

When taking a systematic approach to the creation of an inventory, its objects should be sectoral and territorial proportions of the distribution of productive forces, along with the resulting parameters of the rate of development of socioeconomic processes in Russia.

Many independent experts try to compare the state of the economy of Russia and Western countries. However, they do not take into account that the Russian Empire in 1917 and the USSR in 1991 lost 5.3 mln square km or almost 1/4 of its territories, involving more than 140 mln people or half of the total population, along with two thirds of the production potential and accumulated national wealth. Such huge losses have not known any state for the whole millennial history. If these losses are included in the calculations and ratings, the conclusions will be quite the opposite.

The years of the country's economic development following the destructive years of privatization have demonstrated that the liberal-capitalist model of society lacks unity of views on the integral system of socioeconomic relations. Accordingly, it is unable to realize the effect of synergetic multiplication of productive forces and production relations. Liberal globalization leads only to the loss of sovereignty and prohibitive dependence of the country on the world's transnational corporations. The President of the Russian Federation Vladimir Putin has formulated in the most general form the thesis that dying liberalism[24] and private property[25] [11] do not unite, but rather divide people according to their selfish ends, which will inevitably lead to the failure of the country's economic policy. Liberals throughout the modern historical period have tried to dictate their will to the world. However, since their will proceeded from the interests and values of the rulers of the artificial human habitat represented by the capitalist economy, it constantly conflicts with the natural interests of the majority of people.

In order to follow the course outlined by the President of the Russian Federation Vladimir Putin, the private property that appeared in the course of ill-considered and hasty privatization should be systematically replaced by property that is understood as part of the state, thus functioning as a single integral ensemble. This is the root and quintessence of the country's economic sovereignty.

It is not necessary to prove that, despite the current contradictory Russian reality and series of sanctions against Russia and its citizens, future changes can only be constitutional. Such reforms that take into account real inertia processes and national traditions can be optimal in speed and depth.

[21] https://ratings.moodys.com. Accessed May 07, 2025.

[22] https://fitchratings.com/. Accessed May 07, 2025.

[23] Order of the Government of the Russian Federation No. 4153-r dated December 30, 2024 "On Approval of the General Scheme of Electric Power Industry Facilities Location until 2042." http://government.ru/docs/53923/ (in Russ.). Accessed May 07, 2025.

[24] Interview with the President of the Russian Federation V.V. Putin on the eve of the G-20 summit. http://www.kremlin.ru/events/president/news/60836 (in Russ.). Accessed May 07, 2025.

[25] Private property is a part of national property that has become dependent on capitalists (e.g., the closure of enterprises in Russia). Partial property is the national property that is transferred to private managers who can ensure its most efficient use.

The President of the Russian Federation Vladimir Putin pursues the following line[26]: all processes in Russian society and economy should follow from the consensus of the social contract to become a program of general civil accord, thus uniting the healthy forces of Russian society and its allies on the principles of common sense. Along with the general progress of friendly countries, the success of the electronics industry as the most technologically advanced branch of the country will be characterized by the speed and scope of the universal transition from the present private economy to an economy of pragmatic altruism. The production of various goods with the condition of obligatory reproduction of resources in the natural environment in order to guarantee the basis for sustainable development of future generations should be considered as the norm of future social relations. It is this world outlook criterion that should form the basis for the inventory of the country's productive forces and the elaboration of the general scheme for the development of the economy in general and electronics in particular. We can and should use the systemic global economic crisis as a chance for harmonious development of economy and society in Russia, as well as in countries that share Russia's system of values.

Thus, the object of inventory consists in the entire system of socioeconomic relations in Russia, in which electronics plays an increasing and indispensable role. It is now clear that by grasping this crucial link, it is possible to pull the whole chain to a new phase of progress: the first step should be a nationwide inventory.

The inventory should metrically accurately reflect the real advantages of Russian economy, including the vast natural and skilled human resources used by private owners to barely one-third of their useful capacity. The backbone of the country's former intellectual and military potential has been preserved and recently even multiplied. However, this advantage has not yet been statistically measured, which means that it is difficult to use it effectively as a basis. Progressive improvement of legislative, informational and administrative-technical support of the Russian economy is already yielding tangible results, especially under the conditions of unprecedented sanctions pressure on the country and the economy. Thanks to the persistent implementation of scientific programs, new "windows of opportunity" have been opened for the transition of Russian economy to the sixth mode [12, 13] of future development of Russia and the world. As part of this process, the electronics industry will be assume one of the most prominent positions.

Methods and tools for managing the country's economy and any industrial sector should be chosen depending on the reliability, completeness, and integrity of knowledge about the socioeconomic situation and the objective needs of economic and social development. Currently, no manager starting from the micro-level of enterprises and ending with meso- and macro-levels can be confident in assessing the current state of the managed object and the formation of a winning strategy for further development due to the lack of a holistic picture and the inability to assess the risks beyond the extremely narrow boundary of the sphere of opportunities. Winston Churchill humorously observed that he trusted only those statistics that he himself falsified. Without an inventory, there is no understanding of the extent to which information about the state of affairs in the economy is falsified, or who exactly falsified it and how. Today, there are no longer any proponents of investing the country's reserves in Western financial jurisdictions rather than in the country's productive potential. It is easy to imagine what NATO and the European Union would say now if the frozen USD 300 bn[27] had been invested in the production potential of Russian electronics and related industries.

In his recent articles and speeches, V.M. Simchera authoritatively argued that none of the socioeconomic programs in Russia in the 21st century was ever implemented [14]. Of course, some officials can be accused of incompetence, but the majority of Russian managers and scientists sincerely wished for the fulfillment of the plans. This is the best proof that the specialists who adopted the planned guidelines simply did not realize where they were located.

I would like to emphasize that specialists of economic management bodies present detailed accounts of the true state of affairs in the sphere of their competence, but life goes on in its own way. People move to other jobs, retire, etc. Along with the individual specialists, the knowledge they were carrying also disappears from their offices. New appointees need time to form a holistic idea of the assigned work, which hinders development. For this reason, the inventory, organizational management structure, and general development scheme of productive forces of industries and the economy should

[26] Putin V.V. ASI Forum "Strong Ideas for New Times," 2022. http://www.kremlin.ru/events/president/transcripts/69039 (in Russ.). Accessed May 07, 2025.

[27] https://www.rbc.ru/economics/13/03/2022/622dd6ee9a7947081b63341c?ysclid=m3ujyuye2217113543 (in Russ.) Accessed May 07, 2025.

be formalized in the form of integral, but constantly updated data, which is approved at a high state level. In this case, people may change, but newcomers will have a formalized initial base and material traces of its development by the previous manager. This will significantly increase the efficiency of management, especially at the sectoral meso-level, along with the responsibility of officials for their decisions, which will be reflected as author's innovations in the organizational structure and the General Scheme of Industry Development.

5. MEASURES TO IMPLEMENT THE INVENTORY PROGRAM

The program of inventory of productive forces of the country developed by the group of specialists under the leadership of V.M. Simchera included 77 measures, which should provide the management bodies with reliable information in the context of 280 indicators. Here it is advisable to consider the most significant for electronics provisions.

The electronics industry was seriously underfunded in the period up to 2020, while the demand for its products was growing at a faster rate. As noted above, the right decisions have by now been made to significantly increase capital investments in the industry. Under these conditions, it is especially important to balance them in terms of time, territorial location, and technological level with parallel training of specialists for future new production facilities. Fortunately, sanctions have forced Russian consumers, who previously ordered foreign-made electronics, to turn their attention to Russian manufacturers. The inventory should provide a clear picture of the current and future ratio between the primary factors of production consisting of fixed assets and highly qualified personnel, both temporally and territorially.

One of the bottlenecks in the electronics industry is the rapid obsolescence of the production and technological potential of enterprises, which sometimes significantly outpaces the rate of physical wear and tear of equipment. A complete census and cost estimation of electronic industry equipment will permit an optimization of depreciation charge norms, as well as forming an approach to determining the types of equipment subject to accelerated depreciation. This "accounting" issue is so significant for the electronic industry enterprises that its solution cannot be postponed under any circumstances. Otherwise, the technological lag of the industry will grow and may become catastrophic.

One of the most significant factors of efficiency of electronics and entire economy include specialization, cooperation, and the optimal size of enterprises. Our global competitors are represented by giant transnational corporations that deploy thousands of small and medium satellites around the main economic entity. Privatization, which destroyed sectoral, inter-sectoral cooperation links and clusters of co-operators along the entire chain from research and development (R&D) to the production of finished goods, has not yet been assessed from the position of optimality and efficiency of modern production. Without a comprehensive inventory, the current situation is difficult to assess and consequently almost impossible to improve. In this regard, all existing reports on R&D performed in ministries and departments should be subjected to inventory and deep scientific audit, with the obtained results be put up for auction for their commercialization on the basis of a public–private partnership.

In addition, the inventory will provide a metric for weighing all the factors that influence productivity and form a clear program for generating the required number of high productivity jobs.

A significant development problem consists in the gap between the performance of enterprises, industries, as well as the economy as a whole, as measured in physical and value terms. In addition to solving the problem of assessing the production and technological potential of industries, the proposed inventory will permit the establishment and accounting adjustment of manufactured products to be as close as possible to the final physical and natural results, thus reflecting the real shifts in the economy and the actual situation of people in society. This is not a private task, but a question of manageability, since artificial cost indicators under conditions of galloping inflation and the dominance of the shadow economy reflect little more than errors and mistakes. It will also make it possible to measure the welfare of the population in natural units.

There are already tools that can be used to carry out the first wave of industrial inventory, both in terms of the production capacities of enterprises and the products they produce. For example, a catalog of industrial products manufactured in Russia has been formed on the platform of the State Information System of Industry (SISI)[28]. The catalog contains information on more than 1.6 mln units of products, including more than 360000 units of Russian industrial products with an indication of the manufacturer, the commodity nomenclature of the Eurasian Economic Union, and, with respect to certain Russian radioelectronic

[28] https://gisp.gov.ru/ (in Russ.). Accessed May 07, 2025.

products, the component parts of Russian origin. As for Russian radioelectronic products, the catalog is used as a basis for building the entire system of preferences and state support for the industry. The relevance and completeness of information on the confirmation of Russian origin is realized automatically within the framework of integration interaction with the service of implementation of the Decree of the Government of the Russian Federation dated July 17, 2015, No. 719[29].

SISI also contains tools for describing the production capacities of enterprises, entering information on the volume of production, shipment and sale of goods, including exports, both on the industrial enterprises themselves and the characteristics of their industrial products, taking into account their sectoral affiliation and the level of digital maturity of industrial enterprises. By carrying out verification and operational monitoring of the financial and economic status of systemically important producers of industrial products, it also becomes possible to assess the economic stability of producers in real time.

When supplemented with the necessary industry reliable statistics, including the results of "big data" analysis from open sources, an inventory knowledge base is created having possibilities of seamless integration of the SISI with the accounting systems of enterprises to simplify the mechanism of operational automated collection and processing of the necessary data. The current level of SISI development is already sufficient to start the inventory of industrial products and enterprises producing them in Russia. This will form the basis for territorial and production planning at a strategic depth.

In addition, the basic architecture of the industry decision support system has been designed to date. The complex of "Multi-agent network-centric model of electronics resource management" [15], "Organizational structure of industry business process management," and "General scheme of development and location of productive forces of electronics for the period up to 2050" will form the basis for strategic planning of development of the electronics industry, starting from the detailed goals and objectives facing the national economy (industries, territories), which are formulated by the country's leadership, and ending with the optimization of industry cooperation and logistic interconnection of co-executors of both state tasks and enterprises working in the unregulated market.

In order to obtain the necessary qualitative data, separate systematic analytical studies in the field of development of electronic engineering (including materials, chemistry), photonics technologies, human resources have been carried out in recent years. This formed the basis to approve comprehensive programs for the development of electronic engineering and photonics. However, it is necessary to complete such work in the field of microelectronics technologies, along with power and microwave electronics, passive electronics and electrical engineering, as well as to continue the expansion of comprehensive studies of the state and development prospects of all electronics technologies, the customization of systems of industry and state statistics, and determination of approaches to territorial and production planning and compilation of inter-sectoral balances [16].

The inventory should be the starting point for the fundamental implementation of digital technologies in the management of the electronics industry, the flowchart of which can be visualized as follows (Fig. 5).

CONCLUSIONS

The proposed inventory of the Russian electronics industry and the country's economy as a whole will make it possible to restore the reliability of statistical data, which is currently the subject of considerable doubts. By systematizing and evaluating the obtained data, it also will be possible to more responsibly counteract the leakage of sensitive information from Russia.

In order to prepare, conduct and continue this crucial work it is necessary to restore in Russia the work on operational tracking of the dynamics of the pro-inventorized parameters of the Russian economy and their comparison with the world's best scientific, technical and technological achievements and standards. The necessary revival of methodological and factual work on the formation of the necessary balances should start from individual product graphs linking all co-executors and product-service platforms, which balance the reproduction process on the scale of sub-sectors of the electronics industry, and end with the sectoral balance of ordered results with available resources. This should be carried out in conjunction with the integral inter-sectoral balance of the country's economy. Synchronization of this work with the national inventory will ensure the reliability not only of sectoral management, but also the maintenance of the proportions of the Russian economy as a whole. This approach will make it possible to synergistically accelerate the pace of economic development of the community of friendly countries and introduce a qualitatively new meso-economic management platform in the format of an electronic industry digital twin.

[29] http://government.ru/docs/all/102816/ (in Russ.) Accessed May 07, 2025.

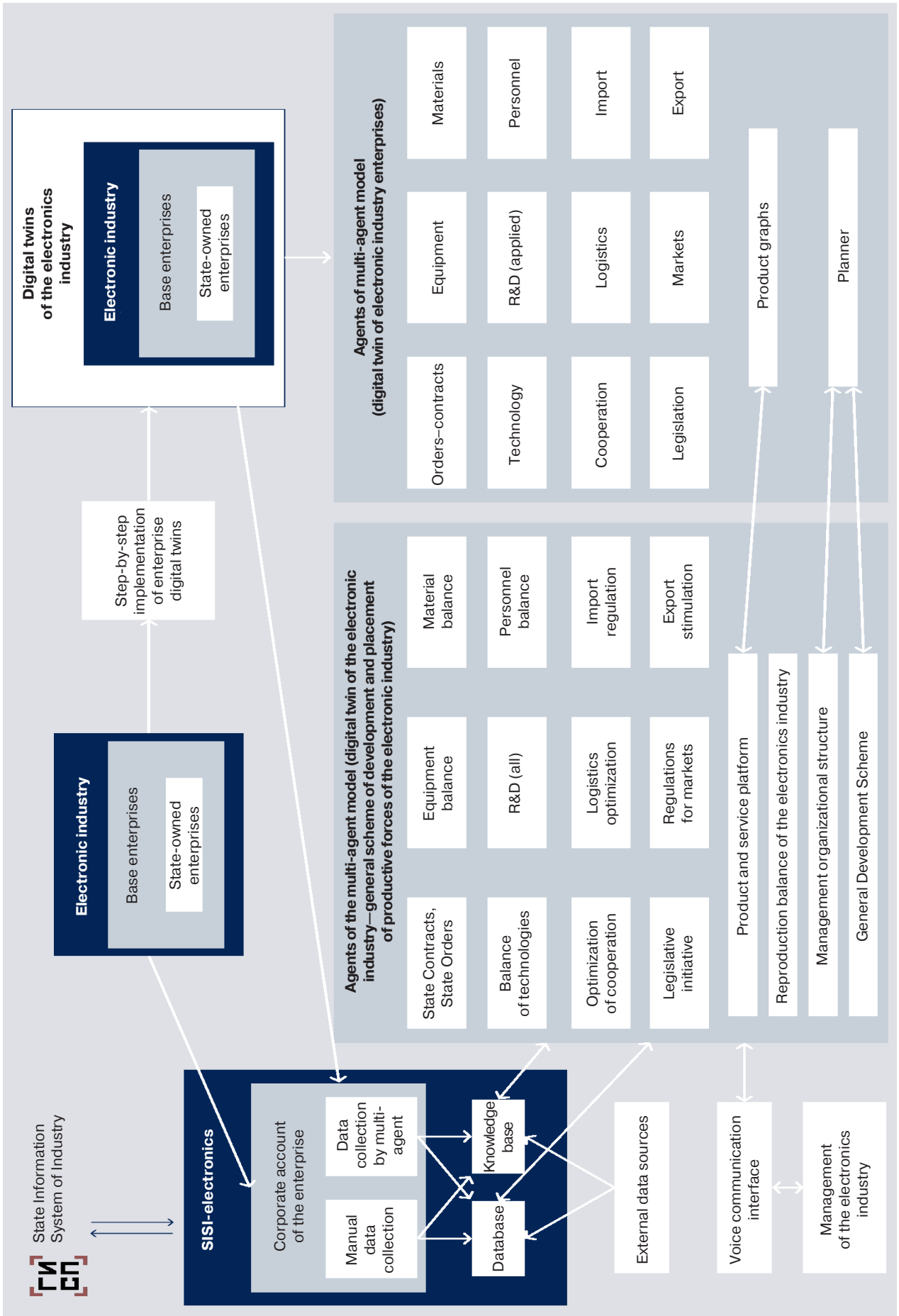

Fig. 5. Block diagram of electronic industry management based on modern digital technologies

REFERENCES

1. Shpak V.V. *Razvitie elektronnoi promyshlennosti v usloviyakh menyayushchegosya mira* (*Development of the Electronics Industry in a Changing World*). Moscow: Tekhnosfera; 2024. 128 p. (in Russ.). ISBN 978-5-94836-708-8
2. Liker J.K. *Dao Toyota: 14 printsipov menedzhmenta vedushchei kompanii mira* (*The Toyota Way: 14 Management Principles from the World's Greatest Manufacturer*): transl. from Engl. Moscow: Alpina Pablisher; 2022. 492 p. (in Russ.) ISBN 978-5-6047582-0-5
   [Liker J.K. *The Toyota Way: 14 Management Principles from the World's Greatest Manufacturer*. NY.: McGraw-Hill; 2004. 352 p. ISBN:0071392319]
3. Maevskii V.I. (Ed.). *Mezoekonomika: sostoyanie i perspektivy*: monografiya (*Mesoeconomics: State and Prospects*: monograph). Moscow: Institute of Economics, RAS; 2018. 314 p. (in Russ.). ISBN 978-5-9940-0642-9
4. Shokin A.A. *Ministr neveroyatnoi promyshlennosti SSSR* (*Minister of Incredible Industry of the USSR*). Moscow: Central Research Institute "Electronics"; 1999. 373 p. (in Russ.).
5. Shokin A.A. *Ministr neveroyatnoi promyshlennosti SSSR* (*Minister of Incredible Industry of the USSR*). Moscow: Tekhnosfera; 2007. 455 p. (in Russ.). ISBN 978-5-94836-151-2
6. Shpak V.V. Formation of the organizational and managerial model for the implementation of the "Strategy for the Development of the Electronics Industry of the Russian Federation for the period up to 2030." *Vestnik Chelyabinskogo gosudarstvennogo universiteta = Bulletin of Chelyabinsk State University*. 2021;3(449):10–23 (in Russ.). https://doi.org/10.47475/1994-2796-2021-10302
7. Shpak V.V. Development Strategy for the Electronics Industry of the Russian Federation and its Financial Support. *Ekonomika nauki = Economics of Science*. 2021;7(3):195–204 (in Russ.). https://doi.org/10.22394/2410-132X-2021-7-3-195-204
8. Simchera V.M. American Censuses. *Uchenye zapiski po statistike AN SSSR*. 1969;18:288–314 (in Russ.).
9. Simchera V.M. Industrial Censuses of the USA. *Vestnik statistiki = Bulletin of Statistics*. 1970;1:45–54 (in Russ.).
10. Shpak V.V. Fundamentals of a Multi-Agent Planning and Logistics Model for Managing the Reproduction Cycle of the Industry in the "Online" Mode. *Fundamental'nye issledovaniya = Fundamental Research*. 2022;3:146–155 (in Russ.). https://doi.org/10.17513/fr.43229
11. Ryazanov A. *Narodnyi sotsializm. Teoriya.* (*People's socialism. Theory*). VI. Moscow: Ritm; 2020. 280 p. (in Russ.). ISBN 978-5-98422-474-1
12. Pereslegin S.B. Technological Order VI: the Space of Opportunities. *Ekonomicheskie strategii = Economic Strategies*. 2019;3:24–33 (in Russ.).
13. Glaz'ev S.Yu. New approaches to the organization of enterprises in the context of changing technological and world economic modes. In: Kleiner G.B. (Ed.). *Strategic Planning and Evolution of Enterprises: Materials. 20th Russian Symposium.* Moscow: CEMI RAS; 2019. P. 7–18 (in Russ.).
14. Kretov S.I., Simchera V.M. What after liberalism? *Izborskii klub = Izborsky Club.* 2020;9(85):90–115 (in Russ.).
15. Galuzin V., Galitskaya A., Grachev S., Laruchkin V., Novichkov D., Skobelev P., Zhilyaev A. The Autonomous Digital Twin of Enterprise: Method and Toolset for Knowledge-Based Multi-Agent Adaptive Management of Tasks and Resources in Real Time. *Mathematics.* 2022;10(10):1662. https://doi.org/10.3390/math10101662
16. Kantorovich L.V. Mathematics in Economics: Achievements, Difficulties, Prospects. (Lecture at the Swedish Academy of Sciences on the Occasion of the Awarding of the Nobel Prize for 1975). *EKO = ECO*. 1976;3:123–133 (in Russ.).

СПИСОК ЛИТЕРАТУРЫ

1. Шпак В.В. *Развитие электронной промышленности в условиях меняющегося мира*. М.: Техносфера; 2024. 128 с. ISBN 978-5-94836-708-8
2. Лайкер Д. *Дао Toyota: 14 принципов менеджмента ведущей компании мира*: пер. с англ. М.: Альпина Паблишер; 2022. 492 с. ISBN 978-5-6047582-0-5
3. *Мезоэкономика: состояние и перспективы*: монография; под ред. Маевского В.И. М.: Институт экономики Российской академии наук; 2018. 314 с. ISBN 978-5-9940-0642-9
4. Шокин А.А. *Министр невероятной промышленности СССР*. М.: ЦНИИ «Электроника»; 1999. 373 с.
5. Шокин А.А. *Министр невероятной промышленности СССР*. М.: Техносфера; 2007. 455 с. ISBN 978-5-94836-151-2
6. Шпак В.В. Формирование организационно-управленческой модели реализации «Стратегии развития электронной промышленности Российской Федерации на период до 2030 года». *Вестник Челябинского государственного университета*. 2021;3(449):10–23. https://doi.org/10.47475/1994-2796-2021-10302
7. Шпак В.В. Стратегия развития электронной промышленности Российской Федерации и ее финансовое обеспечение. *Экономика науки*. 2021;7(3):195–204. https://doi.org/10.22394/2410-132X-2021-7-3-195-204
8. Симчера В.М. Американские цензы. *Ученые записки по статистике АН СССР*. 1969;18:288–314.
9. Симчера В.М. Промышленные цензы США. *Вестник статистики*. 1970;1:45–54.
10. Шпак В.В. Основы мультиагентной планово-логистической модели управления воспроизводственным циклом отрасли в режиме «онлайн». *Фундаментальные исследования*. 2022;3:146–155. https://doi.org/10.17513/fr.43229
11. Рязанов А. *Народный социализм. Теория*. VI. М.: Ритм; 2020. 280 с. ISBN 978-5-98422-474-1
12. Переслегин С.Б. VI технологический уклад: пространство возможностей. *Экономические стратегии.* 2019;3:24–33.

13. Глазьев С.Ю. Новые подходы к организации предприятий в условиях смены технологического и мирохозяйственного укладов. В сб.: *Стратегическое планирование и развитие предприятий: пленарные доклады Двадцатого Всероссийского симпозиума*; под ред. чл.-корр. РАН Г.Б. Клейнера. М.: ЦЭМИ РАН; 2019. С. 7–18.
14. Кретов С.И., Симчера В.М. Что после либерализма? *Общественно-политический журнал «Изборский клуб»*. 2020;9(85):90–115.
15. Galuzin V., Galitskaya A., Grachev S., Laruchkin V., Novichkov D., Skobelev P., Zhilyaev A. The Autonomous Digital Twin of Enterprise: Method and Toolset for Knowledge-Based Multi-Agent Adaptive Management of Tasks and Resources in Real Time. *Mathematics.* 2022;10(10):1662. https://doi.org/10.3390/math10101662
16. Канторович Л.В. Математика в экономике: достижения, трудности, перспективы. (Лекция в Шведской академии наук в связи с присуждением Нобелевской премии за 1975 год). *ЭКО* (*Экономика и организация промышленного производства*). 1976;3:123–133.

About the Author

Vasily V. Shpak, Cand. Sci. (Econ.), Associate Professor, Department of Nanoelectronics, Institute for Advanced Technologies and Industrial Programming, MIREA – Russian Technological University (78, Vernadskogo pr., Moscow, 119454 Russia). E-mail: morser@yandex.ru. https://orcid.org/0009-0002-3548-1070

Об авторе

Шпак Василий Викторович, к.э.н., доцент, кафедра наноэлектроники, Институт перспективных технологий и индустриального программирования, ФГБОУ ВО «МИРЭА – Российский технологический университет» (119454, Россия, Москва, пр-т Вернадского, д. 78). E-mail: morser@yandex.ru. https://orcid.org/0009-0002-3548-1070

Translated from Russian into English by L. Bychkova
Edited for English language and spelling by Thomas A. Beavitt